Acoustic Characterization of Environments (ACE) Challenge Results Technical Report

James Eaton*[1], Nikolay D. Gaubitch†[2], Alastair H. Moore‡[1], and Patrick A. Naylor§[1]

[1]Dept. of Electrical and Electronic Engineering, Imperial College London, UK
[2]SIP Lab, Delft University of Technology, Netherlands, and Pindrop Security

Abstract

This document provides supplementary information, and the results of the tests of acoustic parameter estimation algorithms on the Acoustic Characterization of Environments (ACE) Challenge [1] Evaluation dataset which were subsequently submitted and written up into papers for the Proceedings of the ACE Challenge [2]. This document is supporting material for a forthcoming journal paper on the ACE Challenge which will provide further analysis of the results.

*j.eaton11@imperial.ac.uk
†n.d.gaubitch@tudelft.nl
‡alastair.h.moore@imperial.ac.uk
§p.naylor@imperial.ac.uk

Contents

List of Figures

List of Tables

1 Introduction

This document provides supplementary information and the results of the Acoustic Characterization of Environments (ACE) Challenge Phases 1 and 2 for all the tasks, Reverberation Time (T_{60}) and Direct-to-Reverberant Ratio (DRR) estimation in both fullband and in frequency bands.

1.1 Room recording procedure

The recording procedure in each room involved the following steps:

1. Install recording equipment positioning the microphones in Position 1, and document the room dimensions and the positions of all microphones, sources and seats;
2. Make empty-room Acoustic Impulse Response (AIR) measurements and noise recordings; Empty-room measurements were for verification purposes and do not form part of the published corpus since the set is not complete, although they may be used in future experiments;
3. Participating subjects take their seating positions;
4. Make occupied AIR measurements and noise recordings;
5. Move microphones to Position 2 and document their positions;
6. Make occupied AIR measurements and noise recordings;
7. Participants leave the room;
8. Make unoccupied AIR measurements and noise recordings in the second microphone position;
9. Uninstall recording equipment.

1.2 Room properties

1.2.1 Room dimension and microphone positions

Tables 1 and 2 give the room dimensions and positions of the centre of each microphone array. Also included is the position of the source and each of the fans used to create the fan noise. Between 1 and 3 fans were used depending on the size of the room. The microphone elements in the cruciform. mobile, linear array and Chromebook are assumed to be omnidirectional. The look direction is provided for the source and Eigenmike since these do not have an omnidirectional directivity pattern. This look direction also applies to the orientation of the 8-channel linear array which was always perpendicular to the look direction of the Eigenmike. The 3-element mobile array was mounted with the longer edge with two microphones perpendicular to the look direction of the Eigenmike. The individual elements in the Eigenmike are omnidirectional, but are mounted

on a solid baffle. The look direction is specified in degrees, where 0 degrees is in the direction of $x = \infty$, and a positive angle is towards $y = \infty$ as illustrated in Fig. 1. In the ACE Challenge, the Dev dataset used channel 1 of the 8-channel linear array, whilst for the Eval dataset, channel 1 of

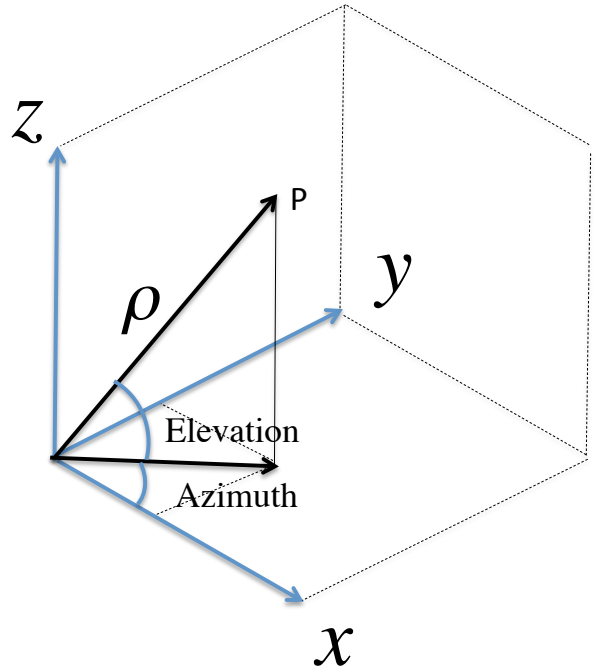

Figure 1: Coordinate system used in tables

the 5-channel cruciform was used. Channel 1 of the 5-channel cruciform was the central microphone which is the same position as for the 5-channel array. Therefore, the position of channel 1 of the 8-channel linear array is provided. Where orientation was possible, fans faced in the same look direction as the source.

1.2.2 Talker positions for babble noise

Table 3 provides each of the talker positions used to produce the babble noise. The z coordinates are not provided since these were not captured. However, the talkers were seated and their mouths were situated at approximately the same height as the microphone arrays which were all at $1.19\,\mathrm{m}$

Table 1: Room dimensions, source, microphone and fan positions

Room Name	Mic. Pos.	Dimensions (L, W, H)	Source Position	Look dir.	5-channel Cruciform	3-channel Mobile	8-channel Linear array
Office 1	1	(3.32, 4.83, 2.95)	(2.06, 1.04, 1.19)	90	(2.66, 2.14, 1.19)	(2.29, 2.15, 1.19)	(1.92, 2.14, 1.19)
Office 1	2	(3.32, 4.83, 2.95)	(2.06, 1.04, 1.19)	90	(2.49, 3.69, 1.19)	(2.15, 3.69, 1.19)	(1.79, 3.67, 1.19)
Office 2	1	(3.22, 5.1, 2.94)	(1.41, 1.73, 1.19)	90	(1.25, 2.81, 1.19)	(1.25, 2.62, 1.19)	(0.84, 2.78, 1.19)
Office 2	2	(3.22, 5.1, 2.94)	(1.41, 1.73, 1.19)	90	(2.25, 4.35, 1.19)	(2.05, 4.16, 1.19)	(1.58, 4.16, 1.19)
Meeting Room 1	1	(6.61, 5.11, 2.95)	(1.39, 1.26, 1.19)	0	(2.74, 0.48, 1.19)	(2.74, 0.82, 1.19)	(2.74, 1.14, 1.19)
Meeting Room 1	2	(6.61, 5.11, 2.95)	(1.39, 1.26, 1.19)	0	(3.96, 0.52, 1.19)	(3.96, 0.85, 1.19)	(3.96, 1.14, 1.19)
Meeting Room 2	1	(10.3, 9.07, 2.63)	(4.65, 4.07, 1.19)	180	(3, 4.39, 1.19)	(3, 3.99, 1.19)	(3, 3.59, 1.19)
Meeting Room 2	2	(10.3, 9.07, 2.63)	(4.65, 4.07, 1.19)	180	(2, 4.39, 1.19)	(2, 3.99, 1.19)	(2, 3.59, 1.19)
Lecture Room 1	1	(6.93, 9.73, 3)	(3.65, 3.73, 1.19)	180	(2.81, 3.84, 1.19)	(2.8, 3.44, 1.19)	(2.89, 3.04, 1.19)
Lecture Room 1	2	(6.93, 9.73, 3)	(3.65, 3.73, 1.19)	180	(1.07, 3.92, 1.19)	(1.07, 3.52, 1.19)	(1.07, 3.12, 1.19)
Lecture Room 2	1	(13.6, 9.29, 2.94)	(6.03, 3.14, 1.19)	180	(5.09, 5.87, 1.19)	(5.09, 5.47, 1.19)	(5.09, 5.07, 1.19)
Lecture Room 2	2	(13.6, 9.29, 2.94)	(6.03, 3.14, 1.19)	180	(3.93, 5.87, 1.19)	(3.93, 5.47, 1.19)	(3.93, 5.07, 1.19)
Building Lobby	1	(4.47, 5.13, 3.18)	(1.98, 0.61, 1.19)	90	(2.69, 2.02, 1.19)	(2.33, 2, 1.19)	(1.95, 2.03, 1.19)
Building Lobby	2	(4.47, 5.13, 3.18)	(1.98, 0.61, 1.19)	90	(2.62, 3.51, 1.19)	(2.25, 3.49, 1.19)	(1.86, 3.54, 1.19)

above the floor.

1.2.3 Distances and look directions

Table 4 provides the source-microphone distances and Direction-of-Arrivals (DoAs) in spherical coordinates, whilst Table 5 provides the fan-microphone distances and DoAs in spherical coordinates.

1.3 Taxonomy of algorithms submitted

There were three main classes of algorithms submitted to the ACE Challenge:

1. Analytical with or without Bias Compensation (ABC);
2. Single Feature with Mapping (SFM);
3. Machine Learning with Multiple Features (MLMF).

Table 2: Room dimensions, source, microphone and fan positions continued

Room Name	Mic. Pos.	32-ch. Eigenmike Position	32-ch. Eigenmike Look dir.	2-channel Chromebook	Ch 1 of 8-ch. linear	Fan 1	Fan 2	Fan 3
Office 1	1	(2.94, 2.15, 1.19)	-90	(3.02, 2.15, 0.68)	(1.68, 2.14, 1.19)	(0.56, 1.43, 1.19)		
Office 1	2	(2.92, 3.69, 1.19)	-90	(2.97, 3.49, 0.68)	(1.55, 3.67, 1.19)	(0.56, 1.43, 1.19)		
Office 2	1	(2.69, 2.84, 1.19)	-90	(2.04, 2.84, 0.68)	(0.6, 2.78, 1.19)	(2.75, 1.25, 1.19)		
Office 2	2	(1.25, 4.25, 1.19)	-90	(0.83, 4.13, 0.68)	(1.34, 4.16, 1.19)	(2.75, 1.25, 1.19)		
Meeting Room 1	1	(2.74, 0.17, 1.19)	180	(2.74, 1.65, 0.68)	(2.74, 1.38, 1.19)	(1.62, 2.2, 1.19)		
Meeting Room 1	2	(3.96, 0.21, 1.19)	180	(3.96, 1.55, 0.68)	(3.96, 1.38, 1.19)	(1.62, 2.2, 1.19)		
Meeting Room 2	1	(3, 4.79, 1.19)	0	(3, 5.19, 0.68)	(3, 3.35, 1.19)	(3.6, 3.15, 0.35)	(3.9, 3.25, 0.35)	
Meeting Room 2	2	(2, 4.79, 1.19)	0	(2, 5.19, 0.68)	(2, 3.35, 1.19)	(3.6, 3.15, 0.35)	(3.9, 3.25, 0.35)	
Lecture Room 1	1	(2.79, 4.24, 1.19)	0	(2.83, 4.64, 0.68)	(2.89, 2.8, 1.19)	(3.65, 3.98, 0.35)	(3.65, 3.48, 0.35)	(3.65, 3.25, 0.1)
Lecture Room 1	2	(1.16, 4.32, 1.19)	0	(1.16, 4.72, 0.68)	(1.07, 2.88, 1.19)	(3.65, 3.98, 0.35)	(3.65, 3.48, 0.35)	(3.65, 3.25, 0.1)
Lecture Room 2	1	(5.09, 6.27, 1.19)	0	(5.09, 6.67, 0.68)	(5.09, 4.83, 1.19)	(6.1, 2.82, 0.35)	(6.1, 3.43, 0.35)	
Lecture Room 2	2	(3.93, 6.27, 1.19)	0	(3.93, 6.67, 0.68)	(3.93, 4.83, 1.19)	(6.1, 2.82, 0.35)	(6.1, 3.43, 0.35)	
Building Lobby	1	(3.1, 2.04, 1.19)	-90	(2.1, 3.49, 0.72)	(1.71, 2.03, 1.19)	(1.74, 0.68, 0.35)		
Building Lobby	2	(2.95, 3.49, 1.19)	-90	(3.35, 3.41, 0.72)	(1.62, 3.54, 1.19)	(1.74, 0.68, 0.35)		

Table 3: Talker positions used to produce babble noise

Room name	Talker ID and associated x-y coordinates 1	2	3	4	5	6	7
Office 1	F6:(2.95, 0.85)	M10:(2.37, 0.65)	M11:(1.64, 0.68)	M17:(1.25, 1.18)			
Office 2	F7:(0.84, 0.55)	M16:(0.6, 1.39)	M10:(0.55, 2.15)	M12:(2.12, 0.4)	M20:(2.07, 1.25)	M15:(2.48, 1.9)	
Meeting Room 1	F7:(0.4, 0.95)	F8:(1.15, 0.4)	M10:(0.65, 3.25)	M11:(0.55, 0.3)	M12:(0.37, 1.78)	M23:(0.37, 2.7)	
Meeting Room 2	F8:(5.8, 4.53)	M10:(4.39, 2.89)	M11:(5.45, 5.32)	M12:(5.45, 2.95)	M13:(4.98, 5.68)	M14:(4.37, 5.96)	M23:(5.65, 3.73)
Lecture Room 1	F6:(4.75, 3.55)	M11:(4.65, 3.25)	M13:(3.65, 5.08)	M14:(4.45, 2.75)	M18:(4.65, 3.9)	M19:(4.55, 4.38)	
Lecture Room 2	F6:(7.2, 2.75)	M10:(6.27, 4.36)	M11:(6.65, 2.12)	M12:(7.07, 3.49)	M13:(6.11, 1.77)	M14:(5.68, 4.52)	M23:(6.82, 4.01)
Building Lobby	M10:(1.23, 0.53)	M13:(2.72, 0.53)	M14:(2.23, 0.53)	M21:(0.93, 0.53)	M22:(3.21, 0.53)		

The ABC approaches derive the estimate for the acoustic parameter directly from the signal without requiring any prior information. Bias compensation may be performed in order to account for noise or specific aspects of the source material. An example of this is the maximum likelihood

Table 4: Source–microphone distances and DoAs in spherical coordinates

		5-ch. cruciform			3-ch. mobile			8-ch. linear			32-ch. Eigenmike			2-ch. Chromebook			Ch-1. of 8-ch. lin.		
		ρ	Azi	Elev	ρ	Azi	Elev	ρ	Azi	Elev	ρ	Azi	Elev	ρ	Azi	Elev	ρ	Azi	Elev
Name	Pos.	(m)	($^\circ$)	($^\circ$)	(m)	($^\circ$)	($^\circ$)	(m)	($^\circ$)	($^\circ$)	(m)	($^\circ$)	($^\circ$)	(m)	($^\circ$)	($^\circ$)	(m)	($^\circ$)	($^\circ$)
Office 1	1	1.25	-28.6	0	1.13	-11.7	0	1.11	7.25	0	1.42	-38.4	0	1.55	-40.9	19.2	1.16	19.1	0
Office 1	2	2.68	-9.22	0	2.65	-1.95	0	2.64	5.86	0	2.79	-18	0	2.66	-20.4	11	2.68	11	0
Office 2	1	1.09	8.43	0	0.904	10.2	0	1.19	28.5	0	1.69	-49.1	0	1.37	-29.6	21.8	1.33	37.6	0
Office 2	2	2.75	-17.8	0	2.51	-14.8	0	2.44	-4	0	2.53	3.63	0	2.52	13.6	11.7	2.43	1.65	0
Meeting Room 1	1	1.55	-30.1	0	1.41	-18.1	0	1.35	-5.07	0	1.73	-39	0	1.49	-344	20.1	1.35	-355	0
Meeting Room 1	2	2.67	-16.1	0	2.59	-9.07	0	2.56	-2.66	0	2.77	-22.2	0	2.63	-354	11.2	2.56	-357	0
Meeting Room 2	1	1.68	-11	0	1.65	2.78	0	1.72	16.2	0	1.8	-23.6	0	2.06	-34.2	14.3	1.8	23.6	0
Meeting Room 2	2	2.67	-6.89	0	2.65	1.73	0	2.69	10.3	0	2.75	-15.2	0	2.92	-22.9	10.1	2.75	15.2	0
Lecture Room 1	1	0.847	-7.46	0	0.898	18.8	0	1.03	42.2	0	1	-30.7	0	1.33	-48	22.6	1.2	50.7	0
Lecture Room 1	2	2.59	-4.21	0	2.59	4.65	0	2.65	13.3	0	2.56	-13.3	0	2.73	-21.7	10.8	2.72	18.2	0
Lecture Room 2	1	2.89	-71	0	2.51	-68	0	2.15	-64	0	3.27	-73.3	0	3.69	-75.1	7.95	1.93	-60.9	0
Lecture Room 2	2	3.44	-52.4	0	3.14	-48	0	2.85	-42.6	0	3.77	-56.1	0	4.14	-59.3	7.08	2.7	-38.8	0
Building Lobby	1	1.58	-26.7	0	1.43	-14.1	0	1.42	1.21	0	1.82	-38.1	0	2.92	-2.39	9.26	1.45	10.8	0
Building Lobby	2	2.97	-12.4	0	2.89	-5.36	0	2.93	2.35	0	3.04	-18.6	0	3.15	-26.1	8.57	2.95	7	0

Table 5: Fan–microphone distances and DoAs

			Crucif			Mobile			Lin8Ch			Eigenmike			Chromebook			Ch-1. of 8-ch. lin.		
			ρ	Azi	Elev	ρ	Azi	Elev	ρ	Azi	Elev	ρ	Azi	Elev	ρ	Azi	Elev	ρ	Azi	Elev
Name	Pos.	Fan	(m)	($^\circ$)	($^\circ$)	(m)	($^\circ$)	($^\circ$)	(m)	($^\circ$)	($^\circ$)	(m)	($^\circ$)	($^\circ$)	(m)	($^\circ$)	($^\circ$)	(m)	($^\circ$)	($^\circ$)
Office 1	1	1	2.22	-71.3	0	1.87	-67.4	0	1.53	-62.4	0	2.49	-73.2	0	2.61	-73.7	11.3	1.33	-57.6	0
Office 1	2	1	2.97	-40.5	0	2.76	-35.1	0	2.56	-28.8	0	3.27	-46.2	0	3.21	-49.5	9.14	2.45	-23.8	0
Office 2	1	1	2.16	43.9	0	2.03	47.6	0	2.45	51.3	0	1.59	2.16	0	1.81	24.1	16.3	2.64	54.6	0
Office 2	2	1	3.14	9.16	0	2.99	13.5	0	3.14	21.9	0	3.35	26.6	0	3.5	33.7	8.38	3.23	25.9	0
Meeting Room 1	1	1	2.05	-56.9	0	1.77	-50.9	0	1.54	-43.4	0	2.32	-61	0	1.35	-26.2	22.3	1.38	-36.2	0
Meeting Room 1	2	1	2.88	-35.7	0	2.7	-29.9	0	2.57	-24.3	0	3.07	-40.3	0	2.48	-15.5	11.9	2.48	-19.3	0
Meeting Room 2	1	1	1.61	-64.2	-31.4	1.33	-54.5	-39.1	1.12	-36.3	-48.5	1.94	-69.9	-25.7	2.15	-73.6	-8.82	1.05	-18.4	-53
Meeting Room 2	1	2	1.68	-51.7	-30	1.44	-39.4	-35.8	1.28	-20.7	-41.1	1.97	-59.7	-25.2	2.16	-65.1	-8.77	1.24	-6.34	-42.8
Meeting Room 2	2	1	2.19	-37.8	-22.5	1.99	-27.7	-24.9	1.86	-15.4	-26.8	2.44	-45.7	-20.1	2.61	-51.9	-7.25	1.82	-7.13	-27.5
Meeting Room 2	2	2	2.37	-31	-20.8	2.21	-21.3	-22.4	2.11	-10.1	-23.5	2.59	-39	-19	2.74	-45.6	-6.93	2.08	-3.01	-23.8
Lecture Room 1	1	1	1.2	9.46	-44.6	1.31	32.4	-39.8	1.47	51	-34.8	1.23	-16.8	-43.1	1.1	-38.8	-17.4	1.64	57.2	-30.9
Lecture Room 1	1	2	1.24	-23.2	-42.6	1.2	2.69	-44.6	1.22	30.1	-43.7	1.42	-41.5	-36.2	1.46	-54.7	-13.1	1.32	41.8	-39.5
Lecture Room 1	1	3	1.5	-35.1	-46.7	1.4	-12.6	-51.4	1.35	15.4	-54.1	1.71	-49	-39.7	1.71	-59.5	-19.8	1.4	30.6	-51
Lecture Room 1	2	1	2.71	1.33	-18	2.75	10.1	-17.8	2.85	18.4	-17.2	2.65	-7.78	-18.5	2.62	-16.6	-7.24	2.93	23.1	-16.7
Lecture Room 1	2	2	2.75	-9.68	-17.8	2.71	-0.888	-18	2.74	7.94	-17.9	2.76	-18.6	-17.7	2.8	-26.5	-6.77	2.78	13.1	-17.6
Lecture Room 1	2	3	2.88	-14.6	-22.2	2.81	-5.97	-22.8	2.8	2.88	-22.9	2.92	-23.3	-21.9	2.95	-30.6	-11.3	2.83	8.16	-22.7
Lecture Room 2	1	1	3.32	-71.7	-14.7	2.96	-69.1	-16.5	2.61	-65.8	-18.8	3.69	-73.7	-13.2	3.99	-75.3	-4.74	2.4	-63.3	-20.5
Lecture Room 2	1	2	2.77	-67.5	-17.6	2.43	-63.7	-20.3	2.1	-58.4	-23.6	3.13	-70.4	-15.6	3.41	-72.7	-5.55	1.92	-54.2	-25.9
Lecture Room 2	2	1	3.84	-54.6	-12.6	3.53	-50.7	-13.8	3.24	-46	-15	4.16	-57.8	-11.6	4.43	-60.6	-4.27	3.07	-42.8	-15.9
Lecture Room 2	2	2	3.37	-48.4	-14.4	3.09	-43.2	-15.8	2.85	-37.1	-17.2	3.67	-52.6	-13.2	3.91	-56.2	-4.84	2.72	-32.8	-18
Building Lobby	1	1	1.84	-35.3	-27.1	1.67	-24.1	-30.2	1.6	-8.84	-31.6	2.1	-45	-23.6	2.86	-7.3	-7.44	1.59	1.27	-31.9
Building Lobby	2	1	3.08	-17.3	-15.8	2.98	-10.3	-16.4	2.98	-2.4	-16.4	3.17	-23.3	-15.4	3.19	-30.5	-6.66	2.98	2.4	-16.4

method [3] which directly produces the T_{60} estimate.

The SFM approaches estimate a parameter from a signal that is correlated with the acoustic parameter to be estimated, and then apply a mapping function to give the acoustic parameter estimate. An example of this is the Spectral Decay Distributions (SDD) method which determines Negative-

Table 6: ACE Challenge participants

Participant	Algorithms submitted (see results tables)	
	T_{60}	DRR
Federal University of Rio de Janeiro	A	α
Friedrich-Alexander-Universität (FAU)	B, C, D, E	
Imperial College London	F, G	v, w, x, y, z
Fraunhofer IDMT	H, I, J, K, L, M, N, O	p, q, r, s, t, u
MuSAELab	O, P, Q, R, S, T, U, V, W	0, 1, 2, 3, 4, 5, 6, 7, 8, 9
Nuance Communications Inc.	X, Y, Z	k, l, m
Microsoft Research	a, b	
University of Auckland/NTT		f, g, h, i, j
Australian National University (ANU)		n

Side Variance (NSV) from STFT bins and then applies a mapping to obtain the T_{60}.

The MLMF approaches typically use many features of the source material to train a neural network which then estimates the acoustic parameter from the features of a test signal. An example of this is the Non-Intrusive Room Acoustics (NIRA) [4] algorithm.

There were no hybrid approaches submitted to the ACE Challenge although several participants applied noise reduction to the source signals before performing parameter estimation.

Algorithms are further classified as being either providing an estimate in Fullband (FB), in frequency bands, or Subbands (SBs).

1.4 Results

The participating institutions in the ACE challenge along with their respective algorithms are listed in Table 6 in order of appearance of their algorithms in the results tables. For the fullband tasks the results are presented as box plots where there is a box shown for each algorithm. Both single and multi-channel algorithms are shown in the same figures and tables. On each box in the box plot, the central notch is the median, the edges of the box are the 25^{th} and 75^{th} percentiles, the whiskers extend to the most extreme data points not considered outliers. Boxes are colour-coded according to algorithm class: ABC: yellow; MLMF: cyan; SFM: green.

Outliers are plotted individually. The algorithms are identified on the box plot by a single character which corresponds to the character in the table after the figure. The results are sorted by the research group which achieved the highest correlation coefficient in the results across all noises and Signal-to-Noise Ratios (SNRs) in fullband. For the T_{60} fullband task, the last three algorithms are those compared in Gaubitch *et al.* [5] and are included as baselines to enable the progress made in blind T_{60} estimation since 2012 to be assessed. Similarly, for the DRR fullband task, Jeub *et*

al. [6] is included as the last algorithm since this was a freely available estimator prior to the ACE Challenge. The correlation coefficient for each algorithm is plotted as a black cross in the same column as the algorithm. The value is provided on the right hand y-axis.

A table of numerical results is also provided following each figure which also provides the legend for the algorithm identifiers, A, B, C, etc. The columns in the table are as follows:

1. Ref., the identifier for each algorithm used on the x-axis of the preceding figure;

2. Algorithm, the name used by the respective ACE Challenge participant to refer to their algorithm;

3. Class, the class of algorithm according to Sec. 1.3;

4. Mic. Config, the microphone configuration of the Evaluation dataset used to test the algorithm. Valid values are Single (1-channel), Chromebook (2-channel), Mobile (3-channel), Crucif (5-channel), Lin8Ch (8-channel), and EM32 (32-channel); Further details of the microphone configurations can be found in [1];

5. Bias, the mean error in the results. ; Let $X = [x_0, x_1, \ldots x_{N-1}]$ equal the set of N ground truth T_{60} and DRR measurements, and let $\hat{X}$ equal the set of estimated results defined similarly. Then
$$\text{Bias} = \frac{1}{N}\sum_{n=0}^{N-1} \hat{x_n} - x_n; \tag{1}$$

6. MSE, the mean squared error in the estimation results defined as
$$\text{MSE} = \frac{1}{N}\sum_{n=0}^{N-1} (\hat{x_n} - x_n)^2. \tag{2}$$

7. ρ, the Pearson correlation coefficient between the estimated and the ground truth results defined as
$$\rho = \frac{E\{\hat{X}X\} - E\{\hat{X}\}E\{X\}}{\sqrt{(E\{\hat{X}^2\} - E\{\hat{X}\}^2)(E\{X^2\} - E\{X\}^2)}}, \tag{3}$$
where $E\{\cdot\}$ is the mathematical expectation;

8. RTF, the real-time factor, the total computation time divided by the total duration of all processed speech files. All implementations were in Matlab except for those marked with a † which used Matlab for feature extraction and C++ for the machine learning-based mapping, and those marked with a ‡ which were implemented entirely in C++.

By considering the bias, MSE, and ρ, it is possible to determine how well the estimator works. For example, an estimator with a low bias and MSE might simply be giving an estimate close to the median for every speech file. However, by examining the ρ, it will be possible to distinguish between such an algorithm, which will have a low correlation, and a better algorithm which is more accurately estimating the parameter concerned which will have a higher correlation. The RTF is useful for determining whether the algorithm has practical applications requiring low computational complexity such as hearing aids and mobile devices.

For the frequency-dependent tasks, a box plot is provided per algorithm with each box representing the performance in a particular frequency band. Frequency dependent algorithms have also been included in the fullband plots. Where those algorithms themselves produce a fullband estimate, this has been used directly as in the case of the DRR Estimation using a Null-Steered Beamformer (DENBE) [7] and Particle Velocity [8] algorithms. Where no fullband estimate is produced, a fullband estimate was obtained by taking the mean of the results over the 400 to $1250\,\mathrm{Hz}$ frequency bands as in the case of the Model-based subband RTE [9] algorithm as recommended in ISO 3382 [10].

2 Overall results summary

2.1 Fullband T_{60} estimation overall results

The overall results for fullband T_{60} estimation are shown in Fig. 2 and Table 7.

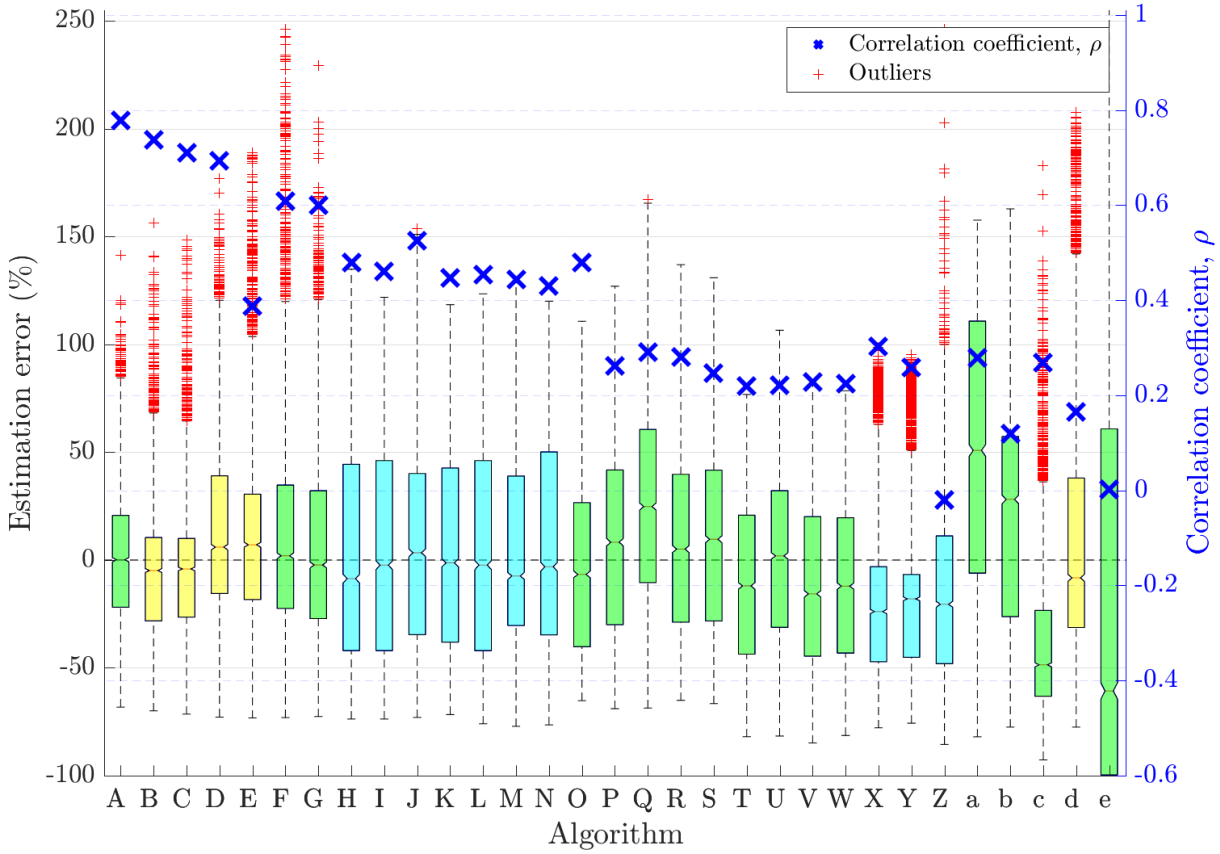

Figure 2: Fullband T_{60} estimation error in all noises for all SNRs

Table 7: T_{60} estimation algorithm performance in all noises for all SNRs

Ref.	Algorithm	Class	Mic. Config.	Bias	MSE	ρ	RTF
A	QA Reverb [11]	SFM	Single	-0.068	0.0648	0.778	0.4
B	Octave SB-based FB RTE [9]	ABC	Single	-0.104	0.0731	0.738	0.939
C	DCT-based FB RTE [9]	ABC	Single	-0.104	0.0766	0.71	1
D	Model-based SB RTE [9]	ABC	Single	-0.0363	0.102	0.693	0.451
E	Baseline algorithm for FB RTE [9]	ABC	Single	-0.0432	0.11	0.387	0.0424
F	SDDSA-G retrained [12]	SFM	Single	0.0167	0.0937	0.608	0.0152
G	SDDSA-G [13]	SFM	Single	-0.0423	0.0803	0.6	0.0164
H	Multi-layer perceptron [14]	MLMF	Single	-0.0967	0.104	0.48	0.0578‡
I	Multi-layer perceptron P2 [14]	MLMF	Single	-0.0497	0.0992	0.46	0.0578‡
J	Multi-layer perceptron P2 [14]	MLMF	Chromebook	-0.054	0.0933	0.525	0.0589‡
K	Multi-layer perceptron P2 [14]	MLMF	Mobile	-0.0299	0.082	0.447	0.0556‡
L	Multi-layer perceptron P2 [14]	MLMF	Crucif	-0.0503	0.1	0.454	0.0569‡
M	Multi-layer perceptron P2 [14]	MLMF	Lin8Ch	-0.0468	0.0868	0.443	0.0618‡
N	Multi-layer perceptron P2 [14]	MLMF	EM32	-0.0602	0.0879	0.43	0.0576‡
O	Per acoust. band SRMR Sec. 2.5. [15]	SFM	Single	-0.114	0.109	0.48	0.578
P	NSRMR Sec. 2.4. [16, 15]	SFM	Single	-0.0646	0.119	0.261	0.571
Q	NSRMR Sec. 2.4. [16, 15]	SFM	Chromebook	0.012	0.116	0.291	1.04
R	NSRMR Sec. 2.4. [16, 15]	SFM	Mobile	-0.0504	0.0958	0.281	1.58
S	NSRMR Sec. 2.4. [16, 15]	SFM	Crucif	-0.0516	0.107	0.246	2.62
T	SRMR Sec. 2.3. [15]	SFM	Single	-0.16	0.144	0.22	0.457
U	SRMR Sec. 2.3. [15]	SFM	Chromebook	-0.105	0.132	0.221	0.829
V	SRMR Sec. 2.3. [15]	SFM	Mobile	-0.153	0.12	0.228	1.26
W	SRMR Sec. 2.3. [15]	SFM	Crucif	-0.153	0.128	0.225	2.09
X	NIRAv3 [4]	MLMF	Single	-0.192	0.151	0.302	0.899†
Y	NIRAv1 [4]	MLMF	Single	-0.184	0.151	0.258	0.899†
Z	NIRAv2 [4]	MLMF	Single	-0.179	0.198	-0.0199	0.907†
a	Blur kernel [17]	SFM	Single	0.173	0.15	0.279	8.46
b	Blur kernel with sliding window [18]	SFM	Single	-0.00555	0.139	0.12	0.421
c	Temporal dynamics [19]	SFM	Single	-0.304	0.211	0.269	0.362
d	Improved blind RTE [3]	ABC	Single	-0.0635	0.165	0.166	0.0259
e	SDD [20]	SFM	Single	0.463	305	0.00158	0.0221

2.2 Fullband DRR estimation overall results

The overall results for fullband DRR estimation are shown in Fig. 3 and Table 8.

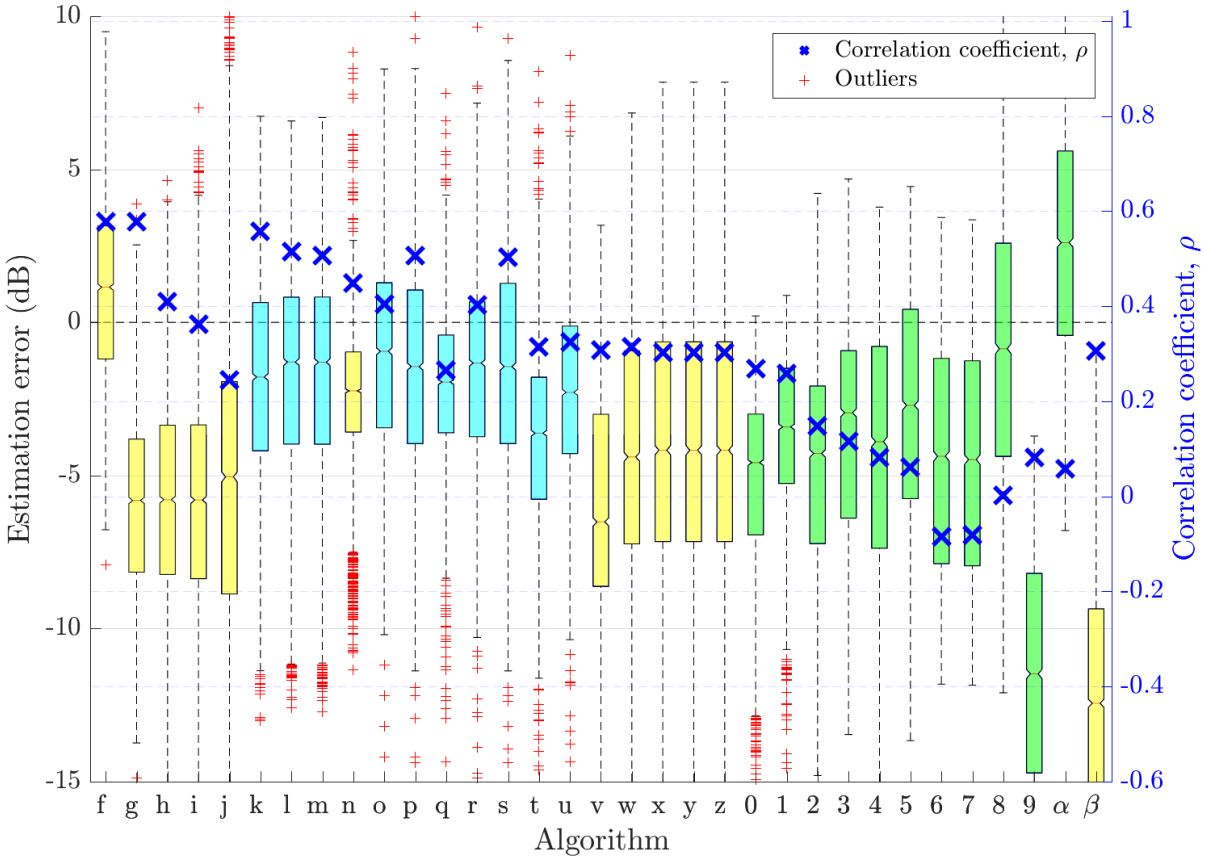

Figure 3: Fullband DRR estimation error in all noises for all SNRs

Table 8: DRR estimation algorithm performance in all noises for all SNRs

Ref.	Algorithm	Class	Mic. Config.	Bias	MSE	ρ	RTF
f	PSD est. in beamspace, bias comp. [21]	ABC	Mobile	1.07	8.14	0.577	0.757
g	PSD est. in beamspace (Raw) [21]	ABC	Mobile	-5.9	41.8	0.577	3.17
h	PSD est. in beamspace v2 [21]	ABC	Mobile	-5.7	43	0.41	0.844
i	PSD est. by twin BF [22]	ABC	Mobile	-5.71	44.9	0.362	0.614
j	Spatial Covariance in matrix mode [23]	ABC	Mobile	-5.37	61.2	0.244	0.627
k	NIRAv2 [4]	MLMF	Single	-1.85	14.8	0.558	$0.899^{\dagger}$
l	NIRAv3 [4]	MLMF	Single	-1.62	14.7	0.515	$0.899^{\dagger}$
m	NIRAv1 [4]	MLMF	Single	-1.64	15	0.507	$0.899^{\dagger}$
n	Particle velocity [8]	ABC	EM32	-2.38	10.4	0.449	0.134
o	Multi-layer perceptron [14]	MLMF	Single	-1.14	15.9	0.405	$0.0578^{\ddagger}$
p	Multi-layer perceptron P2 [14]	MLMF	Single	-1.52	16.1	0.507	$0.0578^{\ddagger}$
q	Multi-layer perceptron P2 [14]	MLMF	Chromebook	-2.43	13.6	0.265	$0.0589^{\ddagger}$
r	Multi-layer perceptron P2 [14]	MLMF	Mobile	-1.67	15	0.403	$0.0556^{\ddagger}$
s	Multi-layer perceptron P2 [14]	MLMF	Crucif	-1.5	16	0.503	$0.0569^{\ddagger}$
t	Multi-layer perceptron P2 [14]	MLMF	Lin8Ch	-3.64	25.7	0.314	$0.0618^{\ddagger}$
u	Multi-layer perceptron P2 [14]	MLMF	EM32	-2.22	14.6	0.325	$0.0576^{\ddagger}$
v	DENBE no noise reduction [24]	ABC	Chromebook	-6.04	51.2	0.308	0.0323
w	DENBE spectral subtraction [7]	ABC	Chromebook	-4.25	34.1	0.314	0.0589
x	DENBE spec. sub. Gerkmann [24]	ABC	Chromebook	-4.01	32.8	0.303	0.0477
y	DENBE filtered subbands [7]	ABC	Chromebook	-4.01	32.8	0.303	0.775
z	DENBE FFT derived subbands [7]	ABC	Chromebook	-4.01	32.8	0.303	0.0449
0	Normalized Overall SRMR (NOSRMR) Sec. 2.2. [15]	SFM	Chromebook	-5.1	34.3	0.269	1.04
1	Overall SRMR (OSRMR) Sec. 2.2. [15]	SFM	Chromebook	-3.71	20.6	0.259	0.829
2	NOSRMR Sec. 2.2. [15]	SFM	Mobile	-4.47	32	0.148	1.58
3	OSRMR Sec. 2.2. [15]	SFM	Mobile	-3.28	22.2	0.116	1.26
4	NOSRMR Sec. 2.2. [15]	SFM	Crucif	-4.05	31.1	0.0814	2.62
5	OSRMR Sec. 2.2. [15]	SFM	Crucif	-2.88	22.3	0.0616	2.09
6	NOSRMR Sec. 2.2. [15]	SFM	Single	-4.16	33.9	-0.0841	0.54
7	OSRMR Sec. 2.2. [15]	SFM	Single	-4.24	34.6	-0.0815	0.446
8	Per acoust. band SRMR Sec. 2.5. [15]	SFM	Single	-0.9	22.8	0.00192	0.578
9	Temporal dynamics [25]	SFM	Single	-11.4	147	0.0815	0.082
α	QA Reverb [11]	SFM	Single	2.51	23.6	0.0576	0.391
β	Blind est. of coherent-to-diffuse energy ratio [6]	ABC	Chromebook	-12.1	162	0.305	0.019

2.2.1 Fullband T_{60} estimation results by parameter

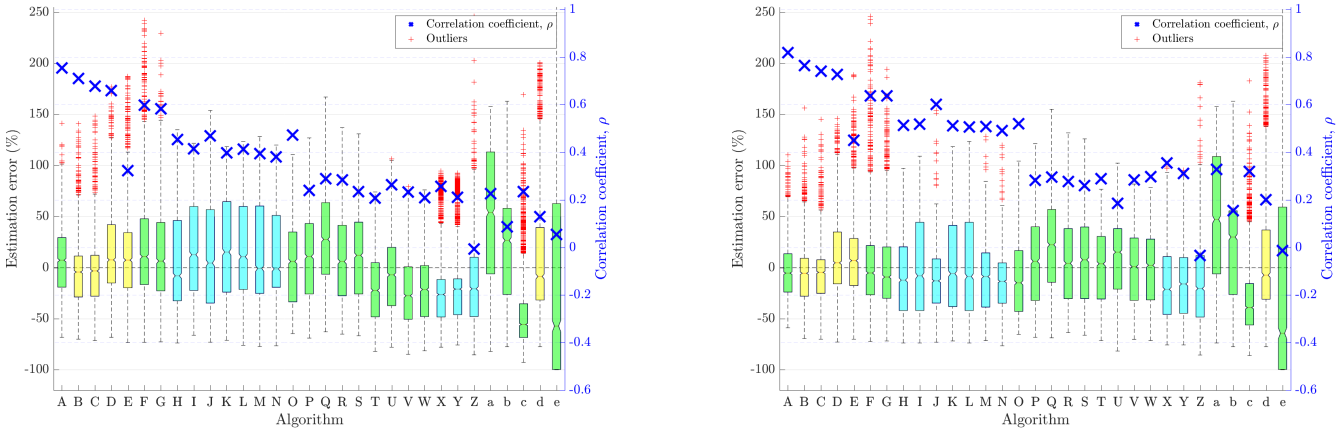

(a) (b)

Figure 4: FB T_{60} estimation error in all noises and all SNRs for a) female talkers and b) male talkers

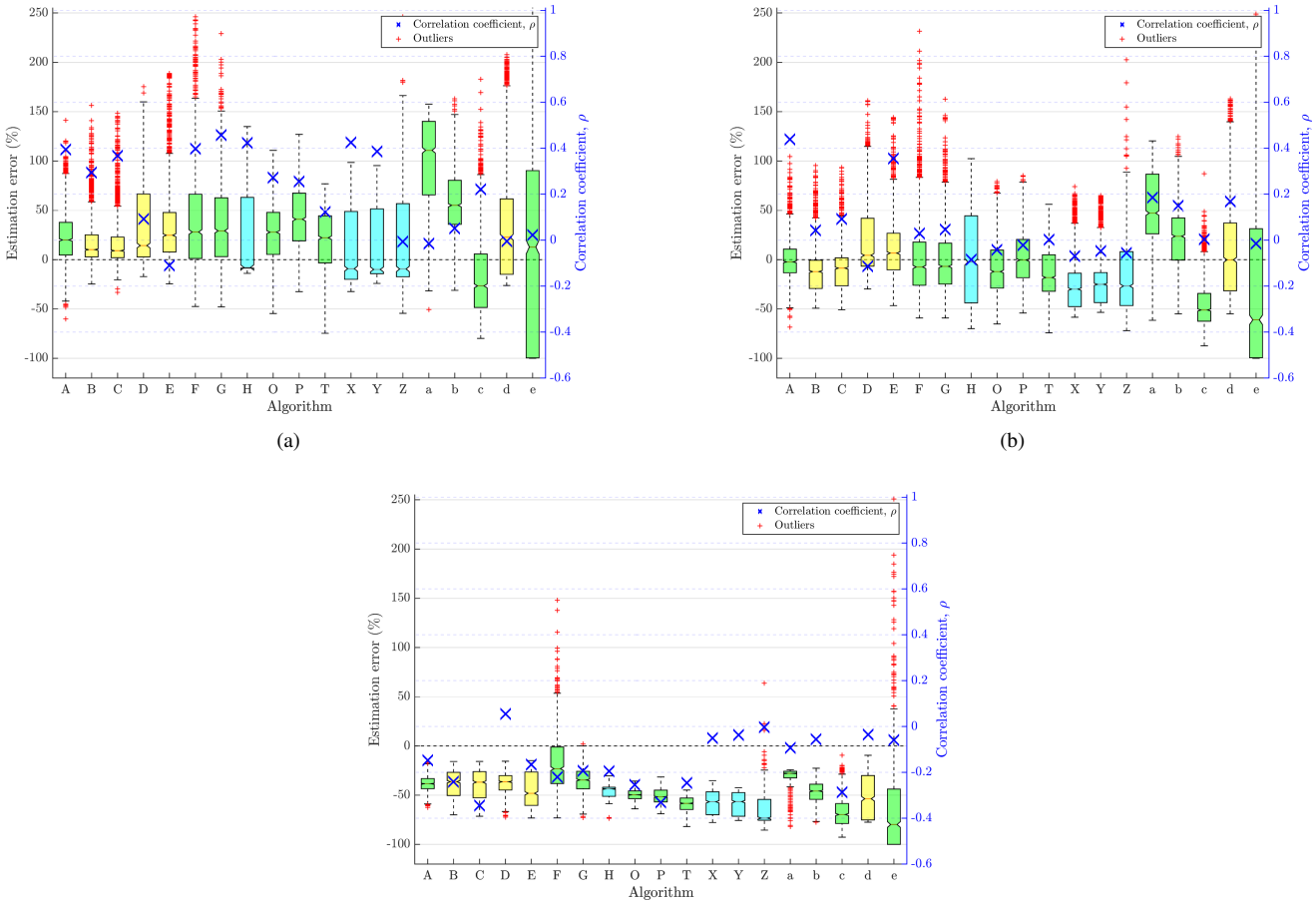

Figure 5: Single channel FB T_{60} estimation error in all noises and all SNRs for a) T_{60} <0.43 s b) $0.43 \leqslant T_{60} < 0.75$ s and c) $T_{60} \geqslant 0.75$ s. Observe that $\rho < 0$ for all except algorithm D

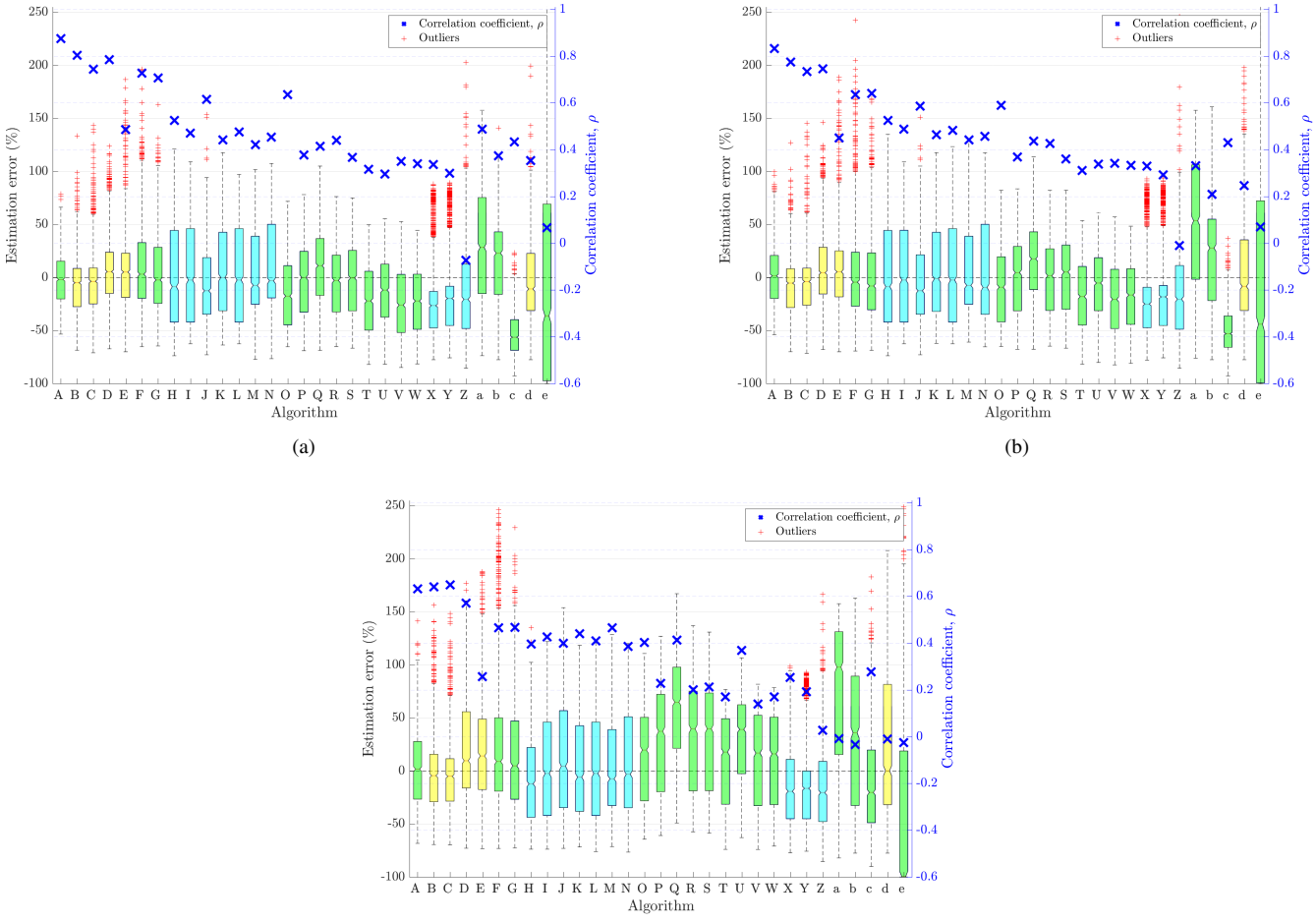

(a)

(b)

(c)

Figure 6: FB T_{60} estimation error in all noises at a), 18 dB SNR, b), 12 dB SNR, and c) -1 dB SNR

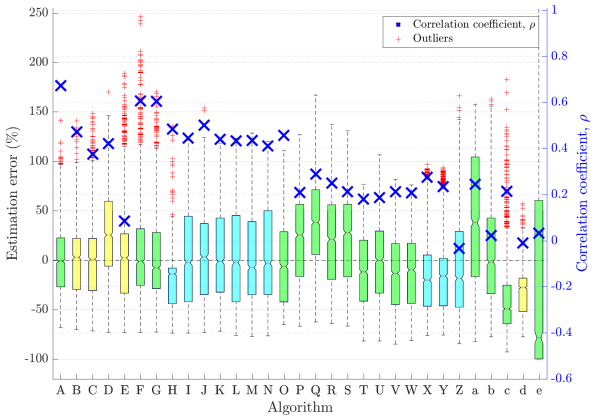

(a)

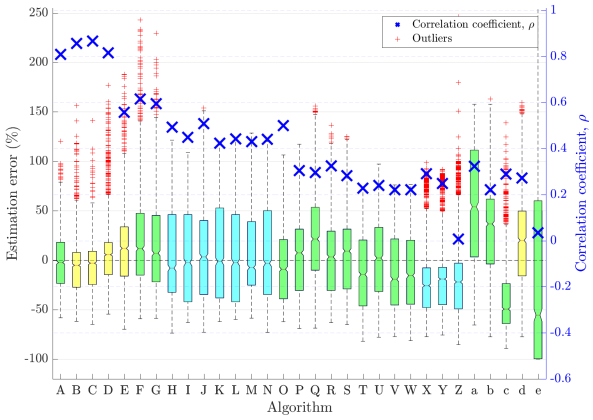

(b)

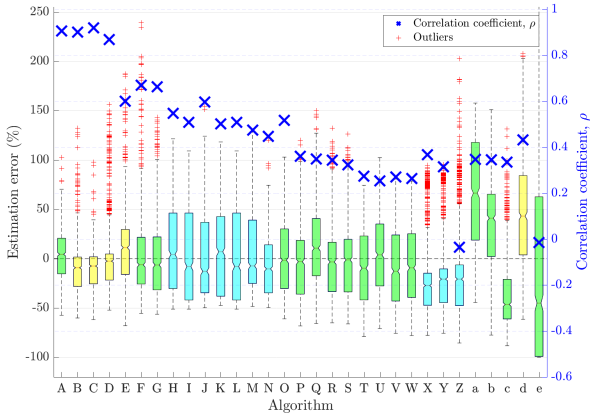

(c)

Figure 7: FB T_{60} estimation error in all noises and all SNRs for a) utterance length $<5\,\mathrm{s}$ b) utterance length $< 15\,\mathrm{s}$ and c) utterance length $\geqslant 15\,\mathrm{s}$

2.2.2 Fullband DRR estimation results by parameter

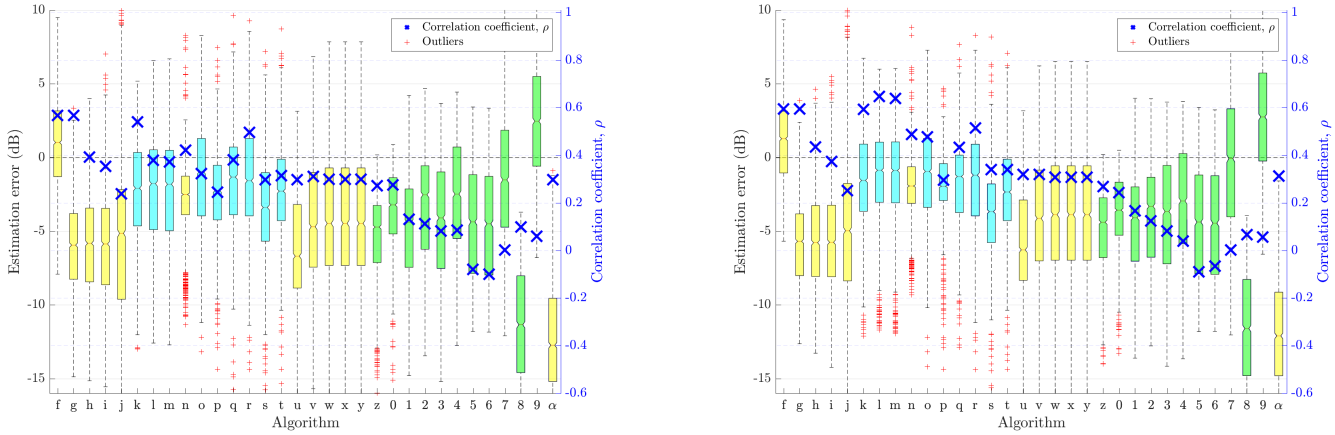

(a) (b)

Figure 8: FB DRR estimation error in all noises and all SNRs for a) female talkers and b) male talkers

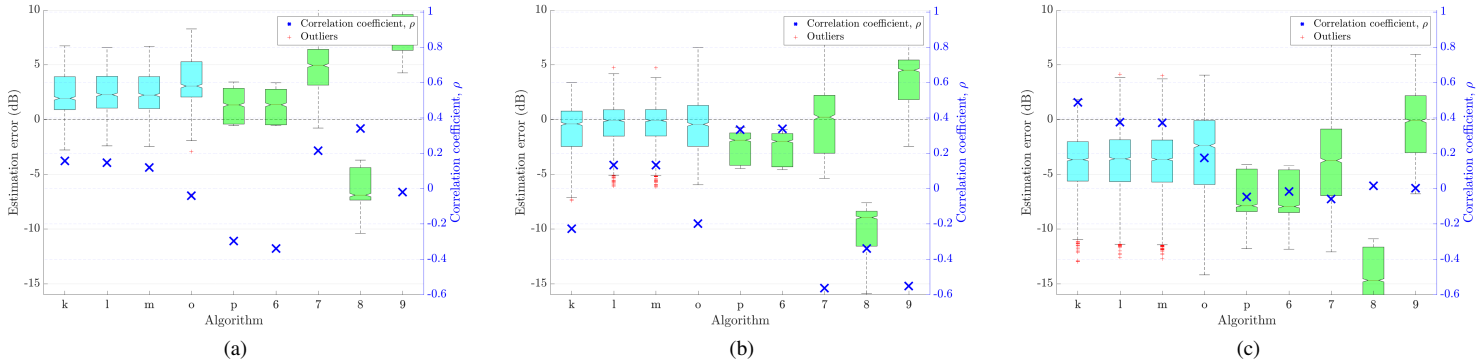

Figure 9: Single channel FB DRR estimation error in all noises and all SNRs for a) DRR $<2\,\mathrm{dB}$ b) $2 \leqslant$DRR $< 5\,\mathrm{dB}$ and c) DRR $\geqslant 5\,\mathrm{dB}$

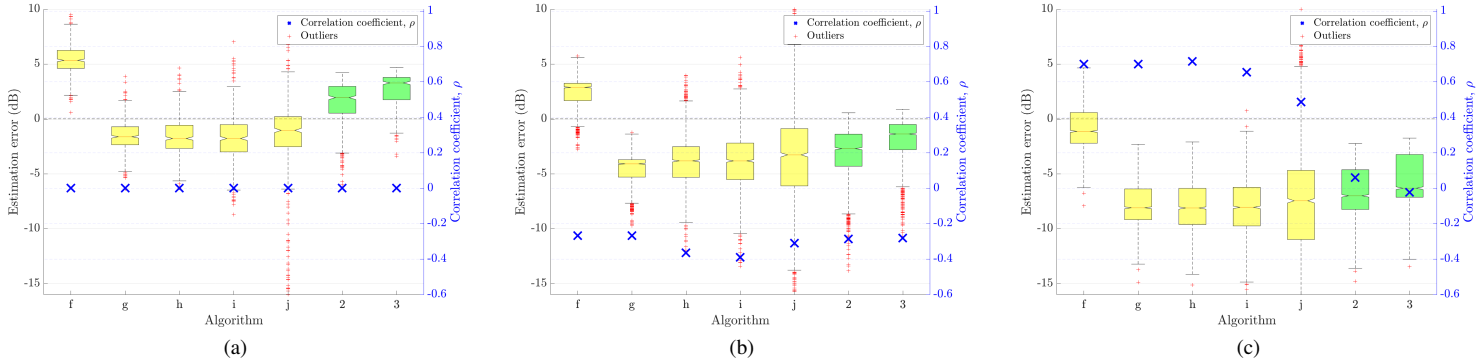

Figure 10: Mobile (3-channel) FB DRR estimation error in all noises and all SNRs for a) DRR $<2\,\mathrm{dB}$ b) $2 \leqslant$DRR $< 5\,\mathrm{dB}$ and c) DRR $\geqslant 5\,\mathrm{dB}$. Note that for b) there are strong negative correlations for all algorithms

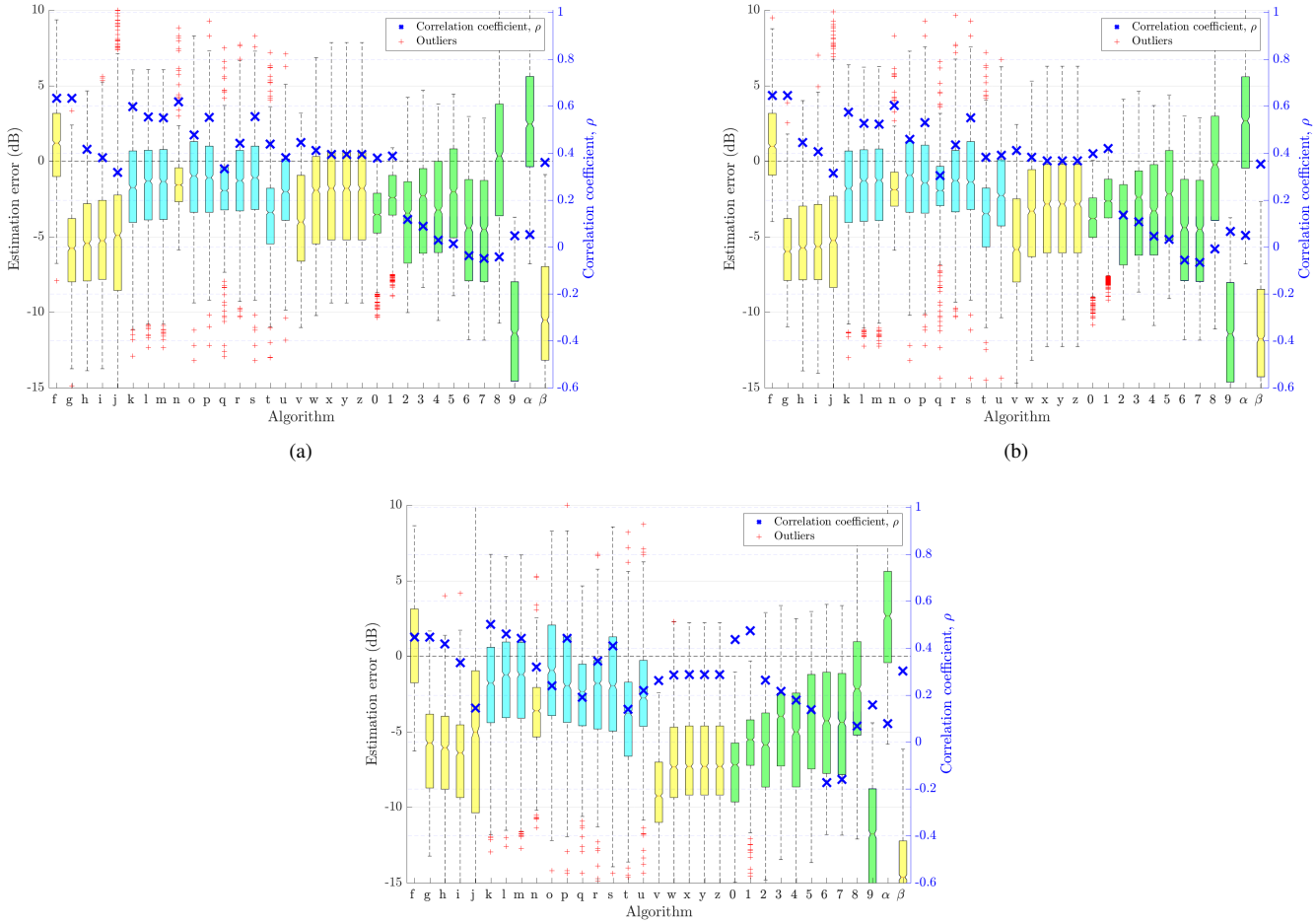

Figure 11: FB DRR estimation error in all noises at a), 18 dB SNR, b), 12 dB SNR, and c) -1 dB SNR

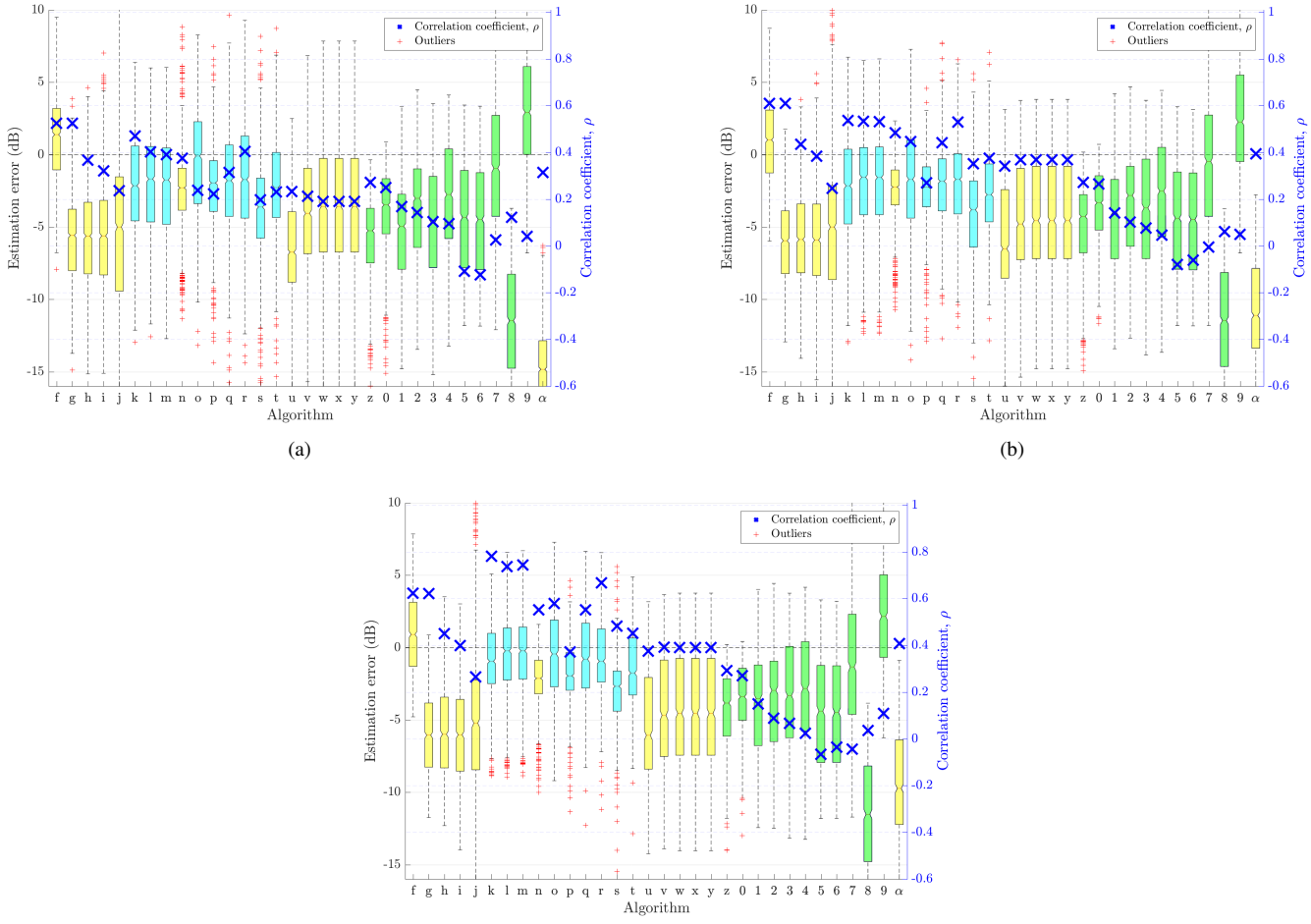

(a) (b)

(c)

Figure 12: FB DRR estimation error in all noises and all SNRs for a) utterance length <5 s b) utterance length < 15 s and c) utterance length $\geqslant 15$ s

3 T_{60} estimation results

3.1 Fullband T_{60} estimation results by noise type

3.1.1 Ambient noise

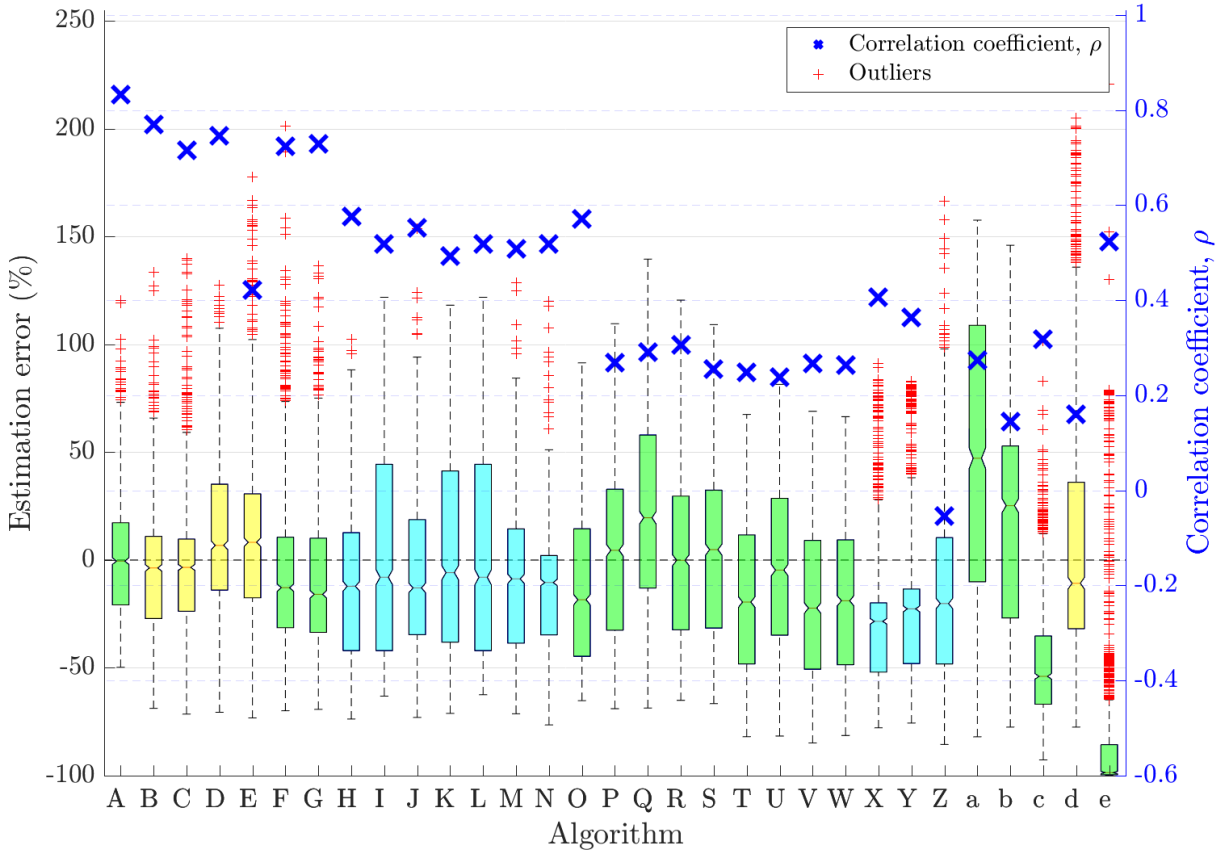

Figure 13: Fullband T_{60} estimation error in ambient noise for all SNRs

Table 9: T_{60} estimation algorithm performance in ambient noise for all SNRs

Ref.	Algorithm	Class	Mic. Config.	Bias	MSE	ρ	RTF
A	QA Reverb [11]	SFM	Single	-0.0682	0.0565	0.833	0.401
B	Octave SB-based FB RTE [9]	ABC	Single	-0.0993	0.068	0.769	1
C	DCT-based FB RTE [9]	ABC	Single	-0.0978	0.0738	0.715	1.04
D	Model-based SB RTE [9]	ABC	Single	-0.0378	0.0936	0.746	0.478
E	Baseline algorithm for FB RTE [9]	ABC	Single	-0.0411	0.105	0.422	0.0421
F	SDDSA-G retrained [12]	SFM	Single	-0.0817	0.0676	0.723	0.0153
G	SDDSA-G [13]	SFM	Single	-0.117	0.0738	0.729	0.0166
H	Multi-layer perceptron [14]	MLMF	Single	-0.125	0.0977	0.576	$0.0578^{\ddagger}$
I	Multi-layer perceptron P2 [14]	MLMF	Single	-0.0844	0.0969	0.518	$0.0578^{\ddagger}$
J	Multi-layer perceptron P2 [14]	MLMF	Chromebook	-0.0704	0.0917	0.553	$0.0589^{\ddagger}$
K	Multi-layer perceptron P2 [14]	MLMF	Mobile	-0.0581	0.0798	0.492	$0.0557^{\ddagger}$
L	Multi-layer perceptron P2 [14]	MLMF	Crucif	-0.0852	0.0971	0.518	$0.0569^{\ddagger}$
M	Multi-layer perceptron P2 [14]	MLMF	Lin8Ch	-0.0818	0.084	0.508	$0.062^{\ddagger}$
N	Multi-layer perceptron P2 [14]	MLMF	EM32	-0.0968	0.084	0.519	$0.0578^{\ddagger}$
O	Per acoust. band SRMR Sec. 2.5. [15]	SFM	Single	-0.16	0.113	0.572	0.58
P	NSRMR Sec. 2.4. [16, 15]	SFM	Single	-0.0964	0.123	0.27	0.571
Q	NSRMR Sec. 2.4. [16, 15]	SFM	Chromebook	-0.00429	0.116	0.291	1.04
R	NSRMR Sec. 2.4. [16, 15]	SFM	Mobile	-0.0837	0.0976	0.306	1.59
S	NSRMR Sec. 2.4. [16, 15]	SFM	Crucif	-0.0838	0.11	0.256	2.63
T	SRMR Sec. 2.3. [15]	SFM	Single	-0.195	0.153	0.249	0.457
U	SRMR Sec. 2.3. [15]	SFM	Chromebook	-0.13	0.136	0.239	0.831
V	SRMR Sec. 2.3. [15]	SFM	Mobile	-0.189	0.129	0.268	1.26
W	SRMR Sec. 2.3. [15]	SFM	Crucif	-0.188	0.137	0.263	2.09
X	NIRAv3 [4]	MLMF	Single	-0.263	0.172	0.406	$0.897^{\dagger}$
Y	NIRAv1 [4]	MLMF	Single	-0.243	0.166	0.363	$0.897^{\dagger}$
Z	NIRAv2 [4]	MLMF	Single	-0.183	0.198	-0.0532	$0.912^{\dagger}$
a	Blur kernel [17]	SFM	Single	0.164	0.15	0.274	8.16
b	Blur kernel with sliding window [18]	SFM	Single	-0.0155	0.137	0.144	0.413
c	Temporal dynamics [19]	SFM	Single	-0.359	0.239	0.319	0.362
d	Improved blind RTE [3]	ABC	Single	-0.0752	0.168	0.159	0.0255
e	SDD [20]	SFM	Single	-0.515	0.355	0.524	0.0219

3.1.2 Babble noise

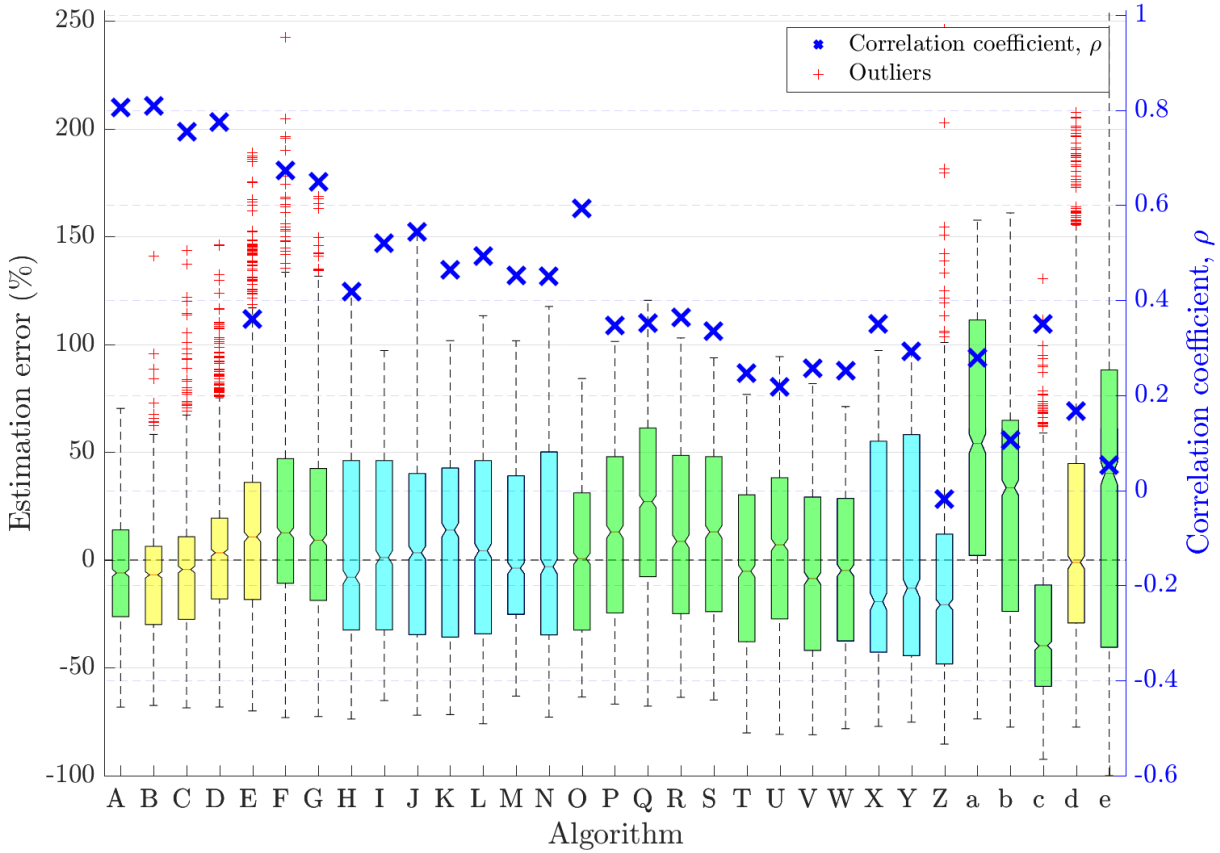

Figure 14: Fullband T_{60} estimation error in babble noise for all SNRs

Table 10: T_{60} estimation algorithm performance in babble noise for all SNRs

Ref.	Algorithm	Class	Mic. Config.	Bias	MSE	ρ	RTF
A	QA Reverb [11]	SFM	Single	-0.109	0.0707	0.805	0.398
B	Octave SB-based FB RTE [9]	ABC	Single	-0.124	0.0701	0.809	0.911
C	DCT-based FB RTE [9]	ABC	Single	-0.106	0.0718	0.755	0.99
D	Model-based SB RTE [9]	ABC	Single	-0.0699	0.0933	0.774	0.443
E	Baseline algorithm for FB RTE [9]	ABC	Single	-0.0236	0.112	0.36	0.0428
F	SDDSA-G retrained [12]	SFM	Single	0.0688	0.0836	0.673	0.0155
G	SDDSA-G [13]	SFM	Single	-0.000784	0.0718	0.649	0.0162
H	Multi-layer perceptron [14]	MLMF	Single	-0.0684	0.106	0.419	$0.0579^{\ddagger}$
I	Multi-layer perceptron P2 [14]	MLMF	Single	-0.045	0.092	0.52	$0.0579^{\ddagger}$
J	Multi-layer perceptron P2 [14]	MLMF	Chromebook	-0.0534	0.0912	0.543	$0.0588^{\ddagger}$
K	Multi-layer perceptron P2 [14]	MLMF	Mobile	-0.0244	0.0796	0.465	$0.0555^{\ddagger}$
L	Multi-layer perceptron P2 [14]	MLMF	Crucif	-0.0432	0.0948	0.494	$0.057^{\ddagger}$
M	Multi-layer perceptron P2 [14]	MLMF	Lin8Ch	-0.0277	0.084	0.452	$0.0618^{\ddagger}$
N	Multi-layer perceptron P2 [14]	MLMF	EM32	-0.0569	0.0853	0.451	$0.0576^{\ddagger}$
O	Per acoust. band SRMR Sec. 2.5. [15]	SFM	Single	-0.0967	0.0992	0.593	0.579
P	NSRMR Sec. 2.4. [16, 15]	SFM	Single	-0.0435	0.11	0.347	0.572
Q	NSRMR Sec. 2.4. [16, 15]	SFM	Chromebook	0.00512	0.11	0.353	1.04
R	NSRMR Sec. 2.4. [16, 15]	SFM	Mobile	-0.0287	0.0873	0.364	1.58
S	NSRMR Sec. 2.4. [16, 15]	SFM	Crucif	-0.03	0.098	0.335	2.63
T	SRMR Sec. 2.3. [15]	SFM	Single	-0.129	0.133	0.246	0.457
U	SRMR Sec. 2.3. [15]	SFM	Chromebook	-0.0928	0.13	0.217	0.833
V	SRMR Sec. 2.3. [15]	SFM	Mobile	-0.12	0.109	0.257	1.26
W	SRMR Sec. 2.3. [15]	SFM	Crucif	-0.121	0.118	0.252	2.1
X	NIRAv3 [4]	MLMF	Single	-0.0965	0.121	0.35	$0.906^{\dagger}$
Y	NIRAv1 [4]	MLMF	Single	-0.0899	0.124	0.292	$0.906^{\dagger}$
Z	NIRAv2 [4]	MLMF	Single	-0.176	0.203	-0.0191	$0.901^{\dagger}$
a	Blur kernel [17]	SFM	Single	0.184	0.152	0.279	8.88
b	Blur kernel with sliding window [18]	SFM	Single	0.0187	0.138	0.106	0.438
c	Temporal dynamics [19]	SFM	Single	-0.257	0.178	0.35	0.365
d	Improved blind RTE [3]	ABC	Single	-0.0357	0.164	0.167	0.0269
e	SDD [20]	SFM	Single	0.593	52.8	0.0524	0.0224

3.1.3 Fan noise

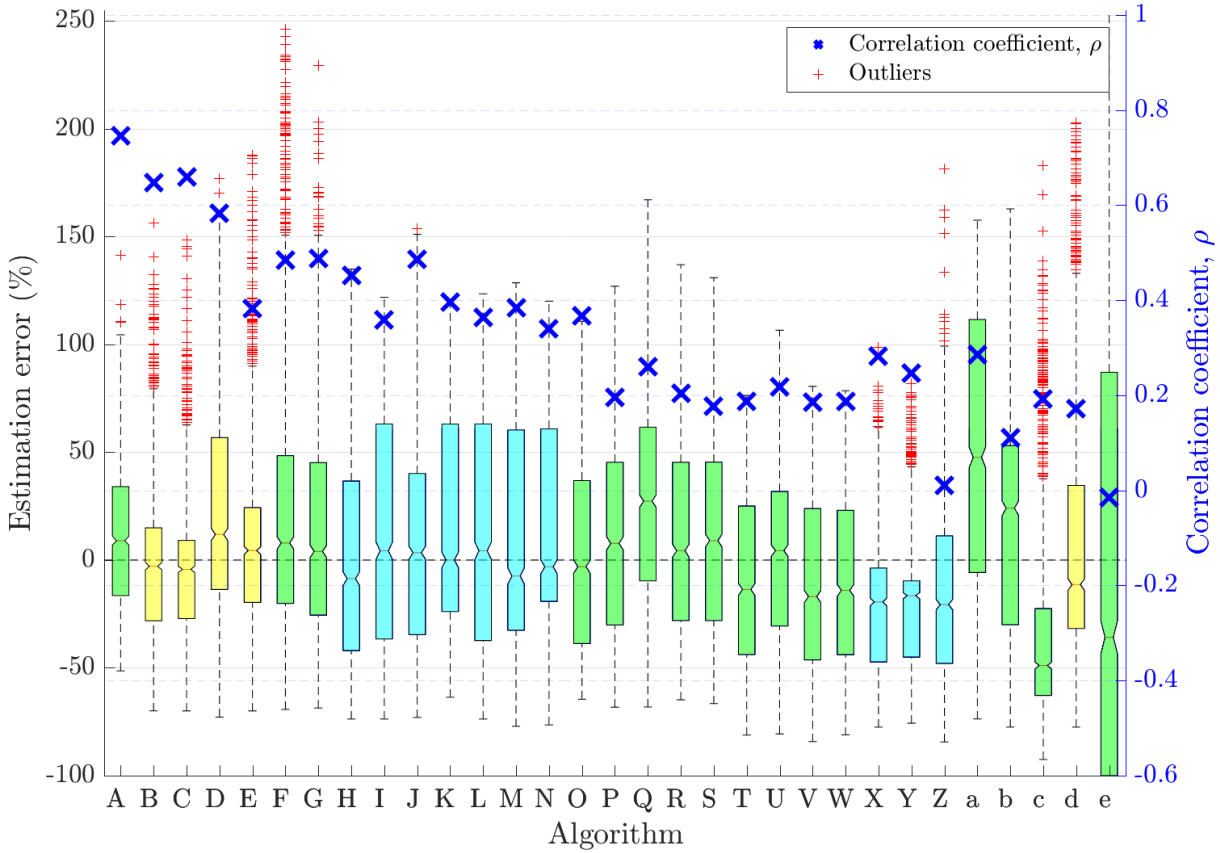

Figure 15: Fullband T_{60} estimation error in fan noise for all SNRs

Table 11: T_{60} estimation algorithm performance in fan noise for all SNRs

Ref.	Algorithm	Class	Mic. Config.	Bias	MSE	ρ	RTF
A	QA Reverb [11]	SFM	Single	-0.0267	0.0672	0.746	0.4
B	Octave SB-based FB RTE [9]	ABC	Single	-0.0881	0.0811	0.647	0.903
C	DCT-based FB RTE [9]	ABC	Single	-0.109	0.0843	0.659	0.984
D	Model-based SB RTE [9]	ABC	Single	-0.00134	0.119	0.583	0.433
E	Baseline algorithm for FB RTE [9]	ABC	Single	-0.065	0.112	0.383	0.0421
F	SDDSA-G retrained [12]	SFM	Single	0.0629	0.13	0.484	0.0148
G	SDDSA-G [13]	SFM	Single	-0.00884	0.0952	0.488	0.0164
H	Multi-layer perceptron [14]	MLMF	Single	-0.097	0.108	0.451	0.0578‡
I	Multi-layer perceptron P2 [14]	MLMF	Single	-0.0197	0.109	0.359	0.0578‡
J	Multi-layer perceptron P2 [14]	MLMF	Chromebook	-0.0382	0.0971	0.486	0.059‡
K	Multi-layer perceptron P2 [14]	MLMF	Mobile	-0.00714	0.0864	0.396	0.0555‡
L	Multi-layer perceptron P2 [14]	MLMF	Crucif	-0.0224	0.108	0.364	0.0569‡
M	Multi-layer perceptron P2 [14]	MLMF	Lin8Ch	-0.031	0.0925	0.384	0.0617‡
N	Multi-layer perceptron P2 [14]	MLMF	EM32	-0.0268	0.0945	0.339	0.0574‡
O	Per acoust. band SRMR Sec. 2.5. [15]	SFM	Single	-0.0853	0.114	0.367	0.576
P	NSRMR Sec. 2.4. [16, 15]	SFM	Single	-0.054	0.125	0.195	0.569
Q	NSRMR Sec. 2.4. [16, 15]	SFM	Chromebook	0.0352	0.122	0.26	1.03
R	NSRMR Sec. 2.4. [16, 15]	SFM	Mobile	-0.0389	0.102	0.204	1.58
S	NSRMR Sec. 2.4. [16, 15]	SFM	Crucif	-0.0411	0.113	0.177	2.61
T	SRMR Sec. 2.3. [15]	SFM	Single	-0.156	0.145	0.188	0.455
U	SRMR Sec. 2.3. [15]	SFM	Chromebook	-0.0922	0.131	0.218	0.824
V	SRMR Sec. 2.3. [15]	SFM	Mobile	-0.149	0.123	0.185	1.26
W	SRMR Sec. 2.3. [15]	SFM	Crucif	-0.149	0.13	0.188	2.08
X	NIRAv3 [4]	MLMF	Single	-0.215	0.159	0.283	0.895†
Y	NIRAv1 [4]	MLMF	Single	-0.22	0.164	0.247	0.895†
Z	NIRAv2 [4]	MLMF	Single	-0.179	0.192	0.0105	0.906†
a	Blur kernel [17]	SFM	Single	0.172	0.149	0.285	8.36
b	Blur kernel with sliding window [18]	SFM	Single	-0.0198	0.142	0.111	0.412
c	Temporal dynamics [19]	SFM	Single	-0.295	0.217	0.191	0.358
d	Improved blind RTE [3]	ABC	Single	-0.0795	0.165	0.172	0.0254
e	SDD [20]	SFM	Single	1.31	861	-0.0141	0.0221

3.2 Fullband T_{60} estimation results by noise type and SNR

3.2.1 Ambient noise at 18 dB SNR

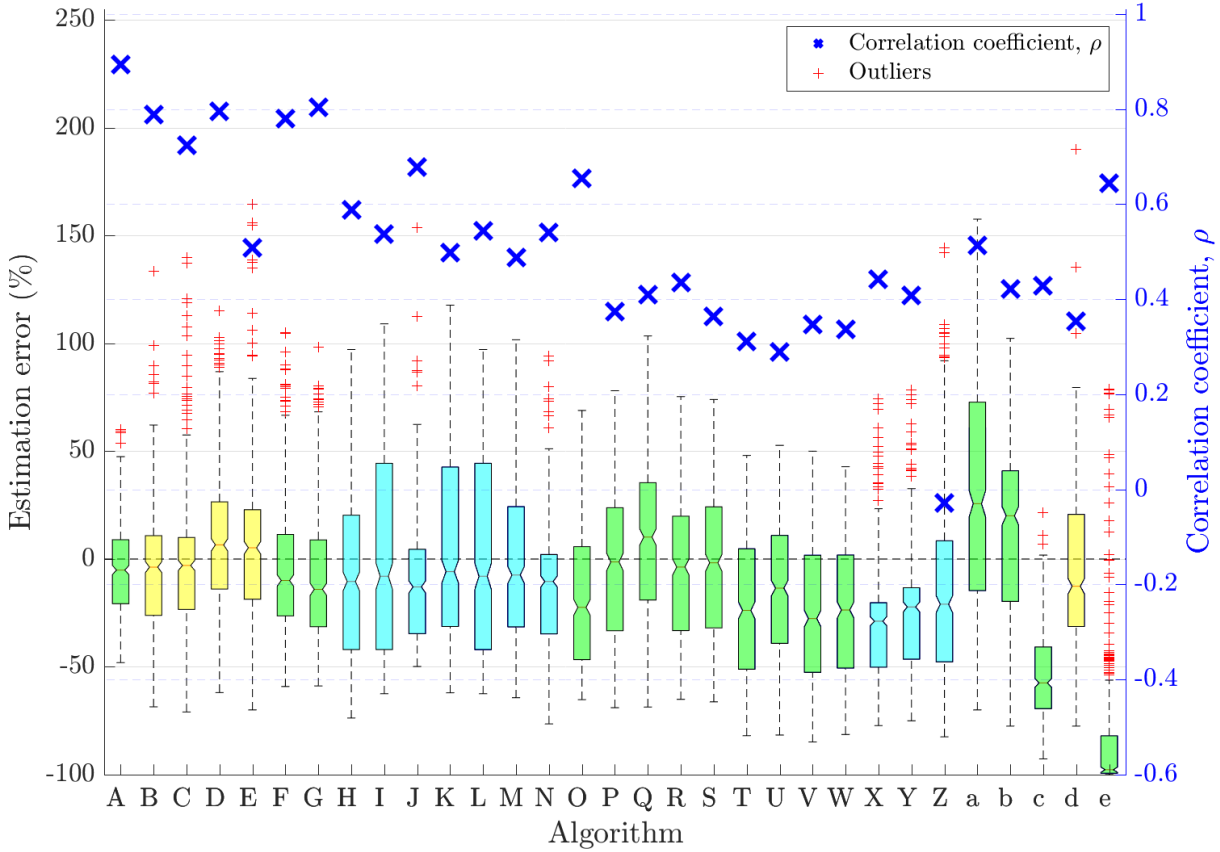

Figure 16: Fullband T_{60} estimation error in ambient noise at 18 dB SNR

Table 12: T_{60} estimation algorithm performance in ambient noise at $18\,\mathrm{dB}$ SNR

Ref.	Algorithm	Class	Mic. Config.	Bias	MSE	ρ	RTF
A	QA Reverb [11]	SFM	Single	-0.0913	0.0519	0.893	0.401
B	Octave SB-based FB RTE [9]	ABC	Single	-0.0979	0.0647	0.788	1
C	DCT-based FB RTE [9]	ABC	Single	-0.0934	0.0712	0.724	1.04
D	Model-based SB RTE [9]	ABC	Single	-0.044	0.0857	0.795	0.478
E	Baseline algorithm for FB RTE [9]	ABC	Single	-0.0705	0.0959	0.509	0.0421
F	SDDSA-G retrained [12]	SFM	Single	-0.0554	0.0593	0.78	0.0153
G	SDDSA-G [13]	SFM	Single	-0.107	0.0591	0.804	0.0166
H	Multi-layer perceptron [14]	MLMF	Single	-0.11	0.0927	0.588	$0.0578^{\ddagger}$
I	Multi-layer perceptron P2 [14]	MLMF	Single	-0.0815	0.0947	0.537	$0.0578^{\ddagger}$
J	Multi-layer perceptron P2 [14]	MLMF	Chromebook	-0.1	0.0816	0.678	$0.0589^{\ddagger}$
K	Multi-layer perceptron P2 [14]	MLMF	Mobile	-0.0493	0.0781	0.499	$0.0557^{\ddagger}$
L	Multi-layer perceptron P2 [14]	MLMF	Crucif	-0.0853	0.0946	0.543	$0.0569^{\ddagger}$
M	Multi-layer perceptron P2 [14]	MLMF	Lin8Ch	-0.0793	0.0855	0.488	$0.062^{\ddagger}$
N	Multi-layer perceptron P2 [14]	MLMF	EM32	-0.0906	0.0806	0.54	$0.0578^{\ddagger}$
O	Per acoust. band SRMR Sec. 2.5. [15]	SFM	Single	-0.191	0.118	0.655	0.58
P	NSRMR Sec. 2.4. [16, 15]	SFM	Single	-0.128	0.123	0.374	0.571
Q	NSRMR Sec. 2.4. [16, 15]	SFM	Chromebook	-0.0736	0.113	0.41	1.04
R	NSRMR Sec. 2.4. [16, 15]	SFM	Mobile	-0.118	0.0961	0.436	1.59
S	NSRMR Sec. 2.4. [16, 15]	SFM	Crucif	-0.115	0.109	0.363	2.63
T	SRMR Sec. 2.3. [15]	SFM	Single	-0.221	0.16	0.312	0.457
U	SRMR Sec. 2.3. [15]	SFM	Chromebook	-0.186	0.15	0.29	0.831
V	SRMR Sec. 2.3. [15]	SFM	Mobile	-0.219	0.136	0.346	1.26
W	SRMR Sec. 2.3. [15]	SFM	Crucif	-0.215	0.144	0.336	2.09
X	NIRAv3 [4]	MLMF	Single	-0.268	0.172	0.442	$0.897^{\dagger}$
Y	NIRAv1 [4]	MLMF	Single	-0.245	0.164	0.408	$0.897^{\dagger}$
Z	NIRAv2 [4]	MLMF	Single	-0.183	0.199	-0.0283	$0.912^{\dagger}$
a	Blur kernel [17]	SFM	Single	0.0888	0.0989	0.513	8.16
b	Blur kernel with sliding window [18]	SFM	Single	-0.045	0.104	0.421	0.413
c	Temporal dynamics [19]	SFM	Single	-0.387	0.253	0.429	0.362
d	Improved blind RTE [3]	ABC	Single	-0.128	0.132	0.354	0.0255
e	SDD [20]	SFM	Single	-0.508	0.329	0.644	0.0219

3.2.2 Ambient noise at 12 dB SNR

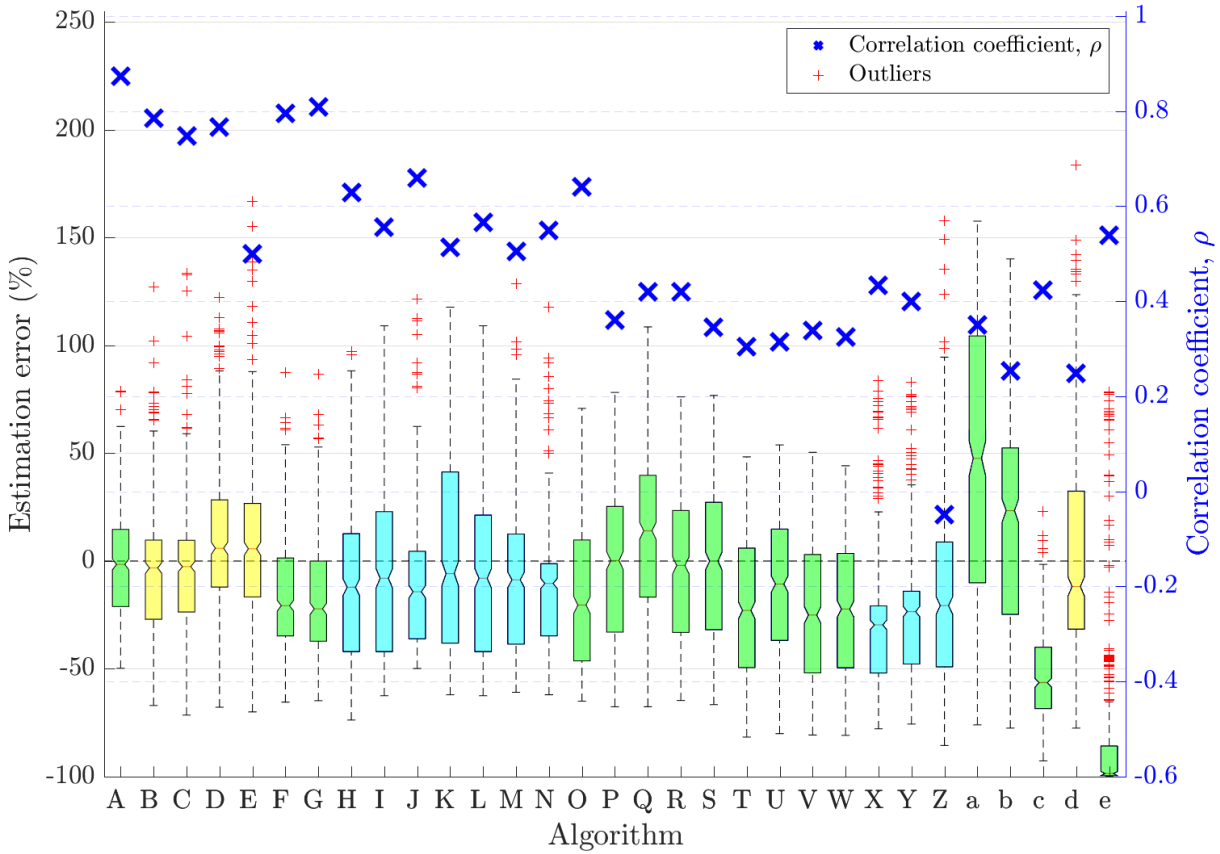

Figure 17: Fullband T_{60} estimation error in ambient noise at 12 dB SNR

Table 13: T_{60} estimation algorithm performance in ambient noise at 12 dB SNR

Ref.	Algorithm	Class	Mic. Config.	Bias	MSE	ρ	RTF
A	QA Reverb [11]	SFM	Single	-0.0795	0.0543	0.873	0.401
B	Octave SB-based FB RTE [9]	ABC	Single	-0.1	0.0657	0.786	1
C	DCT-based FB RTE [9]	ABC	Single	-0.0967	0.069	0.748	1.04
D	Model-based SB RTE [9]	ABC	Single	-0.0433	0.0905	0.767	0.478
E	Baseline algorithm for FB RTE [9]	ABC	Single	-0.0527	0.0955	0.499	0.0421
F	SDDSA-G retrained [12]	SFM	Single	-0.133	0.0629	0.796	0.0153
G	SDDSA-G [13]	SFM	Single	-0.157	0.075	0.808	0.0166
H	Multi-layer perceptron [14]	MLMF	Single	-0.117	0.0888	0.629	0.0578‡
I	Multi-layer perceptron P2 [14]	MLMF	Single	-0.0899	0.0935	0.556	0.0578‡
J	Multi-layer perceptron P2 [14]	MLMF	Chromebook	-0.097	0.0827	0.659	0.0589‡
K	Multi-layer perceptron P2 [14]	MLMF	Mobile	-0.0631	0.0781	0.514	0.0557‡
L	Multi-layer perceptron P2 [14]	MLMF	Crucif	-0.0917	0.0927	0.565	0.0569‡
M	Multi-layer perceptron P2 [14]	MLMF	Lin8Ch	-0.0873	0.0852	0.505	0.062‡
N	Multi-layer perceptron P2 [14]	MLMF	EM32	-0.103	0.0821	0.549	0.0578‡
O	Per acoust. band SRMR Sec. 2.5. [15]	SFM	Single	-0.18	0.115	0.64	0.58
P	NSRMR Sec. 2.4. [16, 15]	SFM	Single	-0.121	0.122	0.36	0.571
Q	NSRMR Sec. 2.4. [16, 15]	SFM	Chromebook	-0.0575	0.11	0.42	1.04
R	NSRMR Sec. 2.4. [16, 15]	SFM	Mobile	-0.111	0.0956	0.42	1.59
S	NSRMR Sec. 2.4. [16, 15]	SFM	Crucif	-0.109	0.109	0.345	2.63
T	SRMR Sec. 2.3. [15]	SFM	Single	-0.215	0.158	0.305	0.457
U	SRMR Sec. 2.3. [15]	SFM	Chromebook	-0.171	0.143	0.314	0.831
V	SRMR Sec. 2.3. [15]	SFM	Mobile	-0.212	0.133	0.338	1.26
W	SRMR Sec. 2.3. [15]	SFM	Crucif	-0.209	0.142	0.324	2.09
X	NIRAv3 [4]	MLMF	Single	-0.273	0.176	0.433	0.897†
Y	NIRAv1 [4]	MLMF	Single	-0.25	0.167	0.399	0.897†
Z	NIRAv2 [4]	MLMF	Single	-0.189	0.196	-0.0487	0.912†
a	Blur kernel [17]	SFM	Single	0.161	0.138	0.35	8.16
b	Blur kernel with sliding window [18]	SFM	Single	-0.0199	0.117	0.254	0.413
c	Temporal dynamics [19]	SFM	Single	-0.382	0.25	0.423	0.362
d	Improved blind RTE [3]	ABC	Single	-0.0994	0.147	0.249	0.0255
e	SDD [20]	SFM	Single	-0.518	0.356	0.539	0.0219

3.2.3 Ambient noise at -1 dB SNR

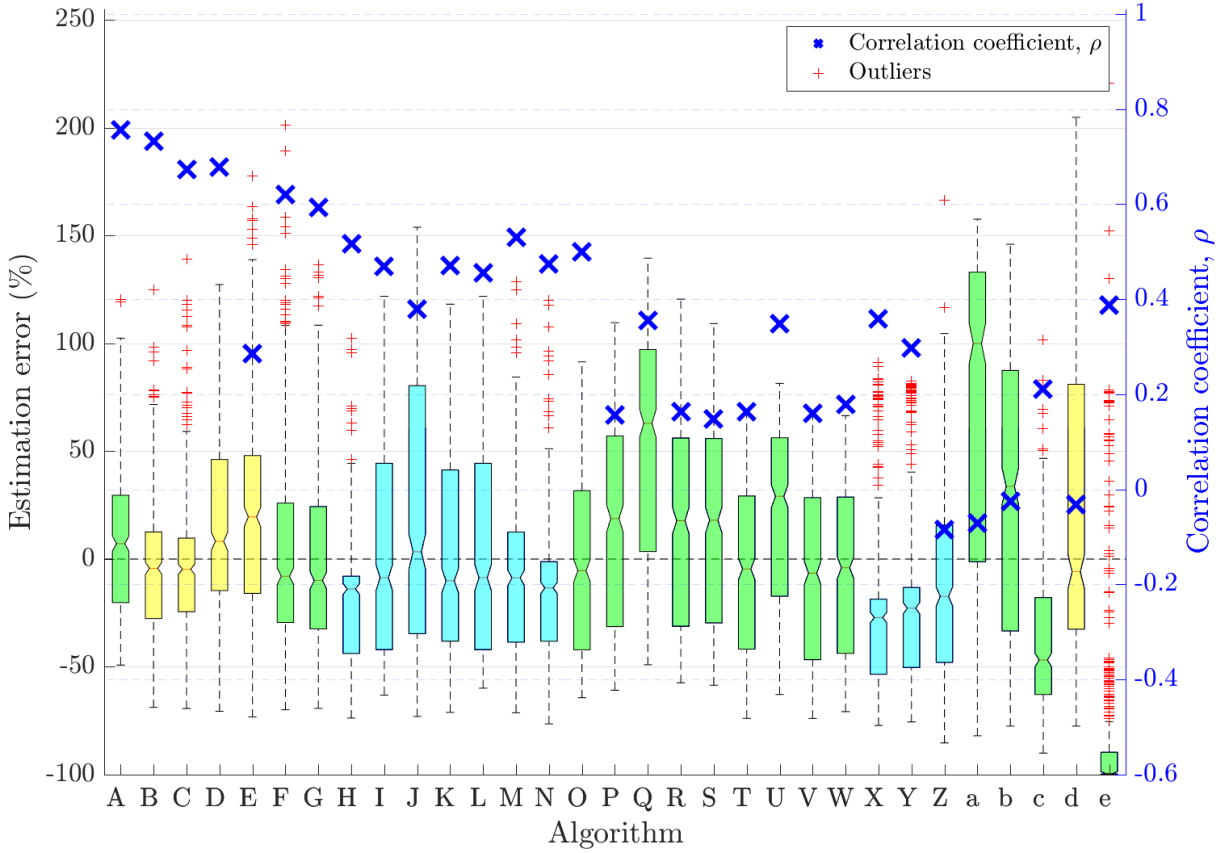

Figure 18: Fullband T_{60} estimation error in ambient noise at -1 dB SNR

Table 14: T_{60} estimation algorithm performance in ambient noise at $-1\,\mathrm{dB}$ SNR

Ref.	Algorithm	Class	Mic. Config.	Bias	MSE	ρ	RTF
A	QA Reverb [11]	SFM	Single	-0.0339	0.0634	0.757	0.401
B	Octave SB-based FB RTE [9]	ABC	Single	-0.0997	0.0735	0.733	1
C	DCT-based FB RTE [9]	ABC	Single	-0.103	0.0812	0.673	1.04
D	Model-based SB RTE [9]	ABC	Single	-0.0259	0.105	0.678	0.478
E	Baseline algorithm for FB RTE [9]	ABC	Single	-0.0001	0.124	0.285	0.0421
F	SDDSA-G retrained [12]	SFM	Single	-0.0564	0.0806	0.62	0.0153
G	SDDSA-G [13]	SFM	Single	-0.0867	0.0874	0.592	0.0166
H	Multi-layer perceptron [14]	MLMF	Single	-0.147	0.112	0.516	$0.0578^{\ddagger}$
I	Multi-layer perceptron P2 [14]	MLMF	Single	-0.0819	0.103	0.47	$0.0578^{\ddagger}$
J	Multi-layer perceptron P2 [14]	MLMF	Chromebook	-0.0138	0.111	0.379	$0.0589^{\ddagger}$
K	Multi-layer perceptron P2 [14]	MLMF	Mobile	-0.0619	0.0834	0.471	$0.0557^{\ddagger}$
L	Multi-layer perceptron P2 [14]	MLMF	Crucif	-0.0787	0.104	0.455	$0.0569^{\ddagger}$
M	Multi-layer perceptron P2 [14]	MLMF	Lin8Ch	-0.0787	0.0812	0.53	$0.062^{\ddagger}$
N	Multi-layer perceptron P2 [14]	MLMF	EM32	-0.0972	0.0894	0.474	$0.0578^{\ddagger}$
O	Per acoust. band SRMR Sec. 2.5. [15]	SFM	Single	-0.108	0.106	0.499	0.58
P	NSRMR Sec. 2.4. [16, 15]	SFM	Single	-0.0403	0.124	0.157	0.571
Q	NSRMR Sec. 2.4. [16, 15]	SFM	Chromebook	0.118	0.125	0.356	1.04
R	NSRMR Sec. 2.4. [16, 15]	SFM	Mobile	-0.022	0.101	0.163	1.59
S	NSRMR Sec. 2.4. [16, 15]	SFM	Crucif	-0.0271	0.111	0.148	2.63
T	SRMR Sec. 2.3. [15]	SFM	Single	-0.148	0.142	0.164	0.457
U	SRMR Sec. 2.3. [15]	SFM	Chromebook	-0.0332	0.114	0.348	0.831
V	SRMR Sec. 2.3. [15]	SFM	Mobile	-0.135	0.117	0.159	1.26
W	SRMR Sec. 2.3. [15]	SFM	Crucif	-0.14	0.126	0.178	2.09
X	NIRAv3 [4]	MLMF	Single	-0.248	0.168	0.359	$0.897^{\dagger}$
Y	NIRAv1 [4]	MLMF	Single	-0.235	0.167	0.298	$0.897^{\dagger}$
Z	NIRAv2 [4]	MLMF	Single	-0.177	0.198	-0.085	$0.912^{\dagger}$
a	Blur kernel [17]	SFM	Single	0.242	0.214	-0.0718	8.16
b	Blur kernel with sliding window [18]	SFM	Single	0.0183	0.188	-0.0244	0.413
c	Temporal dynamics [19]	SFM	Single	-0.307	0.214	0.211	0.362
d	Improved blind RTE [3]	ABC	Single	0.00207	0.224	-0.0319	0.0255
e	SDD [20]	SFM	Single	-0.518	0.381	0.387	0.0219

3.2.4 Babble noise at 18 dB SNR

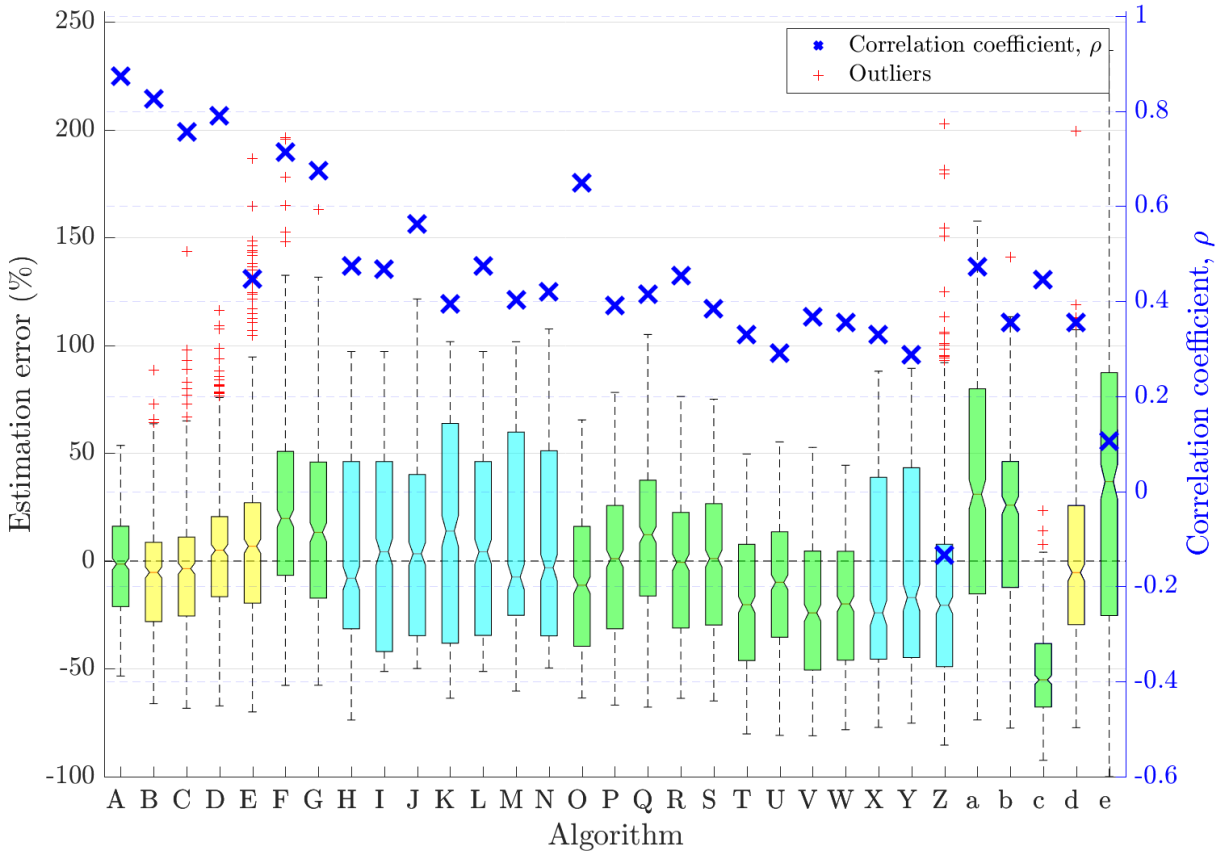

Figure 19: Fullband T_{60} estimation error in babble noise at 18 dB SNR

Table 15: T_{60} estimation algorithm performance in babble noise at $18\,\mathrm{dB}$ SNR

Ref.	Algorithm	Class	Mic. Config.	Bias	MSE	ρ	RTF
A	QA Reverb [11]	SFM	Single	-0.0854	0.058	0.873	0.398
B	Octave SB-based FB RTE [9]	ABC	Single	-0.112	0.064	0.826	0.911
C	DCT-based FB RTE [9]	ABC	Single	-0.1	0.0698	0.756	0.99
D	Model-based SB RTE [9]	ABC	Single	-0.0665	0.0905	0.79	0.443
E	Baseline algorithm for FB RTE [9]	ABC	Single	-0.0546	0.102	0.448	0.0428
F	SDDSA-G retrained [12]	SFM	Single	0.0931	0.0836	0.713	0.0155
G	SDDSA-G [13]	SFM	Single	0.0104	0.0681	0.674	0.0162
H	Multi-layer perceptron [14]	MLMF	Single	-0.054	0.098	0.474	$0.0579^{\ddagger}$
I	Multi-layer perceptron P2 [14]	MLMF	Single	-0.0373	0.0974	0.467	$0.0579^{\ddagger}$
J	Multi-layer perceptron P2 [14]	MLMF	Chromebook	-0.056	0.0891	0.562	$0.0588^{\ddagger}$
K	Multi-layer perceptron P2 [14]	MLMF	Mobile	-0.0197	0.086	0.394	$0.0555^{\ddagger}$
L	Multi-layer perceptron P2 [14]	MLMF	Crucif	-0.0431	0.097	0.474	$0.057^{\ddagger}$
M	Multi-layer perceptron P2 [14]	MLMF	Lin8Ch	-0.0359	0.0897	0.403	$0.0618^{\ddagger}$
N	Multi-layer perceptron P2 [14]	MLMF	EM32	-0.0518	0.0876	0.42	$0.0576^{\ddagger}$
O	Per acoust. band SRMR Sec. 2.5. [15]	SFM	Single	-0.152	0.108	0.648	0.579
P	NSRMR Sec. 2.4. [16, 15]	SFM	Single	-0.116	0.119	0.391	0.572
Q	NSRMR Sec. 2.4. [16, 15]	SFM	Chromebook	-0.0642	0.111	0.414	1.04
R	NSRMR Sec. 2.4. [16, 15]	SFM	Mobile	-0.106	0.0924	0.454	1.58
S	NSRMR Sec. 2.4. [16, 15]	SFM	Crucif	-0.104	0.105	0.385	2.63
T	SRMR Sec. 2.3. [15]	SFM	Single	-0.207	0.152	0.329	0.457
U	SRMR Sec. 2.3. [15]	SFM	Chromebook	-0.173	0.145	0.29	0.833
V	SRMR Sec. 2.3. [15]	SFM	Mobile	-0.204	0.128	0.367	1.26
W	SRMR Sec. 2.3. [15]	SFM	Crucif	-0.2	0.137	0.356	2.1
X	NIRAv3 [4]	MLMF	Single	-0.14	0.133	0.33	$0.906^{\dagger}$
Y	NIRAv1 [4]	MLMF	Single	-0.126	0.132	0.288	$0.906^{\dagger}$
Z	NIRAv2 [4]	MLMF	Single	-0.176	0.228	-0.134	$0.901^{\dagger}$
a	Blur kernel [17]	SFM	Single	0.102	0.107	0.472	8.88
b	Blur kernel with sliding window [18]	SFM	Single	-0.026	0.108	0.356	0.438
c	Temporal dynamics [19]	SFM	Single	-0.375	0.243	0.445	0.365
d	Improved blind RTE [3]	ABC	Single	-0.104	0.126	0.355	0.0269
e	SDD [20]	SFM	Single	0.793	141	0.105	0.0224

3.2.5 Babble noise at 12 dB SNR

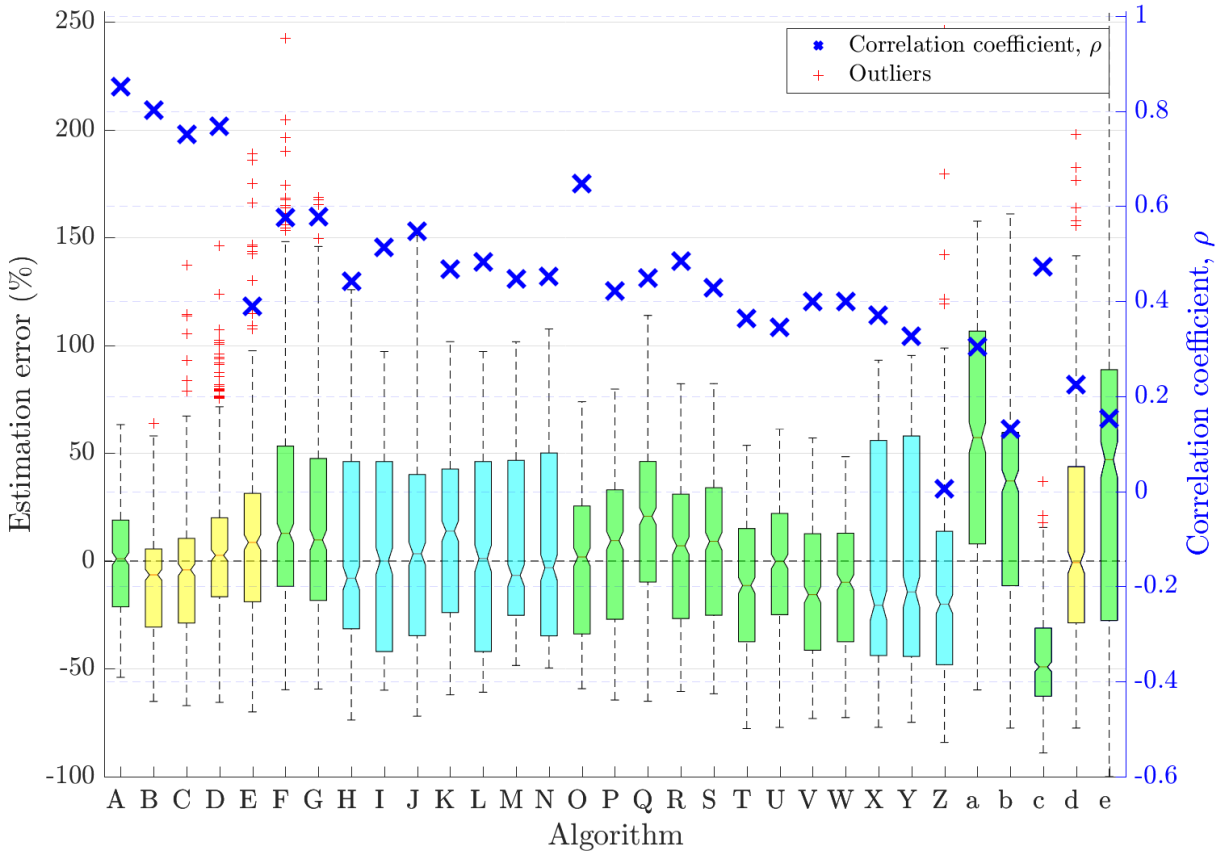

Figure 20: Fullband T_{60} estimation error in babble noise at 12 dB SNR

Table 16: T_{60} estimation algorithm performance in babble noise at $12\,\mathrm{dB}$ SNR

Ref.	Algorithm	Class	Mic. Config.	Bias	MSE	ρ	RTF
A	QA Reverb [11]	SFM	Single	-0.0796	0.0609	0.851	0.398
B	Octave SB-based FB RTE [9]	ABC	Single	-0.128	0.0735	0.802	0.911
C	DCT-based FB RTE [9]	ABC	Single	-0.11	0.0737	0.751	0.99
D	Model-based SB RTE [9]	ABC	Single	-0.0701	0.095	0.768	0.443
E	Baseline algorithm for FB RTE [9]	ABC	Single	-0.0458	0.108	0.389	0.0428
F	SDDSA-G retrained [12]	SFM	Single	0.0875	0.113	0.577	0.0155
G	SDDSA-G [13]	SFM	Single	0.0122	0.0819	0.578	0.0162
H	Multi-layer perceptron [14]	MLMF	Single	-0.0609	0.103	0.443	$0.0579^{\ddagger}$
I	Multi-layer perceptron P2 [14]	MLMF	Single	-0.0513	0.0934	0.514	$0.0579^{\ddagger}$
J	Multi-layer perceptron P2 [14]	MLMF	Chromebook	-0.0474	0.0898	0.548	$0.0588^{\ddagger}$
K	Multi-layer perceptron P2 [14]	MLMF	Mobile	-0.0195	0.079	0.468	$0.0555^{\ddagger}$
L	Multi-layer perceptron P2 [14]	MLMF	Crucif	-0.0445	0.0961	0.483	$0.057^{\ddagger}$
M	Multi-layer perceptron P2 [14]	MLMF	Lin8Ch	-0.0231	0.0843	0.447	$0.0618^{\ddagger}$
N	Multi-layer perceptron P2 [14]	MLMF	EM32	-0.0616	0.0856	0.453	$0.0576^{\ddagger}$
O	Per acoust. band SRMR Sec. 2.5. [15]	SFM	Single	-0.11	0.101	0.647	0.579
P	NSRMR Sec. 2.4. [16, 15]	SFM	Single	-0.0862	0.112	0.422	0.572
Q	NSRMR Sec. 2.4. [16, 15]	SFM	Chromebook	-0.0337	0.107	0.449	1.04
R	NSRMR Sec. 2.4. [16, 15]	SFM	Mobile	-0.0739	0.0856	0.484	1.58
S	NSRMR Sec. 2.4. [16, 15]	SFM	Crucif	-0.0736	0.098	0.429	2.63
T	SRMR Sec. 2.3. [15]	SFM	Single	-0.173	0.138	0.363	0.457
U	SRMR Sec. 2.3. [15]	SFM	Chromebook	-0.135	0.132	0.344	0.833
V	SRMR Sec. 2.3. [15]	SFM	Mobile	-0.166	0.113	0.4	1.26
W	SRMR Sec. 2.3. [15]	SFM	Crucif	-0.164	0.122	0.4	2.1
X	NIRAv3 [4]	MLMF	Single	-0.108	0.12	0.371	$0.906^{\dagger}$
Y	NIRAv1 [4]	MLMF	Single	-0.0969	0.122	0.327	$0.906^{\dagger}$
Z	NIRAv2 [4]	MLMF	Single	-0.167	0.196	0.00486	$0.901^{\dagger}$
a	Blur kernel [17]	SFM	Single	0.187	0.148	0.305	8.88
b	Blur kernel with sliding window [18]	SFM	Single	0.00866	0.127	0.131	0.438
c	Temporal dynamics [19]	SFM	Single	-0.344	0.218	0.472	0.365
d	Improved blind RTE [3]	ABC	Single	-0.0563	0.145	0.224	0.0269
e	SDD [20]	SFM	Single	0.458	5.11	0.153	0.0224

3.2.6 Babble noise at -1 dB SNR

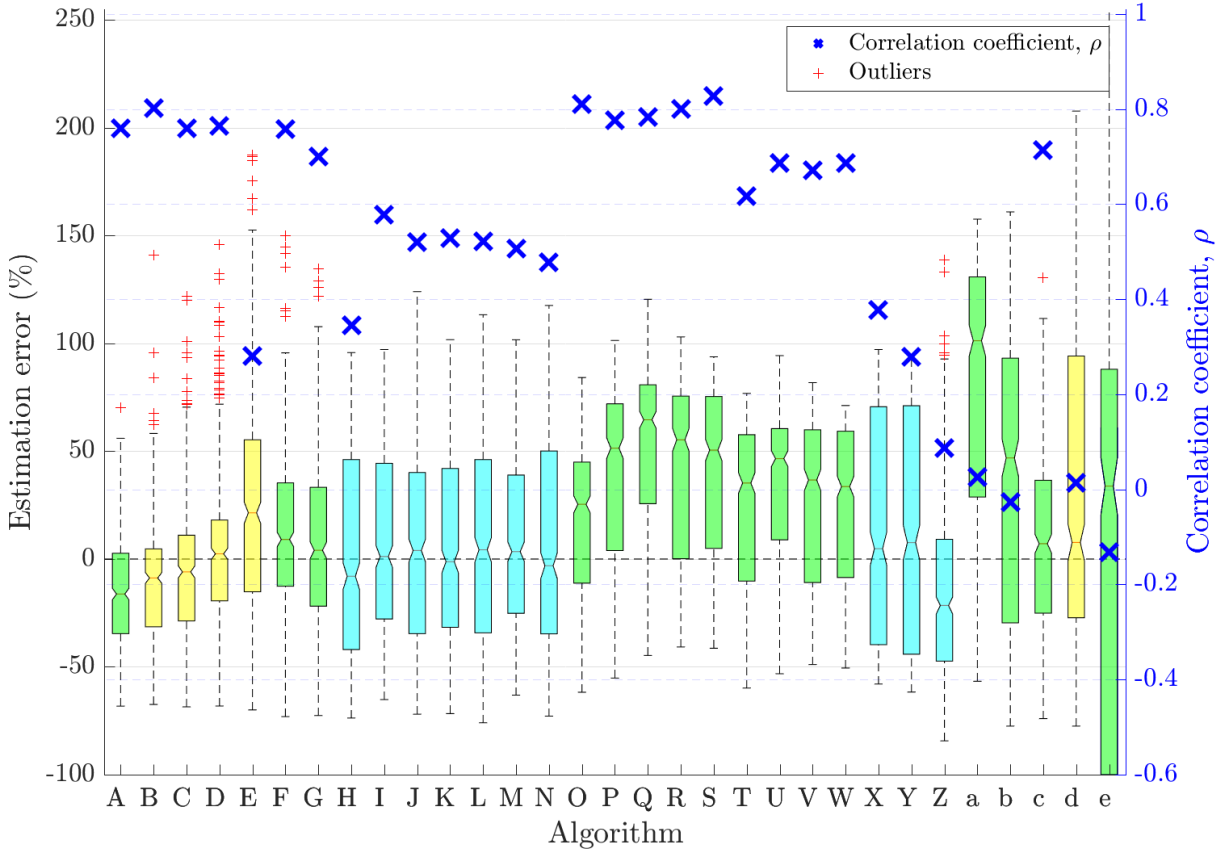

Figure 21: Fullband T_{60} estimation error in babble noise at -1 dB SNR

Table 17: T_{60} estimation algorithm performance in babble noise at -1 dB SNR

Ref.	Algorithm	Class	Mic. Config.	Bias	MSE	ρ	RTF
A	QA Reverb [11]	SFM	Single	-0.162	0.0934	0.759	0.398
B	Octave SB-based FB RTE [9]	ABC	Single	-0.13	0.0727	0.802	0.911
C	DCT-based FB RTE [9]	ABC	Single	-0.108	0.072	0.759	0.99
D	Model-based SB RTE [9]	ABC	Single	-0.073	0.0943	0.765	0.443
E	Baseline algorithm for FB RTE [9]	ABC	Single	0.0297	0.127	0.281	0.0428
F	SDDSA-G retrained [12]	SFM	Single	0.0259	0.0541	0.757	0.0155
G	SDDSA-G [13]	SFM	Single	-0.0249	0.0655	0.7	0.0162
H	Multi-layer perceptron [14]	MLMF	Single	-0.0903	0.119	0.345	0.0579‡
I	Multi-layer perceptron P2 [14]	MLMF	Single	-0.0465	0.0853	0.577	0.0579‡
J	Multi-layer perceptron P2 [14]	MLMF	Chromebook	-0.0568	0.0945	0.52	0.0588‡
K	Multi-layer perceptron P2 [14]	MLMF	Mobile	-0.0339	0.0738	0.528	0.0555‡
L	Multi-layer perceptron P2 [14]	MLMF	Crucif	-0.0419	0.0912	0.523	0.057‡
M	Multi-layer perceptron P2 [14]	MLMF	Lin8Ch	-0.0241	0.078	0.506	0.0618‡
N	Multi-layer perceptron P2 [14]	MLMF	EM32	-0.0572	0.0826	0.478	0.0576‡
O	Per acoust. band SRMR Sec. 2.5. [15]	SFM	Single	-0.0282	0.0888	0.81	0.579
P	NSRMR Sec. 2.4. [16, 15]	SFM	Single	0.0712	0.0987	0.777	0.572
Q	NSRMR Sec. 2.4. [16, 15]	SFM	Chromebook	0.113	0.113	0.783	1.04
R	NSRMR Sec. 2.4. [16, 15]	SFM	Mobile	0.0935	0.0841	0.801	1.58
S	NSRMR Sec. 2.4. [16, 15]	SFM	Crucif	0.0871	0.0905	0.828	2.63
T	SRMR Sec. 2.3. [15]	SFM	Single	-0.00916	0.108	0.617	0.457
U	SRMR Sec. 2.3. [15]	SFM	Chromebook	0.029	0.111	0.687	0.833
V	SRMR Sec. 2.3. [15]	SFM	Mobile	0.00906	0.0867	0.671	1.26
W	SRMR Sec. 2.3. [15]	SFM	Crucif	0.00276	0.0948	0.687	2.1
X	NIRAv3 [4]	MLMF	Single	-0.0413	0.109	0.377	0.906†
Y	NIRAv1 [4]	MLMF	Single	-0.0465	0.119	0.279	0.906†
Z	NIRAv2 [4]	MLMF	Single	-0.184	0.185	0.0865	0.901†
a	Blur kernel [17]	SFM	Single	0.263	0.201	0.0261	8.88
b	Blur kernel with sliding window [18]	SFM	Single	0.0733	0.178	-0.0263	0.438
c	Temporal dynamics [19]	SFM	Single	-0.053	0.0728	0.713	0.365
d	Improved blind RTE [3]	ABC	Single	0.0536	0.219	0.0134	0.0269
e	SDD [20]	SFM	Single	0.529	12.5	-0.131	0.0224

3.2.7 Fan noise at 18 dB SNR

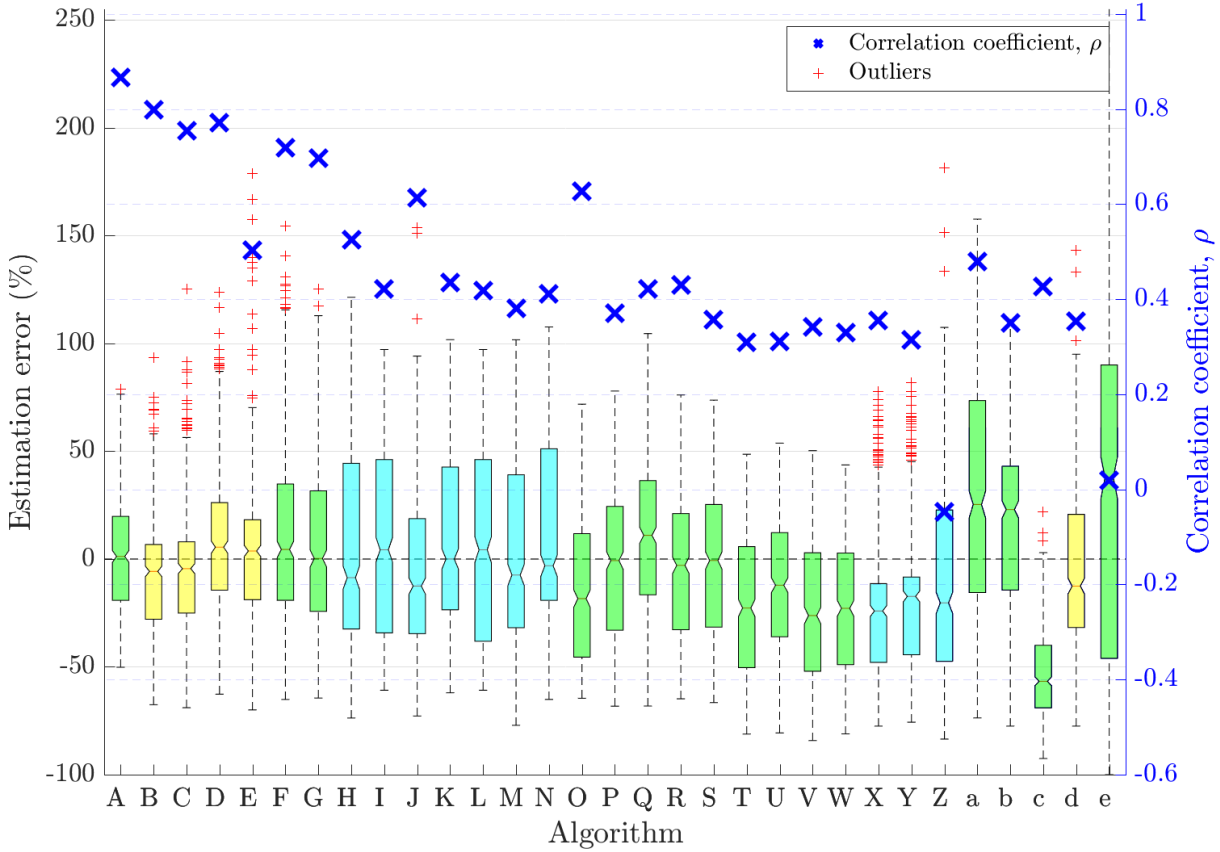

Figure 22: Fullband T_{60} estimation error in fan noise at 18 dB SNR

Table 18: T_{60} estimation algorithm performance in fan noise at $18\,\mathrm{dB}$ SNR

Ref.	Algorithm	Class	Mic. Config.	Bias	MSE	ρ	RTF
A	QA Reverb [11]	SFM	Single	-0.0649	0.055	0.867	0.4
B	Octave SB-based FB RTE [9]	ABC	Single	-0.111	0.0666	0.798	0.903
C	DCT-based FB RTE [9]	ABC	Single	-0.106	0.0705	0.755	0.984
D	Model-based SB RTE [9]	ABC	Single	-0.0527	0.0917	0.772	0.433
E	Baseline algorithm for FB RTE [9]	ABC	Single	-0.079	0.098	0.503	0.0421
F	SDDSA-G retrained [12]	SFM	Single	0.0258	0.0717	0.719	0.0148
G	SDDSA-G [13]	SFM	Single	-0.0387	0.066	0.696	0.0164
H	Multi-layer perceptron [14]	MLMF	Single	-0.0699	0.0938	0.525	0.0578‡
I	Multi-layer perceptron P2 [14]	MLMF	Single	-0.0325	0.102	0.421	0.0578‡
J	Multi-layer perceptron P2 [14]	MLMF	Chromebook	-0.0706	0.0843	0.614	0.059‡
K	Multi-layer perceptron P2 [14]	MLMF	Mobile	-0.0177	0.0821	0.435	0.0555‡
L	Multi-layer perceptron P2 [14]	MLMF	Crucif	-0.0371	0.103	0.418	0.0569‡
M	Multi-layer perceptron P2 [14]	MLMF	Lin8Ch	-0.0477	0.0931	0.381	0.0617‡
N	Multi-layer perceptron P2 [14]	MLMF	EM32	-0.0406	0.0872	0.411	0.0574‡
O	Per acoust. band SRMR Sec. 2.5. [15]	SFM	Single	-0.174	0.115	0.627	0.576
P	NSRMR Sec. 2.4. [16, 15]	SFM	Single	-0.124	0.122	0.37	0.569
Q	NSRMR Sec. 2.4. [16, 15]	SFM	Chromebook	-0.0681	0.111	0.422	1.03
R	NSRMR Sec. 2.4. [16, 15]	SFM	Mobile	-0.114	0.0956	0.431	1.58
S	NSRMR Sec. 2.4. [16, 15]	SFM	Crucif	-0.112	0.109	0.358	2.61
T	SRMR Sec. 2.3. [15]	SFM	Single	-0.217	0.158	0.309	0.455
U	SRMR Sec. 2.3. [15]	SFM	Chromebook	-0.179	0.146	0.312	0.824
V	SRMR Sec. 2.3. [15]	SFM	Mobile	-0.215	0.134	0.342	1.26
W	SRMR Sec. 2.3. [15]	SFM	Crucif	-0.211	0.142	0.33	2.08
X	NIRAv3 [4]	MLMF	Single	-0.223	0.157	0.355	0.895†
Y	NIRAv1 [4]	MLMF	Single	-0.207	0.153	0.315	0.895†
Z	NIRAv2 [4]	MLMF	Single	-0.164	0.201	-0.0474	0.906†
a	Blur kernel [17]	SFM	Single	0.0893	0.103	0.48	8.36
b	Blur kernel with sliding window [18]	SFM	Single	-0.0394	0.109	0.35	0.412
c	Temporal dynamics [19]	SFM	Single	-0.384	0.251	0.427	0.358
d	Improved blind RTE [3]	ABC	Single	-0.134	0.133	0.354	0.0254
e	SDD [20]	SFM	Single	0.666	28.5	0.0185	0.0221

3.2.8 Fan noise at 12 dB SNR

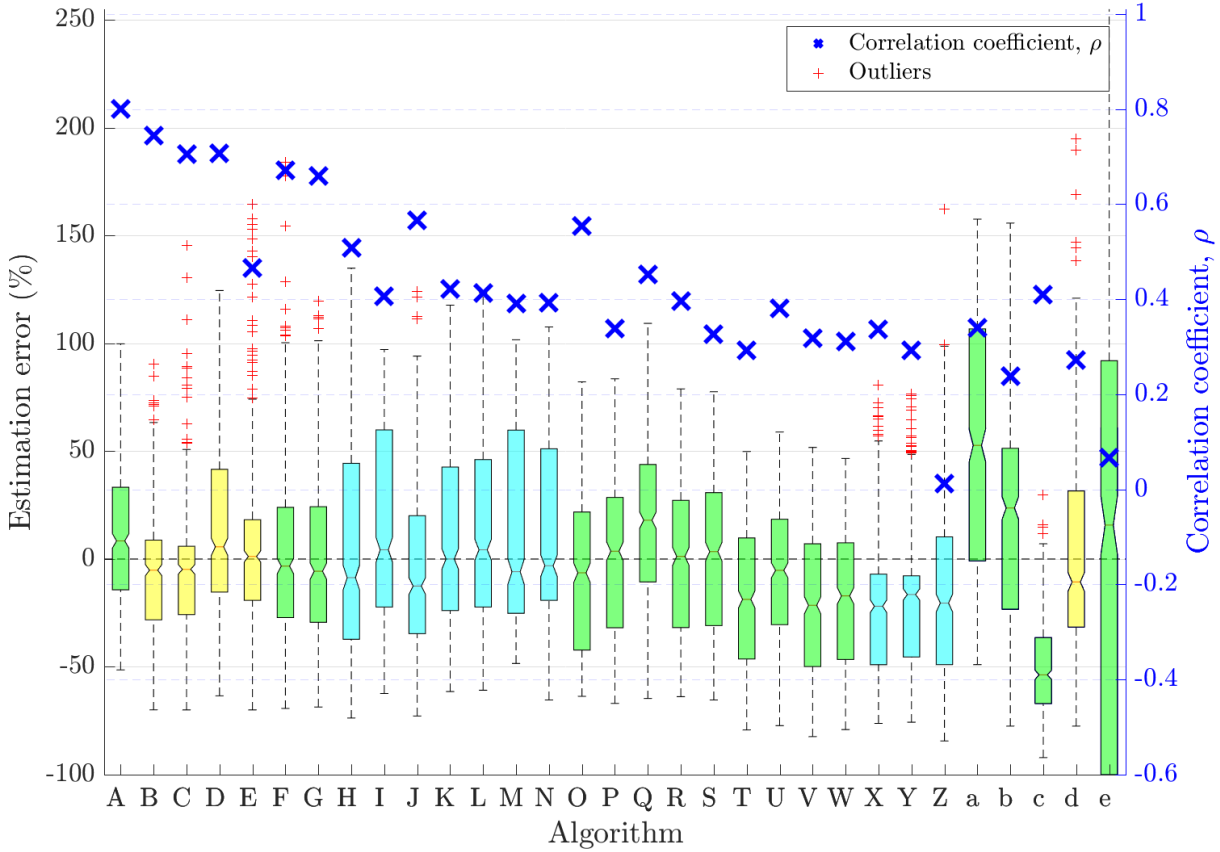

Figure 23: Fullband T_{60} estimation error in fan noise at 12 dB SNR

Table 19: T_{60} estimation algorithm performance in fan noise at $12\,\mathrm{dB}$ SNR

Ref.	Algorithm	Class	Mic. Config.	Bias	MSE	ρ	RTF
A	QA Reverb [11]	SFM	Single	-0.0315	0.0622	0.8	0.4
B	Octave SB-based FB RTE [9]	ABC	Single	-0.114	0.0755	0.744	0.903
C	DCT-based FB RTE [9]	ABC	Single	-0.117	0.0803	0.705	0.984
D	Model-based SB RTE [9]	ABC	Single	-0.0419	0.102	0.706	0.433
E	Baseline algorithm for FB RTE [9]	ABC	Single	-0.0834	0.103	0.465	0.0421
F	SDDSA-G retrained [12]	SFM	Single	-0.05	0.0707	0.671	0.0148
G	SDDSA-G [13]	SFM	Single	-0.0808	0.0782	0.66	0.0164
H	Multi-layer perceptron [14]	MLMF	Single	-0.08	0.0975	0.508	$0.0578^{\ddagger}$
I	Multi-layer perceptron P2 [14]	MLMF	Single	-0.0275	0.103	0.407	$0.0578^{\ddagger}$
J	Multi-layer perceptron P2 [14]	MLMF	Chromebook	-0.0644	0.0894	0.565	$0.059^{\ddagger}$
K	Multi-layer perceptron P2 [14]	MLMF	Mobile	-0.00734	0.0834	0.422	$0.0555^{\ddagger}$
L	Multi-layer perceptron P2 [14]	MLMF	Crucif	-0.0295	0.103	0.414	$0.0569^{\ddagger}$
M	Multi-layer perceptron P2 [14]	MLMF	Lin8Ch	-0.0329	0.0913	0.391	$0.0617^{\ddagger}$
N	Multi-layer perceptron P2 [14]	MLMF	EM32	-0.0338	0.0891	0.392	$0.0574^{\ddagger}$
O	Per acoust. band SRMR Sec. 2.5. [15]	SFM	Single	-0.132	0.109	0.554	0.576
P	NSRMR Sec. 2.4. [16, 15]	SFM	Single	-0.109	0.121	0.339	0.569
Q	NSRMR Sec. 2.4. [16, 15]	SFM	Chromebook	-0.0388	0.106	0.452	1.03
R	NSRMR Sec. 2.4. [16, 15]	SFM	Mobile	-0.0978	0.0944	0.396	1.58
S	NSRMR Sec. 2.4. [16, 15]	SFM	Crucif	-0.0963	0.107	0.326	2.61
T	SRMR Sec. 2.3. [15]	SFM	Single	-0.201	0.153	0.293	0.455
U	SRMR Sec. 2.3. [15]	SFM	Chromebook	-0.149	0.133	0.38	0.824
V	SRMR Sec. 2.3. [15]	SFM	Mobile	-0.197	0.129	0.318	1.26
W	SRMR Sec. 2.3. [15]	SFM	Crucif	-0.195	0.137	0.312	2.08
X	NIRAv3 [4]	MLMF	Single	-0.216	0.155	0.337	$0.895^{\dagger}$
Y	NIRAv1 [4]	MLMF	Single	-0.206	0.155	0.293	$0.895^{\dagger}$
Z	NIRAv2 [4]	MLMF	Single	-0.188	0.188	0.0117	$0.906^{\dagger}$
a	Blur kernel [17]	SFM	Single	0.18	0.143	0.34	8.36
b	Blur kernel with sliding window [18]	SFM	Single	-0.0215	0.119	0.238	0.412
c	Temporal dynamics [19]	SFM	Single	-0.371	0.242	0.409	0.358
d	Improved blind RTE [3]	ABC	Single	-0.106	0.143	0.271	0.0254
e	SDD [20]	SFM	Single	0.918	57.2	0.0662	0.0221

3.2.9 Fan noise at -1 dB SNR

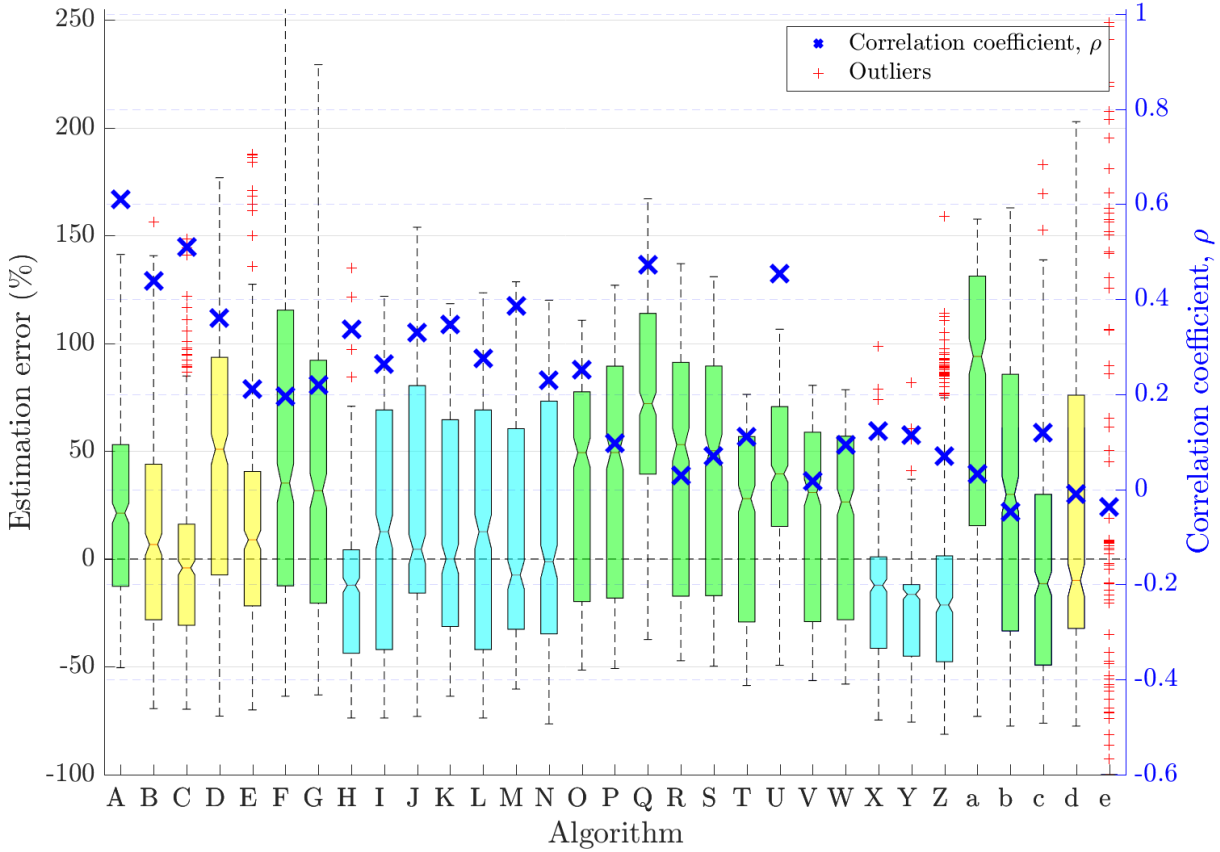

Figure 24: Fullband T_{60} estimation error in fan noise at -1 dB SNR

Table 20: T_{60} estimation algorithm performance in fan noise at $-1\,\mathrm{dB}$ SNR

Ref.	Algorithm	Class	Mic. Config.	Bias	MSE	ρ	RTF
A	QA Reverb [11]	SFM	Single	0.0162	0.0844	0.609	0.4
B	Octave SB-based FB RTE [9]	ABC	Single	-0.0396	0.101	0.438	0.903
C	DCT-based FB RTE [9]	ABC	Single	-0.105	0.102	0.509	0.984
D	Model-based SB RTE [9]	ABC	Single	0.0906	0.162	0.36	0.433
E	Baseline algorithm for FB RTE [9]	ABC	Single	-0.0326	0.135	0.21	0.0421
F	SDDSA-G retrained [12]	SFM	Single	0.213	0.247	0.196	0.0148
G	SDDSA-G [13]	SFM	Single	0.093	0.141	0.22	0.0164
H	Multi-layer perceptron [14]	MLMF	Single	-0.141	0.133	0.337	0.0578‡
I	Multi-layer perceptron P2 [14]	MLMF	Single	0.000904	0.12	0.264	0.0578‡
J	Multi-layer perceptron P2 [14]	MLMF	Chromebook	0.0206	0.118	0.329	0.059‡
K	Multi-layer perceptron P2 [14]	MLMF	Mobile	0.00366	0.0937	0.347	0.0555‡
L	Multi-layer perceptron P2 [14]	MLMF	Crucif	-0.000496	0.119	0.276	0.0569‡
M	Multi-layer perceptron P2 [14]	MLMF	Lin8Ch	-0.0123	0.093	0.386	0.0617‡
N	Multi-layer perceptron P2 [14]	MLMF	EM32	-0.00585	0.107	0.229	0.0574‡
O	Per acoust. band SRMR Sec. 2.5. [15]	SFM	Single	0.0497	0.117	0.251	0.576
P	NSRMR Sec. 2.4. [16, 15]	SFM	Single	0.0712	0.132	0.0973	0.569
Q	NSRMR Sec. 2.4. [16, 15]	SFM	Chromebook	0.212	0.151	0.472	1.03
R	NSRMR Sec. 2.4. [16, 15]	SFM	Mobile	0.0952	0.117	0.0296	1.58
S	NSRMR Sec. 2.4. [16, 15]	SFM	Crucif	0.0847	0.122	0.0702	2.61
T	SRMR Sec. 2.3. [15]	SFM	Single	-0.0493	0.124	0.111	0.455
U	SRMR Sec. 2.3. [15]	SFM	Chromebook	0.0513	0.113	0.454	0.824
V	SRMR Sec. 2.3. [15]	SFM	Mobile	-0.0333	0.105	0.0169	1.26
W	SRMR Sec. 2.3. [15]	SFM	Crucif	-0.0408	0.111	0.0942	2.08
X	NIRAv3 [4]	MLMF	Single	-0.207	0.166	0.122	0.895†
Y	NIRAv1 [4]	MLMF	Single	-0.246	0.184	0.115	0.895†
Z	NIRAv2 [4]	MLMF	Single	-0.185	0.188	0.0698	0.906†
a	Blur kernel [17]	SFM	Single	0.248	0.201	0.0335	8.36
b	Blur kernel with sliding window [18]	SFM	Single	0.00154	0.198	-0.0472	0.412
c	Temporal dynamics [19]	SFM	Single	-0.131	0.158	0.119	0.358
d	Improved blind RTE [3]	ABC	Single	0.000833	0.219	-0.00975	0.0254
e	SDD [20]	SFM	Single	2.35	2.5e+03	-0.0369	0.0221

3.3 Frequency-dependent T_{60} estimation results

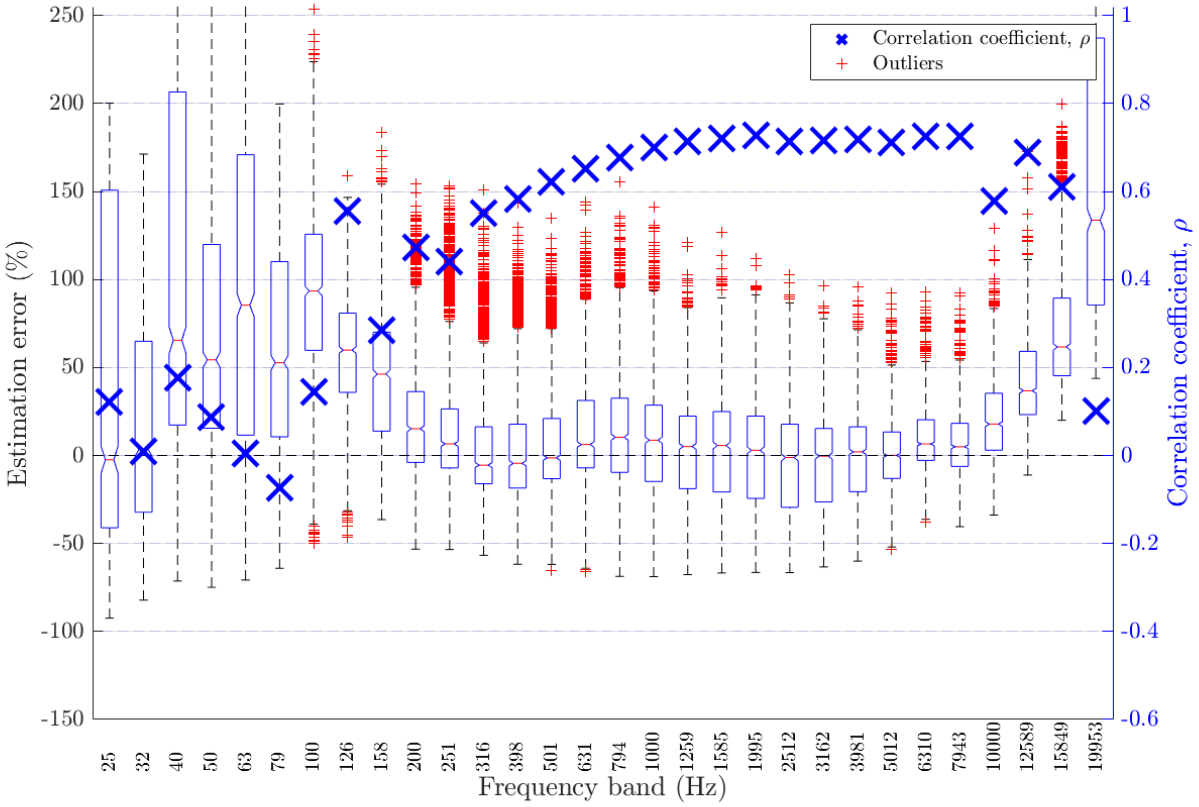

Figure 25: Frequency-dependent T_{60} estimation error in all noises for all SNRs for algorithm Model-based SB RTE [9]

Table 21: T_{60} estimation algorithm performance for all noises for all SNRs

Freq. band	Centre Freq. (Hz)	Bias	MSE	ρ
1	25.12	-0.5197	2.901	0.1224
2	31.62	-0.02769	0.5496	0.009101
3	39.81	0.4369	0.6085	0.177
4	50.12	0.4183	0.5136	0.08707
5	63.10	0.471	0.5336	0.004263
6	79.43	0.3703	0.3121	-0.07279
7	100.00	0.4955	0.3206	0.145
8	125.89	0.3541	0.1641	0.5561
9	158.49	0.2743	0.136	0.2838
10	199.53	0.139	0.08303	0.4733
11	251.19	0.07525	0.08501	0.4412
12	316.23	0.03405	0.06716	0.5516
13	398.11	0.01442	0.07244	0.5838
14	501.19	0.002211	0.08705	0.6224
15	630.96	-0.005208	0.1117	0.651
16	794.33	-0.02265	0.1192	0.6773
17	1000.00	-0.05042	0.128	0.6991
18	1258.93	-0.05597	0.1051	0.7128
19	1584.89	-0.05515	0.09516	0.7203
20	1995.26	-0.06708	0.09227	0.7271
21	2511.89	-0.09857	0.09601	0.7138
22	3162.28	-0.07575	0.0704	0.7165
23	3981.07	-0.04222	0.04788	0.7184
24	5011.87	-0.00961	0.0256	0.7104
25	6309.57	0.0536	0.01633	0.7254
26	7943.28	0.04453	0.01525	0.7262
27	10000.00	0.0958	0.02727	0.5792
28	12589.25	0.1761	0.04667	0.6879
29	15848.93	0.2424	0.07895	0.611
30	19952.62	0.3372	0.1412	0.1018

3.4 Frequency-dependent T_{60} estimation results by noise type

3.4.1 Ambient noise

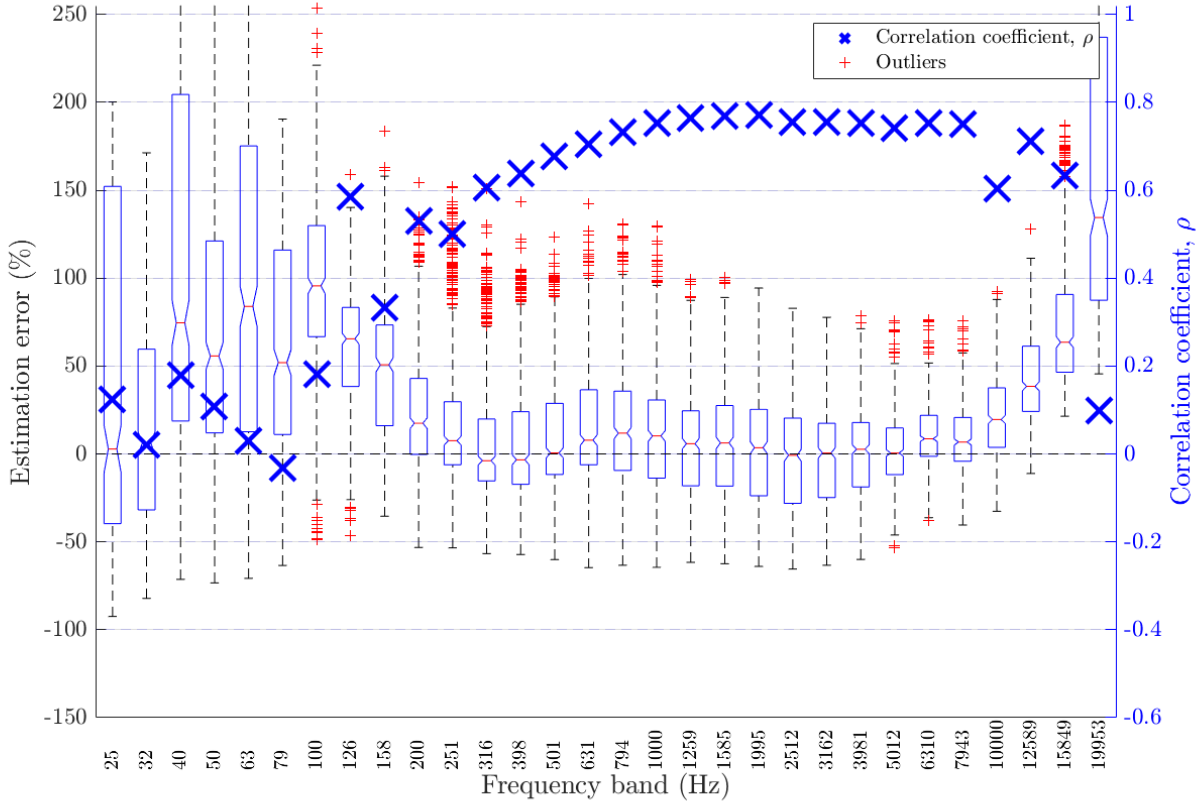

Figure 26: Frequency-dependent T_{60} estimation error in ambient noise for all SNRs for algorithm Model-based SB RTE [9]

Table 22: Frequency-dependent T_{60} estimation error in ambient noise for all SNRs for algorithm Model-based SB RTE [9]

Freq. band	Centre Freq. (Hz)	Bias	MSE	ρ
1	25.12	-0.5118	2.892	0.1237
2	31.62	-0.0155	0.5479	0.02024
3	39.81	0.451	0.6237	0.1794
4	50.12	0.4318	0.5217	0.1085
5	63.10	0.482	0.5402	0.03066
6	79.43	0.3776	0.3146	-0.03175
7	100.00	0.4989	0.3227	0.1825
8	125.89	0.3543	0.1621	0.5862
9	158.49	0.2722	0.1309	0.3326
10	199.53	0.1355	0.0744	0.5299
11	251.19	0.07118	0.07479	0.5004
12	316.23	0.02995	0.05818	0.605
13	398.11	0.01065	0.06323	0.6376
14	501.19	-0.001016	0.07766	0.676
15	630.96	-0.007819	0.1019	0.705
16	794.33	-0.02463	0.1098	0.7319
17	1000.00	-0.0518	0.1192	0.7521
18	1258.93	-0.05678	0.09748	0.7635
19	1584.89	-0.05546	0.08837	0.7677
20	1995.26	-0.06695	0.08603	0.7711
21	2511.89	-0.09804	0.09027	0.7541
22	3162.28	-0.07489	0.06565	0.7539
23	3981.07	-0.04107	0.04412	0.7529
24	5011.87	-0.008213	0.02323	0.7417
25	6309.57	0.05521	0.01547	0.7528
26	7943.28	0.04631	0.01457	0.7503
27	10000.00	0.09773	0.02723	0.6039
28	12589.25	0.1781	0.04744	0.7118
29	15848.93	0.2446	0.08045	0.6337
30	19952.62	0.3395	0.1436	0.09808

3.4.2 Babble noise

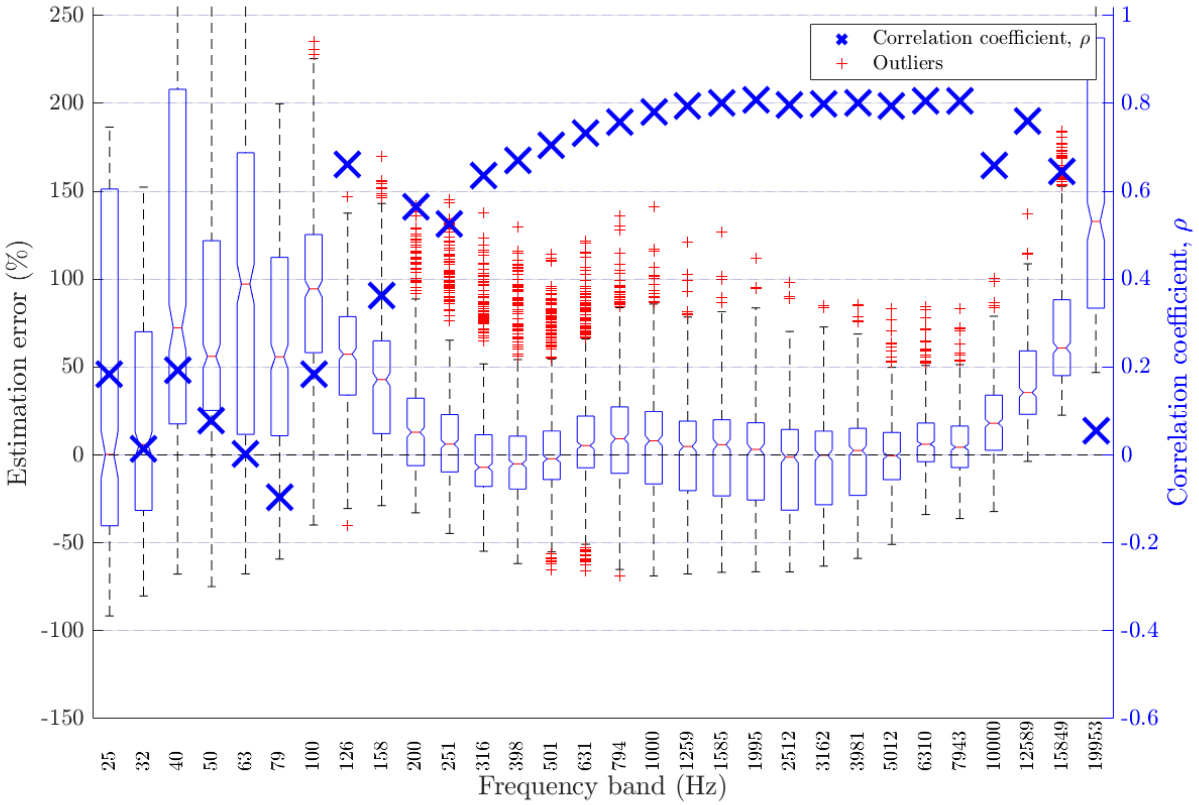

Figure 27: Frequency-dependent T_{60} estimation error in babble noise for all SNRs for algorithm Model-based SB RTE [9]

Table 23: Frequency-dependent T_{60} estimation error in babble noise for all SNRs for algorithm Model-based SB RTE [9]

Freq. band	Centre Freq. (Hz)	Bias	MSE	ρ
1	25.12	-0.5021	2.837	0.1826
2	31.62	0.01671	0.5267	0.01443
3	39.81	0.4939	0.6333	0.1917
4	50.12	0.4729	0.5405	0.07811
5	63.10	0.5109	0.5531	0.001786
6	79.43	0.3889	0.3159	-0.09623
7	100.00	0.4919	0.3071	0.1825
8	125.89	0.3316	0.1374	0.6609
9	158.49	0.2383	0.1079	0.3631
10	199.53	0.09501	0.05918	0.5637
11	251.19	0.0279	0.06538	0.5263
12	316.23	-0.01336	0.05215	0.6363
13	398.11	-0.03105	0.05875	0.6695
14	501.19	-0.04029	0.07434	0.7055
15	630.96	-0.04439	0.09955	0.7309
16	794.33	-0.05855	0.1086	0.7579
17	1000.00	-0.0833	0.1196	0.7795
18	1258.93	-0.08619	0.09809	0.7935
19	1584.89	-0.08311	0.08867	0.8005
20	1995.26	-0.09317	0.08655	0.8077
21	2511.89	-0.1231	0.09174	0.7957
22	3162.28	-0.0991	0.06587	0.7985
23	3981.07	-0.06462	0.0427	0.8006
24	5011.87	-0.03127	0.02038	0.7939
25	6309.57	0.0325	0.01033	0.8055
26	7943.28	0.02386	0.009707	0.8062
27	10000.00	0.07546	0.02013	0.659
28	12589.25	0.156	0.03743	0.7598
29	15848.93	0.2225	0.06813	0.645
30	19952.62	0.3174	0.1277	0.05588

3.4.3 Fan noise

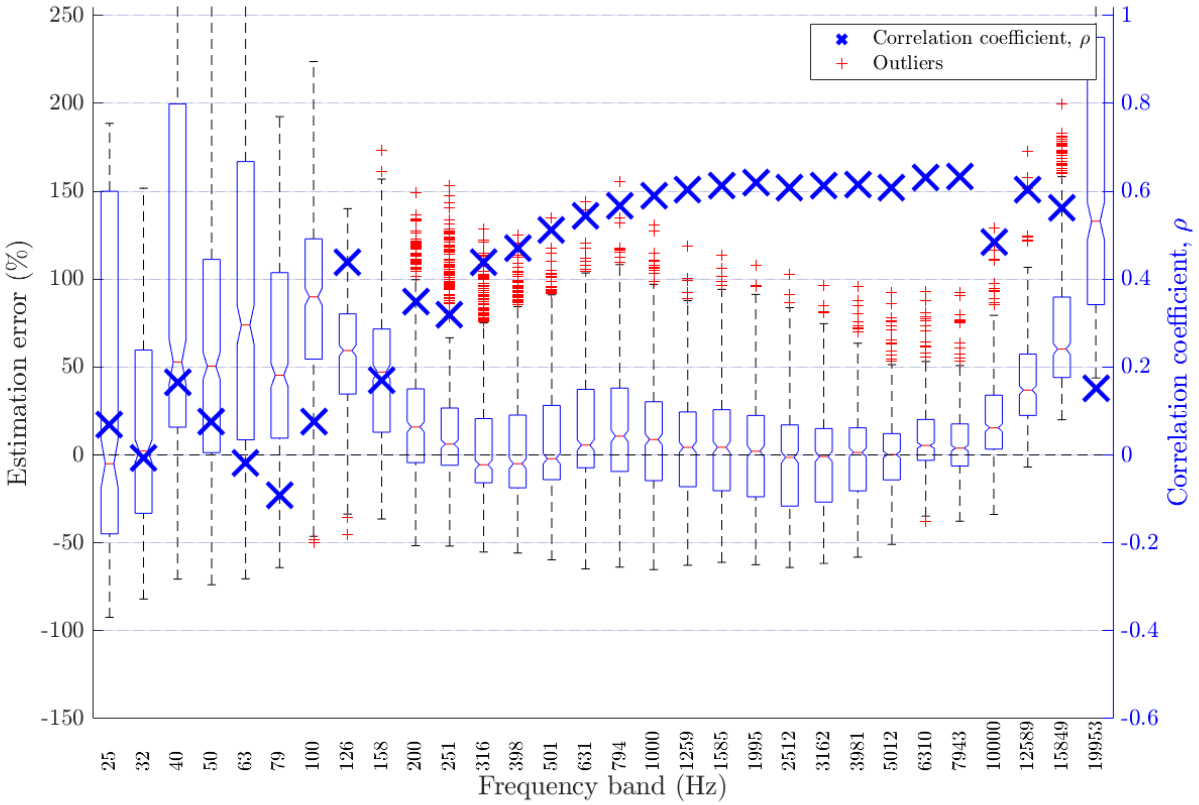

Figure 28: Frequency-dependent T_{60} estimation error in fan noise for all SNRs for algorithm Model-based SB RTE [9]

Table 24: Frequency-dependent T_{60} estimation error in fan noise for all SNRs for algorithm Model-based SB RTE [9]

Freq. band	Centre Freq. (Hz)	Bias	MSE	ρ
1	25.12	-0.5453	2.973	0.06903
2	31.62	-0.08427	0.5741	-0.006387
3	39.81	0.3657	0.5685	0.1654
4	50.12	0.3503	0.4786	0.07602
5	63.10	0.4203	0.5074	-0.01927
6	79.43	0.3445	0.3058	-0.0928
7	100.00	0.4956	0.332	0.07602
8	125.89	0.3763	0.1928	0.4387
9	158.49	0.3124	0.1692	0.17
10	199.53	0.1865	0.1155	0.3485
11	251.19	0.1267	0.1149	0.3184
12	316.23	0.08556	0.09114	0.4388
13	398.11	0.06364	0.09533	0.4702
14	501.19	0.04794	0.1091	0.5121
15	630.96	0.03658	0.1335	0.5428
16	794.33	0.01523	0.1391	0.5671
17	1000.00	-0.01617	0.1454	0.589
18	1258.93	-0.02493	0.1198	0.6031
19	1584.89	-0.02688	0.1085	0.6124
20	1995.26	-0.04114	0.1042	0.6203
21	2511.89	-0.07453	0.106	0.6074
22	3162.28	-0.05326	0.07968	0.6119
23	3981.07	-0.02097	0.05682	0.6155
24	5011.87	0.01065	0.03318	0.6086
25	6309.57	0.07309	0.0232	0.6303
26	7943.28	0.06342	0.02147	0.6341
27	10000.00	0.1142	0.03443	0.4842
28	12589.25	0.1941	0.05513	0.6027
29	15848.93	0.2602	0.08826	0.563
30	19952.62	0.3547	0.1522	0.1521

3.5 Frequency-dependent T_{60} estimation results by noise type and SNR

3.5.1 Ambient noise at 18 dB

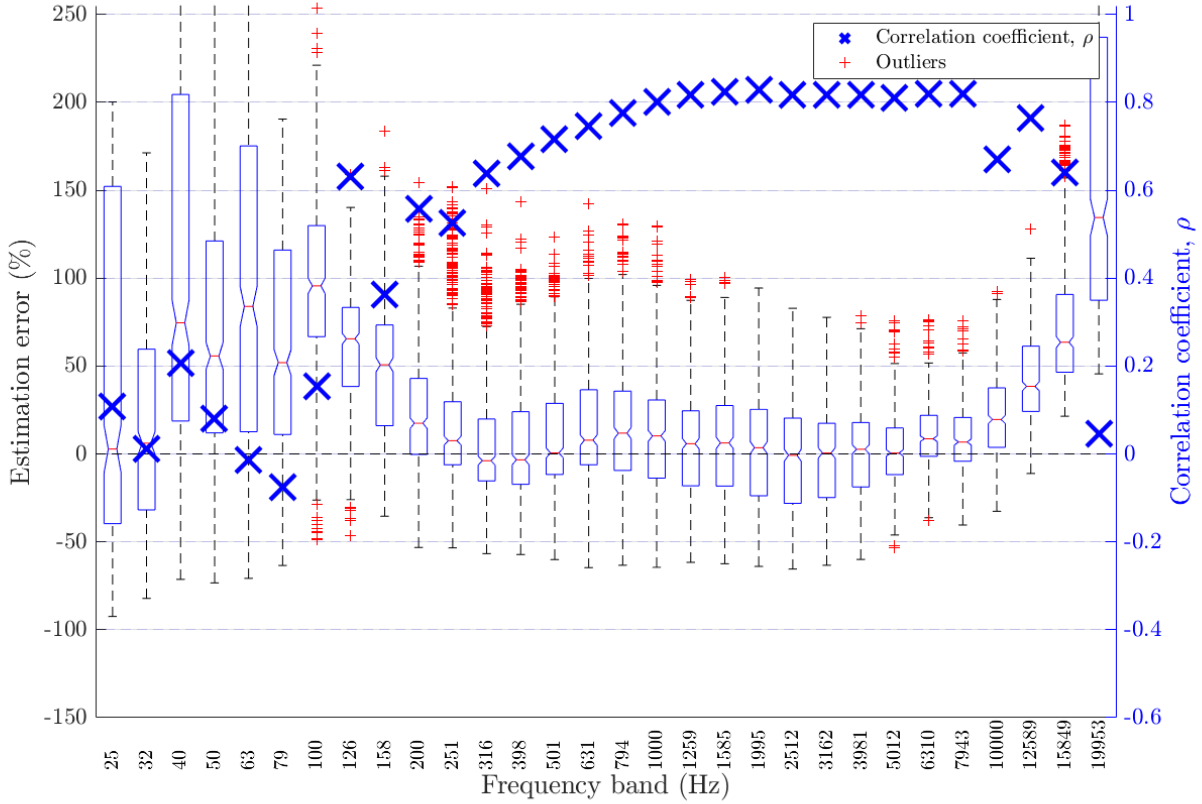

Figure 29: Frequency-dependent T_{60} estimation error in ambient noise at 18 dB SNR for algorithm Model-based SB RTE [9]

Table 25: Frequency-dependent T_{60} estimation error in ambient noise at $18\,\mathrm{dB}$ SNR for algorithm Model-based SB RTE [9]

Freq. band	Centre Freq. (Hz)	Bias	MSE	ρ
1	25.12	-0.492	2.884	0.109
2	31.62	0.0215	0.54	0.01075
3	39.81	0.498	0.6376	0.2061
4	50.12	0.481	0.5514	0.08078
5	63.10	0.5267	0.5733	-0.01295
6	79.43	0.4138	0.3301	-0.07604
7	100.00	0.5253	0.3417	0.1527
8	125.89	0.3714	0.1678	0.6304
9	158.49	0.2818	0.1326	0.3616
10	199.53	0.1397	0.07238	0.5571
11	251.19	0.07161	0.07183	0.5249
12	316.23	0.02794	0.05357	0.6385
13	398.11	0.007045	0.05709	0.6765
14	501.19	-0.005716	0.07074	0.7149
15	630.96	-0.0133	0.09399	0.7461
16	794.33	-0.03069	0.1015	0.7762
17	1000.00	-0.0583	0.1106	0.8008
18	1258.93	-0.06361	0.08942	0.8165
19	1584.89	-0.06253	0.08054	0.8231
20	1995.26	-0.07417	0.07826	0.8294
21	2511.89	-0.1054	0.08277	0.8158
22	3162.28	-0.08224	0.05875	0.8173
23	3981.07	-0.04842	0.03784	0.8173
24	5011.87	-0.01555	0.01819	0.8093
25	6309.57	0.04791	0.01181	0.8193
26	7943.28	0.03906	0.01096	0.8198
27	10000.00	0.09053	0.02404	0.6691
28	12589.25	0.171	0.04441	0.7651
29	15848.93	0.2375	0.07786	0.6411
30	19952.62	0.3324	0.1408	0.04633

3.5.2 Ambient noise at 12 dB

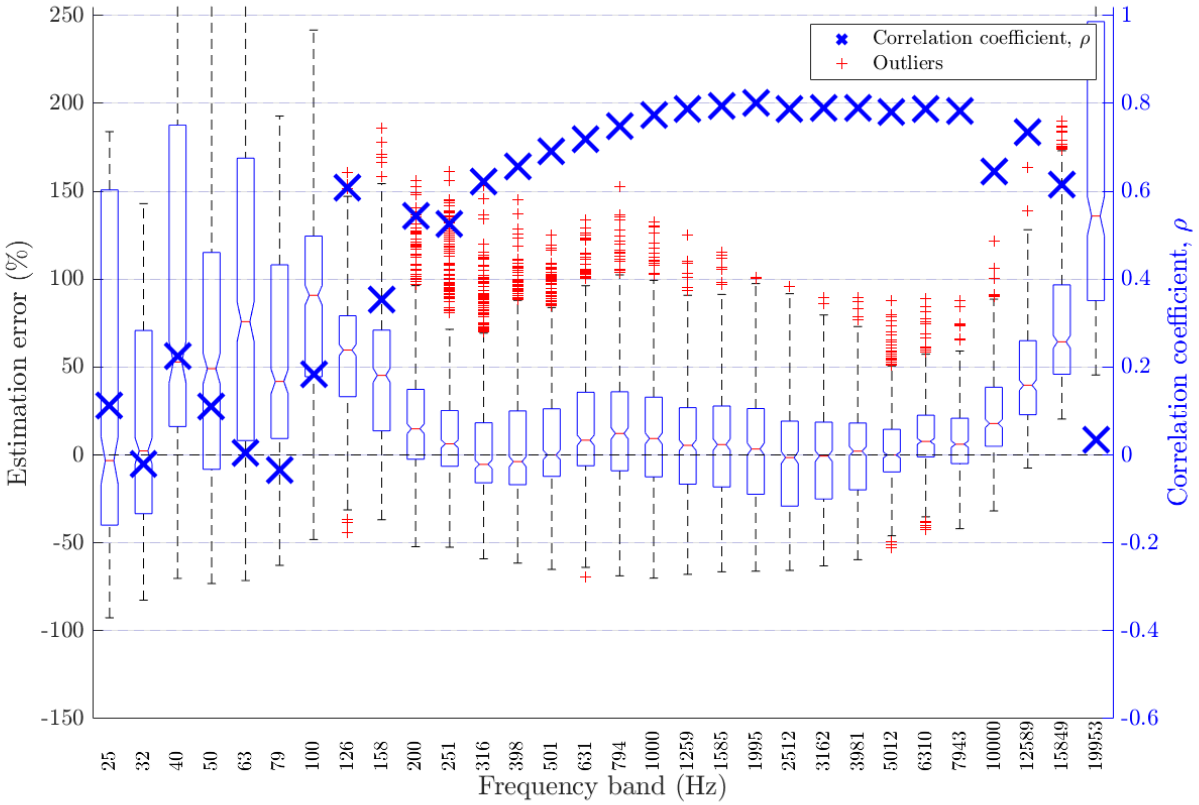

Figure 30: Frequency-dependent T_{60} estimation error in ambient noise at 12 dB SNR for algorithm Model-based SB RTE [9]

Table 26: Frequency-dependent T_{60} estimation error in ambient noise at $12\,\mathrm{dB}$ SNR for algorithm Model-based SB RTE [9]

Freq. band	Centre Freq. (Hz)	Bias	MSE	ρ
1	25.12	-0.5143	2.904	0.1135
2	31.62	-0.01651	0.5708	-0.01967
3	39.81	0.4505	0.6029	0.2257
4	50.12	0.4308	0.5244	0.1093
5	63.10	0.4796	0.5502	0.004409
6	79.43	0.3734	0.315	-0.03412
7	100.00	0.4931	0.3183	0.1834
8	125.89	0.3471	0.1556	0.6079
9	158.49	0.2642	0.1249	0.3536
10	199.53	0.1272	0.06996	0.5449
11	251.19	0.06291	0.06977	0.5247
12	316.23	0.02203	0.05508	0.6214
13	398.11	0.003237	0.06022	0.6552
14	501.19	-0.007883	0.07524	0.6904
15	630.96	-0.01415	0.09982	0.7174
16	794.33	-0.03047	0.1069	0.7491
17	1000.00	-0.05721	0.1159	0.7725
18	1258.93	-0.06186	0.09411	0.7872
19	1584.89	-0.06028	0.08475	0.7943
20	1995.26	-0.07157	0.08228	0.8002
21	2511.89	-0.1025	0.08625	0.7882
22	3162.28	-0.0793	0.06193	0.7889
23	3981.07	-0.04544	0.04072	0.7884
24	5011.87	-0.01257	0.02039	0.78
25	6309.57	0.05084	0.01353	0.7865
26	7943.28	0.04192	0.01275	0.7837
27	10000.00	0.09331	0.0251	0.6454
28	12589.25	0.1737	0.04568	0.7334
29	15848.93	0.2401	0.07893	0.6148
30	19952.62	0.335	0.1421	0.03508

3.5.3 Ambient noise at -1 dB

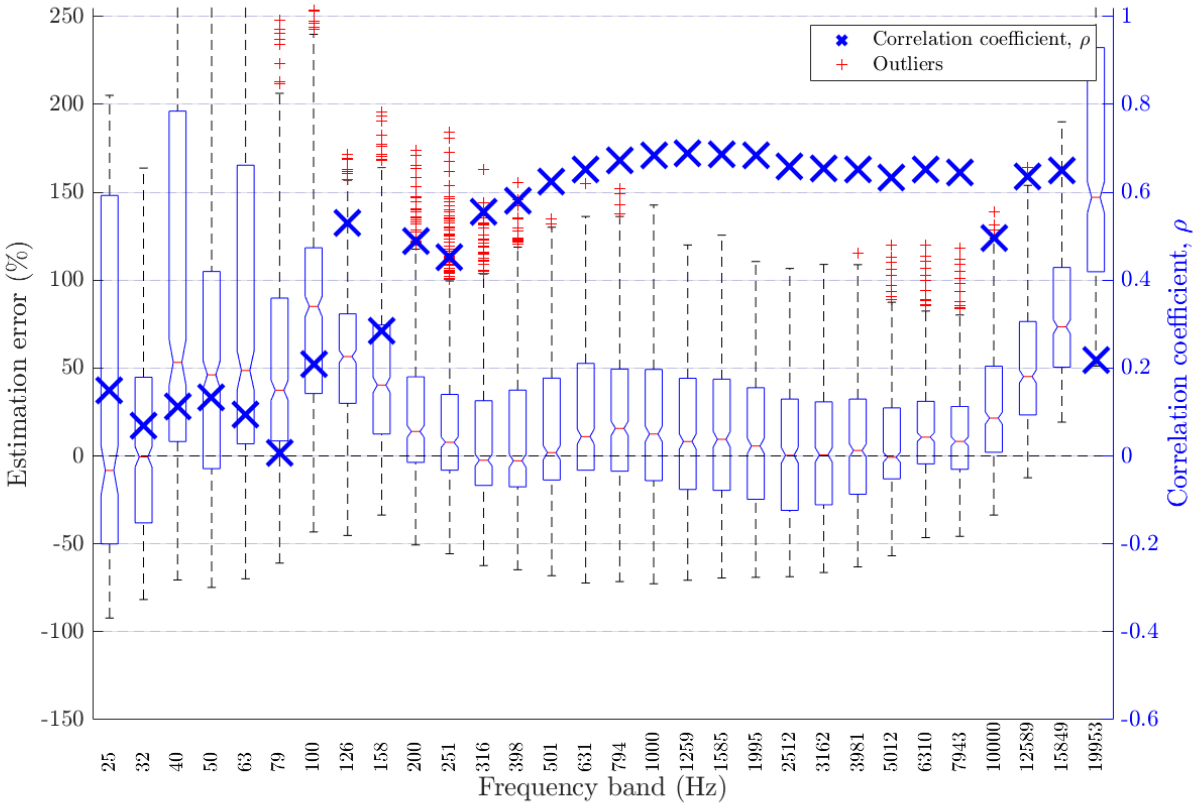

Figure 31: Frequency-dependent T_{60} estimation error in ambient noise at -1 dB SNR for algorithm Model-based SB RTE [9]

Table 27: Frequency-dependent T_{60} estimation error in ambient noise at $-1\,\mathrm{dB}$ SNR for algorithm Model-based SB RTE [9]

Freq. band	Centre Freq. (Hz)	Bias	MSE	ρ
1	25.12	-0.529	2.889	0.1493
2	31.62	-0.05149	0.5329	0.06865
3	39.81	0.4044	0.6307	0.1121
4	50.12	0.3837	0.4894	0.134
5	63.10	0.4396	0.4971	0.094
6	79.43	0.3455	0.2986	0.006754
7	100.00	0.4785	0.3081	0.2094
8	125.89	0.3444	0.1628	0.5294
9	158.49	0.2706	0.1351	0.2846
10	199.53	0.1397	0.08085	0.4884
11	251.19	0.079	0.08276	0.4521
12	316.23	0.03987	0.06589	0.5556
13	398.11	0.02168	0.07236	0.5817
14	501.19	0.01055	0.087	0.6233
15	630.96	0.003987	0.112	0.6525
16	794.33	-0.01273	0.1209	0.6713
17	1000.00	-0.03988	0.131	0.6837
18	1258.93	-0.04487	0.1089	0.6873
19	1584.89	-0.04358	0.09981	0.6859
20	1995.26	-0.0551	0.09755	0.6836
21	2511.89	-0.08624	0.1018	0.6576
22	3162.28	-0.06312	0.07626	0.6543
23	3981.07	-0.02934	0.0538	0.6517
24	5011.87	0.003485	0.03111	0.634
25	6309.57	0.06688	0.02107	0.6511
26	7943.28	0.05796	0.02	0.6456
27	10000.00	0.1094	0.03256	0.4948
28	12589.25	0.1897	0.05224	0.6363
29	15848.93	0.2562	0.08457	0.6484
30	19952.62	0.3511	0.148	0.2188

3.5.4 Babble noise at 18 dB

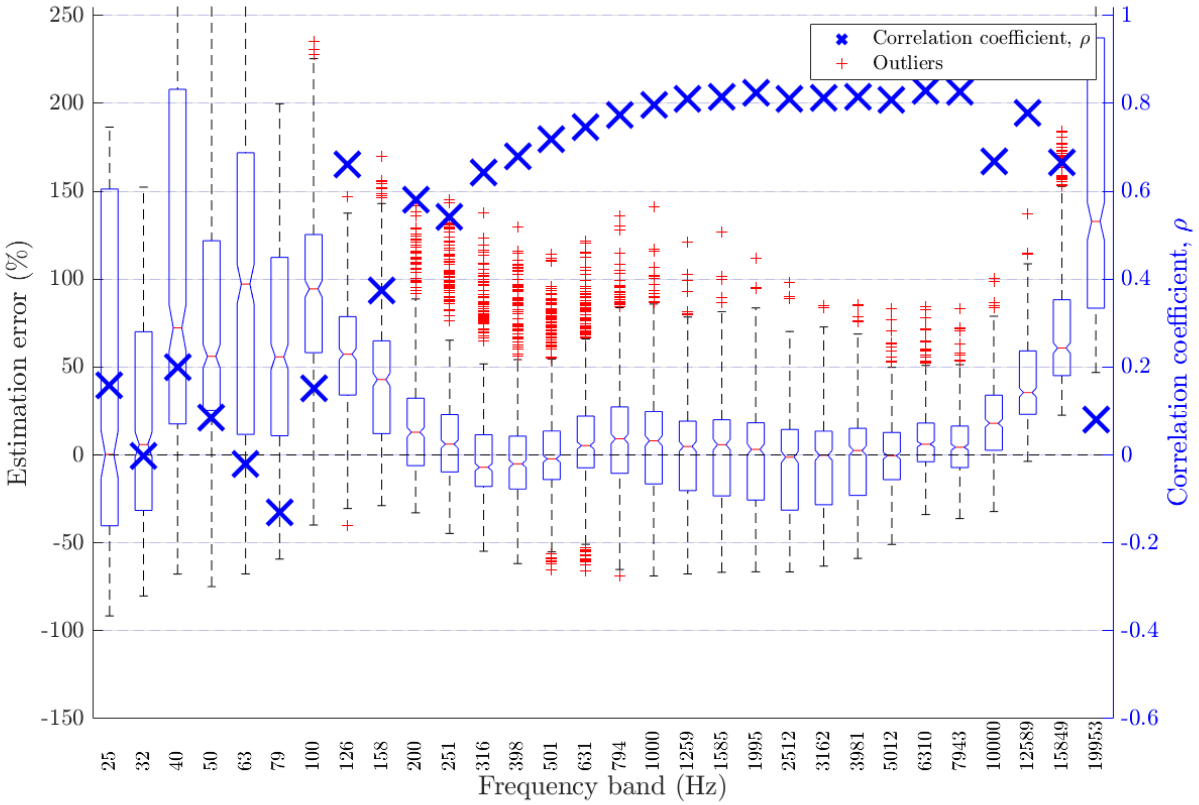

Figure 32: Frequency-dependent T_{60} estimation error in babble noise at 18 dB SNR for algorithm Model-based SB RTE [9]

Table 28: Frequency-dependent T_{60} estimation error in babble noise at $18\,\mathrm{dB}$ SNR for algorithm Model-based SB RTE [9]

Freq. band	Centre Freq. (Hz)	Bias	MSE	ρ
1	25.12	-0.4858	2.839	0.1578
2	31.62	0.0403	0.5332	-0.003286
3	39.81	0.5213	0.6535	0.1986
4	50.12	0.5001	0.5587	0.0844
5	63.10	0.5351	0.579	-0.02045
6	79.43	0.4082	0.332	-0.1301
7	100.00	0.5059	0.321	0.1525
8	125.89	0.341	0.1427	0.6613
9	158.49	0.2442	0.1083	0.3732
10	199.53	0.09864	0.05667	0.5816
11	251.19	0.03031	0.0623	0.5417
12	316.23	-0.01143	0.05043	0.6434
13	398.11	-0.02912	0.05685	0.6797
14	501.19	-0.0381	0.07234	0.7176
15	630.96	-0.04182	0.09694	0.7467
16	794.33	-0.05557	0.1059	0.7736
17	1000.00	-0.07991	0.1163	0.7966
18	1258.93	-0.08241	0.09489	0.8098
19	1584.89	-0.07899	0.08569	0.8149
20	1995.26	-0.08874	0.08324	0.8227
21	2511.89	-0.1184	0.08826	0.809
22	3162.28	-0.09418	0.06279	0.8121
23	3981.07	-0.0595	0.04034	0.8135
24	5011.87	-0.026	0.01891	0.8081
25	6309.57	0.03792	0.009949	0.8278
26	7943.28	0.02939	0.009371	0.8265
27	10000.00	0.08108	0.02127	0.6687
28	12589.25	0.1617	0.0396	0.7775
29	15848.93	0.2283	0.07146	0.6648
30	19952.62	0.3233	0.1322	0.08033

3.5.5 Babble noise at 12 dB

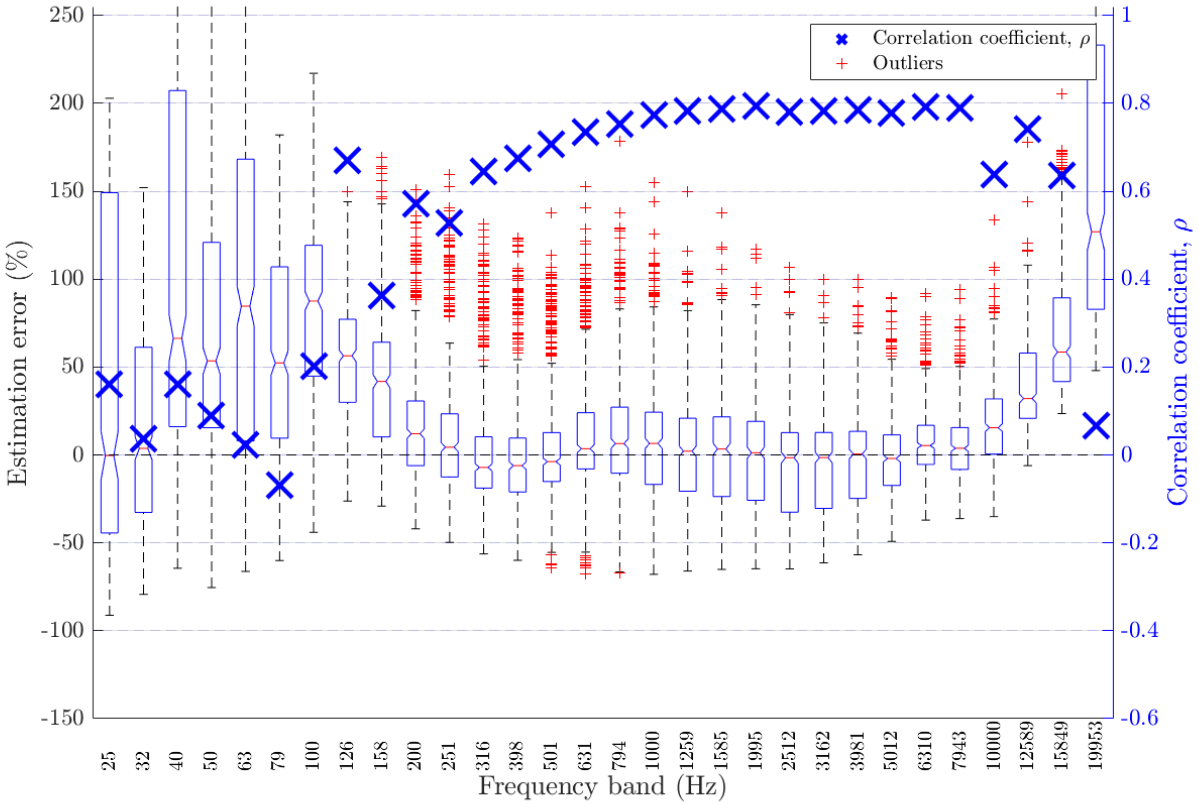

Figure 33: Frequency-dependent T_{60} estimation error in babble noise at 12 dB SNR for algorithm Model-based SB RTE [9]

Table 29: Frequency-dependent T_{60} estimation error in babble noise at $12\,\mathrm{dB}$ SNR for algorithm Model-based SB RTE [9]

Freq. band	Centre Freq. (Hz)	Bias	MSE	ρ
1	25.12	-0.5075	2.858	0.1617
2	31.62	0.008911	0.5158	0.03594
3	39.81	0.485	0.638	0.1617
4	50.12	0.464	0.5279	0.08925
5	63.10	0.5033	0.5386	0.02186
6	79.43	0.3832	0.3057	-0.0682
7	100.00	0.4881	0.3005	0.2029
8	125.89	0.3295	0.1347	0.6701
9	158.49	0.2374	0.1067	0.3634
10	199.53	0.09501	0.05799	0.571
11	251.19	0.02834	0.06502	0.5271
12	316.23	-0.01278	0.05061	0.6459
13	398.11	-0.0305	0.05799	0.6737
14	501.19	-0.03988	0.07403	0.7077
15	630.96	-0.04417	0.0994	0.7336
16	794.33	-0.05855	0.1101	0.7527
17	1000.00	-0.08353	0.1217	0.7726
18	1258.93	-0.08663	0.1008	0.7823
19	1584.89	-0.08376	0.09157	0.7878
20	1995.26	-0.09401	0.08975	0.7933
21	2511.89	-0.1241	0.09515	0.78
22	3162.28	-0.1003	0.06887	0.7823
23	3981.07	-0.06593	0.04512	0.7845
24	5011.87	-0.03272	0.02183	0.7776
25	6309.57	0.03094	0.01047	0.7916
26	7943.28	0.0222	0.009941	0.79
27	10000.00	0.07371	0.01981	0.6373
28	12589.25	0.1542	0.03626	0.7413
29	15848.93	0.2206	0.06609	0.6362
30	19952.62	0.3155	0.1247	0.06677

3.5.6 Babble noise at $-1\,\mathrm{dB}$

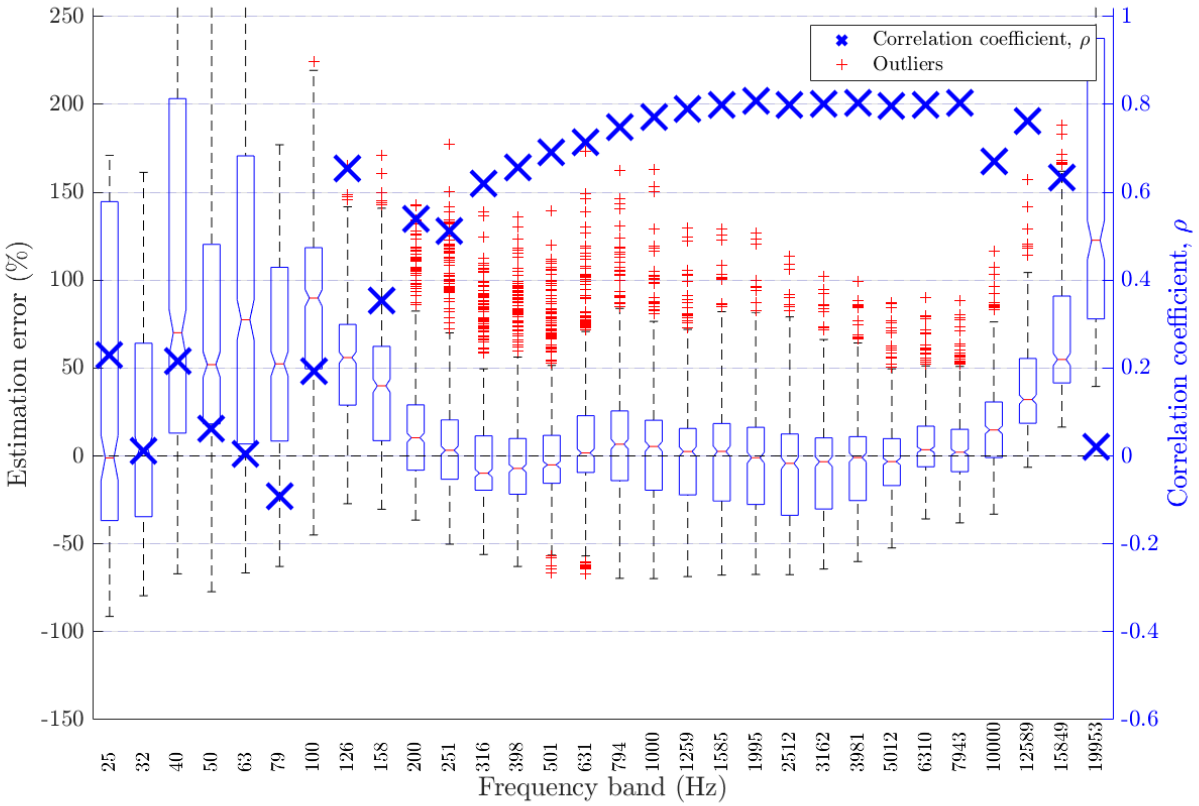

Figure 34: Frequency-dependent T_{60} estimation error in babble noise at $-1\,\mathrm{dB}$ SNR for algorithm Model-based SB RTE [9]

Table 30: Frequency-dependent T_{60} estimation error in babble noise at $-1\,\mathrm{dB}$ SNR for algorithm Model-based SB RTE [9]

Freq. band	Centre Freq. (Hz)	Bias	MSE	ρ
1	25.12	-0.5131	2.813	0.2285
2	31.62	0.0009175	0.5312	0.01062
3	39.81	0.4756	0.6085	0.2152
4	50.12	0.4544	0.5349	0.0614
5	63.10	0.4943	0.5416	0.003491
6	79.43	0.3754	0.31	-0.09157
7	100.00	0.4817	0.2997	0.1922
8	125.89	0.3243	0.1349	0.6534
9	158.49	0.2332	0.1087	0.3537
10	199.53	0.09138	0.0629	0.5397
11	251.19	0.02506	0.0688	0.511
12	316.23	-0.01588	0.05542	0.6203
13	398.11	-0.03353	0.06141	0.6558
14	501.19	-0.04289	0.07666	0.6918
15	630.96	-0.04717	0.1023	0.7134
16	794.33	-0.06153	0.1098	0.7479
17	1000.00	-0.08647	0.1207	0.77
18	1258.93	-0.08953	0.09858	0.7887
19	1584.89	-0.08659	0.08876	0.7991
20	1995.26	-0.09676	0.08667	0.8074
21	2511.89	-0.1268	0.0918	0.7984
22	3162.28	-0.1028	0.06595	0.8014
23	3981.07	-0.06841	0.04263	0.8042
24	5011.87	-0.0351	0.02041	0.7964
25	6309.57	0.02865	0.01057	0.7977
26	7943.28	0.01999	0.009809	0.8025
27	10000.00	0.07158	0.01931	0.6711
28	12589.25	0.1521	0.03644	0.7608
29	15848.93	0.2186	0.06684	0.6344
30	19952.62	0.3136	0.1261	0.02066

3.5.7 **Fan noise at** 18 dB

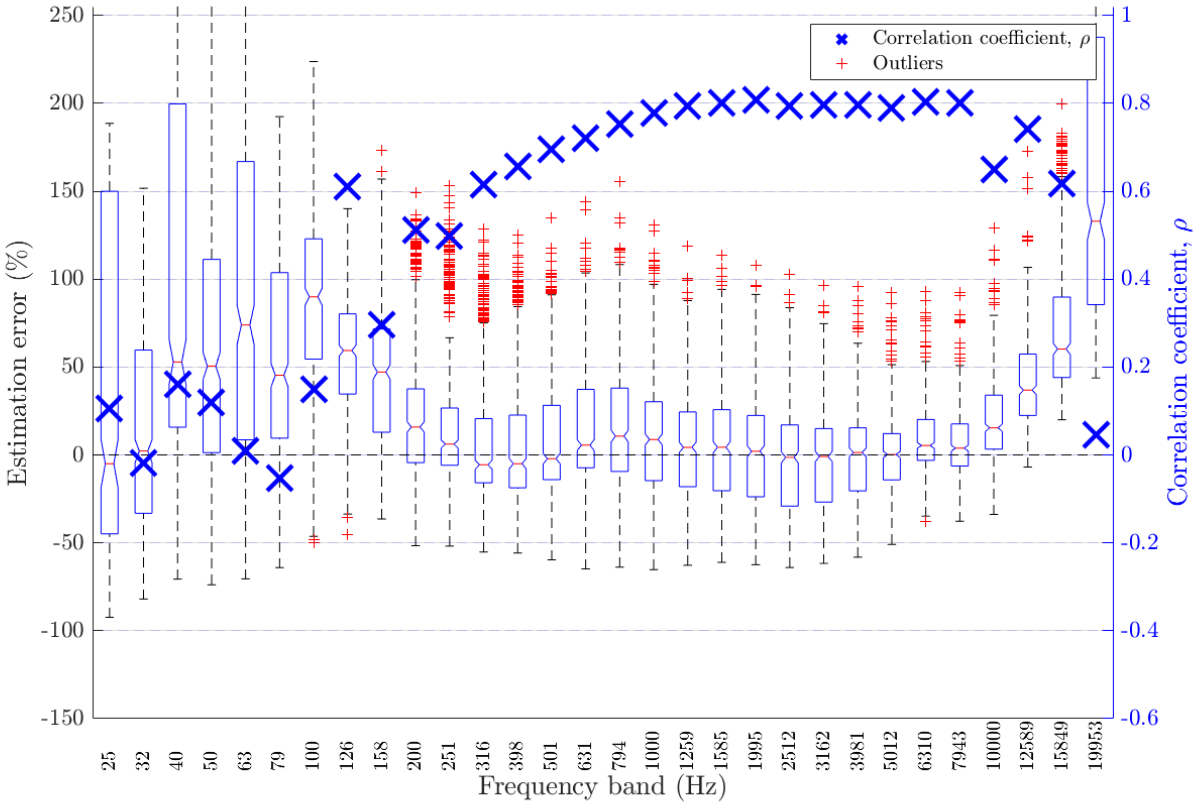

Figure 35: Frequency-dependent T_{60} estimation error in fan noise at 18 dB SNR for algorithm Model-based SB RTE [9]

Table 31: Frequency-dependent T_{60} estimation error in fan noise at $18\,\mathrm{dB}$ SNR for algorithm Model-based SB RTE [9]

Freq. band	Centre Freq. (Hz)	Bias	MSE	ρ
1	25.12	-0.5218	2.916	0.106
2	31.62	-0.02202	0.5605	-0.01754
3	39.81	0.4467	0.6222	0.16
4	50.12	0.4284	0.5049	0.1203
5	63.10	0.4782	0.5333	0.00933
6	79.43	0.3726	0.3054	-0.05196
7	100.00	0.4924	0.3136	0.1494
8	125.89	0.3462	0.1522	0.6111
9	158.49	0.2626	0.1258	0.2967
10	199.53	0.1248	0.07269	0.5116
11	251.19	0.05942	0.07299	0.4974
12	316.23	0.01739	0.05579	0.6146
13	398.11	-0.002582	0.05993	0.6565
14	501.19	-0.01483	0.07473	0.695
15	630.96	-0.02213	0.1003	0.7195
16	794.33	-0.03937	0.1077	0.7533
17	1000.00	-0.06689	0.1177	0.7774
18	1258.93	-0.07216	0.09601	0.7929
19	1584.89	-0.07106	0.08678	0.7998
20	1995.26	-0.0827	0.08452	0.8068
21	2511.89	-0.1139	0.08919	0.7947
22	3162.28	-0.09082	0.06407	0.796
23	3981.07	-0.05704	0.04181	0.796
24	5011.87	-0.0242	0.02017	0.79
25	6309.57	0.03922	0.01118	0.8042
26	7943.28	0.03034	0.01064	0.801
27	10000.00	0.08177	0.02217	0.6486
28	12589.25	0.1622	0.04067	0.7418
29	15848.93	0.2287	0.07238	0.6166
30	19952.62	0.3236	0.133	0.04615

3.5.8 **Fan noise at** 12 dB

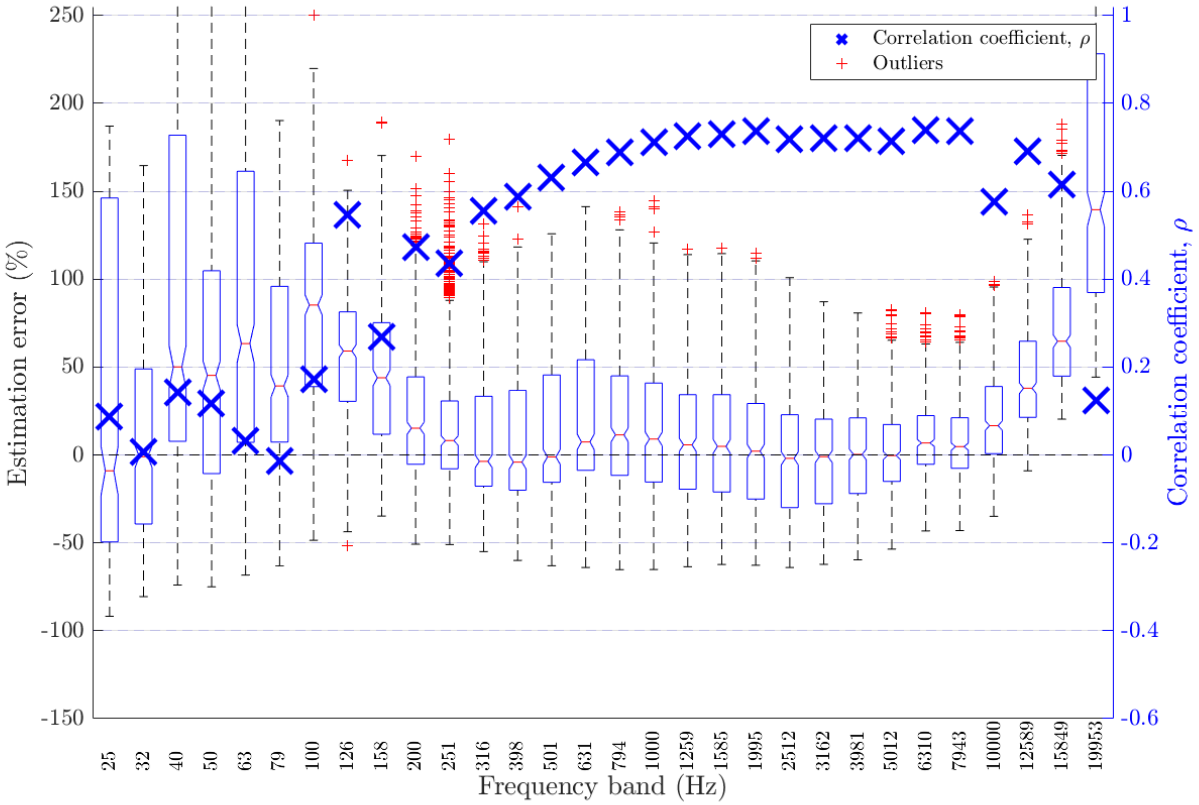

Figure 36: Frequency-dependent T_{60} estimation error in fan noise at 12 dB SNR for algorithm Model-based SB RTE [9]

Table 32: Frequency-dependent T_{60} estimation error in fan noise at $12\,\mathrm{dB}$ SNR for algorithm Model-based SB RTE [9]

Freq. band	Centre Freq. (Hz)	Bias	MSE	ρ
1	25.12	-0.5521	2.964	0.0869
2	31.62	-0.07531	0.5598	0.006393
3	39.81	0.3818	0.5859	0.143
4	50.12	0.3642	0.4662	0.1176
5	63.10	0.4246	0.4877	0.03276
6	79.43	0.3351	0.2795	-0.0127
7	100.00	0.4722	0.2956	0.1716
8	125.89	0.341	0.1547	0.5455
9	158.49	0.2686	0.1315	0.2693
10	199.53	0.1377	0.08082	0.4728
11	251.19	0.07589	0.08383	0.4362
12	316.23	0.03487	0.06505	0.5561
13	398.11	0.01437	0.07111	0.5864
14	501.19	0.0007776	0.08572	0.6304
15	630.96	-0.008209	0.1101	0.666
16	794.33	-0.02718	0.1191	0.6892
17	1000.00	-0.05634	0.1287	0.7125
18	1258.93	-0.06308	0.1062	0.7247
19	1584.89	-0.06325	0.09676	0.7294
20	1995.26	-0.07597	0.09419	0.7359
21	2511.89	-0.1081	0.09894	0.7186
22	3162.28	-0.08569	0.07265	0.7208
23	3981.07	-0.05249	0.04929	0.7209
24	5011.87	-0.02011	0.02566	0.7138
25	6309.57	0.04296	0.01406	0.7384
26	7943.28	0.03379	0.01331	0.7363
27	10000.00	0.08501	0.02439	0.5759
28	12589.25	0.1653	0.04171	0.6908
29	15848.93	0.2316	0.07233	0.6144
30	19952.62	0.3264	0.132	0.124

3.5.9 Fan noise at -1 dB

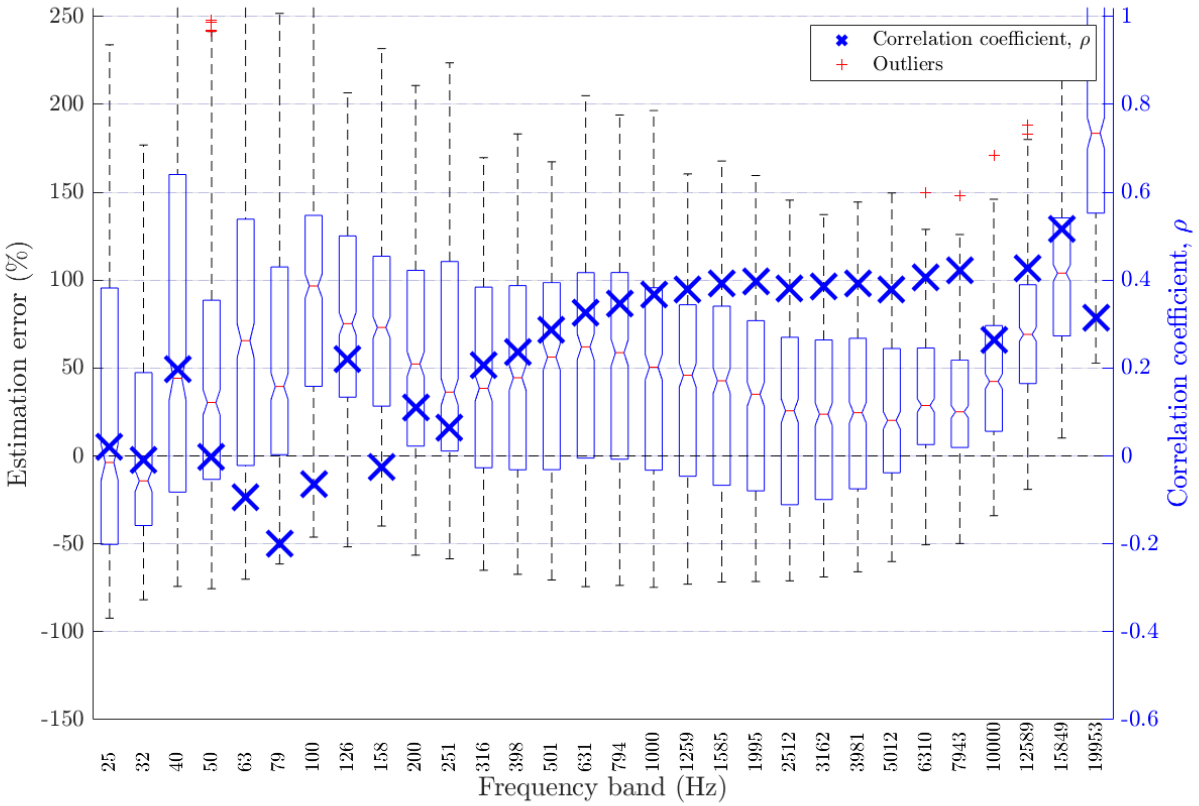

Figure 37: Frequency-dependent T_{60} estimation error in fan noise at -1 dB SNR for algorithm Model-based SB RTE [9]

Table 33: Frequency-dependent T_{60} estimation error in fan noise at $-1\,\mathrm{dB}$ SNR for algorithm Model-based SB RTE [9]

Freq. band	Centre Freq. (Hz)	Bias	MSE	ρ
1	25.12	-0.5619	3.04	0.01991
2	31.62	-0.1555	0.6021	-0.008327
3	39.81	0.2686	0.4974	0.1984
4	50.12	0.2583	0.4648	-0.002017
5	63.10	0.3581	0.5013	-0.09391
6	79.43	0.3256	0.3326	-0.2
7	100.00	0.5222	0.3869	-0.06485
8	125.89	0.4418	0.2714	0.221
9	158.49	0.4061	0.2503	-0.02438
10	199.53	0.2971	0.193	0.1108
11	251.19	0.2447	0.1878	0.06494
12	316.23	0.2044	0.1526	0.2076
13	398.11	0.1791	0.155	0.2356
14	501.19	0.1579	0.167	0.2878
15	630.96	0.1401	0.19	0.3268
16	794.33	0.1122	0.1905	0.3465
17	1000.00	0.07473	0.1897	0.3665
18	1258.93	0.06045	0.1571	0.3794
19	1584.89	0.05367	0.1418	0.3925
20	1995.26	0.03527	0.134	0.398
21	2511.89	-0.001626	0.1299	0.3801
22	3162.28	0.01673	0.1023	0.3858
23	3981.07	0.04662	0.07934	0.3927
24	5011.87	0.07628	0.05372	0.3796
25	6309.57	0.1371	0.04437	0.406
26	7943.28	0.1261	0.04046	0.4213
27	10000.00	0.1758	0.05674	0.265
28	12589.25	0.2549	0.08301	0.4278
29	15848.93	0.3202	0.1201	0.5153
30	19952.62	0.4142	0.1916	0.3153

4 DRR estimation results

4.1 Fullband DRR estimation results by noise type

4.1.1 Ambient noise

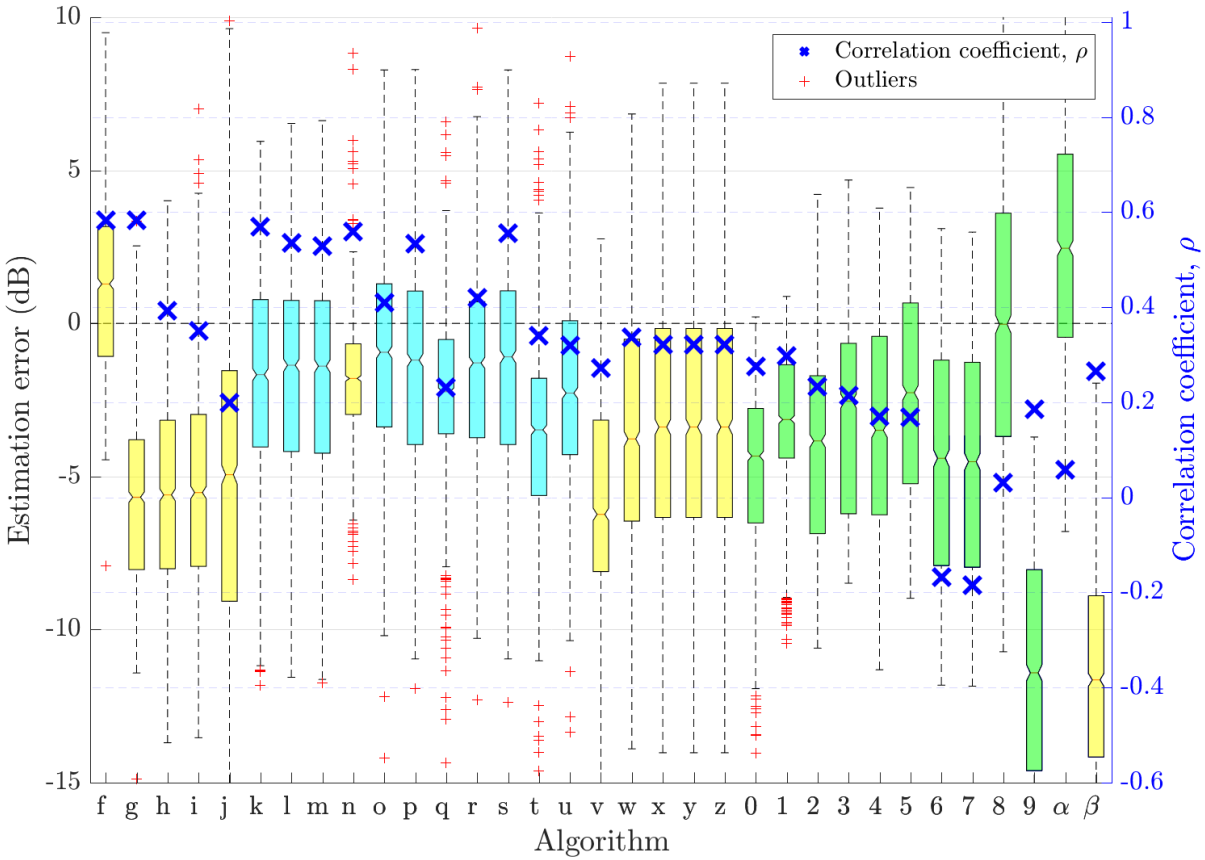

Figure 38: Fullband DRR estimation error in ambient noise for all SNRs

Table 34: DRR estimation algorithm performance in ambient noise for all SNRs

Ref.	Algorithm	Class	Mic. Config.	Bias	MSE	ρ	RTF
f	PSD est. in beamspace, bias comp. [21]	ABC	Mobile	1.21	8.32	0.583	0.757
g	PSD est. in beamspace (Raw) [21]	ABC	Mobile	-5.76	40	0.583	3.15
h	PSD est. in beamspace v2 [21]	ABC	Mobile	-5.46	40.1	0.393	0.844
i	PSD est. by twin BF [22]	ABC	Mobile	-5.34	39.9	0.351	0.614
j	Spatial Covariance in matrix mode [23]	ABC	Mobile	-5.17	65	0.2	0.627
k	NIRAv2 [4]	MLMF	Single	-1.68	14	0.568	$0.897^{\dagger}$
l	NIRAv3 [4]	MLMF	Single	-1.8	15	0.536	$0.897^{\dagger}$
m	NIRAv1 [4]	MLMF	Single	-1.84	15.3	0.528	$0.897^{\dagger}$
n	Particle velocity [8]	ABC	EM32	-1.85	6.62	0.559	0.134
o	Multi-layer perceptron [14]	MLMF	Single	-1.12	16.2	0.409	$0.0578^{\ddagger}$
p	Multi-layer perceptron P2 [14]	MLMF	Single	-1.42	15.4	0.533	$0.0578^{\ddagger}$
q	Multi-layer perceptron P2 [14]	MLMF	Chromebook	-2.58	14.6	0.231	$0.0589^{\ddagger}$
r	Multi-layer perceptron P2 [14]	MLMF	Mobile	-1.36	13.6	0.42	$0.0557^{\ddagger}$
s	Multi-layer perceptron P2 [14]	MLMF	Crucif	-1.33	14.6	0.555	$0.0569^{\ddagger}$
t	Multi-layer perceptron P2 [14]	MLMF	Lin8Ch	-3.57	24.7	0.34	$0.062^{\ddagger}$
u	Multi-layer perceptron P2 [14]	MLMF	EM32	-2.02	13.7	0.32	$0.0578^{\ddagger}$
v	DENBE no noise reduction [24]	ABC	Chromebook	-5.78	46.8	0.272	0.0323
w	DENBE spectral subtraction [7]	ABC	Chromebook	-3.53	25.5	0.337	0.0602
x	DENBE spec. sub. Gerkmann [24]	ABC	Chromebook	-3.24	24.5	0.321	0.0474
y	DENBE filtered subbands [7]	ABC	Chromebook	-3.24	24.5	0.321	0.775
z	DENBE FFT derived subbands [7]	ABC	Chromebook	-3.24	24.5	0.321	0.0449
0	NOSRMR Sec. 2.2. [15]	SFM	Chromebook	-4.75	29.5	0.276	1.04
1	OSRMR Sec. 2.2. [15]	SFM	Chromebook	-3.23	15.6	0.298	0.831
2	NOSRMR Sec. 2.2. [15]	SFM	Mobile	-3.96	25.9	0.233	1.59
3	OSRMR Sec. 2.2. [15]	SFM	Mobile	-2.78	17.7	0.215	1.26
4	NOSRMR Sec. 2.2. [15]	SFM	Crucif	-3.55	25.3	0.171	2.63
5	OSRMR Sec. 2.2. [15]	SFM	Crucif	-2.39	18	0.169	2.09
6	NOSRMR Sec. 2.2. [15]	SFM	Single	-4.19	34.2	-0.168	0.543
7	OSRMR Sec. 2.2. [15]	SFM	Single	-4.28	34.9	-0.185	0.446
8	Per acoust. band SRMR Sec. 2.5. [15]	SFM	Single	-0.0744	22.1	0.0317	0.58
9	Temporal dynamics [25]	SFM	Single	-11.2	142	0.185	0.0819
α	QA Reverb [11]	SFM	Single	2.41	23	0.0583	0.391
β	Blind est. of coherent-to-diffuse energy ratio [6]	ABC	Chromebook	-11.4	146	0.266	0.019

4.1.2 Babble noise

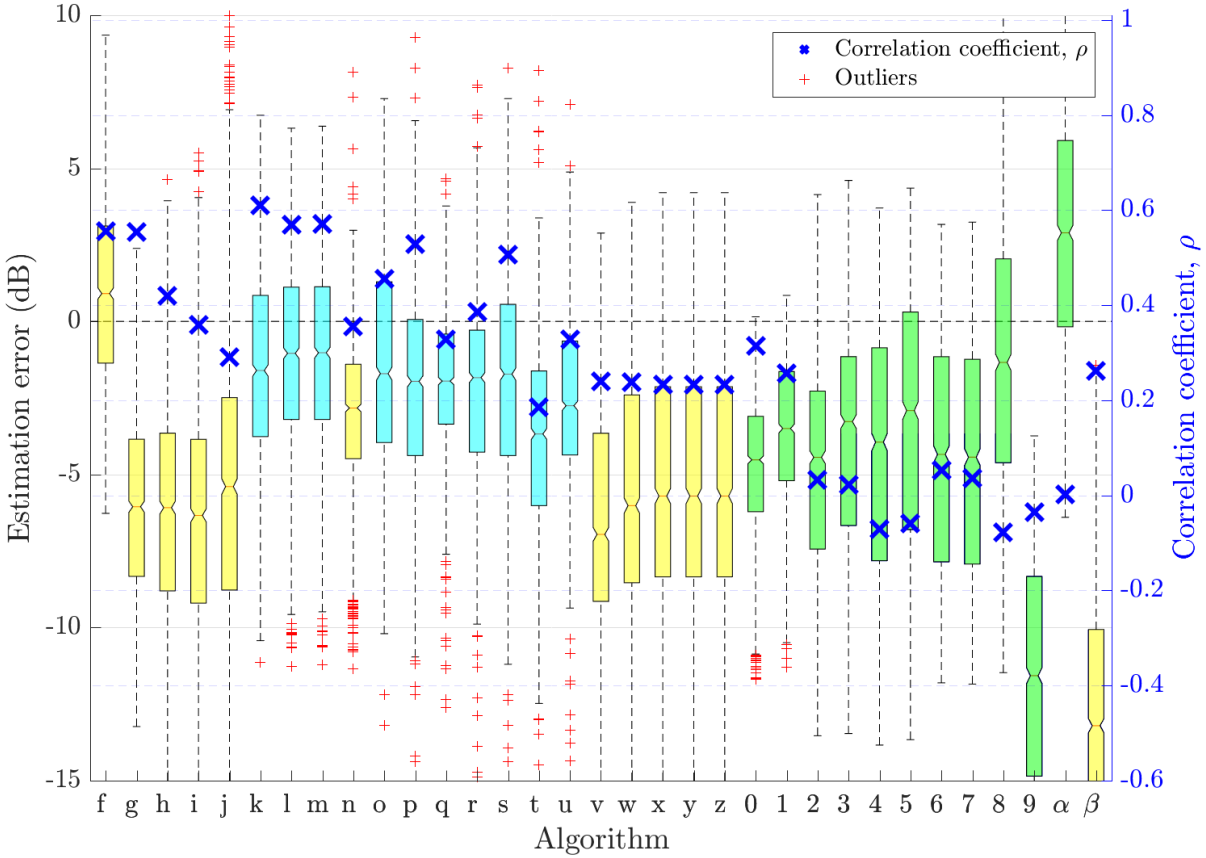

Figure 39: Fullband DRR estimation error in babble noise for all SNRs

Table 35: DRR estimation algorithm performance in babble noise for all SNRs

Ref.	Algorithm	Class	Mic. Config.	Bias	MSE	ρ	RTF
f	PSD est. in beamspace, bias comp. [21]	ABC	Mobile	0.839	8.2	0.555	0.757
g	PSD est. in beamspace (Raw) [21]	ABC	Mobile	-6.13	45	0.555	3.17
h	PSD est. in beamspace v2 [21]	ABC	Mobile	-6.1	48.4	0.42	0.843
i	PSD est. by twin BF [22]	ABC	Mobile	-6.38	54.6	0.358	0.615
j	Spatial Covariance in matrix mode [23]	ABC	Mobile	-5.6	57	0.29	0.627
k	NIRAv2 [4]	MLMF	Single	-1.66	13.2	0.61	$0.906^{\dagger}$
l	NIRAv3 [4]	MLMF	Single	-1.17	12.7	0.57	$0.906^{\dagger}$
m	NIRAv1 [4]	MLMF	Single	-1.14	12.6	0.571	$0.906^{\dagger}$
n	Particle velocity [8]	ABC	EM32	-3.13	16.2	0.356	0.134
o	Multi-layer perceptron [14]	MLMF	Single	-1.53	15.7	0.455	$0.0579^{\ddagger}$
p	Multi-layer perceptron P2 [14]	MLMF	Single	-1.95	17	0.528	$0.0579^{\ddagger}$
q	Multi-layer perceptron P2 [14]	MLMF	Chromebook	-2.31	13	0.328	$0.0588^{\ddagger}$
r	Multi-layer perceptron P2 [14]	MLMF	Mobile	-2.25	17.3	0.386	$0.0555^{\ddagger}$
s	Multi-layer perceptron P2 [14]	MLMF	Crucif	-1.93	17.2	0.506	$0.057^{\ddagger}$
t	Multi-layer perceptron P2 [14]	MLMF	Lin8Ch	-3.75	28.4	0.185	$0.0618^{\ddagger}$
u	Multi-layer perceptron P2 [14]	MLMF	EM32	-2.6	16.4	0.329	$0.0576^{\ddagger}$
v	DENBE no noise reduction [24]	ABC	Chromebook	-6.59	59.3	0.24	0.0323
w	DENBE spectral subtraction [7]	ABC	Chromebook	-5.74	50	0.237	0.0577
x	DENBE spec. sub. Gerkmann [24]	ABC	Chromebook	-5.5	47.6	0.232	0.0476
y	DENBE filtered subbands [7]	ABC	Chromebook	-5.5	47.6	0.232	0.778
z	DENBE FFT derived subbands [7]	ABC	Chromebook	-5.5	47.6	0.232	0.0448
0	NOSRMR Sec. 2.2. [15]	SFM	Chromebook	-4.72	27.7	0.315	1.04
1	OSRMR Sec. 2.2. [15]	SFM	Chromebook	-3.68	19.5	0.257	0.833
2	NOSRMR Sec. 2.2. [15]	SFM	Mobile	-4.71	35.3	0.0325	1.58
3	OSRMR Sec. 2.2. [15]	SFM	Mobile	-3.73	27.2	0.0231	1.26
4	NOSRMR Sec. 2.2. [15]	SFM	Crucif	-4.29	34.6	-0.0707	2.63
5	OSRMR Sec. 2.2. [15]	SFM	Crucif	-3.31	27.1	-0.0591	2.1
6	NOSRMR Sec. 2.2. [15]	SFM	Single	-4.14	33.6	0.0538	0.534
7	OSRMR Sec. 2.2. [15]	SFM	Single	-4.21	34.2	0.0352	0.444
8	Per acoust. band SRMR Sec. 2.5. [15]	SFM	Single	-1.3	22.5	-0.0786	0.579
9	Temporal dynamics [25]	SFM	Single	-11.6	152	-0.0352	0.0823
α	QA Reverb [11]	SFM	Single	2.79	25.5	0.00216	0.392
β	Blind est. of coherent-to-diffuse energy ratio [6]	ABC	Chromebook	-12.8	179	0.261	0.019

4.1.3 Fan noise

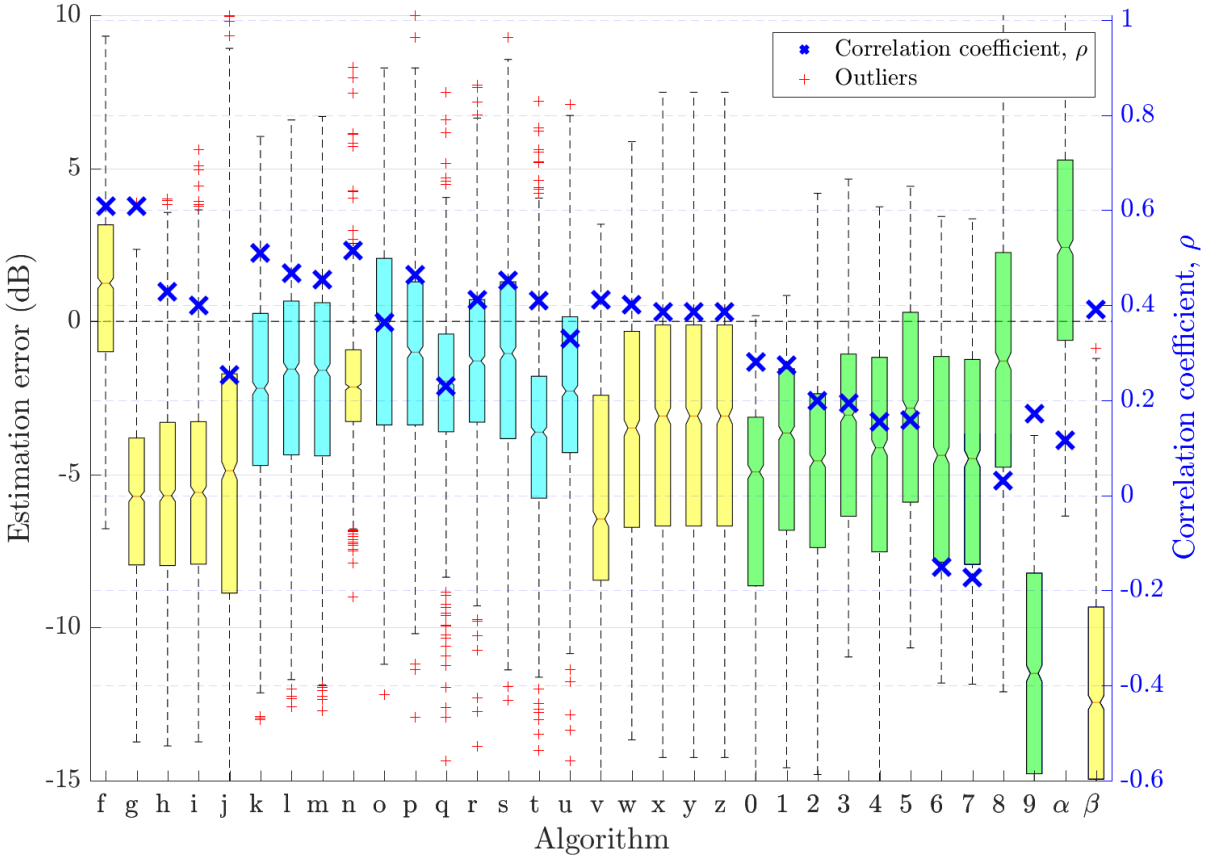

Figure 40: Fullband DRR estimation error in fan noise for all SNRs

Table 36: DRR estimation algorithm performance in fan noise for all SNRs

Ref.	Algorithm	Class	Mic. Config.	Bias	MSE	ρ	RTF
f	PSD est. in beamspace, bias comp. [21]	ABC	Mobile	1.16	7.89	0.608	0.757
g	PSD est. in beamspace (Raw) [21]	ABC	Mobile	-5.8	40.2	0.608	3.18
h	PSD est. in beamspace v2 [21]	ABC	Mobile	-5.54	40.4	0.428	0.844
i	PSD est. by twin BF [22]	ABC	Mobile	-5.42	40	0.4	0.613
j	Spatial Covariance in matrix mode [23]	ABC	Mobile	-5.33	61.4	0.254	0.627
k	NIRAv2 [4]	MLMF	Single	-2.23	17.2	0.511	$0.895^{\dagger}$
l	NIRAv3 [4]	MLMF	Single	-1.88	16.5	0.467	$0.895^{\dagger}$
m	NIRAv1 [4]	MLMF	Single	-1.93	16.9	0.455	$0.895^{\dagger}$
n	Particle velocity [8]	ABC	EM32	-2.15	8.28	0.515	0.134
o	Multi-layer perceptron [14]	MLMF	Single	-0.773	15.9	0.363	$0.0578^{\ddagger}$
p	Multi-layer perceptron P2 [14]	MLMF	Single	-1.2	15.9	0.465	$0.0578^{\ddagger}$
q	Multi-layer perceptron P2 [14]	MLMF	Chromebook	-2.41	13.4	0.23	$0.059^{\ddagger}$
r	Multi-layer perceptron P2 [14]	MLMF	Mobile	-1.39	13.9	0.412	$0.0555^{\ddagger}$
s	Multi-layer perceptron P2 [14]	MLMF	Crucif	-1.24	16.3	0.451	$0.0569^{\ddagger}$
t	Multi-layer perceptron P2 [14]	MLMF	Lin8Ch	-3.62	24.2	0.41	$0.0617^{\ddagger}$
u	Multi-layer perceptron P2 [14]	MLMF	EM32	-2.04	13.9	0.33	$0.0574^{\ddagger}$
v	DENBE no noise reduction [24]	ABC	Chromebook	-5.77	47.4	0.411	0.0322
w	DENBE spectral subtraction [7]	ABC	Chromebook	-3.48	26.9	0.401	0.0588
x	DENBE spec. sub. Gerkmann [24]	ABC	Chromebook	-3.27	26.4	0.386	0.048
y	DENBE filtered subbands [7]	ABC	Chromebook	-3.27	26.4	0.386	0.774
z	DENBE FFT derived subbands [7]	ABC	Chromebook	-3.27	26.4	0.386	0.0452
0	NOSRMR Sec. 2.2. [15]	SFM	Chromebook	-5.82	45.6	0.281	1.03
1	OSRMR Sec. 2.2. [15]	SFM	Chromebook	-4.21	26.8	0.275	0.824
2	NOSRMR Sec. 2.2. [15]	SFM	Mobile	-4.74	34.9	0.199	1.58
3	OSRMR Sec. 2.2. [15]	SFM	Mobile	-3.33	21.8	0.193	1.26
4	NOSRMR Sec. 2.2. [15]	SFM	Crucif	-4.3	33.2	0.155	2.61
5	OSRMR Sec. 2.2. [15]	SFM	Crucif	-2.93	21.6	0.158	2.08
6	NOSRMR Sec. 2.2. [15]	SFM	Single	-4.14	33.8	-0.151	0.543
7	OSRMR Sec. 2.2. [15]	SFM	Single	-4.24	34.6	-0.173	0.447
8	Per acoust. band SRMR Sec. 2.5. [15]	SFM	Single	-1.33	23.7	0.0307	0.576
9	Temporal dynamics [25]	SFM	Single	-11.4	147	0.173	0.0818
α	QA Reverb [11]	SFM	Single	2.34	22.1	0.116	0.391
β	Blind est. of coherent-to-diffuse energy ratio [6]	ABC	Chromebook	-12	160	0.391	0.019

4.2 Fullband DRR estimation results by noise type and SNR

4.2.1 Ambient noise at 18 dB SNR

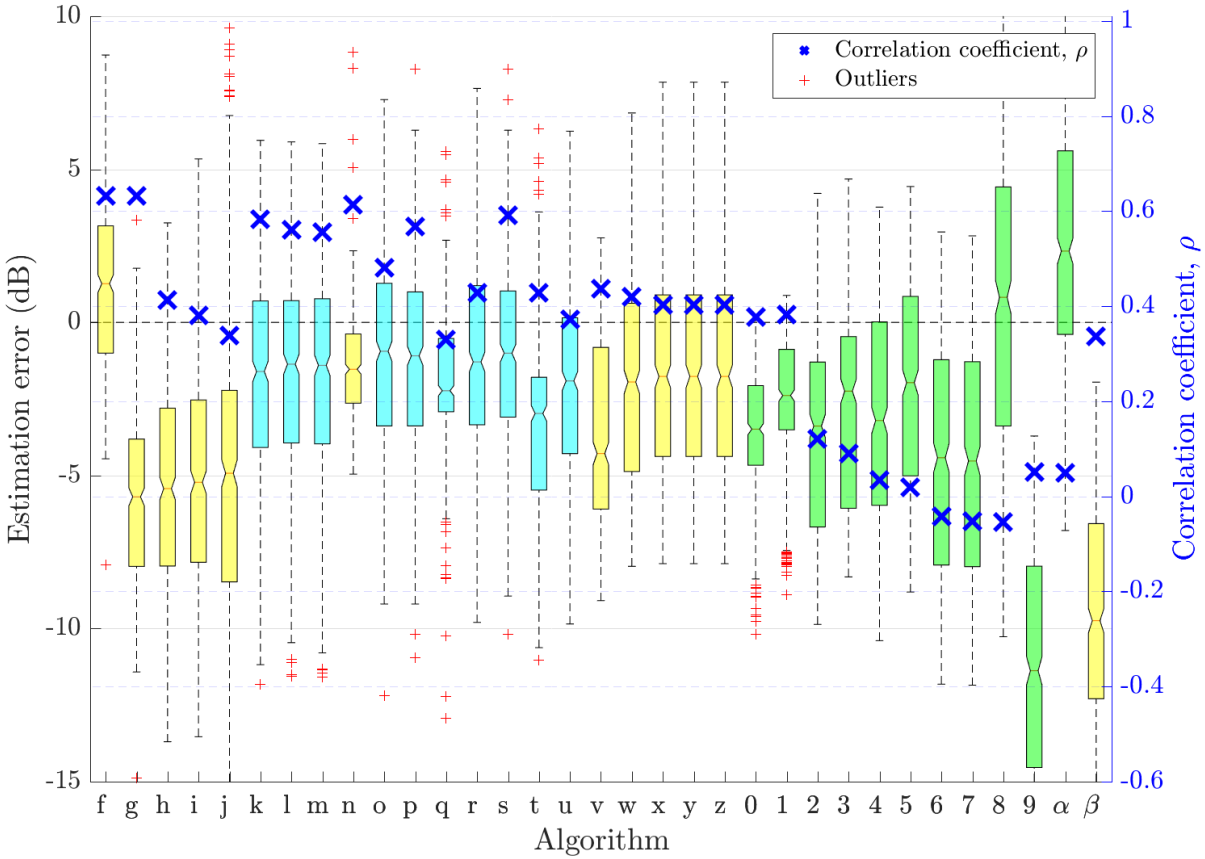

Figure 41: Fullband DRR estimation error in ambient noise at 18 dB SNR

Table 37: DRR estimation algorithm performance in ambient noise at $18\,\mathrm{dB}$ SNR

Ref.	Algorithm	Class	Mic. Config.	Bias	MSE	ρ	RTF
f	PSD est. in beamspace, bias comp. [21]	ABC	Mobile	1.14	7.81	0.632	0.757
g	PSD est. in beamspace (Raw) [21]	ABC	Mobile	-5.82	40.4	0.632	3.15
h	PSD est. in beamspace v2 [21]	ABC	Mobile	-5.37	40.7	0.413	0.844
i	PSD est. by twin BF [22]	ABC	Mobile	-5.11	39.2	0.381	0.614
j	Spatial Covariance in matrix mode [23]	ABC	Mobile	-5.22	53	0.339	0.627
k	NIRAv2 [4]	MLMF	Single	-1.73	13.9	0.582	$0.897^{\dagger}$
l	NIRAv3 [4]	MLMF	Single	-1.81	14.6	0.561	$0.897^{\dagger}$
m	NIRAv1 [4]	MLMF	Single	-1.84	14.8	0.557	$0.897^{\dagger}$
n	Particle velocity [8]	ABC	EM32	-1.44	4.89	0.613	0.134
o	Multi-layer perceptron [14]	MLMF	Single	-1.14	15.4	0.48	$0.0578^{\ddagger}$
p	Multi-layer perceptron P2 [14]	MLMF	Single	-1.29	14.3	0.567	$0.0578^{\ddagger}$
q	Multi-layer perceptron P2 [14]	MLMF	Chromebook	-2.28	11.6	0.331	$0.0589^{\ddagger}$
r	Multi-layer perceptron P2 [14]	MLMF	Mobile	-1.17	12.8	0.428	$0.0557^{\ddagger}$
s	Multi-layer perceptron P2 [14]	MLMF	Crucif	-1.16	13.5	0.592	$0.0569^{\ddagger}$
t	Multi-layer perceptron P2 [14]	MLMF	Lin8Ch	-3.37	21.1	0.428	$0.062^{\ddagger}$
u	Multi-layer perceptron P2 [14]	MLMF	EM32	-1.93	11.9	0.373	$0.0578^{\ddagger}$
v	DENBE no noise reduction [24]	ABC	Chromebook	-3.51	21.4	0.437	0.0323
w	DENBE spectral subtraction [7]	ABC	Chromebook	-1.91	14.2	0.42	0.0602
x	DENBE spec. sub. Gerkmann [24]	ABC	Chromebook	-1.58	13.8	0.403	0.0474
y	DENBE filtered subbands [7]	ABC	Chromebook	-1.58	13.8	0.403	0.775
z	DENBE FFT derived subbands [7]	ABC	Chromebook	-1.58	13.8	0.403	0.0449
0	NOSRMR Sec. 2.2. [15]	SFM	Chromebook	-3.66	17.8	0.377	1.04
1	OSRMR Sec. 2.2. [15]	SFM	Chromebook	-2.51	10.7	0.382	0.831
2	NOSRMR Sec. 2.2. [15]	SFM	Mobile	-3.53	23.2	0.121	1.59
3	OSRMR Sec. 2.2. [15]	SFM	Mobile	-2.53	16.8	0.0908	1.26
4	NOSRMR Sec. 2.2. [15]	SFM	Crucif	-3.16	23.3	0.0351	2.63
5	OSRMR Sec. 2.2. [15]	SFM	Crucif	-2.15	17.5	0.0185	2.09
6	NOSRMR Sec. 2.2. [15]	SFM	Single	-4.22	34.3	-0.0427	0.543
7	OSRMR Sec. 2.2. [15]	SFM	Single	-4.3	35	-0.0515	0.446
8	Per acoust. band SRMR Sec. 2.5. [15]	SFM	Single	0.511	24.1	-0.0548	0.58
9	Temporal dynamics [25]	SFM	Single	-11.1	140	0.0515	0.0819
α	QA Reverb [11]	SFM	Single	2.41	23.5	0.0488	0.391
β	Blind est. of coherent-to-diffuse energy ratio [6]	ABC	Chromebook	-9.71	109	0.337	0.019

4.2.2 Ambient noise at 12 dB SNR

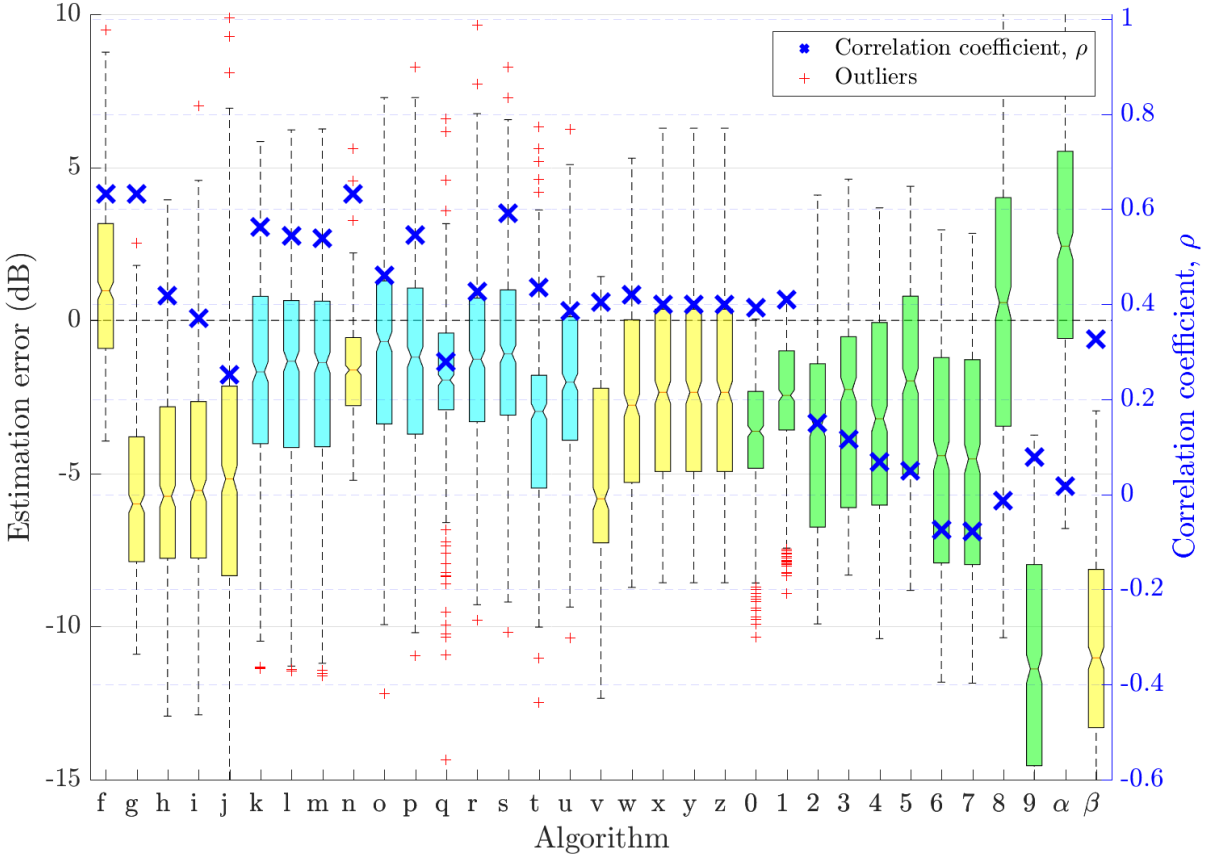

Figure 42: Fullband DRR estimation error in ambient noise at 12 dB SNR

Table 38: DRR estimation algorithm performance in ambient noise at 12 dB SNR

Ref.	Algorithm	Class	Mic. Config.	Bias	MSE	ρ	RTF
f	PSD est. in beamspace, bias comp. [21]	ABC	Mobile	1.18	7.63	0.632	0.757
g	PSD est. in beamspace (Raw) [21]	ABC	Mobile	-5.79	39.8	0.632	3.15
h	PSD est. in beamspace v2 [21]	ABC	Mobile	-5.38	39.2	0.419	0.844
i	PSD est. by twin BF [22]	ABC	Mobile	-5.16	38.1	0.37	0.614
j	Spatial Covariance in matrix mode [23]	ABC	Mobile	-5.11	52.6	0.251	0.627
k	NIRAv2 [4]	MLMF	Single	-1.71	14.2	0.562	$0.897^{\dagger}$
l	NIRAv3 [4]	MLMF	Single	-1.82	14.9	0.543	$0.897^{\dagger}$
m	NIRAv1 [4]	MLMF	Single	-1.84	15.1	0.539	$0.897^{\dagger}$
n	Particle velocity [8]	ABC	EM32	-1.64	5.2	0.632	0.134
o	Multi-layer perceptron [14]	MLMF	Single	-1.06	15.2	0.46	$0.0578^{\ddagger}$
p	Multi-layer perceptron P2 [14]	MLMF	Single	-1.33	15	0.545	$0.0578^{\ddagger}$
q	Multi-layer perceptron P2 [14]	MLMF	Chromebook	-2.27	12.2	0.279	$0.0589^{\ddagger}$
r	Multi-layer perceptron P2 [14]	MLMF	Mobile	-1.1	12.8	0.426	$0.0557^{\ddagger}$
s	Multi-layer perceptron P2 [14]	MLMF	Crucif	-1.15	13.2	0.592	$0.0569^{\ddagger}$
t	Multi-layer perceptron P2 [14]	MLMF	Lin8Ch	-3.37	21.5	0.435	$0.062^{\ddagger}$
u	Multi-layer perceptron P2 [14]	MLMF	EM32	-1.88	11.8	0.386	$0.0578^{\ddagger}$
v	DENBE no noise reduction [24]	ABC	Chromebook	-4.96	33.2	0.404	0.0323
w	DENBE spectral subtraction [7]	ABC	Chromebook	-2.68	16.6	0.42	0.0602
x	DENBE spec. sub. Gerkmann [24]	ABC	Chromebook	-2.28	15.2	0.399	0.0474
y	DENBE filtered subbands [7]	ABC	Chromebook	-2.28	15.2	0.399	0.775
z	DENBE FFT derived subbands [7]	ABC	Chromebook	-2.28	15.2	0.399	0.0449
0	NOSRMR Sec. 2.2. [15]	SFM	Chromebook	-3.83	19	0.392	1.04
1	OSRMR Sec. 2.2. [15]	SFM	Chromebook	-2.62	11.2	0.41	0.831
2	NOSRMR Sec. 2.2. [15]	SFM	Mobile	-3.6	23.4	0.15	1.59
3	OSRMR Sec. 2.2. [15]	SFM	Mobile	-2.56	16.9	0.116	1.26
4	NOSRMR Sec. 2.2. [15]	SFM	Crucif	-3.22	23.5	0.0688	2.63
5	OSRMR Sec. 2.2. [15]	SFM	Crucif	-2.18	17.5	0.0496	2.09
6	NOSRMR Sec. 2.2. [15]	SFM	Single	-4.22	34.3	-0.0748	0.543
7	OSRMR Sec. 2.2. [15]	SFM	Single	-4.29	35	-0.0777	0.446
8	Per acoust. band SRMR Sec. 2.5. [15]	SFM	Single	0.283	22.8	-0.0139	0.58
9	Temporal dynamics [25]	SFM	Single	-11.1	140	0.0777	0.0819
α	QA Reverb [11]	SFM	Single	2.37	23.5	0.0171	0.391
β	Blind est. of coherent-to-diffuse energy ratio [6]	ABC	Chromebook	-10.9	131	0.327	0.019

4.2.3 Ambient noise at -1 dB SNR

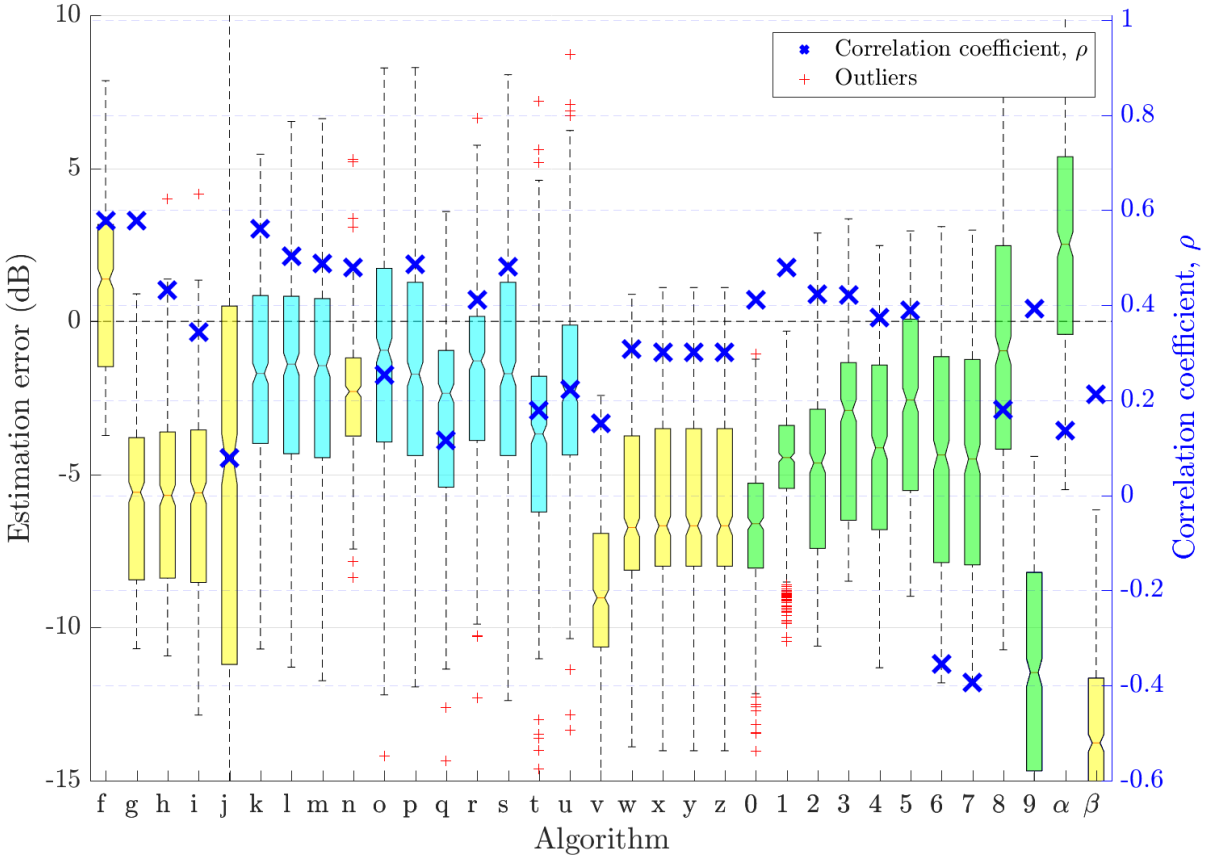

Figure 43: Fullband DRR estimation error in ambient noise at -1 dB SNR

Table 39: DRR estimation algorithm performance in ambient noise at $-1\,\mathrm{dB}$ SNR

Ref.	Algorithm	Class	Mic. Config.	Bias	MSE	ρ	RTF
f	PSD est. in beamspace, bias comp. [21]	ABC	Mobile	1.3	9.51	0.578	0.757
g	PSD est. in beamspace (Raw) [21]	ABC	Mobile	-5.67	39.9	0.578	3.15
h	PSD est. in beamspace v2 [21]	ABC	Mobile	-5.63	40.2	0.431	0.844
i	PSD est. by twin BF [22]	ABC	Mobile	-5.76	42.4	0.344	0.614
j	Spatial Covariance in matrix mode [23]	ABC	Mobile	-5.17	89.4	0.0787	0.627
k	NIRAv2 [4]	MLMF	Single	-1.6	13.9	0.561	$0.897^{\dagger}$
l	NIRAv3 [4]	MLMF	Single	-1.78	15.5	0.503	$0.897^{\dagger}$
m	NIRAv1 [4]	MLMF	Single	-1.86	16.1	0.488	$0.897^{\dagger}$
n	Particle velocity [8]	ABC	EM32	-2.48	9.77	0.479	0.134
o	Multi-layer perceptron [14]	MLMF	Single	-1.15	17.9	0.253	$0.0578^{\ddagger}$
p	Multi-layer perceptron P2 [14]	MLMF	Single	-1.63	17	0.486	$0.0578^{\ddagger}$
q	Multi-layer perceptron P2 [14]	MLMF	Chromebook	-3.17	20	0.116	$0.0589^{\ddagger}$
r	Multi-layer perceptron P2 [14]	MLMF	Mobile	-1.81	15.2	0.412	$0.0557^{\ddagger}$
s	Multi-layer perceptron P2 [14]	MLMF	Crucif	-1.66	17.1	0.481	$0.0569^{\ddagger}$
t	Multi-layer perceptron P2 [14]	MLMF	Lin8Ch	-3.97	31.4	0.178	$0.062^{\ddagger}$
u	Multi-layer perceptron P2 [14]	MLMF	EM32	-2.23	17.4	0.223	$0.0578^{\ddagger}$
v	DENBE no noise reduction [24]	ABC	Chromebook	-8.85	85.7	0.152	0.0323
w	DENBE spectral subtraction [7]	ABC	Chromebook	-5.99	45.8	0.308	0.0602
x	DENBE spec. sub. Gerkmann [24]	ABC	Chromebook	-5.88	44.5	0.302	0.0474
y	DENBE filtered subbands [7]	ABC	Chromebook	-5.88	44.5	0.302	0.775
z	DENBE FFT derived subbands [7]	ABC	Chromebook	-5.88	44.5	0.302	0.0449
0	NOSRMR Sec. 2.2. [15]	SFM	Chromebook	-6.77	51.5	0.411	1.04
1	OSRMR Sec. 2.2. [15]	SFM	Chromebook	-4.55	24.8	0.479	0.831
2	NOSRMR Sec. 2.2. [15]	SFM	Mobile	-4.74	31	0.423	1.59
3	OSRMR Sec. 2.2. [15]	SFM	Mobile	-3.26	19.3	0.422	1.26
4	NOSRMR Sec. 2.2. [15]	SFM	Crucif	-4.28	29.2	0.374	2.63
5	OSRMR Sec. 2.2. [15]	SFM	Crucif	-2.84	19	0.389	2.09
6	NOSRMR Sec. 2.2. [15]	SFM	Single	-4.14	34	-0.355	0.543
7	OSRMR Sec. 2.2. [15]	SFM	Single	-4.25	34.8	-0.393	0.446
8	Per acoust. band SRMR Sec. 2.5. [15]	SFM	Single	-1.02	19.3	0.181	0.58
9	Temporal dynamics [25]	SFM	Single	-11.4	145	0.393	0.0819
α	QA Reverb [11]	SFM	Single	2.43	22.2	0.137	0.391
β	Blind est. of coherent-to-diffuse energy ratio [6]	ABC	Chromebook	-13.8	199	0.212	0.019

4.2.4 Babble noise at 18 dB SNR

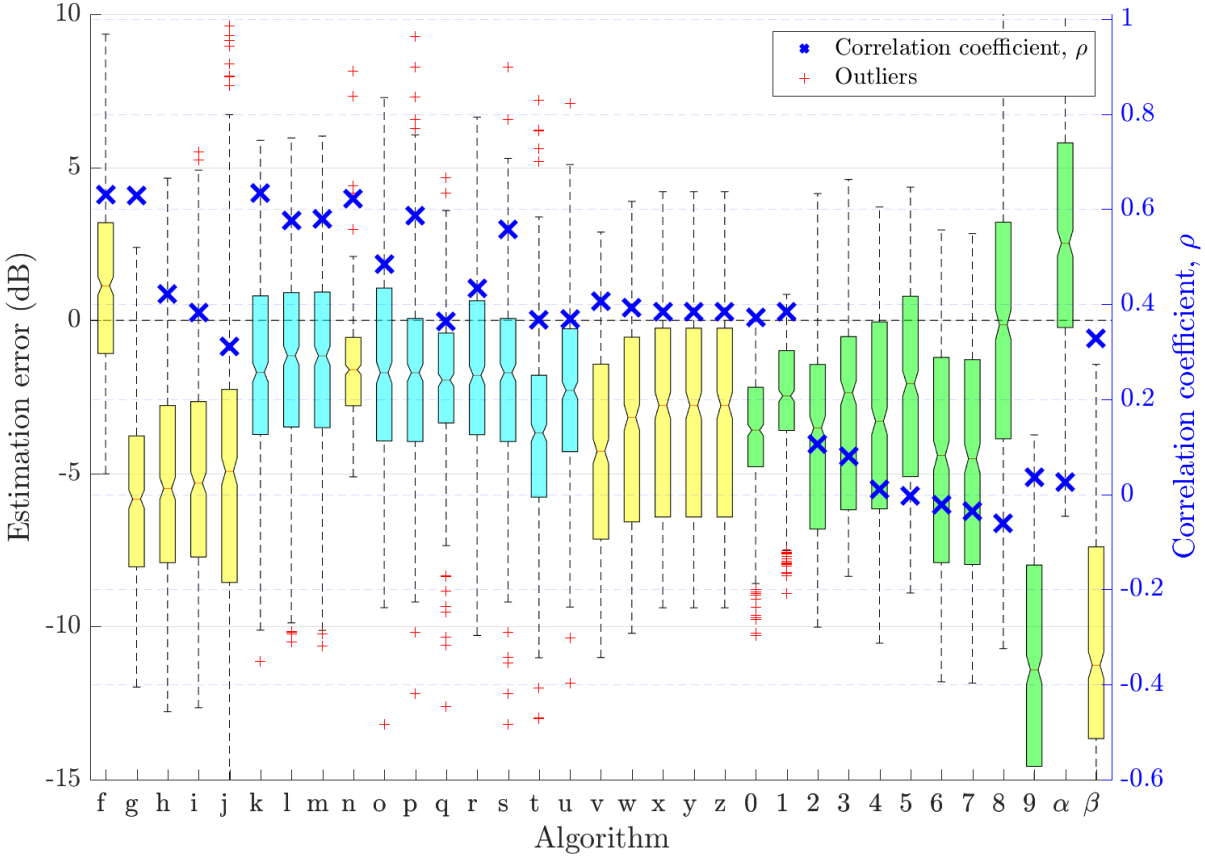

Figure 44: Fullband DRR estimation error in babble noise at 18 dB SNR

Table 40: DRR estimation algorithm performance in babble noise at $18\,\mathrm{dB}$ SNR

Ref.	Algorithm	Class	Mic. Config.	Bias	MSE	ρ	RTF
f	PSD est. in beamspace, bias comp. [21]	ABC	Mobile	1.12	7.96	0.631	0.757
g	PSD est. in beamspace (Raw) [21]	ABC	Mobile	-5.85	40.9	0.629	3.17
h	PSD est. in beamspace v2 [21]	ABC	Mobile	-5.38	41.2	0.422	0.843
i	PSD est. by twin BF [22]	ABC	Mobile	-5.13	40	0.382	0.615
j	Spatial Covariance in matrix mode [23]	ABC	Mobile	-5.09	51.7	0.312	0.627
k	NIRAv2 [4]	MLMF	Single	-1.67	12.8	0.633	$0.906^{\dagger}$
l	NIRAv3 [4]	MLMF	Single	-1.35	13	0.576	$0.906^{\dagger}$
m	NIRAv1 [4]	MLMF	Single	-1.35	12.9	0.579	$0.906^{\dagger}$
n	Particle velocity [8]	ABC	EM32	-1.62	5.28	0.623	0.134
o	Multi-layer perceptron [14]	MLMF	Single	-1.54	15.5	0.485	$0.0579^{\ddagger}$
p	Multi-layer perceptron P2 [14]	MLMF	Single	-1.6	14.1	0.586	$0.0579^{\ddagger}$
q	Multi-layer perceptron P2 [14]	MLMF	Chromebook	-2.16	11.1	0.363	$0.0588^{\ddagger}$
r	Multi-layer perceptron P2 [14]	MLMF	Mobile	-1.76	13.8	0.434	$0.0555^{\ddagger}$
s	Multi-layer perceptron P2 [14]	MLMF	Crucif	-1.62	14.6	0.557	$0.057^{\ddagger}$
t	Multi-layer perceptron P2 [14]	MLMF	Lin8Ch	-3.56	23.3	0.368	$0.0618^{\ddagger}$
u	Multi-layer perceptron P2 [14]	MLMF	EM32	-2.2	13.5	0.369	$0.0576^{\ddagger}$
v	DENBE no noise reduction [24]	ABC	Chromebook	-4.11	27.4	0.406	0.0323
w	DENBE spectral subtraction [7]	ABC	Chromebook	-3.27	22	0.393	0.0577
x	DENBE spec. sub. Gerkmann [24]	ABC	Chromebook	-3.02	20.6	0.385	0.0476
y	DENBE filtered subbands [7]	ABC	Chromebook	-3.02	20.6	0.385	0.778
z	DENBE FFT derived subbands [7]	ABC	Chromebook	-3.02	20.6	0.385	0.0448
0	NOSRMR Sec. 2.2. [15]	SFM	Chromebook	-3.76	18.5	0.373	1.04
1	OSRMR Sec. 2.2. [15]	SFM	Chromebook	-2.6	11.1	0.384	0.833
2	NOSRMR Sec. 2.2. [15]	SFM	Mobile	-3.66	24.2	0.106	1.58
3	OSRMR Sec. 2.2. [15]	SFM	Mobile	-2.62	17.4	0.0805	1.26
4	NOSRMR Sec. 2.2. [15]	SFM	Crucif	-3.28	24.3	0.0103	2.63
5	OSRMR Sec. 2.2. [15]	SFM	Crucif	-2.24	18	-0.00234	2.1
6	NOSRMR Sec. 2.2. [15]	SFM	Single	-4.21	34.3	-0.0213	0.534
7	OSRMR Sec. 2.2. [15]	SFM	Single	-4.29	34.9	-0.0354	0.444
8	Per acoust. band SRMR Sec. 2.5. [15]	SFM	Single	-0.337	21.5	-0.0605	0.579
9	Temporal dynamics [25]	SFM	Single	-11.1	141	0.0354	0.0823
α	QA Reverb [11]	SFM	Single	2.63	24.8	0.0256	0.392
β	Blind est. of coherent-to-diffuse energy ratio [6]	ABC	Chromebook	-10.8	133	0.329	0.019

4.2.5 Babble noise at 12 dB SNR

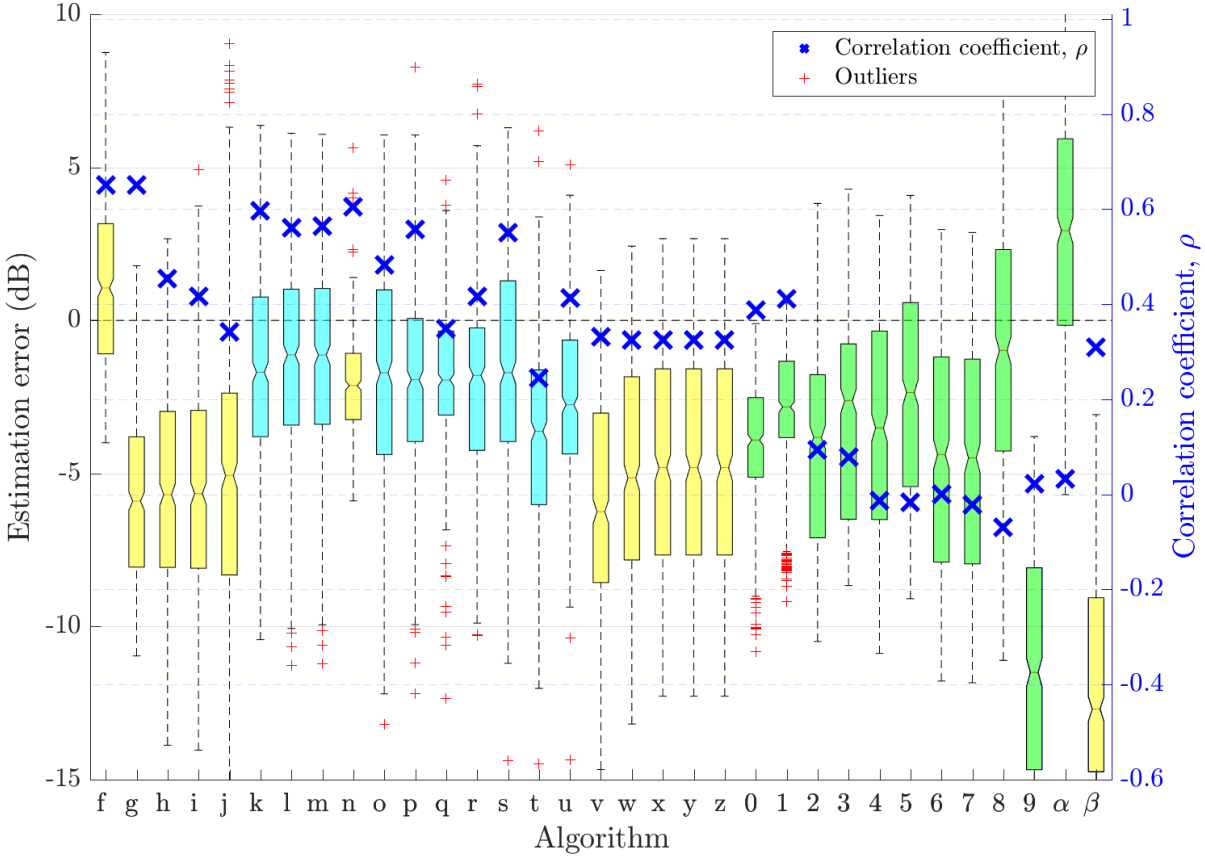

Figure 45: Fullband DRR estimation error in babble noise at 12 dB SNR

Table 41: DRR estimation algorithm performance in babble noise at $12\,\mathrm{dB}$ SNR

Ref.	Algorithm	Class	Mic. Config.	Bias	MSE	ρ	RTF
f	PSD est. in beamspace, bias comp. [21]	ABC	Mobile	1.11	7.41	0.651	0.757
g	PSD est. in beamspace (Raw) [21]	ABC	Mobile	-5.86	40.5	0.651	3.17
h	PSD est. in beamspace v2 [21]	ABC	Mobile	-5.49	40.9	0.454	0.843
i	PSD est. by twin BF [22]	ABC	Mobile	-5.4	40.8	0.416	0.615
j	Spatial Covariance in matrix mode [23]	ABC	Mobile	-5.2	48.4	0.342	0.627
k	NIRAv2 [4]	MLMF	Single	-1.73	13.7	0.596	$0.906^{\dagger}$
l	NIRAv3 [4]	MLMF	Single	-1.26	13	0.561	$0.906^{\dagger}$
m	NIRAv1 [4]	MLMF	Single	-1.23	12.9	0.564	$0.906^{\dagger}$
n	Particle velocity [8]	ABC	EM32	-2.15	7.25	0.604	0.134
o	Multi-layer perceptron [14]	MLMF	Single	-1.57	15.4	0.483	$0.0579^{\ddagger}$
p	Multi-layer perceptron P2 [14]	MLMF	Single	-1.8	15.5	0.558	$0.0579^{\ddagger}$
q	Multi-layer perceptron P2 [14]	MLMF	Chromebook	-2.11	11.3	0.349	$0.0588^{\ddagger}$
r	Multi-layer perceptron P2 [14]	MLMF	Mobile	-2.01	15.6	0.416	$0.0555^{\ddagger}$
s	Multi-layer perceptron P2 [14]	MLMF	Crucif	-1.64	14.8	0.551	$0.057^{\ddagger}$
t	Multi-layer perceptron P2 [14]	MLMF	Lin8Ch	-3.64	25.8	0.246	$0.0618^{\ddagger}$
u	Multi-layer perceptron P2 [14]	MLMF	EM32	-2.51	14.1	0.413	$0.0576^{\ddagger}$
v	DENBE no noise reduction [24]	ABC	Chromebook	-5.91	46	0.331	0.0323
w	DENBE spectral subtraction [7]	ABC	Chromebook	-4.9	35.7	0.325	0.0577
x	DENBE spec. sub. Gerkmann [24]	ABC	Chromebook	-4.62	33	0.324	0.0476
y	DENBE filtered subbands [7]	ABC	Chromebook	-4.62	33	0.324	0.778
z	DENBE FFT derived subbands [7]	ABC	Chromebook	-4.62	33	0.324	0.0448
0	NOSRMR Sec. 2.2. [15]	SFM	Chromebook	-4.09	21.1	0.388	1.04
1	OSRMR Sec. 2.2. [15]	SFM	Chromebook	-2.88	12.6	0.411	0.833
2	NOSRMR Sec. 2.2. [15]	SFM	Mobile	-4	27	0.0937	1.58
3	OSRMR Sec. 2.2. [15]	SFM	Mobile	-2.88	18.8	0.0782	1.26
4	NOSRMR Sec. 2.2. [15]	SFM	Crucif	-3.59	26.7	-0.014	2.63
5	OSRMR Sec. 2.2. [15]	SFM	Crucif	-2.49	19.3	-0.0169	2.1
6	NOSRMR Sec. 2.2. [15]	SFM	Single	-4.19	34	-0.000435	0.534
7	OSRMR Sec. 2.2. [15]	SFM	Single	-4.27	34.8	-0.0218	0.444
8	Per acoust. band SRMR Sec. 2.5. [15]	SFM	Single	-1.12	21.2	-0.0696	0.579
9	Temporal dynamics [25]	SFM	Single	-11.2	143	0.0218	0.0823
α	QA Reverb [11]	SFM	Single	2.8	25.5	0.0333	0.392
β	Blind est. of coherent-to-diffuse energy ratio [6]	ABC	Chromebook	-12.2	163	0.31	0.019

4.2.6 Babble noise at -1 dB SNR

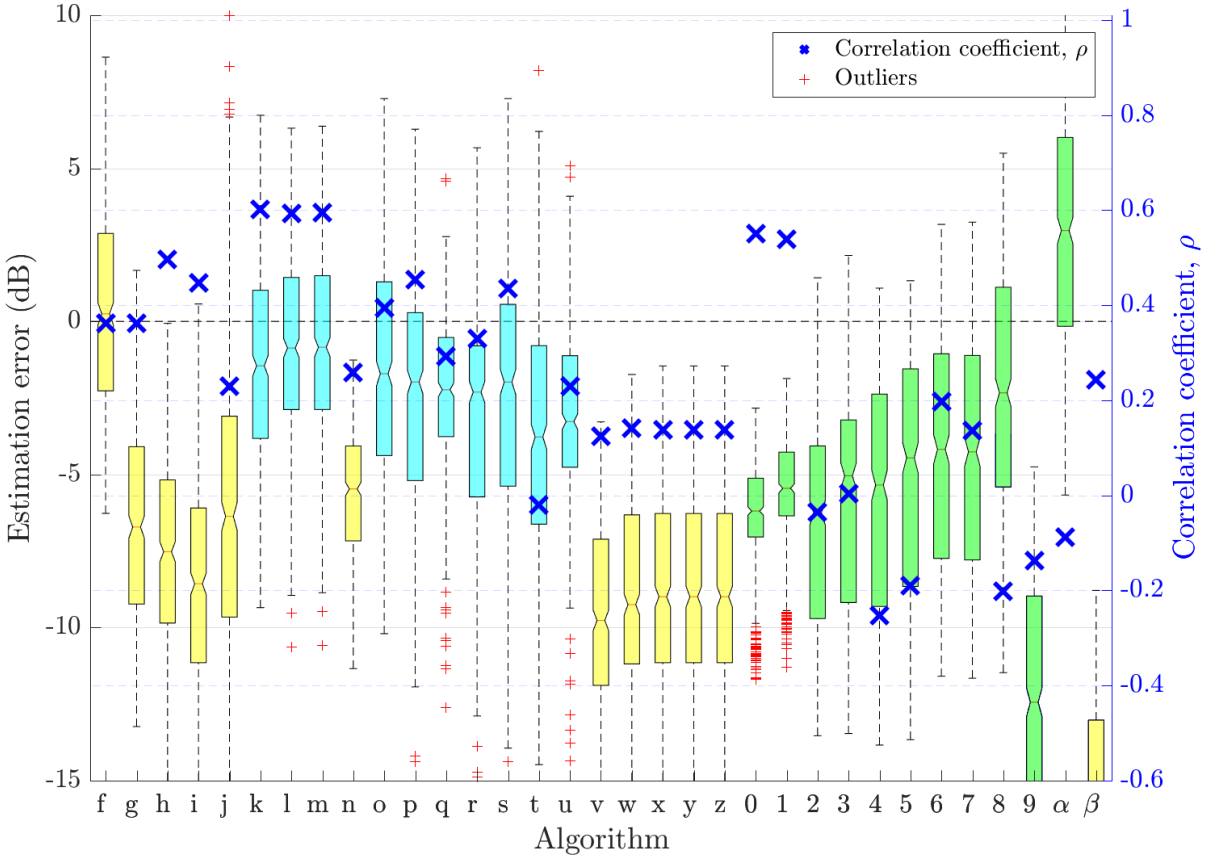

Figure 46: Fullband DRR estimation error in babble noise at -1 dB SNR

Table 42: DRR estimation algorithm performance in babble noise at $-1\,\mathrm{dB}$ SNR

Ref.	Algorithm	Class	Mic. Config.	Bias	MSE	ρ	RTF
f	PSD est. in beamspace, bias comp. [21]	ABC	Mobile	0.289	9.23	0.362	0.757
g	PSD est. in beamspace (Raw) [21]	ABC	Mobile	-6.67	53.7	0.362	3.17
h	PSD est. in beamspace v2 [21]	ABC	Mobile	-7.42	63.1	0.496	0.843
i	PSD est. by twin BF [22]	ABC	Mobile	-8.61	83.1	0.447	0.615
j	Spatial Covariance in matrix mode [23]	ABC	Mobile	-6.51	71	0.23	0.627
k	NIRAv2 [4]	MLMF	Single	-1.58	13.1	0.601	0.906†
l	NIRAv3 [4]	MLMF	Single	-0.885	12.1	0.594	0.906†
m	NIRAv1 [4]	MLMF	Single	-0.848	12.1	0.595	0.906†
n	Particle velocity [8]	ABC	EM32	-5.63	36.2	0.259	0.134
o	Multi-layer perceptron [14]	MLMF	Single	-1.46	16.1	0.395	0.0579‡
p	Multi-layer perceptron P2 [14]	MLMF	Single	-2.45	21.5	0.454	0.0579‡
q	Multi-layer perceptron P2 [14]	MLMF	Chromebook	-2.66	16.5	0.293	0.0588‡
r	Multi-layer perceptron P2 [14]	MLMF	Mobile	-2.99	22.6	0.331	0.0555‡
s	Multi-layer perceptron P2 [14]	MLMF	Crucif	-2.54	22.2	0.434	0.057‡
t	Multi-layer perceptron P2 [14]	MLMF	Lin8Ch	-4.04	36	-0.0201	0.0618‡
u	Multi-layer perceptron P2 [14]	MLMF	EM32	-3.07	21.5	0.23	0.0576‡
v	DENBE no noise reduction [24]	ABC	Chromebook	-9.74	105	0.124	0.0323
w	DENBE spectral subtraction [7]	ABC	Chromebook	-9.03	92.2	0.142	0.0577
x	DENBE spec. sub. Gerkmann [24]	ABC	Chromebook	-8.87	89.1	0.137	0.0476
y	DENBE filtered subbands [7]	ABC	Chromebook	-8.87	89.1	0.137	0.778
z	DENBE FFT derived subbands [7]	ABC	Chromebook	-8.87	89.1	0.137	0.0448
0	NOSRMR Sec. 2.2. [15]	SFM	Chromebook	-6.33	43.6	0.551	1.04
1	OSRMR Sec. 2.2. [15]	SFM	Chromebook	-5.57	34.7	0.539	0.833
2	NOSRMR Sec. 2.2. [15]	SFM	Mobile	-6.47	54.7	-0.0348	1.58
3	OSRMR Sec. 2.2. [15]	SFM	Mobile	-5.69	45.3	0.00456	1.26
4	NOSRMR Sec. 2.2. [15]	SFM	Crucif	-5.99	52.9	-0.253	2.63
5	OSRMR Sec. 2.2. [15]	SFM	Crucif	-5.21	44.1	-0.19	2.1
6	NOSRMR Sec. 2.2. [15]	SFM	Single	-4.02	32.5	0.197	0.534
7	OSRMR Sec. 2.2. [15]	SFM	Single	-4.07	32.9	0.136	0.444
8	Per acoust. band SRMR Sec. 2.5. [15]	SFM	Single	-2.45	24.9	-0.201	0.579
9	Temporal dynamics [25]	SFM	Single	-12.4	172	-0.136	0.0823
α	QA Reverb [11]	SFM	Single	2.96	26.3	-0.0876	0.392
β	Blind est. of coherent-to-diffuse energy ratio [6]	ABC	Chromebook	-15.3	241	0.244	0.019

4.2.7 Fan noise at 18 dB SNR

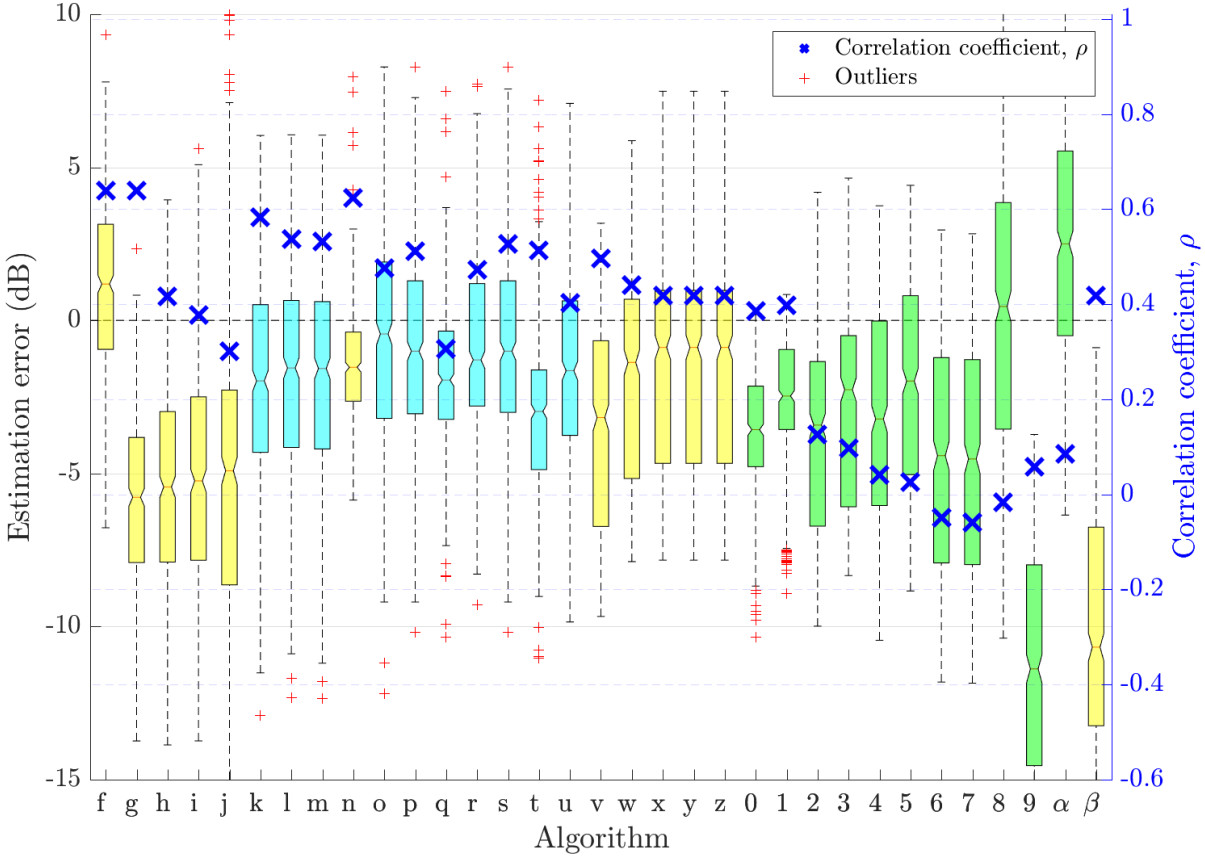

Figure 47: Fullband DRR estimation error in fan noise at 18 dB SNR

Table 43: DRR estimation algorithm performance in fan noise at $18\,\mathrm{dB}$ SNR

Ref.	Algorithm	Class	Mic. Config.	Bias	MSE	ρ	RTF
f	PSD est. in beamspace, bias comp. [21]	ABC	Mobile	1.13	7.67	0.638	0.757
g	PSD est. in beamspace (Raw) [21]	ABC	Mobile	-5.83	40.4	0.639	3.18
h	PSD est. in beamspace v2 [21]	ABC	Mobile	-5.38	40.9	0.416	0.844
i	PSD est. by twin BF [22]	ABC	Mobile	-5.09	39.4	0.378	0.613
j	Spatial Covariance in matrix mode [23]	ABC	Mobile	-5.18	52.6	0.301	0.627
k	NIRAv2 [4]	MLMF	Single	-1.97	14.8	0.583	$0.895^{\dagger}$
l	NIRAv3 [4]	MLMF	Single	-1.85	15.1	0.537	$0.895^{\dagger}$
m	NIRAv1 [4]	MLMF	Single	-1.86	15.3	0.531	$0.895^{\dagger}$
n	Particle velocity [8]	ABC	EM32	-1.45	4.9	0.624	0.134
o	Multi-layer perceptron [14]	MLMF	Single	-0.829	14.4	0.476	$0.0578^{\ddagger}$
p	Multi-layer perceptron P2 [14]	MLMF	Single	-0.883	14.3	0.512	$0.0578^{\ddagger}$
q	Multi-layer perceptron P2 [14]	MLMF	Chromebook	-2.09	10.8	0.306	$0.059^{\ddagger}$
r	Multi-layer perceptron P2 [14]	MLMF	Mobile	-0.997	11.7	0.472	$0.0555^{\ddagger}$
s	Multi-layer perceptron P2 [14]	MLMF	Crucif	-0.985	14.3	0.526	$0.0569^{\ddagger}$
t	Multi-layer perceptron P2 [14]	MLMF	Lin8Ch	-3.19	19.3	0.514	$0.0617^{\ddagger}$
u	Multi-layer perceptron P2 [14]	MLMF	EM32	-1.61	11.2	0.403	$0.0574^{\ddagger}$
v	DENBE no noise reduction [24]	ABC	Chromebook	-3.49	22.8	0.497	0.0322
w	DENBE spectral subtraction [7]	ABC	Chromebook	-1.83	15.5	0.439	0.0588
x	DENBE spec. sub. Gerkmann [24]	ABC	Chromebook	-1.55	15.2	0.418	0.048
y	DENBE filtered subbands [7]	ABC	Chromebook	-1.55	15.2	0.418	0.774
z	DENBE FFT derived subbands [7]	ABC	Chromebook	-1.55	15.2	0.418	0.0452
0	NOSRMR Sec. 2.2. [15]	SFM	Chromebook	-3.72	18.2	0.386	1.03
1	OSRMR Sec. 2.2. [15]	SFM	Chromebook	-2.56	10.9	0.398	0.824
2	NOSRMR Sec. 2.2. [15]	SFM	Mobile	-3.58	23.4	0.127	1.58
3	OSRMR Sec. 2.2. [15]	SFM	Mobile	-2.55	16.9	0.0964	1.26
4	NOSRMR Sec. 2.2. [15]	SFM	Crucif	-3.2	23.5	0.0412	2.61
5	OSRMR Sec. 2.2. [15]	SFM	Crucif	-2.17	17.6	0.0261	2.08
6	NOSRMR Sec. 2.2. [15]	SFM	Single	-4.22	34.3	-0.0485	0.543
7	OSRMR Sec. 2.2. [15]	SFM	Single	-4.3	35	-0.0587	0.447
8	Per acoust. band SRMR Sec. 2.5. [15]	SFM	Single	0.136	22.2	-0.0161	0.576
9	Temporal dynamics [25]	SFM	Single	-11.1	140	0.0587	0.0818
α	QA Reverb [11]	SFM	Single	2.39	22.9	0.086	0.391
β	Blind est. of coherent-to-diffuse energy ratio [6]	ABC	Chromebook	-10.2	120	0.419	0.019

4.2.8 Fan noise at 12 dB SNR

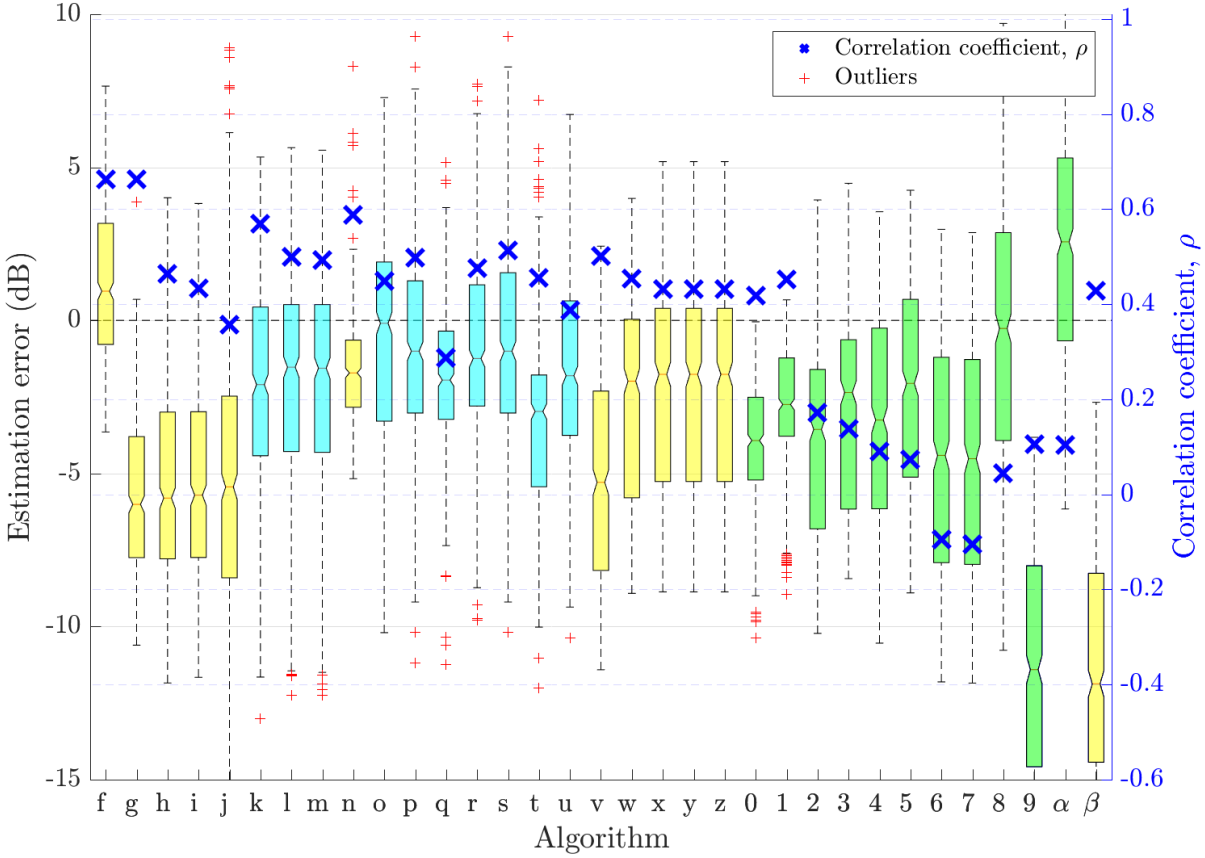

Figure 48: Fullband DRR estimation error in fan noise at 12 dB SNR

Table 44: DRR estimation algorithm performance in fan noise at 12 dB SNR

Ref.	Algorithm	Class	Mic. Config.	Bias	MSE	ρ	RTF
f	PSD est. in beamspace, bias comp. [21]	ABC	Mobile	1.15	7.15	0.662	0.757
g	PSD est. in beamspace (Raw) [21]	ABC	Mobile	-5.81	39.6	0.662	3.18
h	PSD est. in beamspace v2 [21]	ABC	Mobile	-5.48	39.7	0.464	0.844
i	PSD est. by twin BF [22]	ABC	Mobile	-5.3	38.6	0.434	0.613
j	Spatial Covariance in matrix mode [23]	ABC	Mobile	-5.4	50.5	0.357	0.627
k	NIRAv2 [4]	MLMF	Single	-2.04	15.3	0.57	0.895†
l	NIRAv3 [4]	MLMF	Single	-1.92	16.1	0.5	0.895†
m	NIRAv1 [4]	MLMF	Single	-1.93	16.3	0.493	0.895†
n	Particle velocity [8]	ABC	EM32	-1.67	5.69	0.589	0.134
o	Multi-layer perceptron [14]	MLMF	Single	-0.743	14.4	0.449	0.0578‡
p	Multi-layer perceptron P2 [14]	MLMF	Single	-0.941	14.7	0.498	0.0578‡
q	Multi-layer perceptron P2 [14]	MLMF	Chromebook	-2.06	10.1	0.288	0.059‡
r	Multi-layer perceptron P2 [14]	MLMF	Mobile	-0.905	11.7	0.476	0.0555‡
s	Multi-layer perceptron P2 [14]	MLMF	Crucif	-0.893	14	0.513	0.0569‡
t	Multi-layer perceptron P2 [14]	MLMF	Lin8Ch	-3.22	20.5	0.456	0.0617‡
u	Multi-layer perceptron P2 [14]	MLMF	EM32	-1.65	11.8	0.388	0.0574‡
v	DENBE no noise reduction [24]	ABC	Chromebook	-5.06	36.3	0.501	0.0322
w	DENBE spectral subtraction [7]	ABC	Chromebook	-2.58	17.6	0.455	0.0588
x	DENBE spec. sub. Gerkmann [24]	ABC	Chromebook	-2.21	16.4	0.432	0.048
y	DENBE filtered subbands [7]	ABC	Chromebook	-2.21	16.4	0.432	0.774
z	DENBE FFT derived subbands [7]	ABC	Chromebook	-2.21	16.4	0.432	0.0452
0	NOSRMR Sec. 2.2. [15]	SFM	Chromebook	-4.07	20.8	0.418	1.03
1	OSRMR Sec. 2.2. [15]	SFM	Chromebook	-2.78	11.9	0.452	0.824
2	NOSRMR Sec. 2.2. [15]	SFM	Mobile	-3.74	24.4	0.172	1.58
3	OSRMR Sec. 2.2. [15]	SFM	Mobile	-2.65	17.3	0.137	1.26
4	NOSRMR Sec. 2.2. [15]	SFM	Crucif	-3.36	24.3	0.09	2.61
5	OSRMR Sec. 2.2. [15]	SFM	Crucif	-2.27	17.8	0.0731	2.08
6	NOSRMR Sec. 2.2. [15]	SFM	Single	-4.21	34.3	-0.0954	0.543
7	OSRMR Sec. 2.2. [15]	SFM	Single	-4.29	34.9	-0.105	0.447
8	Per acoust. band SRMR Sec. 2.5. [15]	SFM	Single	-0.669	20.3	0.0451	0.576
9	Temporal dynamics [25]	SFM	Single	-11.2	141	0.105	0.0818
α	QA Reverb [11]	SFM	Single	2.41	22.7	0.104	0.391
β	Blind est. of coherent-to-diffuse energy ratio [6]	ABC	Chromebook	-11.5	147	0.428	0.019

4.2.9 Fan noise at -1 dB SNR

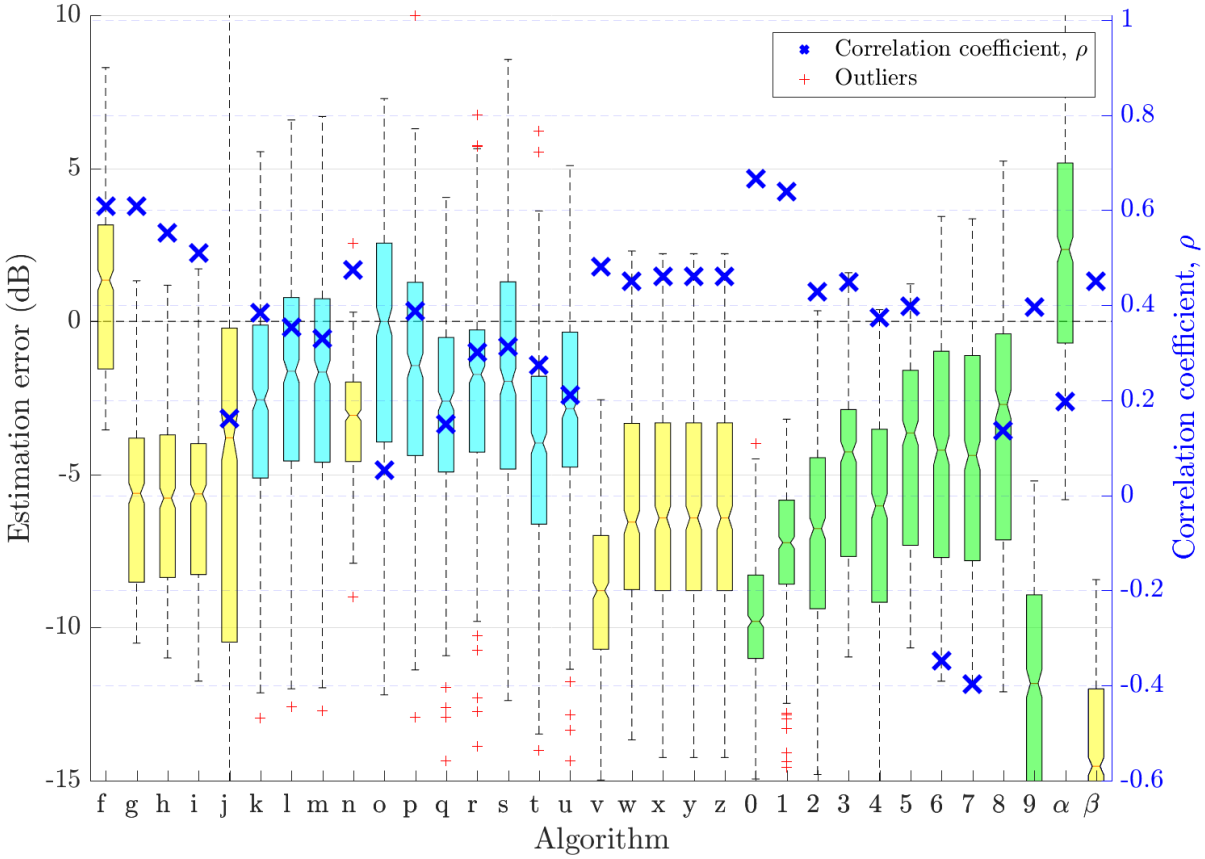

Figure 49: Fullband DRR estimation error in fan noise at -1 dB SNR

Table 45: DRR estimation algorithm performance in fan noise at $-1\,\mathrm{dB}$ SNR

Ref.	Algorithm	Class	Mic. Config.	Bias	MSE	ρ	RTF
f	PSD est. in beamspace, bias comp. [21]	ABC	Mobile	1.2	8.85	0.609	0.757
g	PSD est. in beamspace (Raw) [21]	ABC	Mobile	-5.76	40.6	0.609	3.18
h	PSD est. in beamspace v2 [21]	ABC	Mobile	-5.75	40.6	0.553	0.844
i	PSD est. by twin BF [22]	ABC	Mobile	-5.86	42.1	0.51	0.613
j	Spatial Covariance in matrix mode [23]	ABC	Mobile	-5.4	81.2	0.161	0.627
k	NIRAv2 [4]	MLMF	Single	-2.67	21.5	0.384	$0.895^{\dagger}$
l	NIRAv3 [4]	MLMF	Single	-1.89	18.3	0.354	$0.895^{\dagger}$
m	NIRAv1 [4]	MLMF	Single	-1.98	19.1	0.33	$0.895^{\dagger}$
n	Particle velocity [8]	ABC	EM32	-3.32	14.3	0.474	0.134
o	Multi-layer perceptron [14]	MLMF	Single	-0.747	18.7	0.053	$0.0578^{\ddagger}$
p	Multi-layer perceptron P2 [14]	MLMF	Single	-1.77	18.7	0.387	$0.0578^{\ddagger}$
q	Multi-layer perceptron P2 [14]	MLMF	Chromebook	-3.08	19.2	0.149	$0.059^{\ddagger}$
r	Multi-layer perceptron P2 [14]	MLMF	Mobile	-2.26	18.3	0.302	$0.0555^{\ddagger}$
s	Multi-layer perceptron P2 [14]	MLMF	Crucif	-1.83	20.6	0.312	$0.0569^{\ddagger}$
t	Multi-layer perceptron P2 [14]	MLMF	Lin8Ch	-4.44	32.6	0.274	$0.0617^{\ddagger}$
u	Multi-layer perceptron P2 [14]	MLMF	EM32	-2.86	18.6	0.212	$0.0574^{\ddagger}$
v	DENBE no noise reduction [24]	ABC	Chromebook	-8.75	83	0.481	0.0322
w	DENBE spectral subtraction [7]	ABC	Chromebook	-6.05	47.6	0.45	0.0588
x	DENBE spec. sub. Gerkmann [24]	ABC	Chromebook	-6.05	47.5	0.46	0.048
y	DENBE filtered subbands [7]	ABC	Chromebook	-6.05	47.5	0.46	0.774
z	DENBE FFT derived subbands [7]	ABC	Chromebook	-6.05	47.5	0.46	0.0452
0	NOSRMR Sec. 2.2. [15]	SFM	Chromebook	-9.66	97.8	0.667	1.03
1	OSRMR Sec. 2.2. [15]	SFM	Chromebook	-7.29	57.5	0.639	0.824
2	NOSRMR Sec. 2.2. [15]	SFM	Mobile	-6.9	57	0.429	1.58
3	OSRMR Sec. 2.2. [15]	SFM	Mobile	-4.78	31.1	0.449	1.26
4	NOSRMR Sec. 2.2. [15]	SFM	Crucif	-6.34	52	0.374	2.61
5	OSRMR Sec. 2.2. [15]	SFM	Crucif	-4.35	29.5	0.398	2.08
6	NOSRMR Sec. 2.2. [15]	SFM	Single	-3.99	32.9	-0.347	0.543
7	OSRMR Sec. 2.2. [15]	SFM	Single	-4.13	34	-0.397	0.447
8	Per acoust. band SRMR Sec. 2.5. [15]	SFM	Single	-3.44	28.6	0.136	0.576
9	Temporal dynamics [25]	SFM	Single	-12.1	160	0.397	0.0818
α	QA Reverb [11]	SFM	Single	2.22	20.8	0.198	0.391
β	Blind est. of coherent-to-diffuse energy ratio [6]	ABC	Chromebook	-14.3	211	0.451	0.019

4.3 Frequency-dependent DRR estimation results

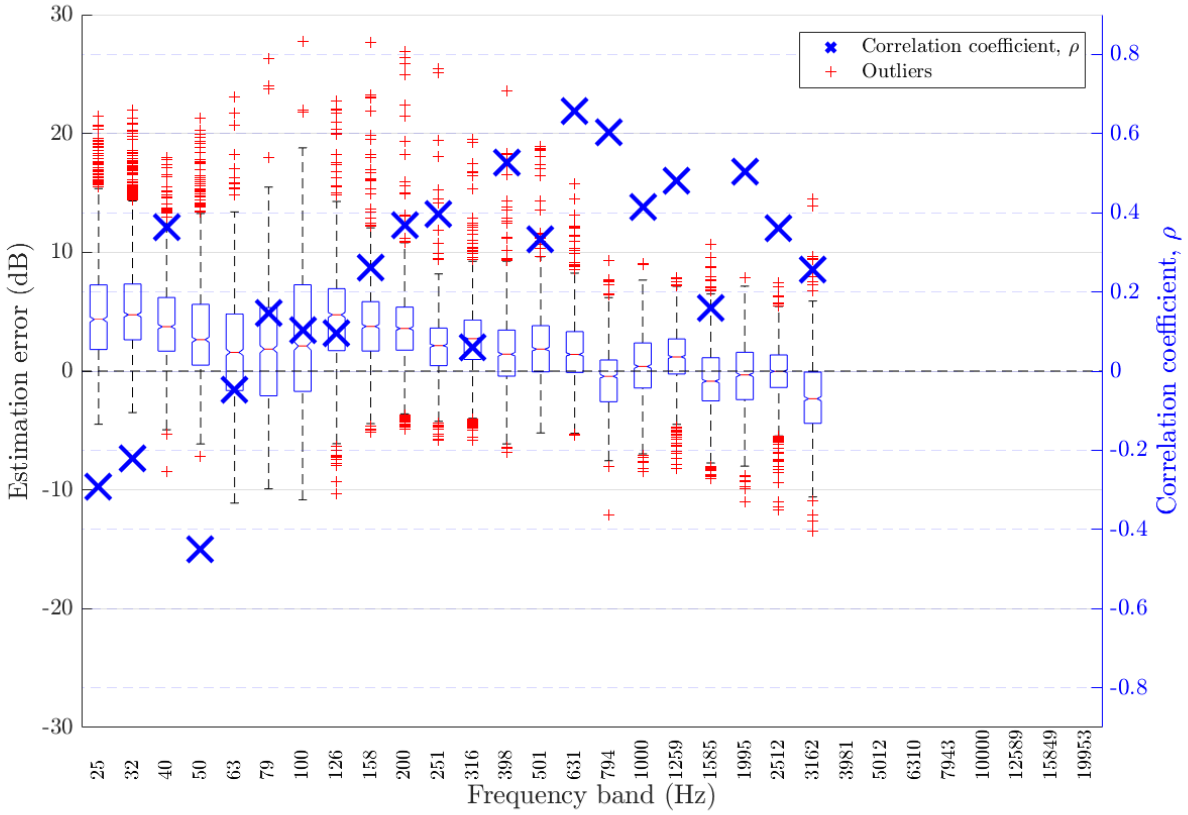

Figure 50: Frequency-dependent DRR estimation error in all noises for all SNRs for algorithm Particle Velocity [8]

Table 46: Frequency-dependent DRR estimation error in all noises for all SNRs for algorithm Particle Velocity [8]

Freq. band	Centre Freq. (Hz)	Bias	MSE	ρ
1	25.12	5.915	59.49	-0.2928
2	31.62	6.399	62.41	-0.2196
3	39.81	4.915	40.5	0.3622
4	50.12	3.624	37.37	-0.4494
5	63.10	1.311	23.91	-0.04796
6	79.43	0.6641	20.28	0.1454
7	100.00	1.154	25.77	0.104
8	125.89	1.867	27.15	0.09463
9	158.49	2.251	20.78	0.2602
10	199.53	2.809	18.57	0.3691
11	251.19	1.455	11.06	0.3971
12	316.23	1.66	14.86	0.05926
13	398.11	1.008	12.1	0.5263
14	501.19	1.512	14.1	0.334
15	630.96	1.12	11.15	0.6573
16	794.33	-1.25	11.12	0.6027
17	1000.00	-0.2177	10.31	0.4151
18	1258.93	0.6023	9.464	0.4811
19	1584.89	-1.002	10.28	0.1604
20	1995.26	-0.8029	8.668	0.5033
21	2511.89	-0.7828	8.903	0.3599
22	3162.28	-2.95	22.64	0.2575

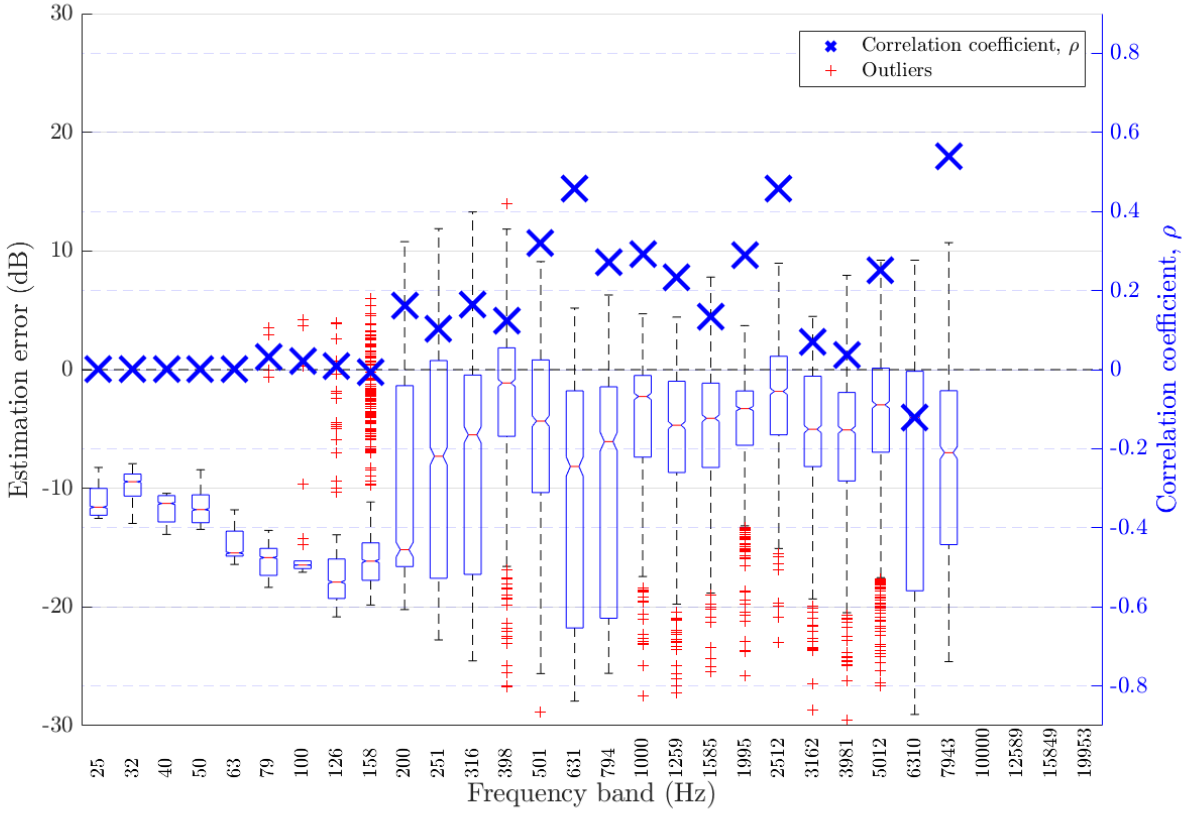

Figure 51: Frequency-dependent DRR estimation error in all noises for all SNRs for algorithm DENBE with FFT derived subbands [7]

Table 47: Frequency-dependent DRR estimation error in all noises for all SNRs for algorithm DENBE with FFT derived subbands [7]

Freq. band	Centre Freq. (Hz)	Bias	MSE	ρ
1	25.12	-11.07	124.4	0
2	31.62	-9.93	100.8	0
3	39.81	-11.69	138.1	0
4	50.12	-11.55	135.4	0
5	63.10	-14.82	221.5	0
6	79.43	-16.07	260.2	0.0318
7	100.00	-16.16	262.3	0.02187
8	125.89	-17.68	317.1	0.009427
9	158.49	-16.39	276.4	-0.005167
10	199.53	-13.75	231.9	0.1624
11	251.19	-12.72	233	0.1023
12	316.23	-14.05	275.1	0.1637
13	398.11	-10.56	228.8	0.1242
14	501.19	-11.52	237.1	0.3193
15	630.96	-14.88	312.2	0.4584
16	794.33	-13.78	282.8	0.2725
17	1000.00	-10.74	211.8	0.2908
18	1258.93	-10.4	187.5	0.2331
19	1584.89	-8.162	140.1	0.1336
20	1995.26	-7.311	102.7	0.2892
21	2511.89	-5.217	74.37	0.4572
22	3162.28	-6.642	82.46	0.07081
23	3981.07	-7.008	81.94	0.03811
24	5011.87	-6.333	95.62	0.2504
25	6309.57	-9.64	207.7	-0.1221
26	7943.28	-9.647	166.5	0.5396

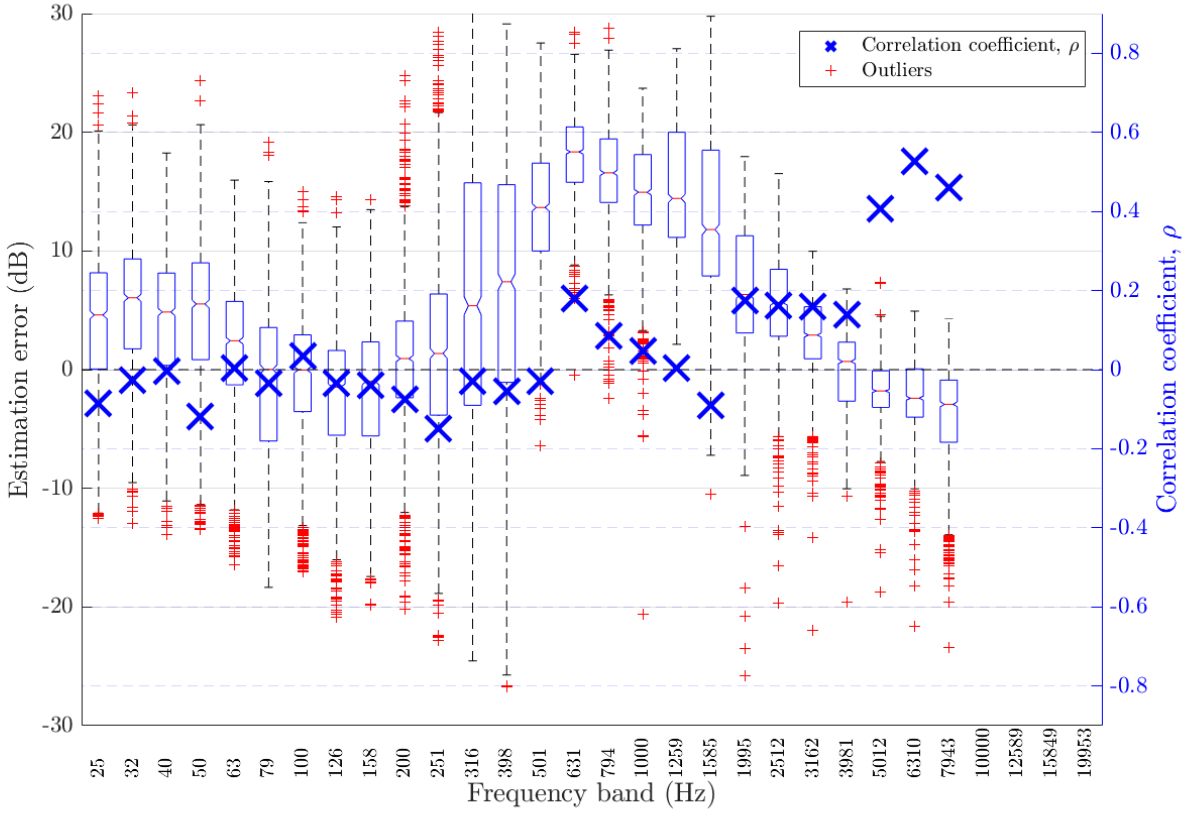

Figure 52: Frequency-dependent DRR estimation error in all noises for all SNRs for algorithm DENBE with filtered subbands [7]

Table 48: Frequency-dependent DRR estimation error in all noises for all SNRs for algorithm DENBE with filtered subbands [7]

Freq. band	Centre Freq. (Hz)	Bias	MSE	ρ
1	25.12	2.367	60.71	-0.08501
2	31.62	3.618	64.55	-0.0276
3	39.81	2.117	52.78	-0.004386
4	50.12	2.7	61.79	-0.1188
5	63.10	-0.01441	47.99	0.004362
6	79.43	-2.464	67.34	-0.03461
7	100.00	-2.482	50.57	0.03417
8	125.89	-3.691	58.41	-0.03403
9	158.49	-3.092	59.07	-0.03996
10	199.53	-1.593	51.98	-0.07489
11	251.19	-1.831	81.92	-0.1493
12	316.23	1.369	128	-0.0298
13	398.11	1.402	121.7	-0.0544
14	501.19	6.935	135.3	-0.02971
15	630.96	12.77	215.3	0.179
16	794.33	11.48	195.7	0.08491
17	1000.00	9.2	157.1	0.04596
18	1258.93	11.13	184.6	0.003646
19	1584.89	8.951	153.7	-0.0894
20	1995.26	3.492	68.87	0.1737
21	2511.89	2.02	57.47	0.1612
22	3162.28	-0.5084	40.61	0.16
23	3981.07	-2.036	27	0.1399
24	5011.87	-3.013	25.41	0.4063
25	6309.57	-3.702	30.21	0.5259
26	7943.28	-5.567	56.88	0.4599

4.4 Frequency-dependent DRR estimation results by noise type

4.4.1 Ambient noise

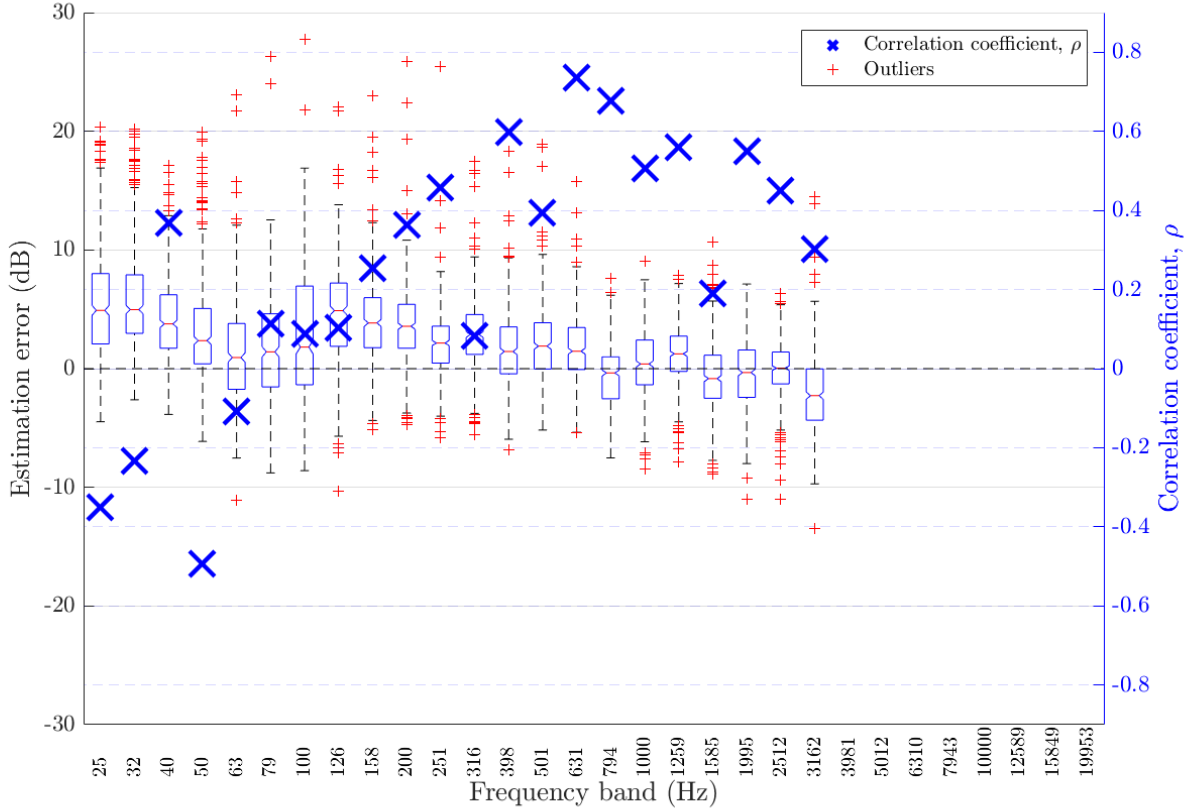

Figure 53: Frequency-dependent DRR estimation error in ambient noise for all SNRs for algorithm Particle Velocity [8]

Table 49: Frequency-dependent DRR estimation error in ambient noise for all SNRs for algorithm Particle Velocity [8]

Freq. band	Centre Freq. (Hz)	Bias	MSE	ρ
1	25.12	6.214	63.74	-0.3506
2	31.62	6.689	66.26	-0.2323
3	39.81	5.141	42.68	0.3684
4	50.12	3.689	37.53	-0.4925
5	63.10	1.167	21.71	-0.109
6	79.43	0.511	17.14	0.1127
7	100.00	1.343	23.59	0.08844
8	125.89	2.361	26.85	0.103
9	158.49	2.723	21.22	0.2526
10	199.53	3.108	19.59	0.3639
11	251.19	1.817	11.37	0.4577
12	316.23	2.511	15.81	0.0833
13	398.11	1.649	11.81	0.5972
14	501.19	2.16	15.08	0.3946
15	630.96	1.818	10.86	0.7346
16	794.33	-0.6569	7.836	0.6764
17	1000.00	0.4372	7.952	0.5051
18	1258.93	1.151	8.026	0.5595
19	1584.89	-0.7626	9.359	0.1898
20	1995.26	-0.4096	7.21	0.55
21	2511.89	-0.2113	6.052	0.451
22	3162.28	-2.222	16.39	0.302

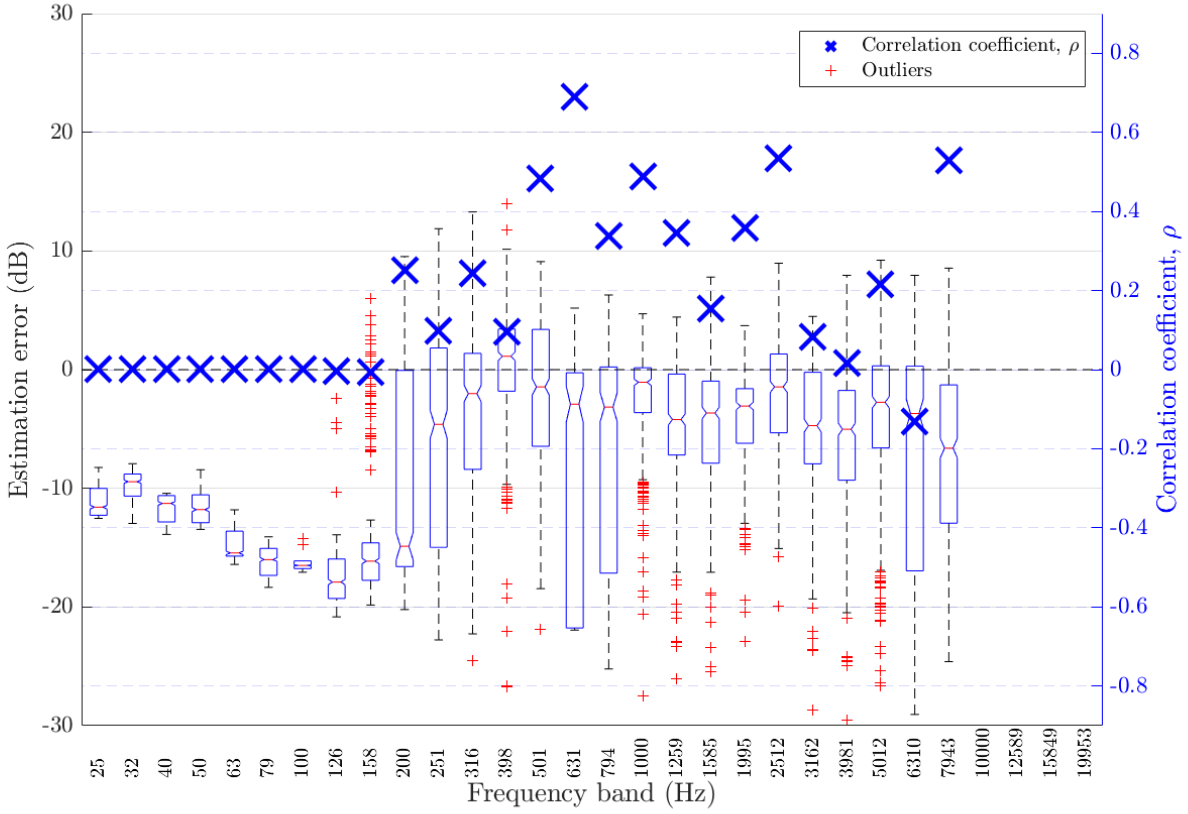

Figure 54: Frequency-dependent DRR estimation error in ambient noise for all SNRs for algorithm DENBE with FFT derived subbands [7]

Table 50: Frequency-dependent DRR estimation error in ambient noise for all SNRs for algorithm DENBE with FFT derived subbands [7]

Freq. band	Centre Freq. (Hz)	Bias	MSE	ρ
1	25.12	-11.07	124.4	0
2	31.62	-9.93	100.8	0
3	39.81	-11.69	138.1	0
4	50.12	-11.55	135.4	0
5	63.10	-14.82	221.5	0
6	79.43	-16.09	260.6	0
7	100.00	-16.18	262.6	0
8	125.89	-17.71	317.6	-0.002839
9	158.49	-16.36	276.1	-0.006109
10	199.53	-13.14	222	0.2499
11	251.19	-11.33	212.9	0.09857
12	316.23	-11.3	218	0.2435
13	398.11	-5.595	135.9	0.0947
14	501.19	-5.816	112.4	0.4825
15	630.96	-10.64	209.3	0.6889
16	794.33	-9.63	187.8	0.339
17	1000.00	-6.313	104.9	0.4895
18	1258.93	-7.227	107.4	0.3443
19	1584.89	-5.902	86.14	0.1545
20	1995.26	-5.517	58.78	0.359
21	2511.89	-3.762	45.75	0.5346
22	3162.28	-5.89	69.48	0.0819
23	3981.07	-6.871	82	0.01629
24	5011.87	-5.961	90.28	0.2161
25	6309.57	-9.023	193.2	-0.1301
26	7943.28	-8.983	151.1	0.529

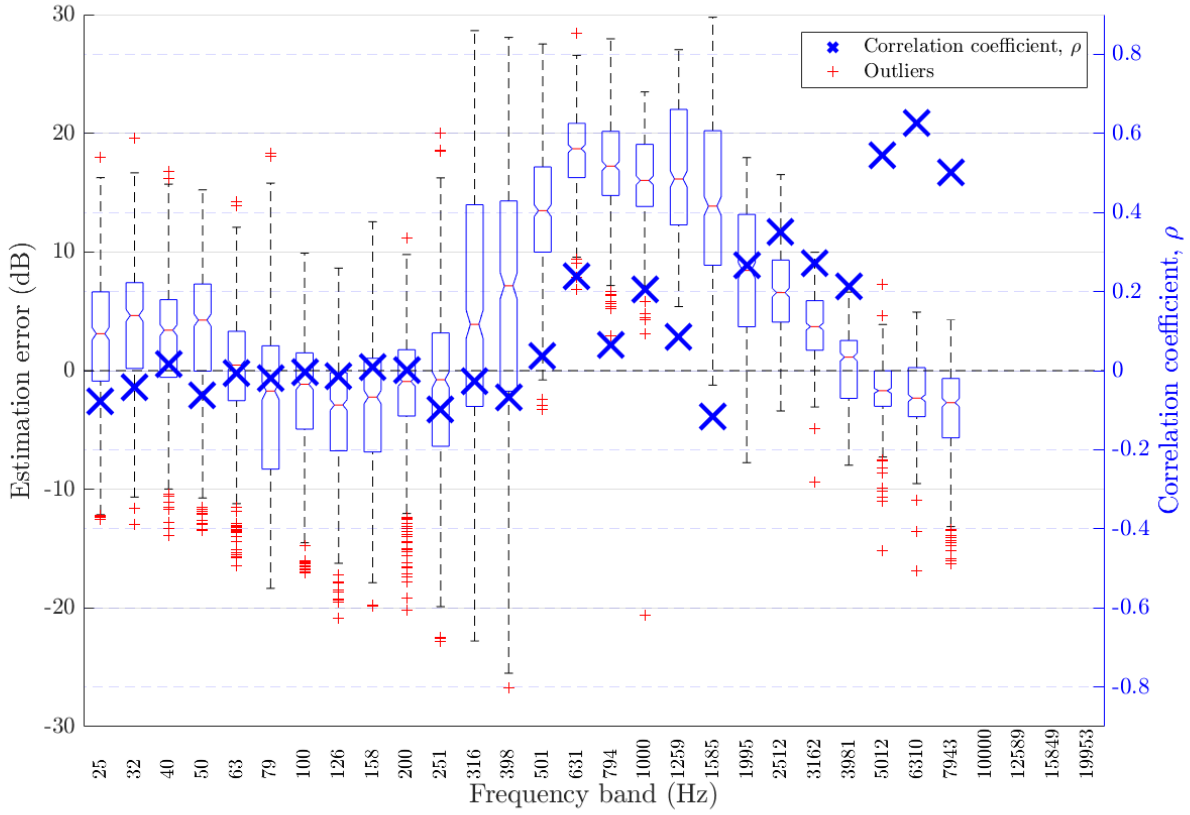

Figure 55: Frequency-dependent DRR estimation error in ambient noise for all SNRs for algorithm DENBE with filtered subbands [7]

Table 51: Frequency-dependent DRR estimation error in ambient noise for all SNRs for algorithm DENBE with filtered subbands [7]

Freq. band	Centre Freq. (Hz)	Bias	MSE	ρ
1	25.12	1.66	54.97	-0.07702
2	31.62	2.713	53.7	-0.04108
3	39.81	1.356	42.18	0.01744
4	50.12	1.582	50.25	-0.06225
5	63.10	-1.442	43.29	-0.006312
6	79.43	-3.108	68.75	-0.01959
7	100.00	-3.231	49.12	-0.003524
8	125.89	-4.595	60.49	-0.01394
9	158.49	-3.882	60.76	0.008567
10	199.53	-2.874	44.48	0.002132
11	251.19	-3.767	69.47	-0.0971
12	316.23	0.3985	112.6	-0.02558
13	398.11	0.7077	118.2	-0.06832
14	501.19	6.848	131.9	0.03671
15	630.96	13.44	229.6	0.2388
16	794.33	12.93	227.2	0.0649
17	1000.00	12.07	193.2	0.2053
18	1258.93	14.78	247.4	0.08421
19	1584.89	12.73	207.5	-0.1166
20	1995.26	6.81	80.34	0.2655
21	2511.89	5.048	51.05	0.3499
22	3162.28	1.967	24.94	0.2718
23	3981.07	-0.7185	14.42	0.2117
24	5011.87	-2.156	14.58	0.544
25	6309.57	-2.896	19.87	0.6265
26	7943.28	-4.729	43.81	0.5001

4.4.2 Babble noise

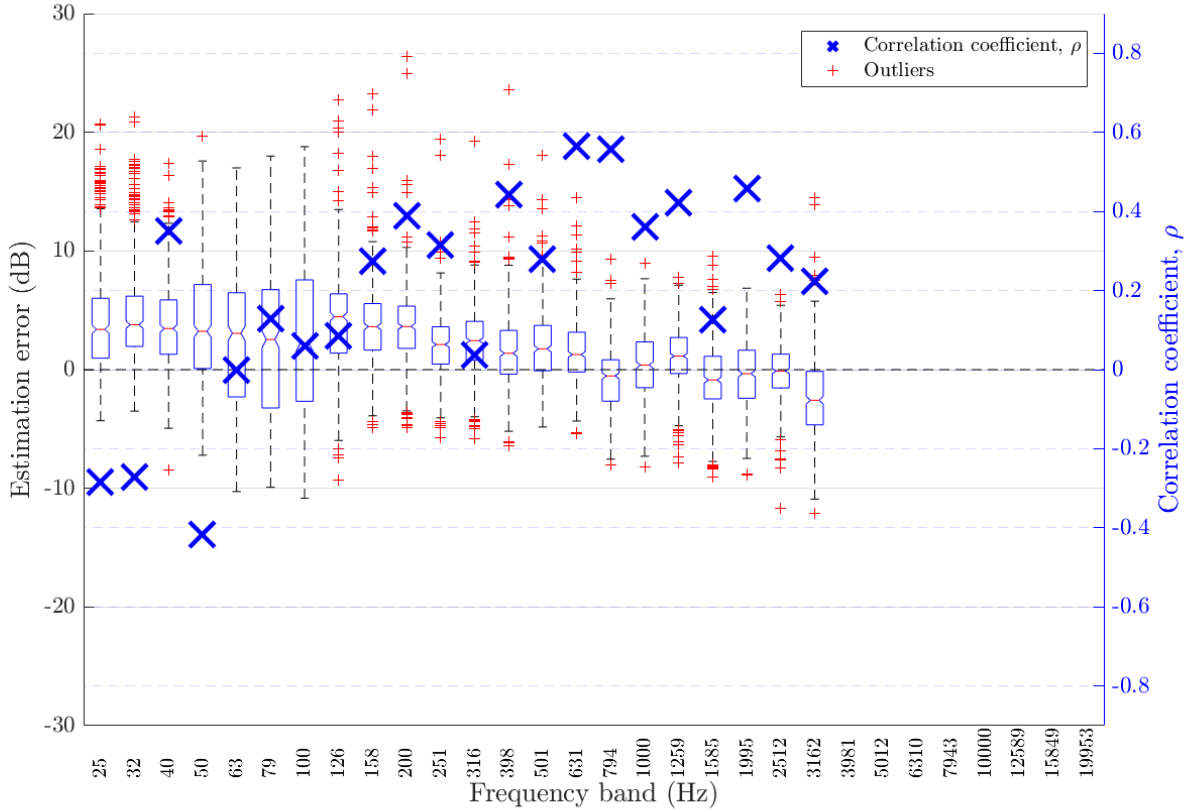

Figure 56: Frequency-dependent DRR estimation error in babble noise for all SNRs for algorithm Particle Velocity [8]

Table 52: Frequency-dependent DRR estimation error in babble noise for all SNRs for algorithm Particle Velocity [8]

Freq. band	Centre Freq. (Hz)	Bias	MSE	ρ
1	25.12	5.283	53.02	-0.2852
2	31.62	5.764	55.5	-0.2719
3	39.81	4.42	36.07	0.35
4	50.12	3.432	37.01	-0.4171
5	63.10	1.334	27.61	-0.0008789
6	79.43	0.4524	25.49	0.1279
7	100.00	0.4457	29.46	0.0596
8	125.89	0.9477	27.44	0.08608
9	158.49	1.447	19.41	0.2753
10	199.53	2.22	16.05	0.3898
11	251.19	0.7781	10.82	0.3151
12	316.23	0.4684	14.71	0.03585
13	398.11	0.1692	13.43	0.4431
14	501.19	0.6781	13.49	0.2792
15	630.96	0.1452	12.36	0.5645
16	794.33	-1.864	14.5	0.5561
17	1000.00	-0.8126	12.97	0.3599
18	1258.93	-0.05593	11.58	0.4217
19	1584.89	-1.384	12.04	0.1265
20	1995.26	-1.305	10.75	0.4583
21	2511.89	-1.619	13.53	0.2812
22	3162.28	-3.902	31.41	0.2219

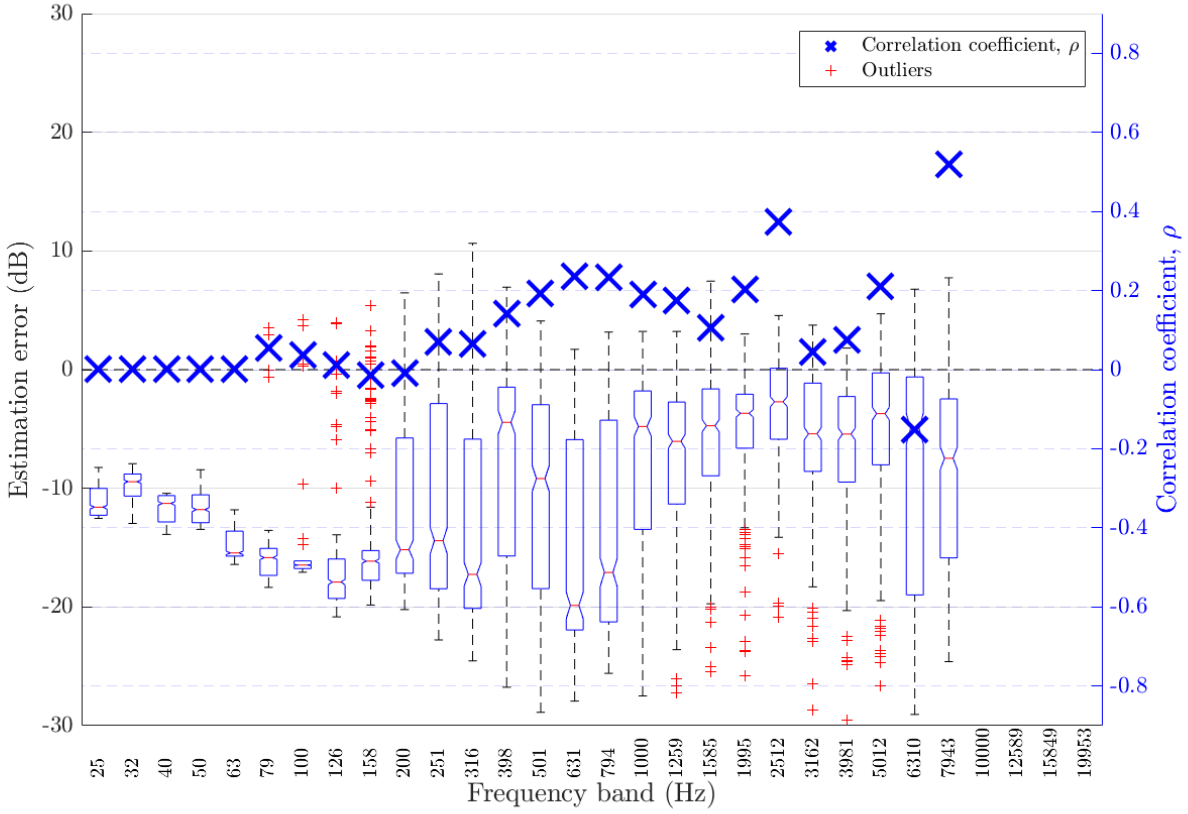

Figure 57: Frequency-dependent DRR estimation error in babble noise for all SNRs for algorithm DENBE with FFT derived subbands [7]

Table 53: Frequency-dependent DRR estimation error in babble noise for all SNRs for algorithm DENBE with FFT derived subbands [7]

Freq. band	Centre Freq. (Hz)	Bias	MSE	ρ
1	25.12	-11.07	124.4	0
2	31.62	-9.93	100.8	0
3	39.81	-11.69	138.1	0
4	50.12	-11.55	135.4	0
5	63.10	-14.82	221.5	0
6	79.43	-16.03	259.6	0.05514
7	100.00	-16.12	261.6	0.03793
8	125.89	-17.62	316	0.01081
9	158.49	-16.47	278	-0.01475
10	199.53	-14.94	252.4	-0.009532
11	251.19	-15.14	272.3	0.07024
12	316.23	-17.67	353.7	0.06498
13	398.11	-16.26	345.6	0.1415
14	501.19	-17.53	378.2	0.1929
15	630.96	-19.54	428.4	0.237
16	794.33	-18.05	382.3	0.2328
17	1000.00	-15.23	321.6	0.1888
18	1258.93	-14.58	290.9	0.1744
19	1584.89	-11.62	222.4	0.1068
20	1995.26	-10.08	173.3	0.2017
21	2511.89	-7.693	123.8	0.3742
22	3162.28	-8.071	109.7	0.04468
23	3981.07	-7.607	88.77	0.07405
24	5011.87	-7.238	104.3	0.2093
25	6309.57	-11.01	231.9	-0.1509
26	7943.28	-11.06	193.3	0.519

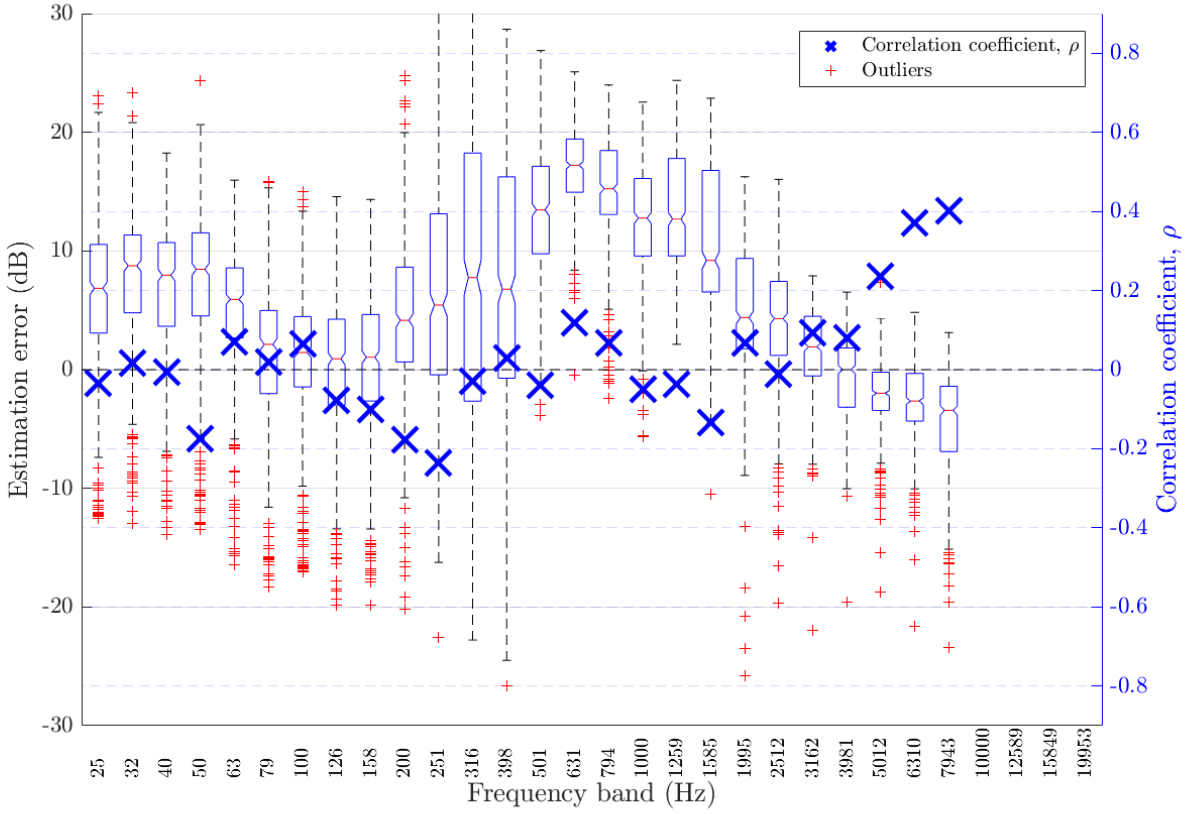

Figure 58: Frequency-dependent DRR estimation error in babble noise for all SNRs for algorithm DENBE with filtered subbands [7]

Table 54: Frequency-dependent DRR estimation error in babble noise for all SNRs for algorithm DENBE with filtered subbands [7]

Freq. band	Centre Freq. (Hz)	Bias	MSE	ρ
1	25.12	3.769	68.3	-0.03378
2	31.62	5.437	76.85	0.01647
3	39.81	4.093	62.42	-0.00727
4	50.12	5.104	76.03	-0.1741
5	63.10	2.715	46.94	0.06954
6	79.43	-1.091	55.54	0.01963
7	100.00	-1.016	42.39	0.06502
8	125.89	-1.576	39.75	-0.07832
9	158.49	-1.467	47.49	-0.09999
10	199.53	1.03	52.19	-0.1781
11	251.19	1.692	94.37	-0.2364
12	316.23	2.913	147.8	-0.03055
13	398.11	1.472	123.6	0.02826
14	501.19	6.685	135.6	-0.03896
15	630.96	10.94	179.4	0.1174
16	794.33	8.818	151.9	0.06773
17	1000.00	5.442	119.5	-0.05079
18	1258.93	6.697	124.4	-0.03634
19	1584.89	4.199	105	-0.133
20	1995.26	-0.5712	68.04	0.06788
21	2511.89	-1.244	73.39	-0.01247
22	3162.28	-3.337	63.95	0.09364
23	3981.07	-4.13	49.48	0.07909
24	5011.87	-4.5	46.33	0.2359
25	6309.57	-4.977	47.57	0.3699
26	7943.28	-7.132	82.14	0.4012

4.4.3 Fan noise

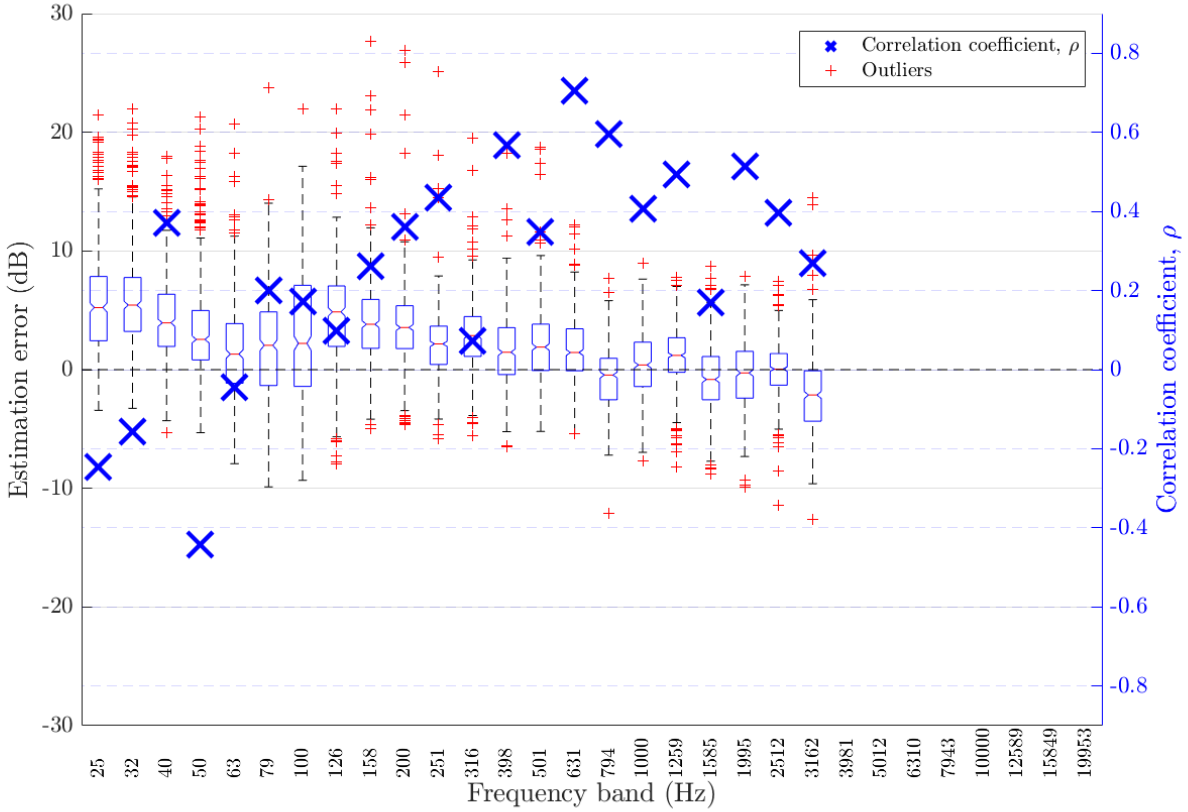

Figure 59: Frequency-dependent DRR estimation error in fan noise for all SNRs for algorithm Particle Velocity [8]

Table 55: Frequency-dependent DRR estimation error in fan noise for all SNRs for algorithm Particle Velocity [8]

Freq. band	Centre Freq. (Hz)	Bias	MSE	ρ
1	25.12	6.247	61.73	-0.2465
2	31.62	6.743	65.47	-0.1562
3	39.81	5.183	42.73	0.3718
4	50.12	3.751	37.56	-0.4414
5	63.10	1.432	22.4	-0.04497
6	79.43	1.029	18.2	0.2009
7	100.00	1.672	24.28	0.172
8	125.89	2.291	27.15	0.0991
9	158.49	2.585	21.72	0.2602
10	199.53	3.098	20.07	0.3609
11	251.19	1.77	11.01	0.4359
12	316.23	2	14.07	0.07199
13	398.11	1.204	11.06	0.5675
14	501.19	1.697	13.72	0.3477
15	630.96	1.398	10.22	0.7052
16	794.33	-1.228	11.02	0.5956
17	1000.00	-0.2778	10.02	0.4073
18	1258.93	0.7117	8.782	0.4946
19	1584.89	-0.8601	9.44	0.1695
20	1995.26	-0.6946	8.04	0.515
21	2511.89	-0.5183	7.125	0.3956
22	3162.28	-2.725	20.13	0.2696

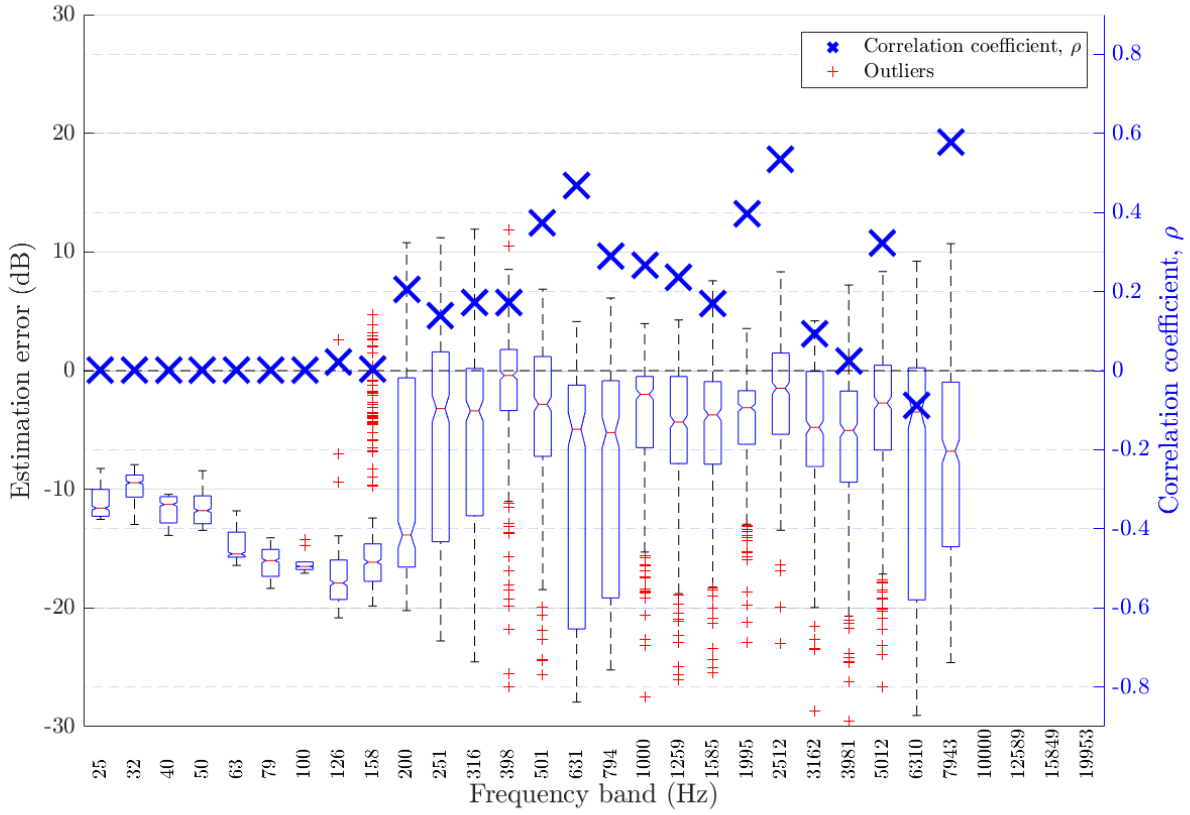

Figure 60: Frequency-dependent DRR estimation error in fan noise for all SNRs for algorithm DENBE with FFT derived subbands [7]

Table 56: Frequency-dependent DRR estimation error in fan noise for all SNRs for algorithm DENBE with FFT derived subbands [7]

Freq. band	Centre Freq. (Hz)	Bias	MSE	ρ
1	25.12	-11.07	124.4	0
2	31.62	-9.93	100.8	0
3	39.81	-11.69	138.1	0
4	50.12	-11.55	135.4	0
5	63.10	-14.82	221.5	0
6	79.43	-16.09	260.6	0
7	100.00	-16.18	262.6	0
8	125.89	-17.71	317.7	0.02099
9	158.49	-16.32	275.2	0.003448
10	199.53	-13.16	221.2	0.2047
11	251.19	-11.67	213.8	0.1388
12	316.23	-13.19	253.5	0.1732
13	398.11	-9.816	205	0.1723
14	501.19	-11.2	220.7	0.3728
15	630.96	-14.46	298.9	0.4677
16	794.33	-13.67	278.3	0.2903
17	1000.00	-10.67	209	0.2675
18	1258.93	-9.385	164.2	0.236
19	1584.89	-6.966	111.6	0.1705
20	1995.26	-6.339	76	0.3956
21	2511.89	-4.197	53.6	0.5345
22	3162.28	-5.964	68.26	0.09377
23	3981.07	-6.548	75.06	0.02546
24	5011.87	-5.8	92.28	0.322
25	6309.57	-8.89	198	-0.08916
26	7943.28	-8.902	155	0.5775

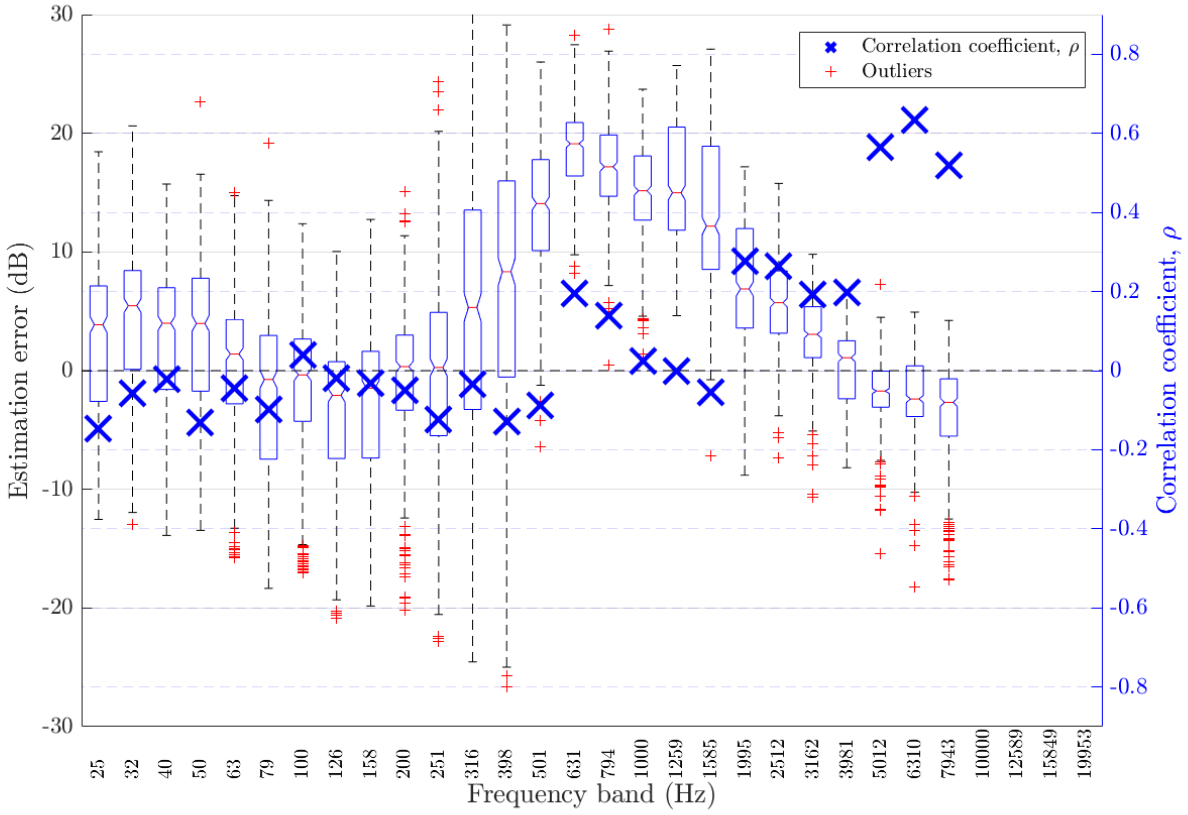

Figure 61: Frequency-dependent DRR estimation error in fan noise for all SNRs for algorithm DENBE with filtered subbands [7]

Table 57: Frequency-dependent DRR estimation error in fan noise for all SNRs for algorithm DENBE with filtered subbands [7]

Freq. band	Centre Freq. (Hz)	Bias	MSE	ρ
1	25.12	1.672	58.87	-0.1467
2	31.62	2.705	63.12	-0.05782
3	39.81	0.9042	53.73	-0.0211
4	50.12	1.413	59.08	-0.1302
5	63.10	-1.317	53.74	-0.04346
6	79.43	-3.195	77.74	-0.09915
7	100.00	-3.199	60.21	0.04029
8	125.89	-4.903	74.99	-0.01795
9	158.49	-3.928	68.95	-0.0327
10	199.53	-2.936	59.26	-0.04891
11	251.19	-3.417	81.91	-0.124
12	316.23	0.7962	123.5	-0.0336
13	398.11	2.026	123.4	-0.1288
14	501.19	7.271	138.6	-0.08914
15	630.96	13.94	237	0.196
16	794.33	12.71	208	0.1394
17	1000.00	10.09	158.5	0.02309
18	1258.93	11.91	182	-0.001627
19	1584.89	9.922	148.6	-0.05414
20	1995.26	4.237	58.22	0.2764
21	2511.89	2.256	47.98	0.2649
22	3162.28	-0.1546	32.93	0.1915
23	3981.07	-1.258	17.11	0.1974
24	5011.87	-2.383	15.33	0.5647
25	6309.57	-3.232	23.2	0.6342
26	7943.28	-4.841	44.68	0.5195

4.5 Frequency-dependent DRR estimation results by noise type and SNR

4.5.1 Ambient noise at 18 dB

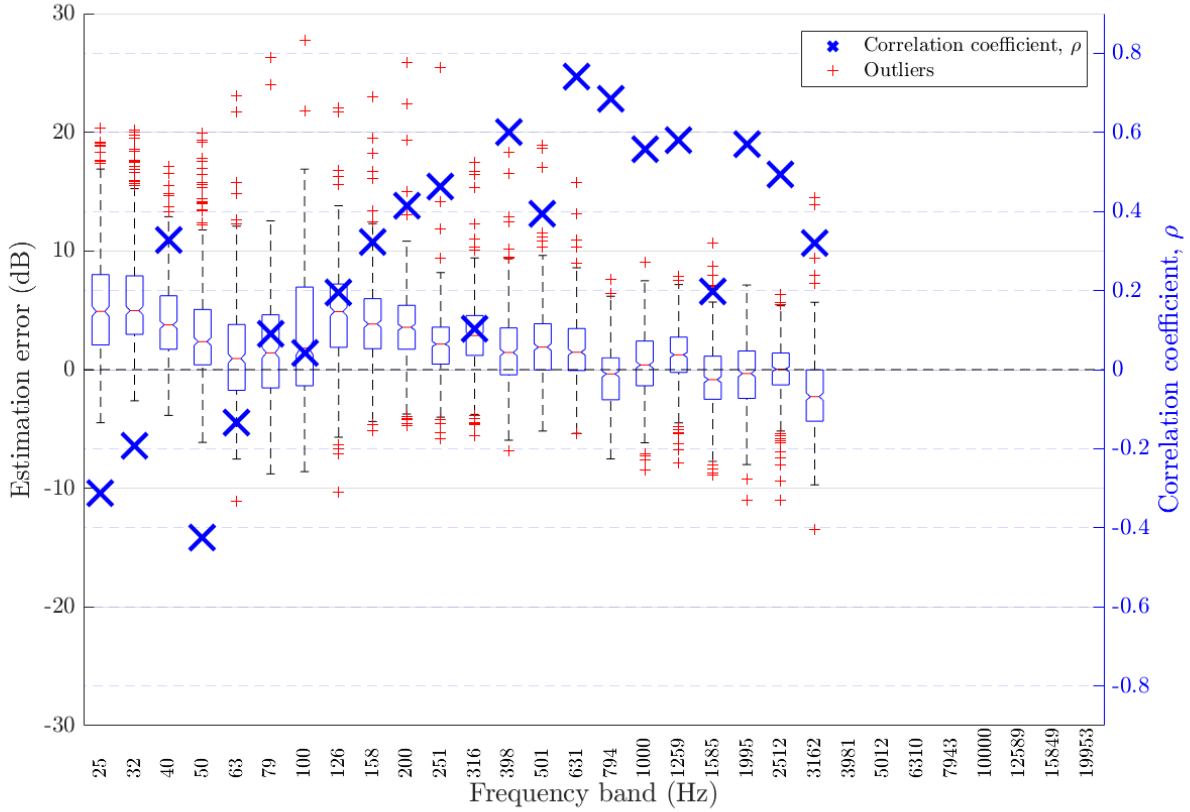

Figure 62: Frequency-dependent DRR estimation error in ambient noise at 18 dB SNR for algorithm Particle Velocity [8]

Table 58: Frequency-dependent DRR estimation error in ambient noise at $18\,\mathrm{dB}$ SNR for algorithm Particle Velocity [8]

Freq. band	Centre Freq. (Hz)	Bias	MSE	ρ
1	25.12	5.406	50.56	-0.3128
2	31.62	5.76	50.42	-0.1923
3	39.81	4.176	30.1	0.3286
4	50.12	3.073	26.77	-0.4243
5	63.10	1.351	19.74	-0.1328
6	79.43	1.491	21.83	0.08933
7	100.00	2.656	35.8	0.04144
8	125.89	4.562	38.54	0.1947
9	158.49	4.027	27.7	0.3228
10	199.53	3.599	22.6	0.4139
11	251.19	2.115	11.63	0.4632
12	316.23	2.923	16.9	0.1038
13	398.11	1.741	11.87	0.6015
14	501.19	2.165	14.94	0.3948
15	630.96	1.808	10.65	0.7419
16	794.33	-0.5607	7.33	0.6849
17	1000.00	0.5146	7.047	0.5579
18	1258.93	1.212	7.82	0.5805
19	1584.89	-0.7134	9.087	0.1987
20	1995.26	-0.4129	6.879	0.5693
21	2511.89	-0.07927	5.183	0.4921
22	3162.28	-2.098	15.07	0.3196

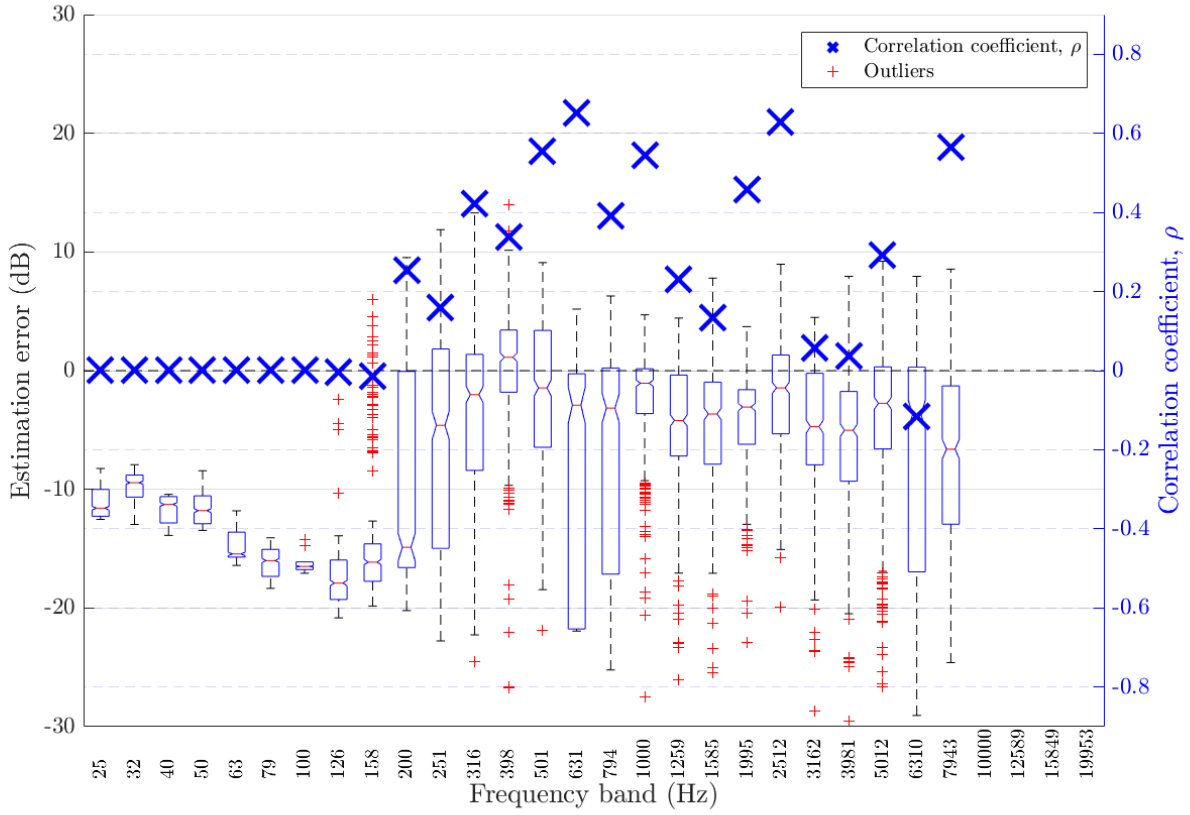

Figure 63: Frequency-dependent DRR estimation error in ambient noise at 18 dB SNR for algorithm DENBE with FFT derived subbands [7]

Table 59: Frequency-dependent DRR estimation error in ambient noise at $18\,\mathrm{dB}$ SNR for algorithm DENBE with FFT derived subbands [7]

Freq. band	Centre Freq. (Hz)	Bias	MSE	ρ
1	25.12	-11.07	124.4	0
2	31.62	-9.93	100.8	0
3	39.81	-11.69	138.1	0
4	50.12	-11.55	135.4	0
5	63.10	-14.82	221.5	0
6	79.43	-16.09	260.6	0
7	100.00	-16.18	262.6	0
8	125.89	-17.64	316.2	-0.004931
9	158.49	-15.71	264.6	-0.01359
10	199.53	-9.331	164.4	0.2525
11	251.19	-6.262	131.6	0.1594
12	316.23	-4.357	78.91	0.4217
13	398.11	0.1566	32.37	0.3379
14	501.19	-2.666	60.08	0.5553
15	630.96	-8.696	173.6	0.6512
16	794.33	-6.646	126.9	0.391
17	1000.00	-2.447	27.52	0.5453
18	1258.93	-4.887	58.83	0.2303
19	1584.89	-4.395	55.2	0.1331
20	1995.26	-4.28	33.51	0.4573
21	2511.89	-2.04	20.88	0.6292
22	3162.28	-5.056	58.67	0.05753
23	3981.07	-6.156	71.91	0.0363
24	5011.87	-5.07	88.46	0.2912
25	6309.57	-8.196	196.5	-0.1169
26	7943.28	-8.268	154.6	0.5657

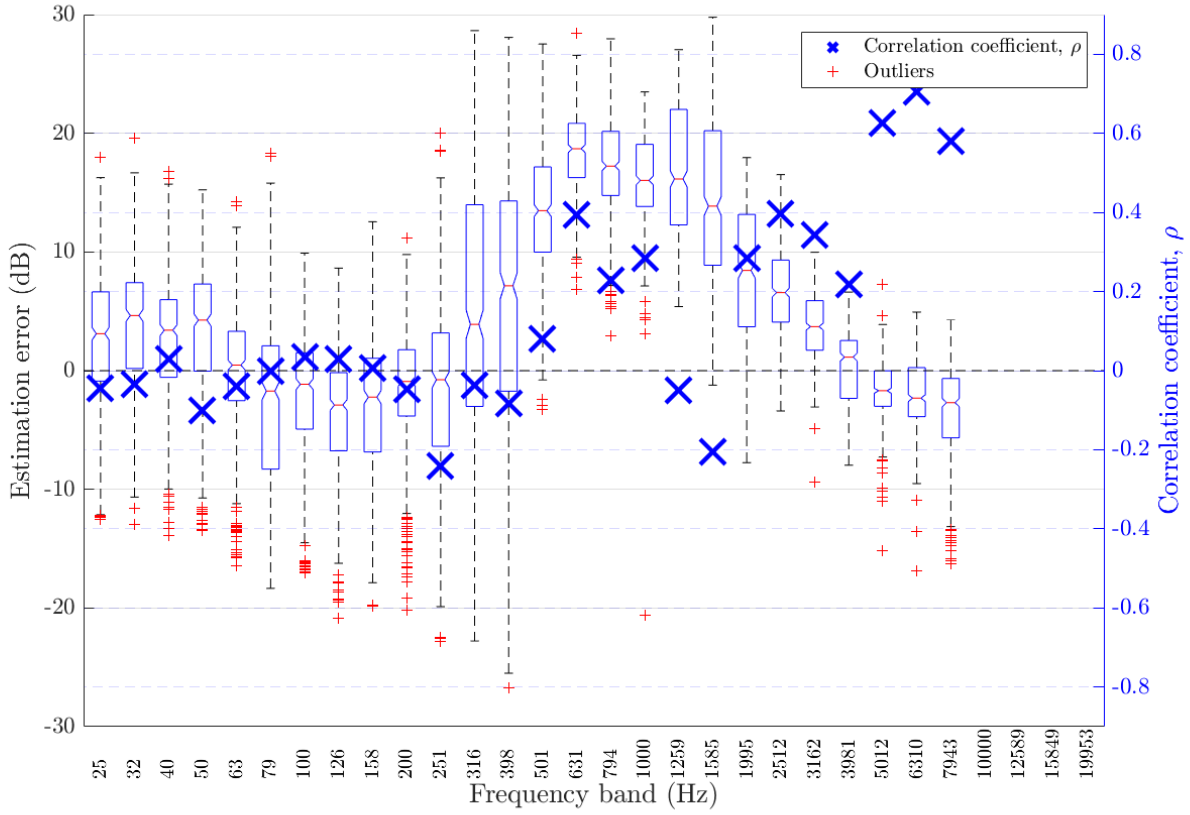

Figure 64: Frequency-dependent DRR estimation error in ambient noise at 18 dB SNR for algorithm DENBE with filtered subbands [7]

Table 60: Frequency-dependent DRR estimation error in ambient noise at $18\,\mathrm{dB}$ SNR for algorithm DENBE with filtered subbands [7]

Freq. band	Centre Freq. (Hz)	Bias	MSE	ρ
1	25.12	1.837	52.38	-0.04507
2	31.62	2.974	52.09	-0.03439
3	39.81	1.954	43.64	0.02952
4	50.12	2.518	51.84	-0.1013
5	63.10	-0.764	39.38	-0.03964
6	79.43	-3.26	68.83	-0.001419
7	100.00	-2.692	45.76	0.0342
8	125.89	-4.244	56.44	0.0283
9	158.49	-3.707	59.23	0.006268
10	199.53	-1.979	36.98	-0.04766
11	251.19	-2.019	66.38	-0.2408
12	316.23	5.004	155.8	-0.0357
13	398.11	6.548	147.9	-0.0831
14	501.19	13.46	207.7	0.08096
15	630.96	18.42	351	0.393
16	794.33	17.29	315.8	0.2286
17	1000.00	16.12	276.1	0.2841
18	1258.93	16.81	311.4	-0.04852
19	1584.89	13.99	238.4	-0.2051
20	1995.26	8.126	92.09	0.2834
21	2511.89	6.96	63.24	0.3958
22	3162.28	3.66	20.4	0.3438
23	3981.07	0.1298	8.961	0.2187
24	5011.87	-1.568	9.029	0.6269
25	6309.57	-2.109	12.11	0.7049
26	7943.28	-3.563	28.85	0.5793

4.5.2 Ambient noise at 12 dB

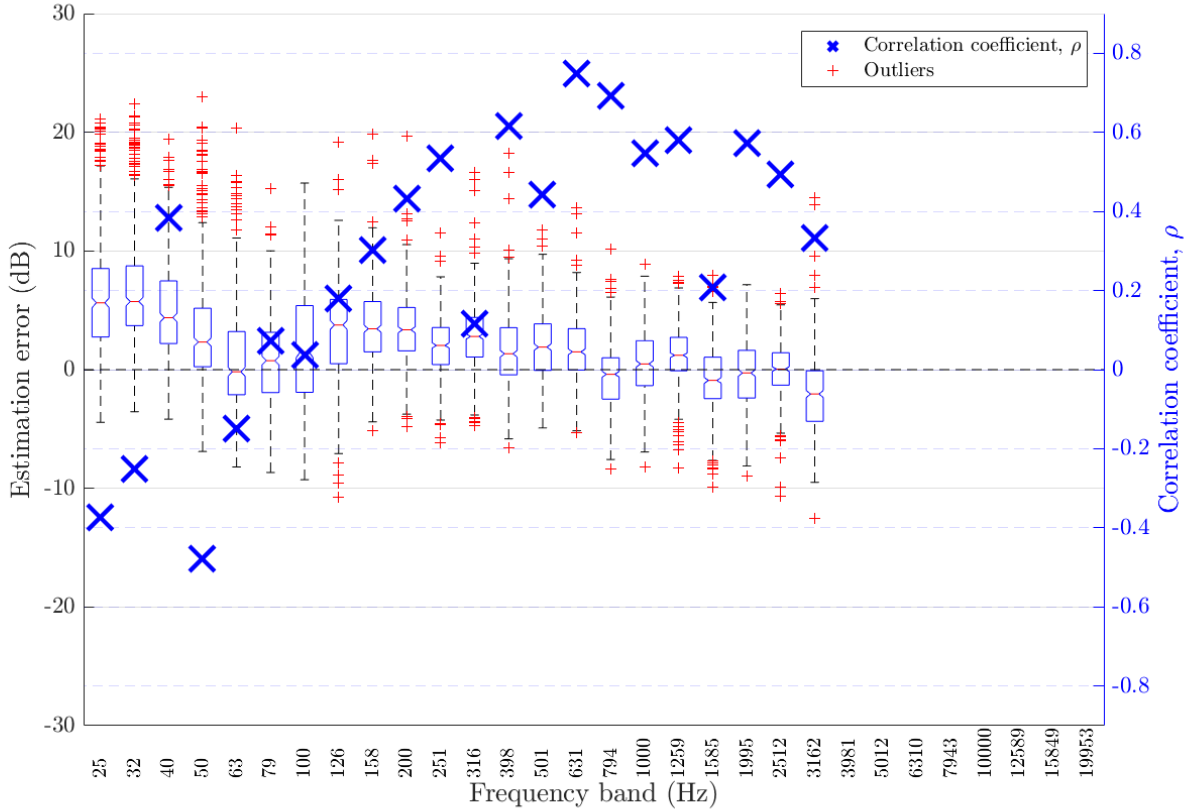

Figure 65: Frequency-dependent DRR estimation error in ambient noise at 12 dB SNR for algorithm Particle Velocity [8]

Table 61: Frequency-dependent DRR estimation error in ambient noise at $12\,\mathrm{dB}$ SNR for algorithm Particle Velocity [8]

Freq. band	Centre Freq. (Hz)	Bias	MSE	ρ
1	25.12	6.359	65.55	-0.3728
2	31.62	6.785	67.38	-0.2514
3	39.81	5.078	41.35	0.3833
4	50.12	3.373	34.39	-0.477
5	63.10	0.9007	19.91	-0.148
6	79.43	0.7675	13.97	0.07313
7	100.00	1.702	23.86	0.03628
8	125.89	3.146	26.96	0.1796
9	158.49	3.641	23.7	0.3027
10	199.53	3.398	19.63	0.4324
11	251.19	1.981	9.75	0.5344
12	316.23	2.793	15.63	0.1157
13	398.11	1.74	11.58	0.615
14	501.19	2.094	13.31	0.4419
15	630.96	1.844	10.64	0.7478
16	794.33	-0.5516	7.374	0.6916
17	1000.00	0.5537	7.12	0.5468
18	1258.93	1.225	7.833	0.5796
19	1584.89	-0.7749	8.803	0.207
20	1995.26	-0.3684	6.802	0.5722
21	2511.89	-0.07648	5.207	0.4929
22	3162.28	-2.103	14.93	0.3319

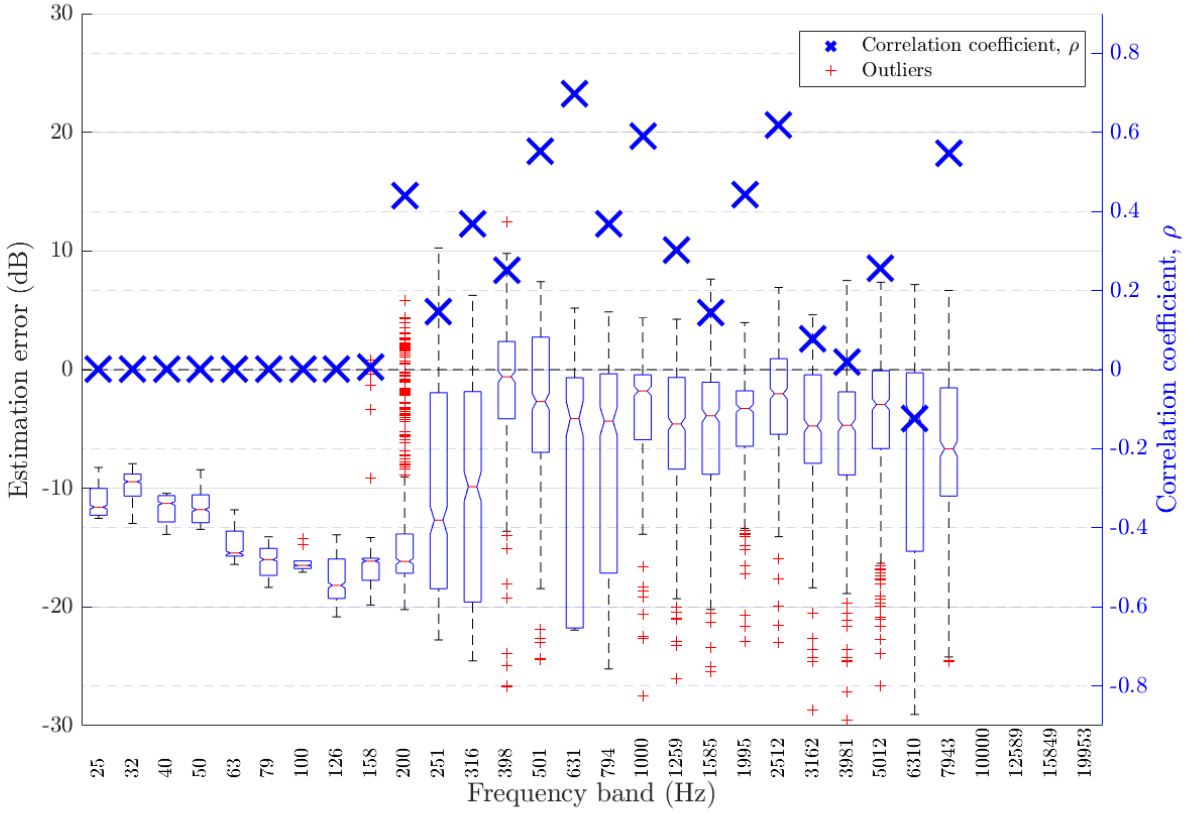

Figure 66: Frequency-dependent DRR estimation error in ambient noise at 12 dB SNR for algorithm DENBE with FFT derived subbands [7]

Table 62: Frequency-dependent DRR estimation error in ambient noise at $12\,\mathrm{dB}$ SNR for algorithm DENBE with FFT derived subbands [7]

Freq. band	Centre Freq. (Hz)	Bias	MSE	ρ
1	25.12	-11.07	124.4	0
2	31.62	-9.93	100.8	0
3	39.81	-11.69	138.1	0
4	50.12	-11.55	135.4	0
5	63.10	-14.82	221.5	0
6	79.43	-16.09	260.6	0
7	100.00	-16.18	262.6	0
8	125.89	-17.74	318.4	0
9	158.49	-16.61	280.5	0.005537
10	199.53	-13.41	220.1	0.441
11	251.19	-10.38	190	0.1459
12	316.23	-9.938	174.8	0.3679
13	398.11	-1.624	44.07	0.252
14	501.19	-3.547	67.21	0.5522
15	630.96	-9.559	187.6	0.6975
16	794.33	-7.938	149.4	0.3693
17	1000.00	-4.081	53.3	0.5898
18	1258.93	-5.65	72.35	0.3011
19	1584.89	-4.762	61.11	0.1436
20	1995.26	-4.527	37.28	0.4416
21	2511.89	-2.455	24.07	0.6174
22	3162.28	-5.193	61.14	0.07716
23	3981.07	-6.199	73.04	0.02002
24	5011.87	-5.401	89.86	0.2552
25	6309.57	-8.351	189.6	-0.1232
26	7943.28	-8.355	147.1	0.548

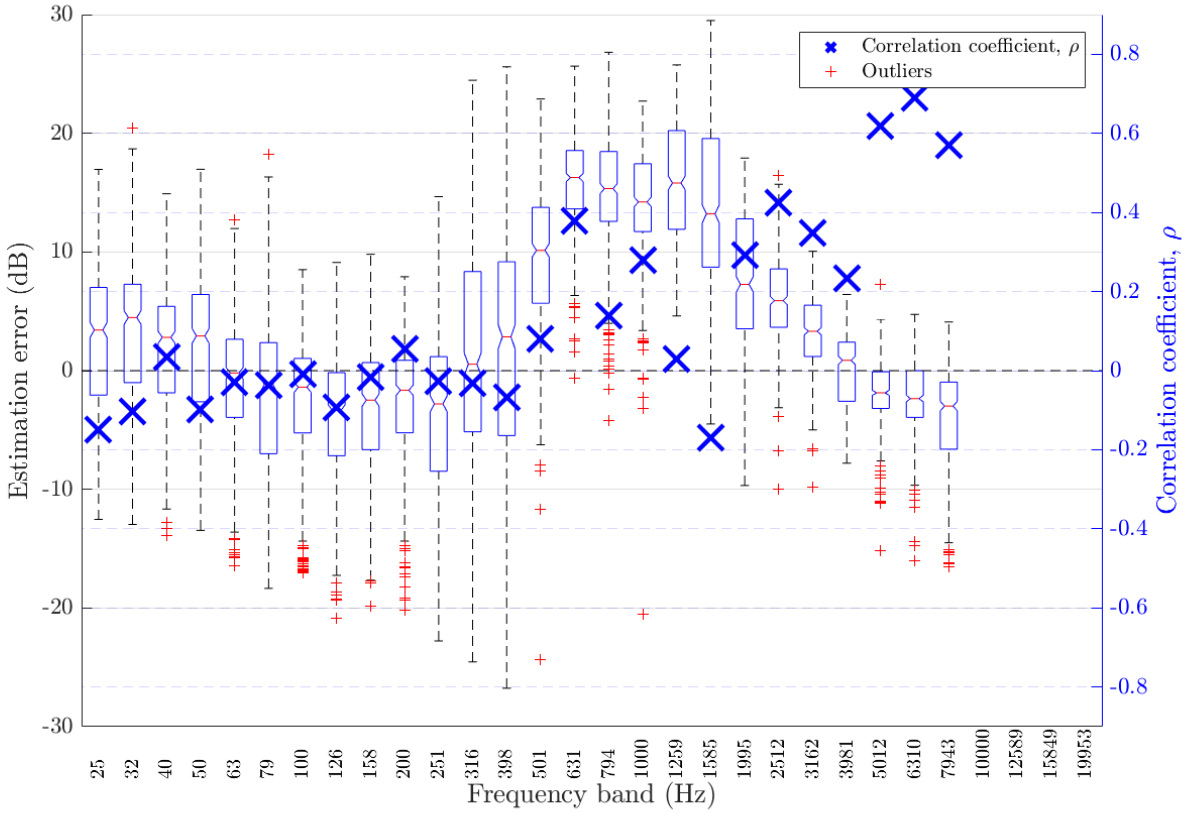

Figure 67: Frequency-dependent DRR estimation error in ambient noise at 12 dB SNR for algorithm DENBE with filtered subbands [7]

Table 63: Frequency-dependent DRR estimation error in ambient noise at $12\,\mathrm{dB}$ SNR for algorithm DENBE with filtered subbands [7]

Freq. band	Centre Freq. (Hz)	Bias	MSE	ρ
1	25.12	1.669	58.18	-0.1503
2	31.62	2.594	56.2	-0.1029
3	39.81	0.9571	42.32	0.03507
4	50.12	1.207	50.29	-0.0987
5	63.10	-1.482	45.9	-0.03009
6	79.43	-2.647	66.96	-0.03601
7	100.00	-3.125	49.47	-0.008729
8	125.89	-4.407	58.81	-0.09237
9	158.49	-3.911	59.85	-0.01577
10	199.53	-3.022	44.1	0.05573
11	251.19	-4.229	70.15	-0.0268
12	316.23	1.125	107.4	-0.03246
13	398.11	2.161	96.84	-0.06773
14	501.19	9.611	127.5	0.0791
15	630.96	15.92	268.8	0.378
16	794.33	15.2	257.1	0.1393
17	1000.00	14.07	220.2	0.2787
18	1258.93	16.03	280.8	0.0291
19	1584.89	13.58	225.9	-0.1685
20	1995.26	7.663	85.47	0.291
21	2511.89	6.253	54.61	0.424
22	3162.28	3.143	18.42	0.3489
23	3981.07	-0.07644	9.101	0.2326
24	5011.87	-1.73	9.988	0.6178
25	6309.57	-2.318	13.71	0.6894
26	7943.28	-3.937	32.1	0.571

4.5.3 Ambient noise at $-1\,\mathrm{dB}$

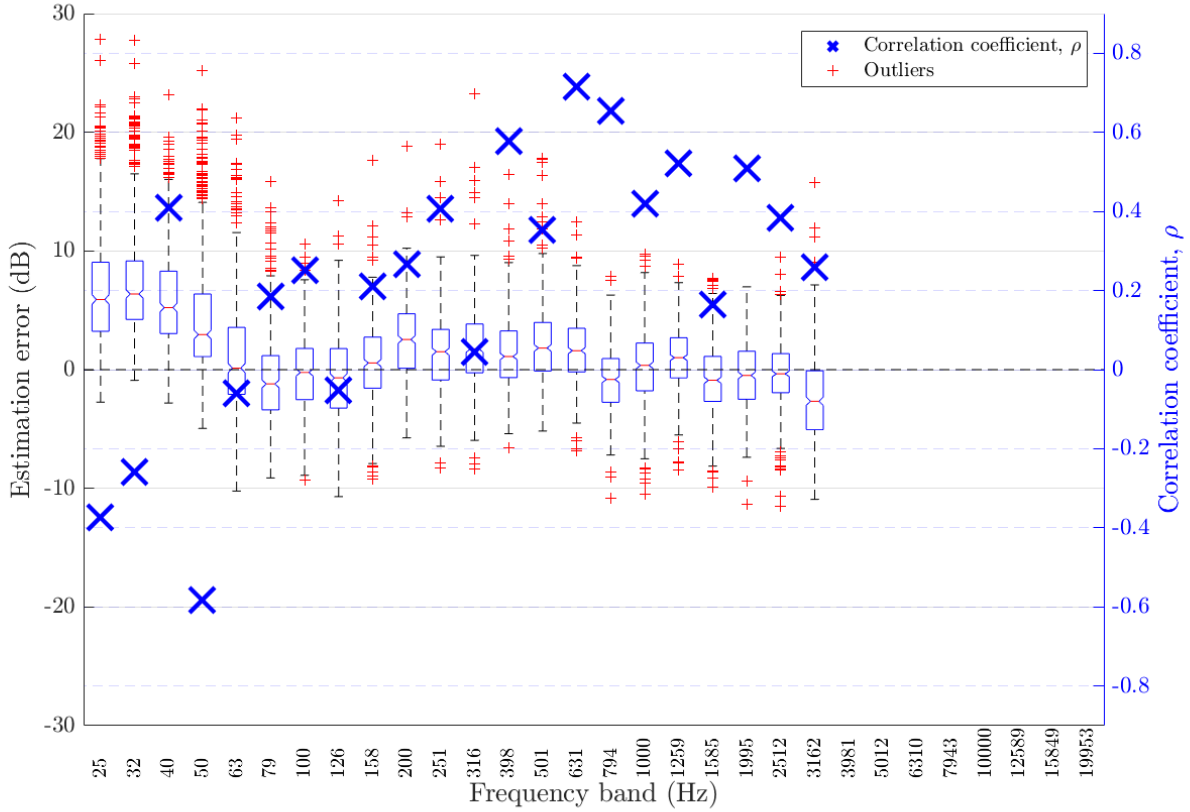

Figure 68: Frequency-dependent DRR estimation error in ambient noise at $-1\,\mathrm{dB}$ SNR for algorithm Particle Velocity [8]

Table 64: Frequency-dependent DRR estimation error in ambient noise at $-1\,\mathrm{dB}$ SNR for algorithm Particle Velocity [8]

Freq. band	Centre Freq. (Hz)	Bias	MSE	ρ
1	25.12	6.877	75.1	-0.3746
2	31.62	7.523	81	-0.2588
3	39.81	6.169	56.59	0.4088
4	50.12	4.622	51.43	-0.5833
5	63.10	1.25	25.48	-0.05929
6	79.43	-0.7251	15.61	0.1846
7	100.00	-0.3289	11.11	0.2517
8	125.89	-0.6238	15.06	-0.05141
9	158.49	0.5003	12.24	0.2103
10	199.53	2.328	16.54	0.2667
11	251.19	1.354	12.72	0.4064
12	316.23	1.816	14.92	0.04348
13	398.11	1.468	11.99	0.5772
14	501.19	2.222	16.97	0.3531
15	630.96	1.801	11.3	0.7141
16	794.33	-0.8585	8.804	0.6549
17	1000.00	0.2432	9.689	0.4193
18	1258.93	1.016	8.424	0.5203
19	1584.89	-0.7994	10.19	0.1657
20	1995.26	-0.4474	7.949	0.5098
21	2511.89	-0.4781	7.765	0.3828
22	3162.28	-2.465	19.17	0.26

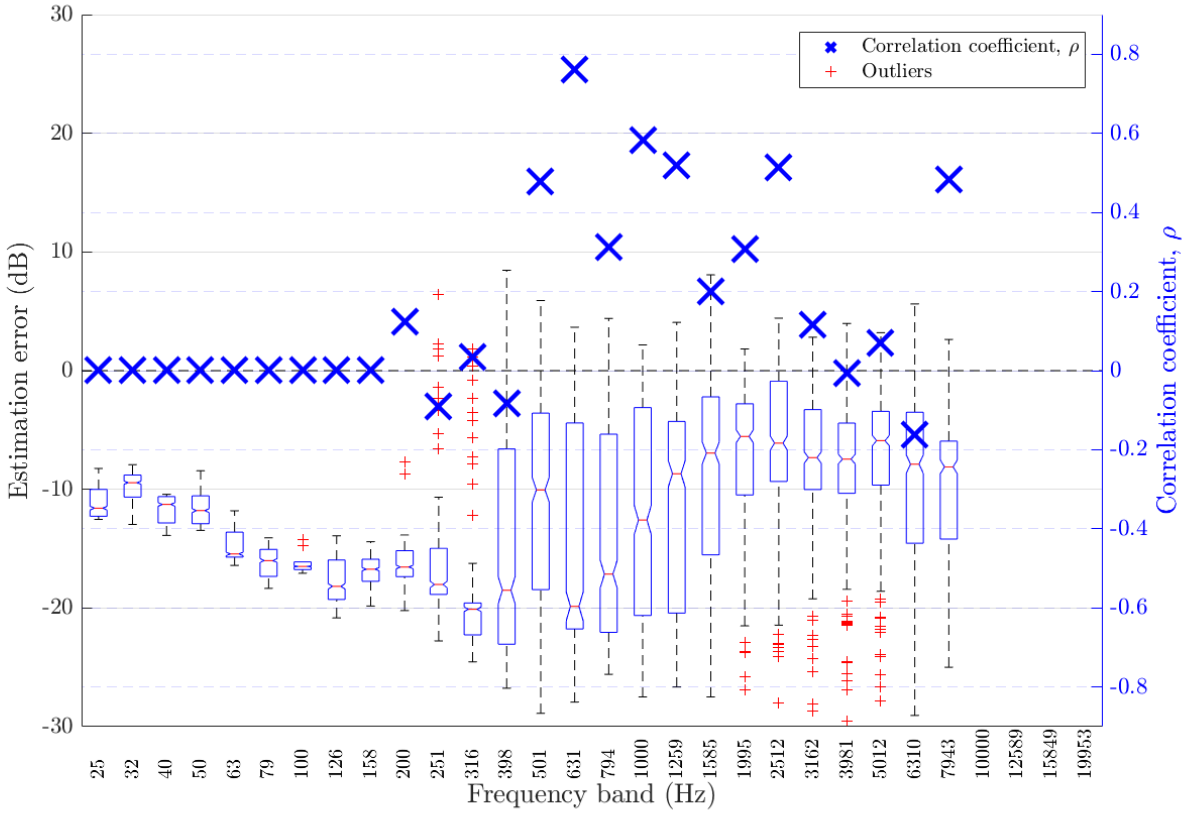

Figure 69: Frequency-dependent DRR estimation error in ambient noise at -1 dB SNR for algorithm DENBE with FFT derived subbands [7]

Table 65: Frequency-dependent DRR estimation error in ambient noise at $-1\,\mathrm{dB}$ SNR for algorithm DENBE with FFT derived subbands [7]

Freq. band	Centre Freq. (Hz)	Bias	MSE	ρ
1	25.12	-11.07	124.4	0
2	31.62	-9.93	100.8	0
3	39.81	-11.69	138.1	0
4	50.12	-11.55	135.4	0
5	63.10	-14.82	221.5	0
6	79.43	-16.09	260.6	0
7	100.00	-16.18	262.6	0
8	125.89	-17.74	318.4	0
9	158.49	-16.76	283.2	0
10	199.53	-16.67	281.5	0.1229
11	251.19	-17.36	317	-0.09157
12	316.23	-19.59	400.4	0.03542
13	398.11	-15.32	331.3	-0.08202
14	501.19	-11.24	210	0.4774
15	630.96	-13.65	266.7	0.7611
16	794.33	-14.31	287.1	0.3133
17	1000.00	-12.41	234	0.5832
18	1258.93	-11.14	191	0.5185
19	1584.89	-8.548	142.1	0.1992
20	1995.26	-7.744	105.6	0.307
21	2511.89	-6.79	92.29	0.5136
22	3162.28	-7.42	88.62	0.1148
23	3981.07	-8.258	101.1	-0.007562
24	5011.87	-7.411	92.54	0.06913
25	6309.57	-10.52	193.5	-0.1615
26	7943.28	-10.32	151.4	0.4823

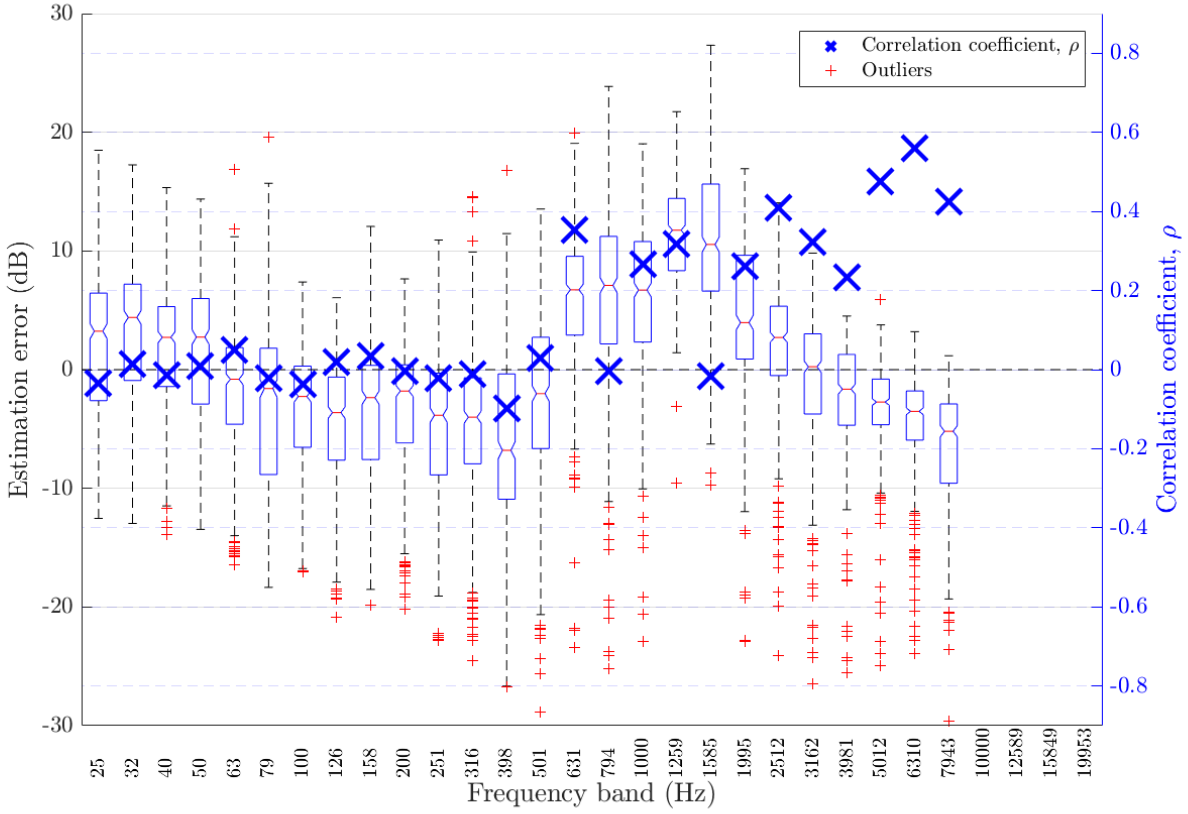

Figure 70: Frequency-dependent DRR estimation error in ambient noise at $-1\,\mathrm{dB}$ SNR for algorithm DENBE with filtered subbands [7]

Table 66: Frequency-dependent DRR estimation error in ambient noise at $-1\,\mathrm{dB}$ SNR for algorithm DENBE with filtered subbands [7]

Freq. band	Centre Freq. (Hz)	Bias	MSE	ρ
1	25.12	1.475	54.36	-0.034
2	31.62	2.572	52.8	0.01495
3	39.81	1.155	40.57	-0.013
4	50.12	1.02	48.62	0.01018
5	63.10	-2.08	44.58	0.05004
6	79.43	-3.417	70.46	-0.02126
7	100.00	-3.875	52.12	-0.03701
8	125.89	-5.134	66.23	0.01959
9	158.49	-4.026	63.19	0.03421
10	199.53	-3.621	52.36	-0.004437
11	251.19	-5.054	71.9	-0.02234
12	316.23	-4.934	74.52	-0.01068
13	398.11	-6.586	109.8	-0.09895
14	501.19	-2.527	60.51	0.02878
15	630.96	5.978	68.93	0.3528
16	794.33	6.295	108.7	-0.004775
17	1000.00	6.022	83.15	0.2673
18	1258.93	11.5	150.1	0.3178
19	1584.89	10.63	158.3	-0.0164
20	1995.26	4.64	63.46	0.2619
21	2511.89	1.932	35.3	0.41
22	3162.28	-0.9033	36.01	0.3213
23	3981.07	-2.209	25.19	0.2336
24	5011.87	-3.17	24.71	0.4751
25	6309.57	-4.261	33.77	0.5598
26	7943.28	-6.688	70.49	0.4238

4.5.4 Babble noise at 18 dB

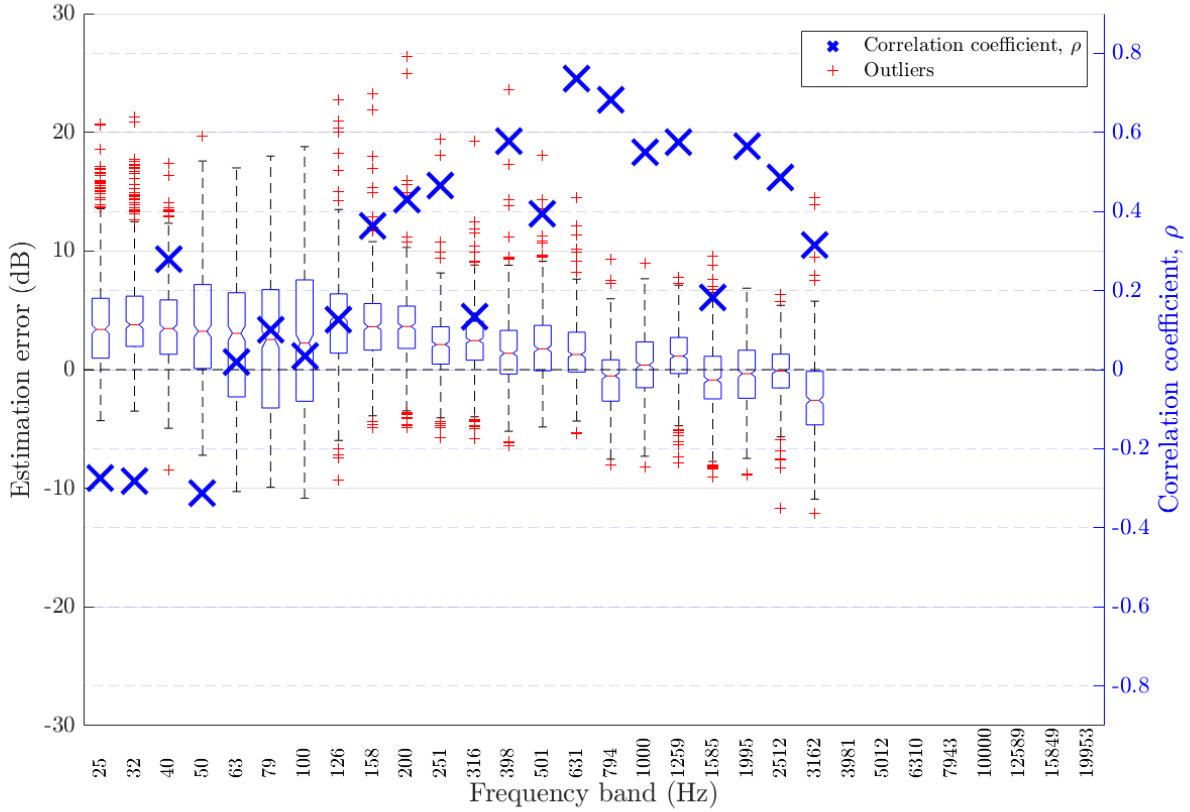

Figure 71: Frequency-dependent DRR estimation error in babble noise at 18 dB SNR for algorithm Particle Velocity [8]

Table 67: Frequency-dependent DRR estimation error in babble noise at $18\,\mathrm{dB}$ SNR for algorithm Particle Velocity [8]

Freq. band	Centre Freq. (Hz)	Bias	MSE	ρ
1	25.12	4.045	36.66	-0.2731
2	31.62	4.636	38.22	-0.2818
3	39.81	3.781	27.1	0.2794
4	50.12	3.692	34.92	-0.3127
5	63.10	2.471	33.61	0.02033
6	79.43	1.976	35.13	0.1008
7	100.00	2.378	40.53	0.03389
8	125.89	3.913	34.6	0.1254
9	158.49	3.809	25.51	0.3629
10	199.53	3.569	22.52	0.429
11	251.19	2.058	11.08	0.4648
12	316.23	2.475	13.74	0.135
13	398.11	1.681	12.31	0.5766
14	501.19	2.033	13.76	0.3938
15	630.96	1.622	9.909	0.7345
16	794.33	-0.6727	7.534	0.6814
17	1000.00	0.4143	7.104	0.5483
18	1258.93	1.114	7.761	0.5754
19	1584.89	-0.7544	9.169	0.1823
20	1995.26	-0.4273	6.97	0.5643
21	2511.89	-0.2249	5.301	0.4866
22	3162.28	-2.361	17.19	0.3143

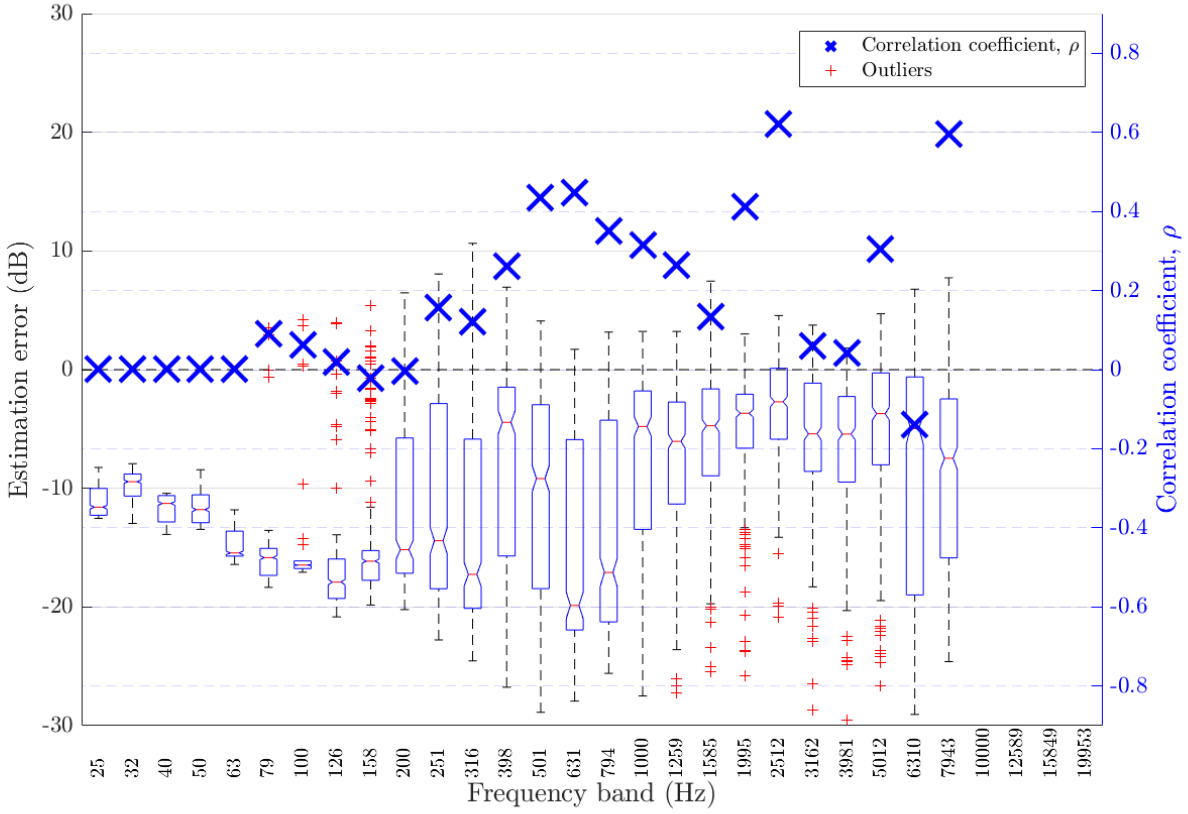

Figure 72: Frequency-dependent DRR estimation error in babble noise at 18 dB SNR for algorithm DENBE with FFT derived subbands [7]

Table 68: Frequency-dependent DRR estimation error in babble noise at $18\,\mathrm{dB}$ SNR for algorithm DENBE with FFT derived subbands [7]

Freq. band	Centre Freq. (Hz)	Bias	MSE	ρ
1	25.12	-11.07	124.4	0
2	31.62	-9.93	100.8	0
3	39.81	-11.69	138.1	0
4	50.12	-11.55	135.4	0
5	63.10	-14.82	221.5	0
6	79.43	-15.93	258	0.08941
7	100.00	-16.01	260.1	0.06148
8	125.89	-17.43	312.4	0.01814
9	158.49	-15.95	268.6	-0.02279
10	199.53	-12.17	204.7	-0.003117
11	251.19	-11.13	194	0.1571
12	316.23	-13.89	263.9	0.1212
13	398.11	-7.772	133.8	0.2609
14	501.19	-10.58	185.7	0.4345
15	630.96	-14.55	282.7	0.448
16	794.33	-13.03	248.9	0.3505
17	1000.00	-8.092	135.7	0.315
18	1258.93	-7.993	116.8	0.2627
19	1584.89	-5.421	70.28	0.1349
20	1995.26	-4.894	42.14	0.4116
21	2511.89	-3.024	27.58	0.6217
22	3162.28	-5.777	64.58	0.05932
23	3981.07	-6.629	74.89	0.0429
24	5011.87	-5.767	88.67	0.3052
25	6309.57	-9.303	208.7	-0.1381
26	7943.28	-9.405	165.6	0.5956

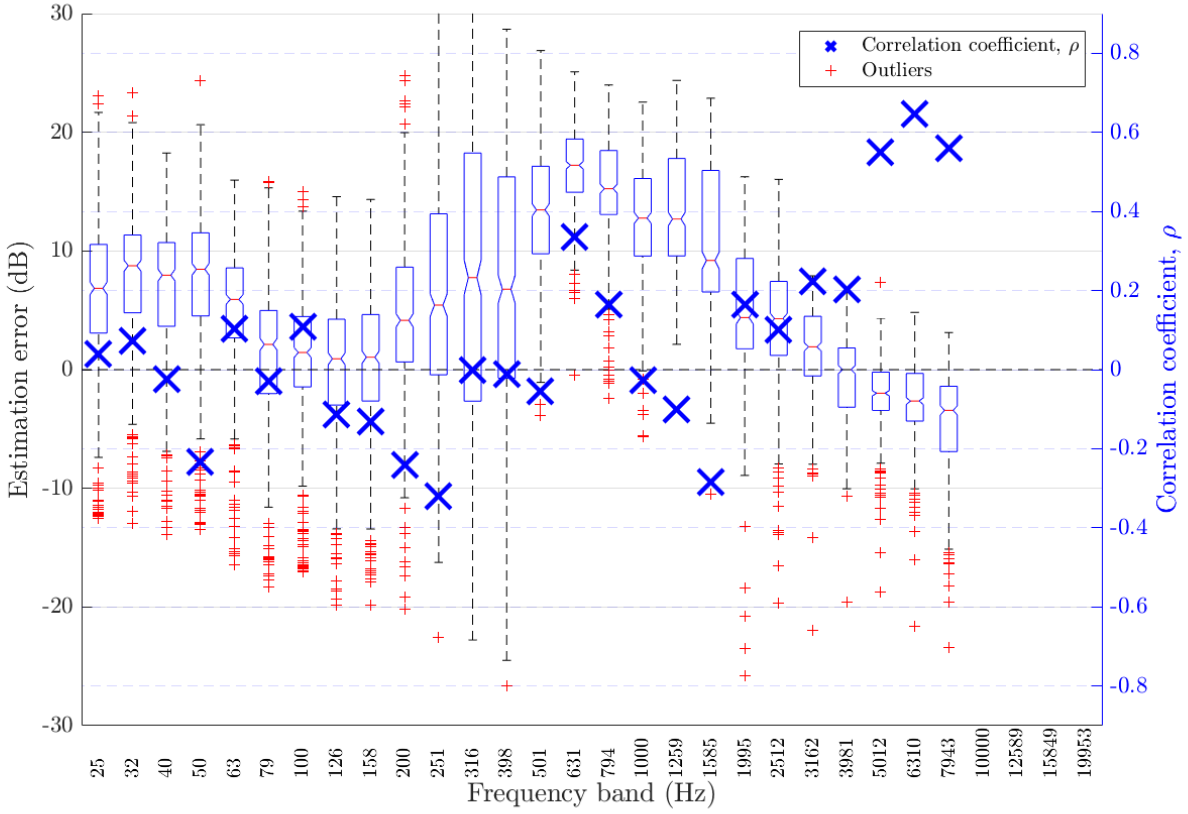

Figure 73: Frequency-dependent DRR estimation error in babble noise at 18 dB SNR for algorithm DENBE with filtered subbands [7]

Table 69: Frequency-dependent DRR estimation error in babble noise at $18\,\mathrm{dB}$ SNR for algorithm DENBE with filtered subbands [7]

Freq. band	Centre Freq. (Hz)	Bias	MSE	ρ
1	25.12	5.806	87.23	0.03839
2	31.62	7.379	102	0.07329
3	39.81	6.041	84.26	-0.02312
4	50.12	6.841	101.5	-0.2325
5	63.10	4.888	59.84	0.1023
6	79.43	0.7027	51.13	-0.02964
7	100.00	0.5538	42.13	0.1081
8	125.89	0.3938	32.13	-0.1125
9	158.49	0.007819	48.47	-0.1312
10	199.53	4.481	68.56	-0.2401
11	251.19	6.531	130.1	-0.3197
12	316.23	8.028	203.7	-0.00221
13	398.11	7.136	156.2	-0.0126
14	501.19	13.5	214	-0.05445
15	630.96	16.96	298	0.3353
16	794.33	15.16	248.7	0.1636
17	1000.00	12.61	184.9	-0.027
18	1258.93	13.49	205.5	-0.09952
19	1584.89	10.46	149.7	-0.2832
20	1995.26	5.049	56.02	0.165
21	2511.89	4.132	46.24	0.1014
22	3162.28	1.57	16.45	0.2225
23	3981.07	-0.7083	10.32	0.202
24	5011.87	-1.98	12.09	0.5492
25	6309.57	-2.584	15.93	0.6471
26	7943.28	-4.422	37.51	0.5584

4.5.5 Babble noise at 12 dB

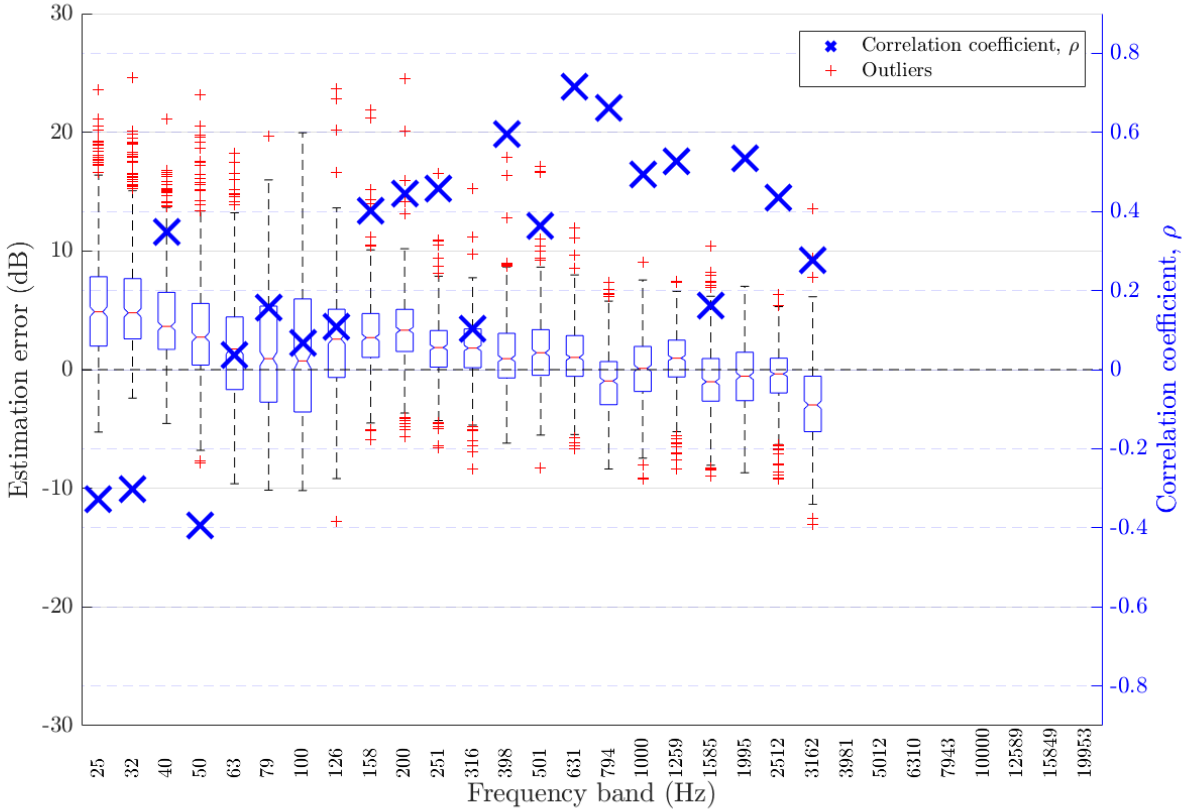

Figure 74: Frequency-dependent DRR estimation error in babble noise at 12 dB SNR for algorithm Particle Velocity [8]

Table 70: Frequency-dependent DRR estimation error in babble noise at $12\,\mathrm{dB}$ SNR for algorithm Particle Velocity [8]

Freq. band	Centre Freq. (Hz)	Bias	MSE	ρ
1	25.12	5.482	55.83	-0.3274
2	31.62	5.822	56.2	-0.3022
3	39.81	4.336	34.14	0.3476
4	50.12	3.396	33.47	-0.3935
5	63.10	1.658	24.62	0.03637
6	79.43	1.107	25	0.1574
7	100.00	1.103	32.27	0.06681
8	125.89	2.188	24.99	0.1081
9	158.49	2.996	18.72	0.4028
10	199.53	3.309	19.73	0.4446
11	251.19	1.789	9.746	0.4576
12	316.23	1.709	10.74	0.1024
13	398.11	1.258	9.83	0.5957
14	501.19	1.646	12.84	0.3629
15	630.96	1.158	8.498	0.7151
16	794.33	-1.016	8.382	0.6615
17	1000.00	0.07851	7.85	0.493
18	1258.93	0.8271	8.021	0.5276
19	1584.89	-0.86	9.62	0.1607
20	1995.26	-0.6218	7.38	0.5351
21	2511.89	-0.5907	6.343	0.4349
22	3162.28	-2.899	20.86	0.2771

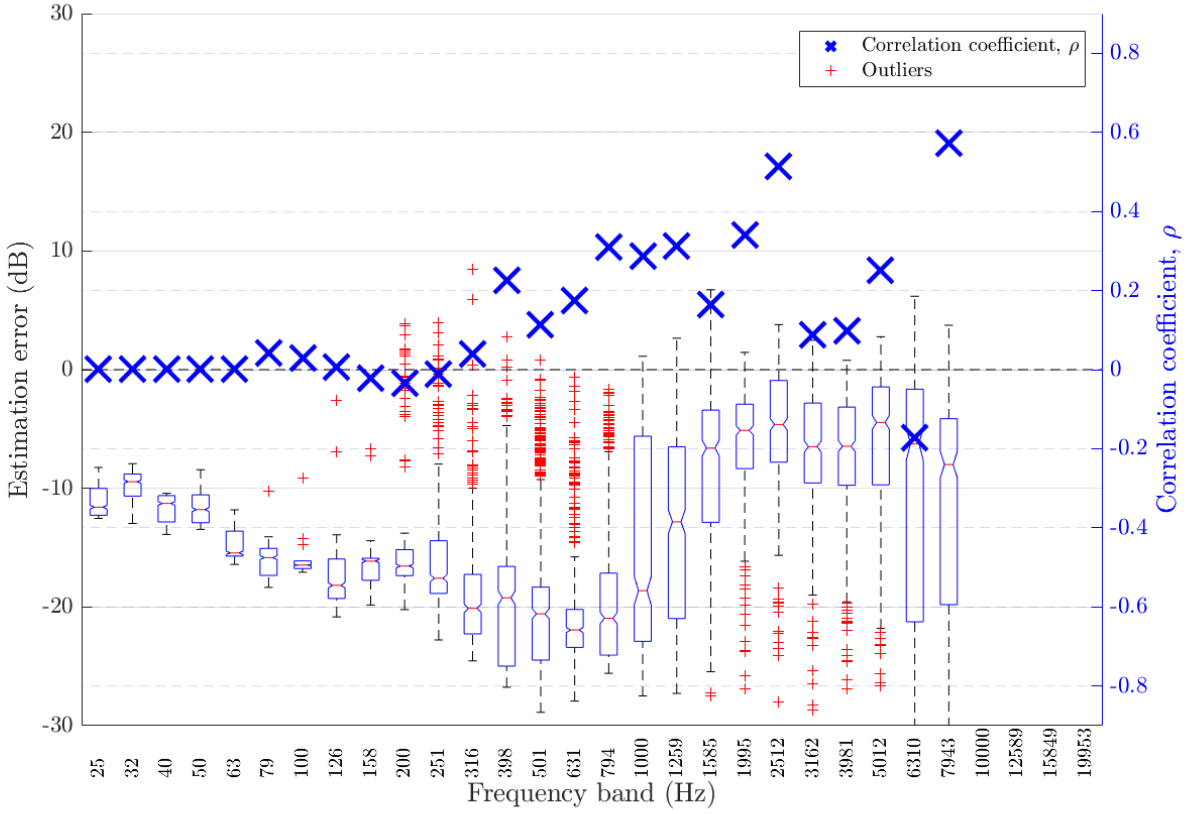

Figure 75: Frequency-dependent DRR estimation error in babble noise at 12 dB SNR for algorithm DENBE with FFT derived subbands [7]

Table 71: Frequency-dependent DRR estimation error in babble noise at $12\,\mathrm{dB}$ SNR for algorithm DENBE with FFT derived subbands [7]

Freq. band	Centre Freq. (Hz)	Bias	MSE	ρ
1	25.12	-11.07	124.4	0
2	31.62	-9.93	100.8	0
3	39.81	-11.69	138.1	0
4	50.12	-11.55	135.4	0
5	63.10	-14.82	221.5	0
6	79.43	-16.08	260.2	0.04283
7	100.00	-16.17	262.2	0.02861
8	125.89	-17.69	317.2	0.005174
9	158.49	-16.71	282.2	-0.02086
10	199.53	-15.94	269.6	-0.03566
11	251.19	-16.65	301.1	-0.01128
12	316.23	-19.11	387.2	0.03975
13	398.11	-18.8	396.7	0.2256
14	501.19	-19.24	420.6	0.1147
15	630.96	-21.17	472.8	0.1755
16	794.33	-18.92	396.4	0.3108
17	1000.00	-14.59	291.2	0.2861
18	1258.93	-13.35	243.5	0.3114
19	1584.89	-8.363	129.6	0.1655
20	1995.26	-6.422	68.93	0.3393
21	2511.89	-5.361	65.83	0.5141
22	3162.28	-7.194	90.5	0.08875
23	3981.07	-7.182	78.57	0.09841
24	5011.87	-6.73	97.75	0.2507
25	6309.57	-10.37	222.9	-0.1724
26	7943.28	-10.38	177.2	0.5722

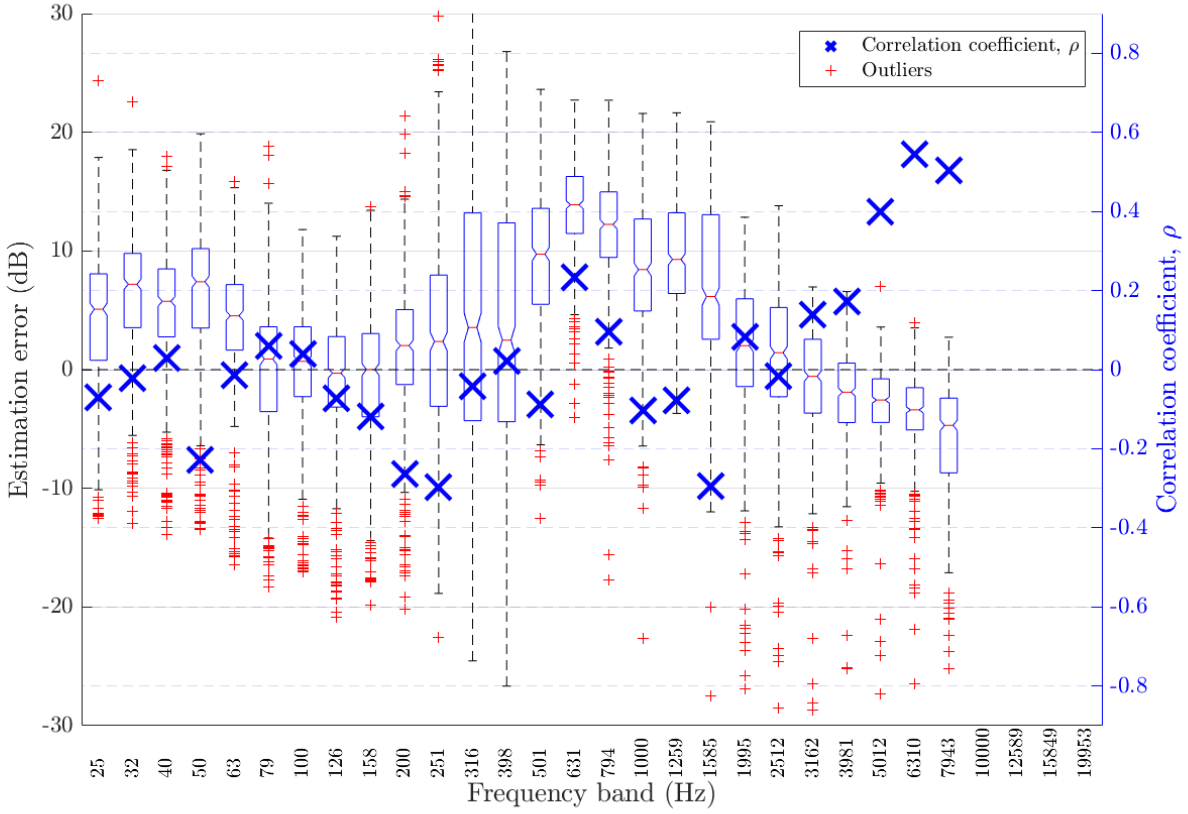

Figure 76: Frequency-dependent DRR estimation error in babble noise at 12 dB SNR for algorithm DENBE with filtered subbands [7]

Table 72: Frequency-dependent DRR estimation error in babble noise at $12\,\mathrm{dB}$ SNR for algorithm DENBE with filtered subbands [7]

Freq. band	Centre Freq. (Hz)	Bias	MSE	ρ
1	25.12	3.524	66.65	-0.06888
2	31.62	5.514	77.91	-0.02182
3	39.81	4.343	61.66	0.02824
4	50.12	5.904	80.68	-0.2271
5	63.10	3.685	49.25	-0.01334
6	79.43	-0.9334	53.69	0.06042
7	100.00	-0.5737	42.67	0.03834
8	125.89	-0.8532	34.69	-0.0728
9	158.49	-1.069	42.45	-0.1184
10	199.53	1.487	43.47	-0.2627
11	251.19	2.52	83.89	-0.2978
12	316.23	4.068	154.6	-0.04307
13	398.11	2.982	117.9	0.02072
14	501.19	9.457	129.7	-0.08717
15	630.96	13.69	202.7	0.2336
16	794.33	11.74	165.6	0.09492
17	1000.00	8.25	105	-0.1032
18	1258.93	9.81	119	-0.07773
19	1584.89	6.89	94.54	-0.2943
20	1995.26	1.502	44.69	0.08286
21	2511.89	0.6092	51.5	-0.01732
22	3162.28	-1.282	28.89	0.1388
23	3981.07	-2.301	19.14	0.1732
24	5011.87	-2.819	20.37	0.399
25	6309.57	-3.532	24.85	0.5454
26	7943.28	-6.014	59.4	0.5041

4.5.6 Babble noise at $-1\,\mathrm{dB}$

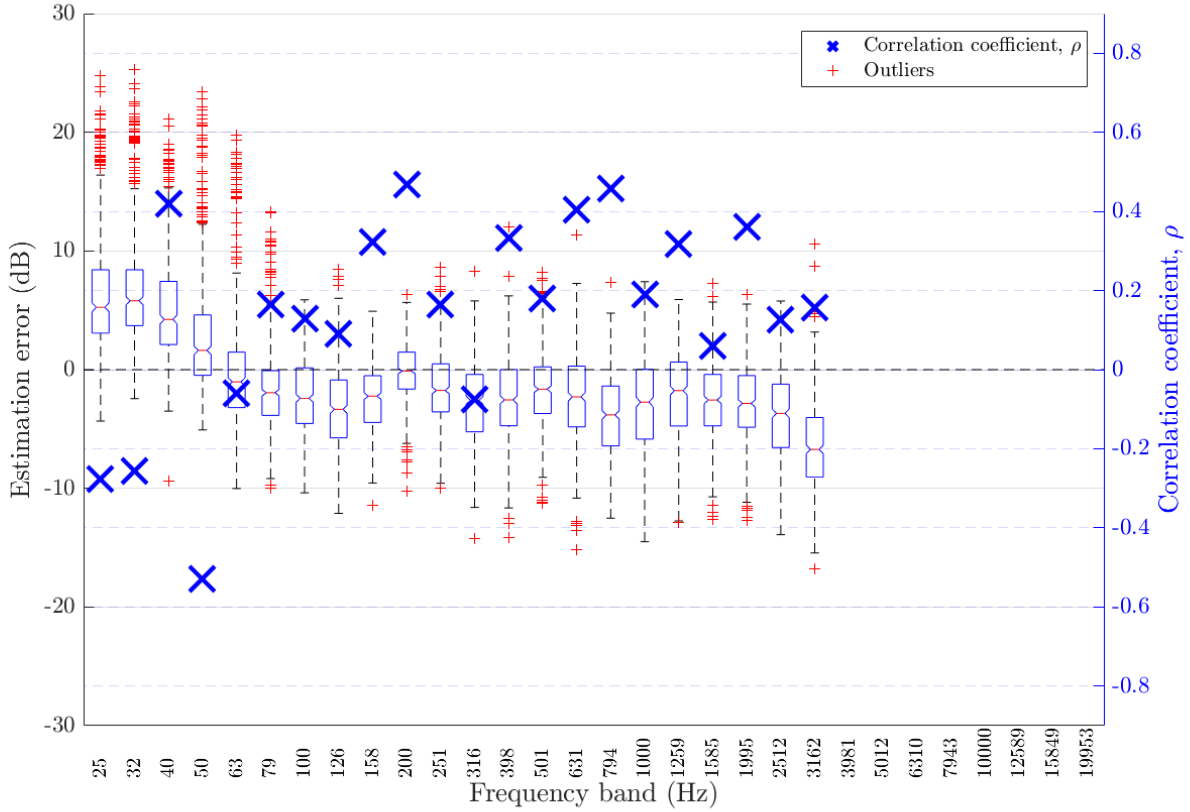

Figure 77: Frequency-dependent DRR estimation error in babble noise at $-1\,\mathrm{dB}$ SNR for algorithm Particle Velocity [8]

Table 73: Frequency-dependent DRR estimation error in babble noise at $-1\,\mathrm{dB}$ SNR for algorithm Particle Velocity [8]

Freq. band	Centre Freq. (Hz)	Bias	MSE	ρ
1	25.12	6.323	66.56	-0.2761
2	31.62	6.835	72.08	-0.2555
3	39.81	5.145	46.98	0.4187
4	50.12	3.207	42.64	-0.5288
5	63.10	-0.1255	24.6	-0.06066
6	79.43	-1.725	16.34	0.1651
7	100.00	-2.144	15.57	0.1279
8	125.89	-3.258	22.74	0.09127
9	158.49	-2.464	14.01	0.3215
10	199.53	-0.2192	5.897	0.4681
11	251.19	-1.513	11.62	0.1635
12	316.23	-2.78	19.64	-0.07476
13	398.11	-2.431	18.16	0.3329
14	501.19	-1.644	13.88	0.1786
15	630.96	-2.345	18.68	0.4048
16	794.33	-3.904	27.58	0.4582
17	1000.00	-2.931	23.96	0.1891
18	1258.93	-2.109	18.97	0.3171
19	1584.89	-2.538	17.33	0.05895
20	1995.26	-2.865	17.91	0.3615
21	2511.89	-4.041	28.95	0.1254
22	3162.28	-6.447	56.19	0.1557

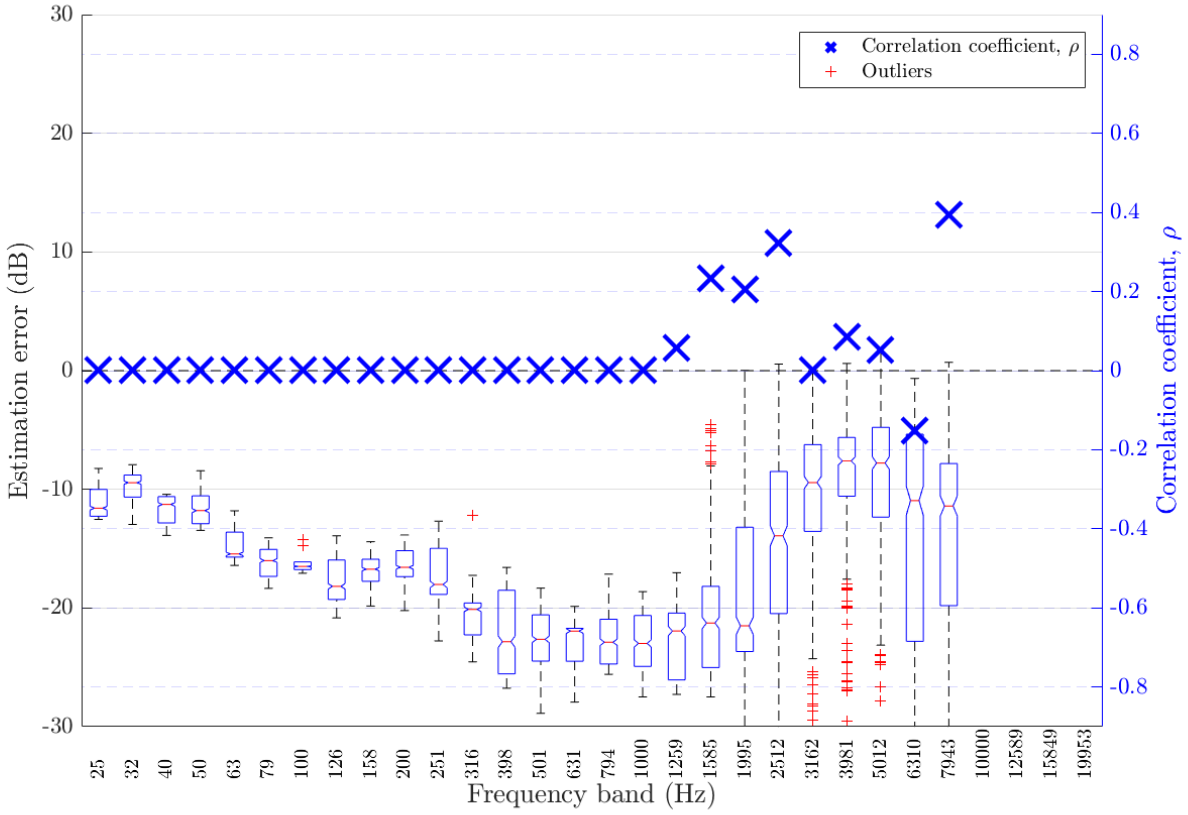

Figure 78: Frequency-dependent DRR estimation error in babble noise at -1 dB SNR for algorithm DENBE with FFT derived subbands [7]

Table 74: Frequency-dependent DRR estimation error in babble noise at $-1\,\mathrm{dB}$ SNR for algorithm DENBE with FFT derived subbands [7]

Freq. band	Centre Freq. (Hz)	Bias	MSE	ρ
1	25.12	-11.07	124.4	0
2	31.62	-9.93	100.8	0
3	39.81	-11.69	138.1	0
4	50.12	-11.55	135.4	0
5	63.10	-14.82	221.5	0
6	79.43	-16.09	260.6	0
7	100.00	-16.18	262.6	0
8	125.89	-17.74	318.4	0
9	158.49	-16.76	283.2	0
10	199.53	-16.72	282.9	0
11	251.19	-17.66	321.9	0
12	316.23	-19.99	410	0
13	398.11	-22.2	506.2	0
14	501.19	-22.78	528.4	0
15	630.96	-22.89	529.6	0
16	794.33	-22.2	501.5	0
17	1000.00	-23.01	537.8	0
18	1258.93	-22.4	512.4	0.05738
19	1584.89	-21.07	467.4	0.2331
20	1995.26	-18.92	408.7	0.206
21	2511.89	-14.69	277.9	0.3235
22	3162.28	-11.24	173.9	0.001717
23	3981.07	-9.009	112.8	0.08607
24	5011.87	-9.218	126.4	0.05141
25	6309.57	-13.35	263.9	-0.1515
26	7943.28	-13.38	237.1	0.3941

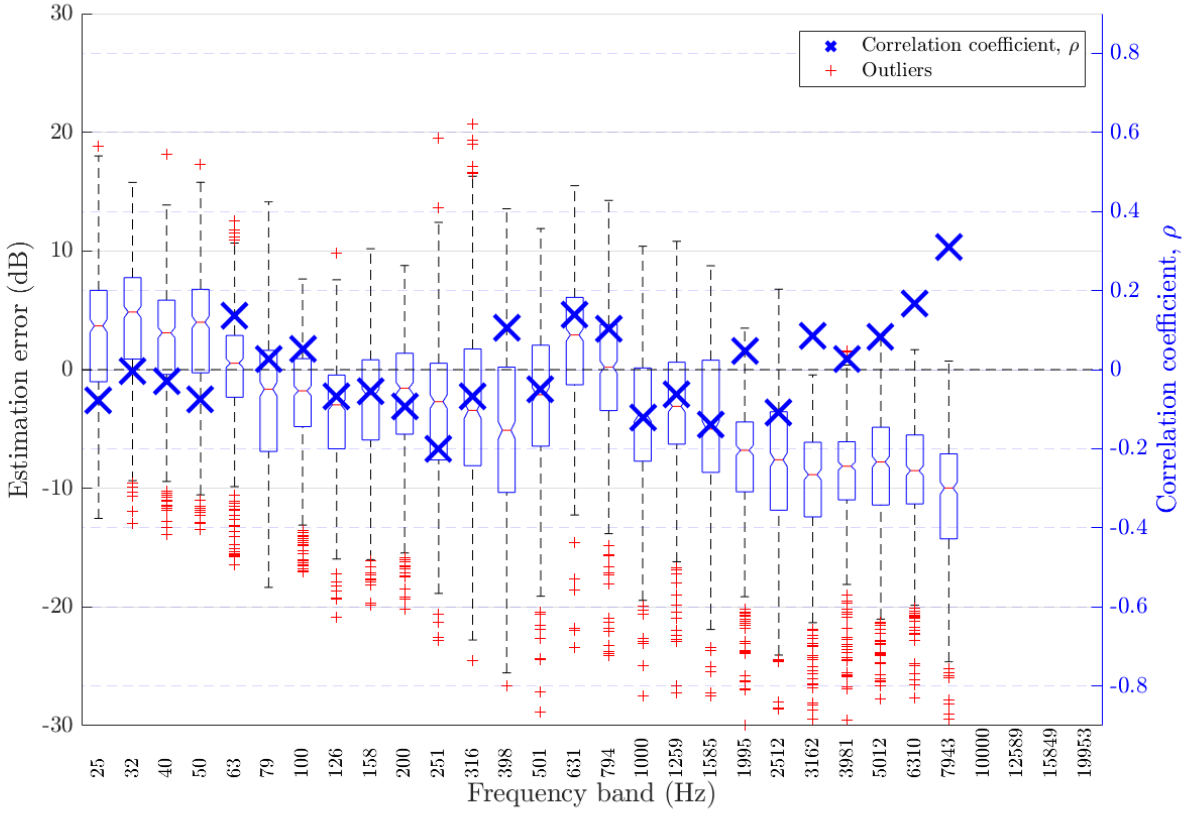

Figure 79: Frequency-dependent DRR estimation error in babble noise at -1 dB SNR for algorithm DENBE with filtered subbands [7]

Table 75: Frequency-dependent DRR estimation error in babble noise at $-1\,\mathrm{dB}$ SNR for algorithm DENBE with filtered subbands [7]

Freq. band	Centre Freq. (Hz)	Bias	MSE	ρ
1	25.12	1.979	51.03	-0.07764
2	31.62	3.419	50.61	-0.00371
3	39.81	1.894	41.34	-0.02848
4	50.12	2.567	45.96	-0.07436
5	63.10	-0.4269	31.73	0.1359
6	79.43	-3.042	61.8	0.02766
7	100.00	-3.029	42.37	0.05269
8	125.89	-4.269	52.43	-0.06707
9	158.49	-3.339	51.56	-0.05568
10	199.53	-2.879	44.53	-0.09246
11	251.19	-3.977	69.08	-0.2014
12	316.23	-3.357	85.18	-0.06781
13	398.11	-5.701	96.52	0.1071
14	501.19	-2.899	63.08	-0.05049
15	630.96	2.181	37.39	0.1397
16	794.33	-0.4429	41.57	0.1041
17	1000.00	-4.534	68.66	-0.1207
18	1258.93	-3.205	48.64	-0.06257
19	1584.89	-4.756	70.9	-0.1387
20	1995.26	-8.265	103.4	0.04785
21	2511.89	-8.472	122.4	-0.1081
22	3162.28	-10.3	146.5	0.08453
23	3981.07	-9.382	119	0.02584
24	5011.87	-8.7	106.5	0.08226
25	6309.57	-8.815	101.9	0.1664
26	7943.28	-10.96	149.5	0.31

4.5.7 **Fan noise at** 18 dB

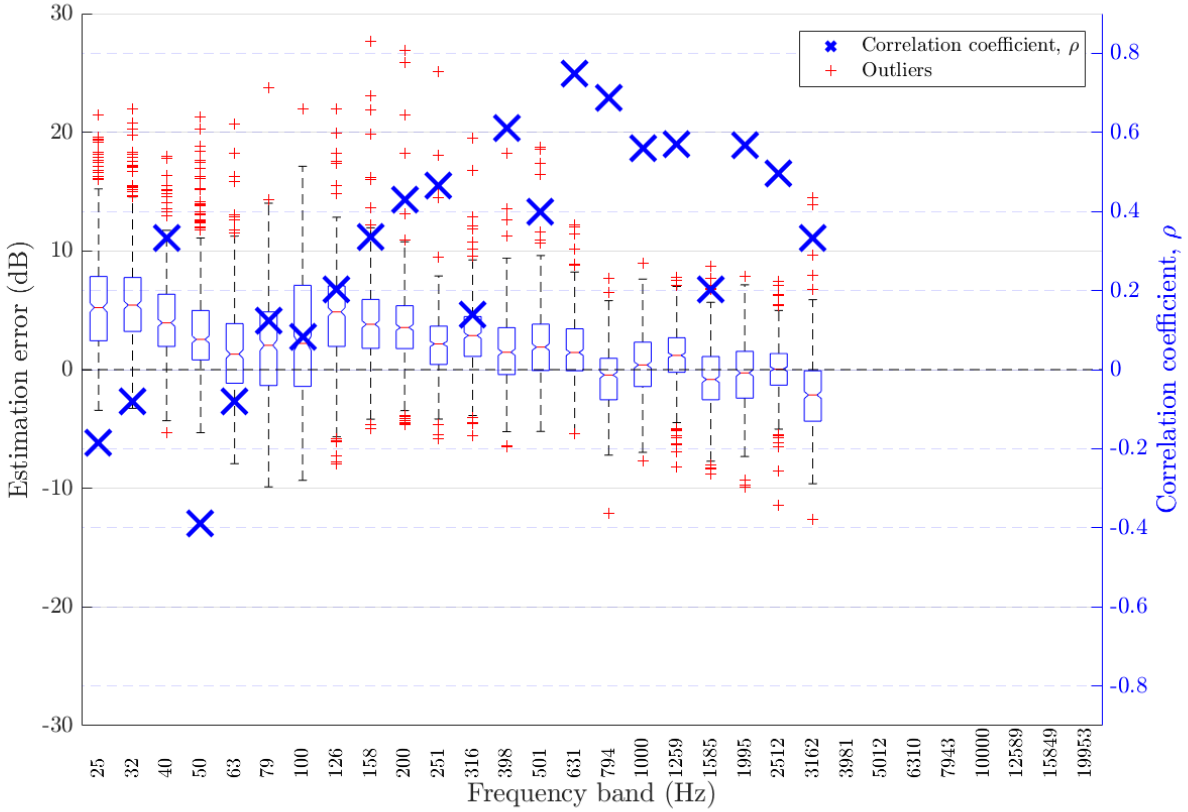

Figure 80: Frequency-dependent DRR estimation error in fan noise at 18 dB SNR for algorithm Particle Velocity [8]

Table 76: Frequency-dependent DRR estimation error in fan noise at $18\,\mathrm{dB}$ SNR for algorithm Particle Velocity [8]

Freq. band	Centre Freq. (Hz)	Bias	MSE	ρ
1	25.12	5.568	49.61	-0.186
2	31.62	5.965	50.92	-0.08042
3	39.81	4.347	31.19	0.3321
4	50.12	3.23	26.9	-0.3896
5	63.10	1.687	19.34	-0.0814
6	79.43	1.879	22.24	0.1236
7	100.00	2.695	34.55	0.08174
8	125.89	4.451	36.98	0.2025
9	158.49	4.048	28.93	0.3348
10	199.53	3.646	24.23	0.429
11	251.19	2.164	12.43	0.4663
12	316.23	2.854	16.33	0.1379
13	398.11	1.763	11.81	0.6109
14	501.19	2.169	15.36	0.3992
15	630.96	1.783	10.47	0.7474
16	794.33	-0.5915	7.34	0.6872
17	1000.00	0.4346	6.893	0.5591
18	1258.93	1.174	7.707	0.569
19	1584.89	-0.7393	8.931	0.2038
20	1995.26	-0.3955	6.943	0.5677
21	2511.89	-0.07322	5.205	0.496
22	3162.28	-2.109	14.92	0.3336

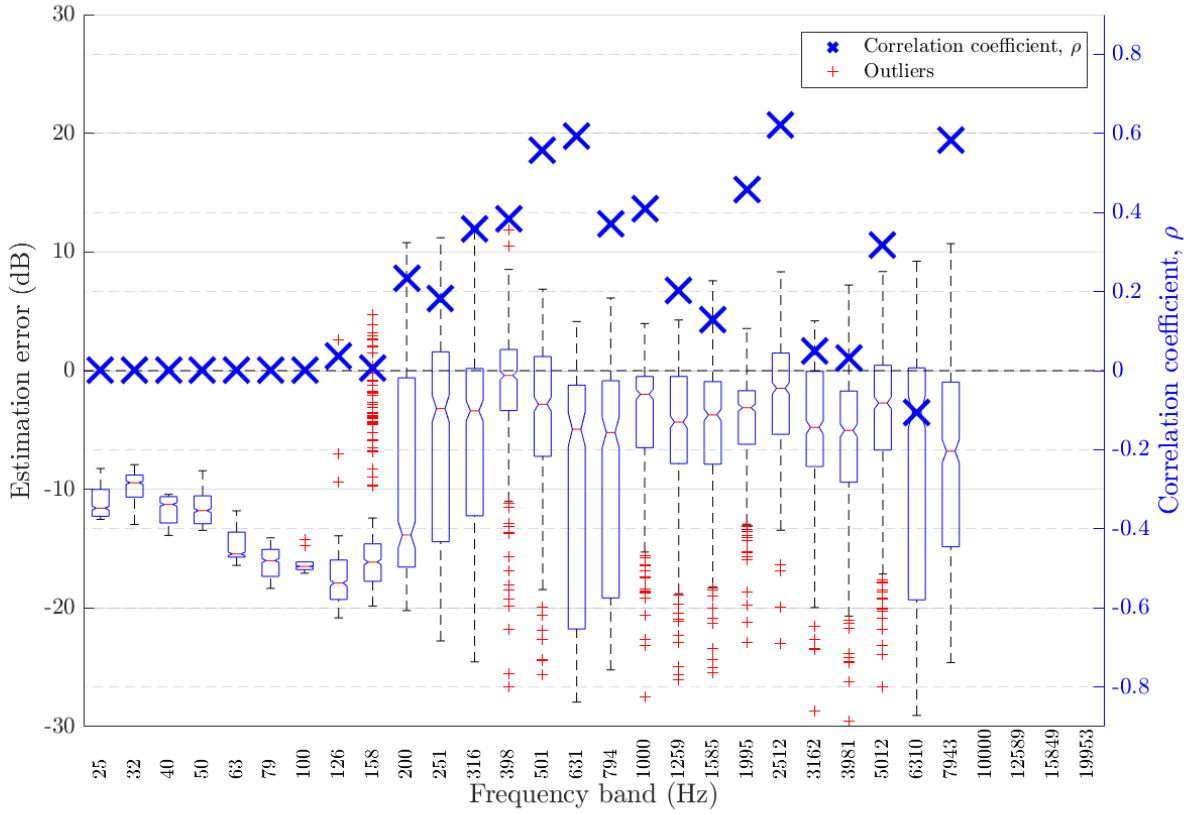

Figure 81: Frequency-dependent DRR estimation error in fan noise at 18 dB SNR for algorithm DENBE with FFT derived subbands [7]

Table 77: Frequency-dependent DRR estimation error in fan noise at $18\,\mathrm{dB}$ SNR for algorithm DENBE with FFT derived subbands [7]

Freq. band	Centre Freq. (Hz)	Bias	MSE	ρ
1	25.12	-11.07	124.4	0
2	31.62	-9.93	100.8	0
3	39.81	-11.69	138.1	0
4	50.12	-11.55	135.4	0
5	63.10	-14.82	221.5	0
6	79.43	-16.09	260.6	0
7	100.00	-16.18	262.6	0
8	125.89	-17.65	316.3	0.03643
9	158.49	-15.56	260.9	0.006855
10	199.53	-8.973	155.2	0.234
11	251.19	-5.995	120.8	0.1831
12	316.23	-5.986	96.83	0.3581
13	398.11	-1.476	33.87	0.3833
14	501.19	-4.451	71.67	0.5581
15	630.96	-10.04	193.9	0.5922
16	794.33	-8.864	165.3	0.3703
17	1000.00	-4.469	61.2	0.4102
18	1258.93	-5.349	70.01	0.2037
19	1584.89	-4.49	57.63	0.1294
20	1995.26	-4.358	34.73	0.4578
21	2511.89	-2.074	22.13	0.6219
22	3162.28	-5.059	58.43	0.05027
23	3981.07	-6.16	72.68	0.03261
24	5011.87	-5.025	90.52	0.3185
25	6309.57	-8.276	202.8	-0.1055
26	7943.28	-8.321	158.4	0.5825

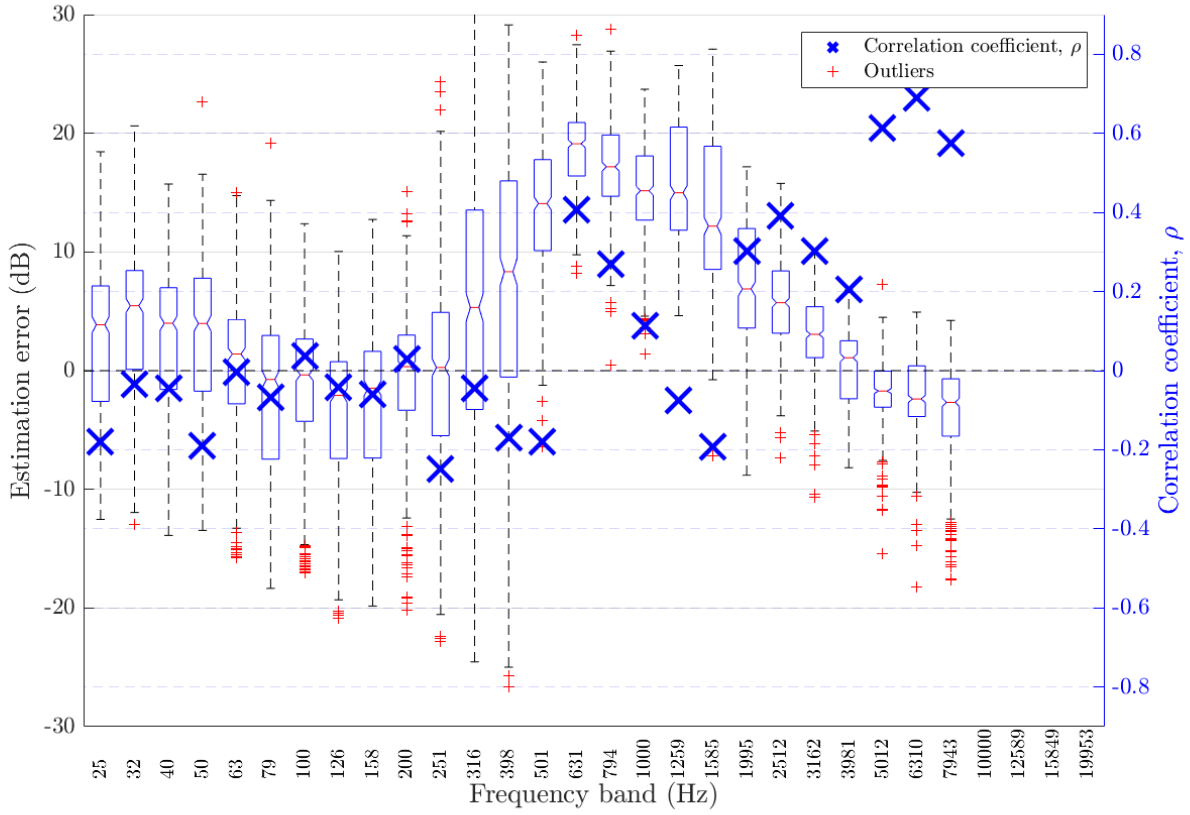

Figure 82: Frequency-dependent DRR estimation error in fan noise at 18 dB SNR for algorithm DENBE with filtered subbands [7]

Table 78: Frequency-dependent DRR estimation error in fan noise at $18\,\mathrm{dB}$ SNR for algorithm DENBE with filtered subbands [7]

Freq. band	Centre Freq. (Hz)	Bias	MSE	ρ
1	25.12	1.877	59.57	-0.18
2	31.62	3.281	65.71	-0.03397
3	39.81	1.818	56.53	-0.04415
4	50.12	1.93	66.65	-0.1904
5	63.10	-0.3509	50.46	-0.004009
6	79.43	-2.634	69.71	-0.06639
7	100.00	-2.127	52.01	0.03706
8	125.89	-4.104	67.28	-0.04096
9	158.49	-3.5	64.13	-0.05915
10	199.53	-1.274	46.11	0.02888
11	251.19	-0.8414	75.93	-0.249
12	316.23	5.042	166.6	-0.04575
13	398.11	7.572	164.5	-0.1703
14	501.19	13.87	223.2	-0.1801
15	630.96	18.65	358.2	0.4069
16	794.33	17.12	307.6	0.2691
17	1000.00	15.18	246.9	0.1132
18	1258.93	15.73	271.9	-0.07646
19	1584.89	13.04	207.9	-0.192
20	1995.26	7.297	77.76	0.3027
21	2511.89	5.92	51.58	0.3914
22	3162.28	2.992	17.82	0.3029
23	3981.07	0.08042	9.421	0.2053
24	5011.87	-1.62	9.631	0.6133
25	6309.57	-2.155	13.15	0.6909
26	7943.28	-3.579	29.57	0.5761

4.5.8 Fan noise at 12 dB

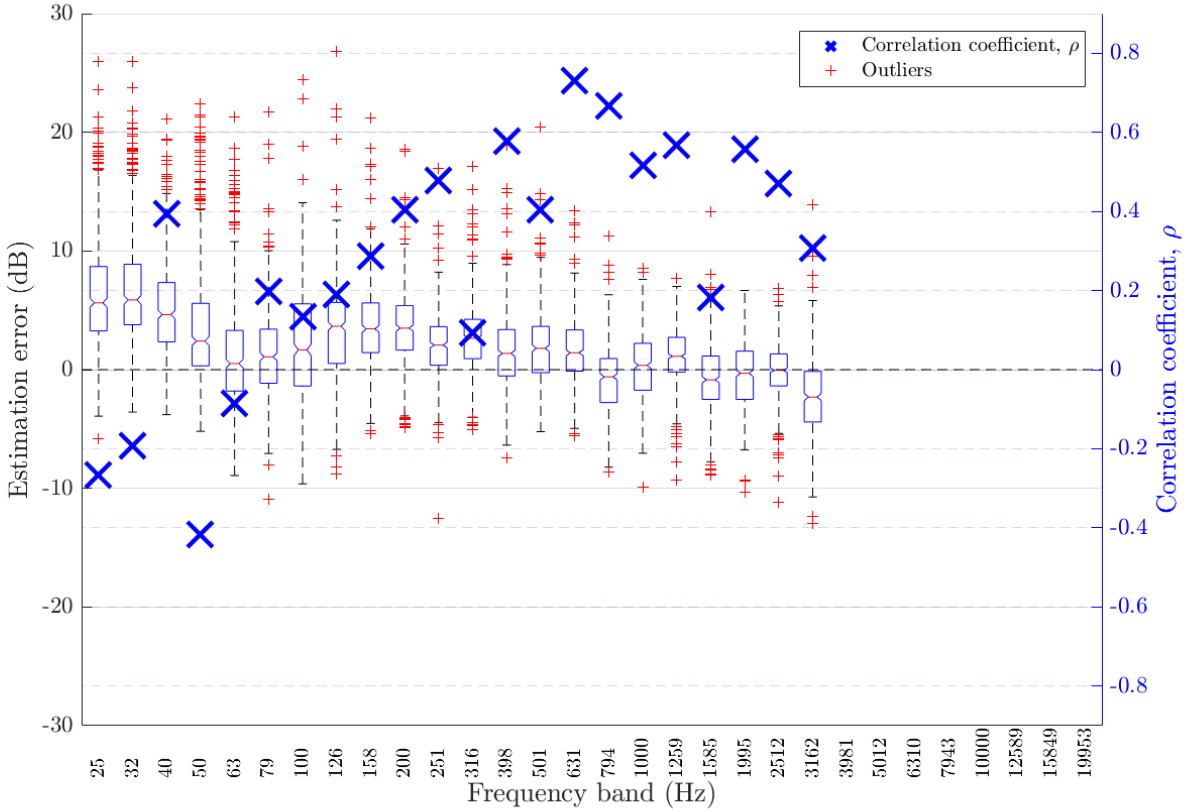

Figure 83: Frequency-dependent DRR estimation error in fan noise at 12 dB SNR for algorithm Particle Velocity [8]

Table 79: Frequency-dependent DRR estimation error in fan noise at 12 dB SNR for algorithm Particle Velocity [8]

Freq. band	Centre Freq. (Hz)	Bias	MSE	ρ
1	25.12	6.373	63.43	-0.2652
2	31.62	6.808	66.57	-0.1931
3	39.81	5.128	41.74	0.393
4	50.12	3.517	35.93	-0.4176
5	63.10	1.242	22.04	-0.08476
6	79.43	1.304	16.38	0.1981
7	100.00	2.093	26.43	0.1344
8	125.89	3.115	27.96	0.1907
9	158.49	3.676	25.06	0.2859
10	199.53	3.561	21.94	0.4053
11	251.19	2.027	11.1	0.4792
12	316.23	2.664	15.53	0.0931
13	398.11	1.649	12.23	0.5775
14	501.19	2.012	14.11	0.403
15	630.96	1.736	10.56	0.7308
16	794.33	-0.7317	8.364	0.6664
17	1000.00	0.3256	7.451	0.5155
18	1258.93	1.141	7.829	0.5666
19	1584.89	-0.7265	9.257	0.1824
20	1995.26	-0.4448	7.139	0.5573
21	2511.89	-0.1216	5.385	0.4696
22	3162.28	-2.204	15.46	0.3065

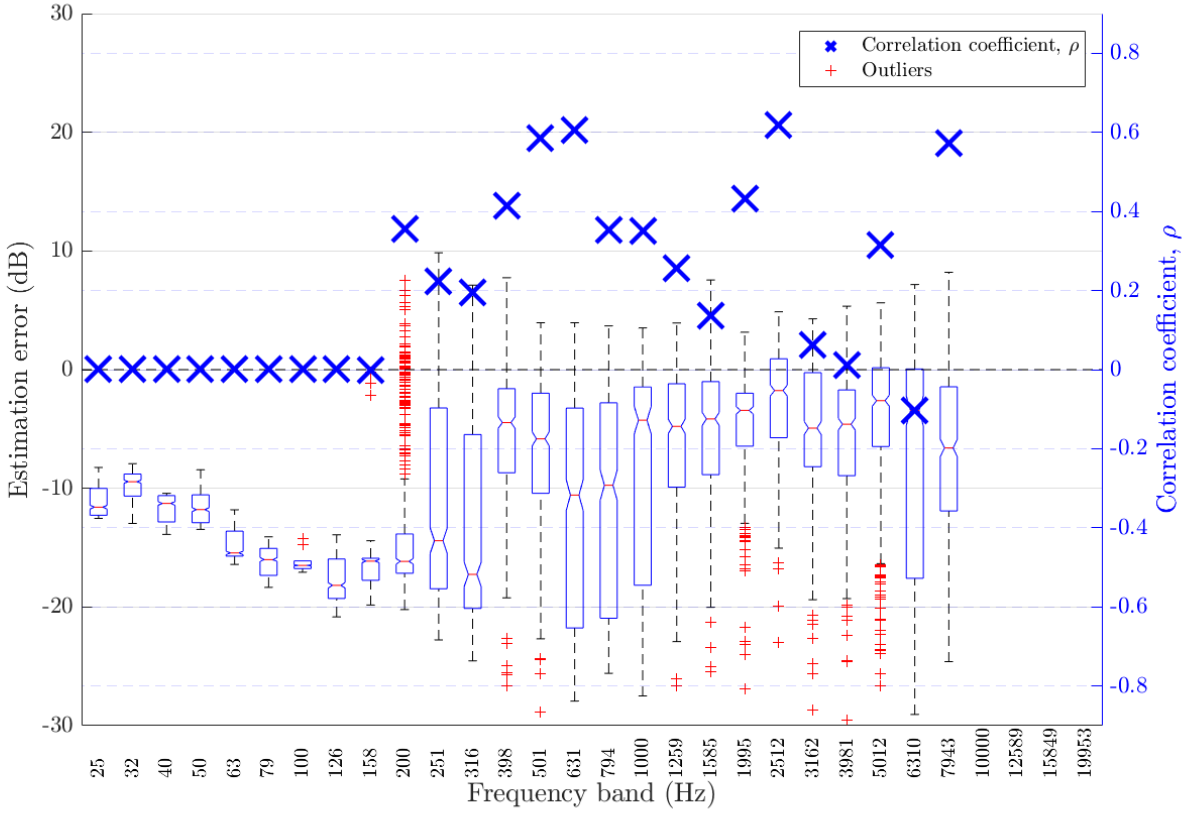

Figure 84: Frequency-dependent DRR estimation error in fan noise at 12 dB SNR for algorithm DENBE with FFT derived subbands [7]

Table 80: Frequency-dependent DRR estimation error in fan noise at 12 dB SNR for algorithm DENBE with FFT derived subbands [7]

Freq. band	Centre Freq. (Hz)	Bias	MSE	ρ
1	25.12	-11.07	124.4	0
2	31.62	-9.93	100.8	0
3	39.81	-11.69	138.1	0
4	50.12	-11.55	135.4	0
5	63.10	-14.82	221.5	0
6	79.43	-16.09	260.6	0
7	100.00	-16.18	262.6	0
8	125.89	-17.74	318.4	0
9	158.49	-16.66	281.5	-0.001611
10	199.53	-13.78	225.6	0.3551
11	251.19	-11.38	199.2	0.2235
12	316.23	-13.58	253.6	0.1957
13	398.11	-5.869	78.75	0.414
14	501.19	-7.438	106.1	0.5862
15	630.96	-12.22	230.3	0.6053
16	794.33	-11.73	223.1	0.3537
17	1000.00	-8.183	144	0.3512
18	1258.93	-6.818	99.92	0.2574
19	1584.89	-4.966	65.99	0.1365
20	1995.26	-4.839	43.62	0.4311
21	2511.89	-2.527	25.36	0.6183
22	3162.28	-5.205	60.28	0.0624
23	3981.07	-6.064	71.88	0.0111
24	5011.87	-5.174	90.29	0.3143
25	6309.57	-8.275	195.9	-0.1023
26	7943.28	-8.247	151.4	0.5723

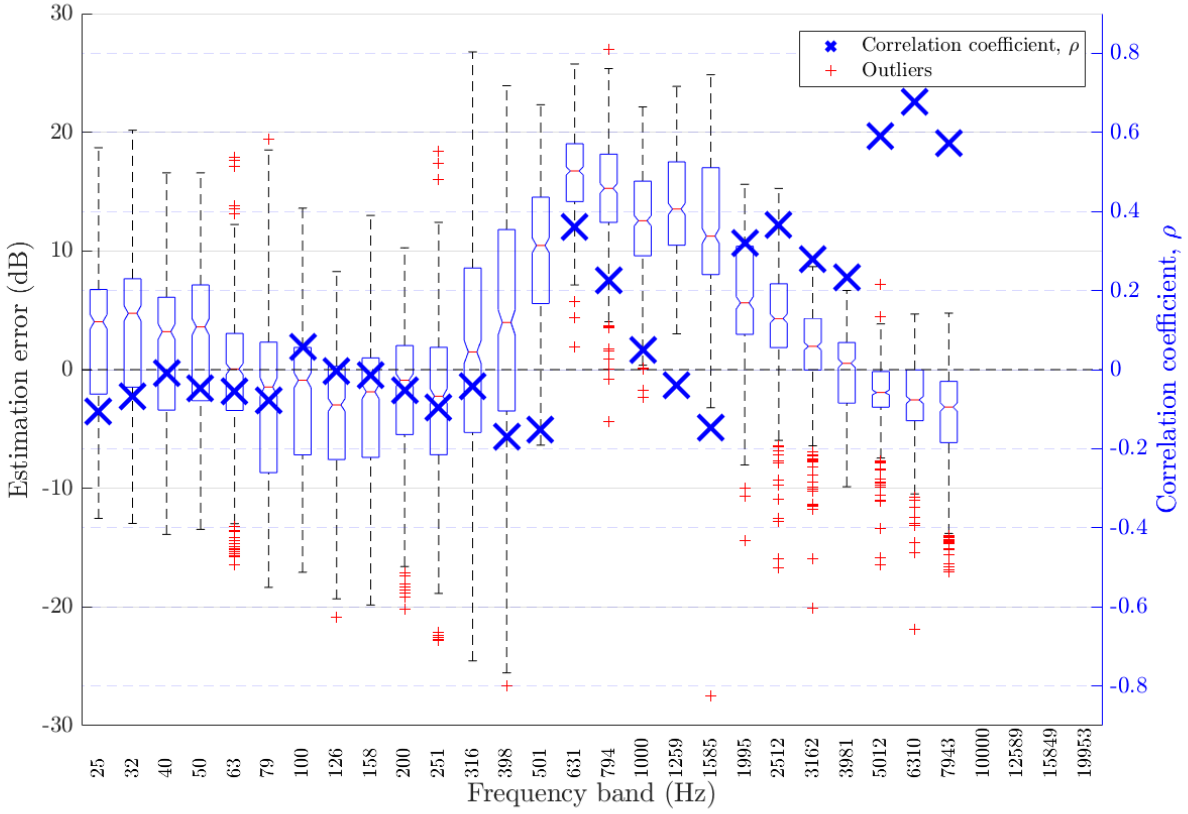

Figure 85: Frequency-dependent DRR estimation error in fan noise at 12 dB SNR for algorithm DENBE with filtered subbands [7]

Table 81: Frequency-dependent DRR estimation error in fan noise at $12\,\mathrm{dB}$ SNR for algorithm DENBE with filtered subbands [7]

Freq. band	Centre Freq. (Hz)	Bias	MSE	ρ
1	25.12	1.945	57.33	-0.1064
2	31.62	2.648	61.43	-0.06851
3	39.81	0.732	50.87	-0.009295
4	50.12	1.479	55.93	-0.04758
5	63.10	-1.065	47.53	-0.05469
6	79.43	-3.138	76.39	-0.07837
7	100.00	-3.221	60.88	0.05739
8	125.89	-4.621	67.87	-0.003219
9	158.49	-3.731	64.3	-0.01393
10	199.53	-2.962	56.44	-0.05119
11	251.19	-3.522	73.98	-0.09599
12	316.23	1.612	118.3	-0.0424
13	398.11	3.888	110.4	-0.1705
14	501.19	9.92	134.4	-0.1507
15	630.96	16.39	281.5	0.3608
16	794.33	14.98	244	0.2259
17	1000.00	12.57	180.4	0.05034
18	1258.93	13.99	215.4	-0.03996
19	1584.89	11.76	175.6	-0.1455
20	1995.26	6.072	61.61	0.3206
21	2511.89	4.316	41.11	0.3652
22	3162.28	1.643	17.93	0.2787
23	3981.07	-0.2957	10.14	0.2337
24	5011.87	-1.847	11.5	0.5915
25	6309.57	-2.485	16.07	0.6766
26	7943.28	-3.96	32.92	0.5712

4.5.9 Fan noise at -1 dB

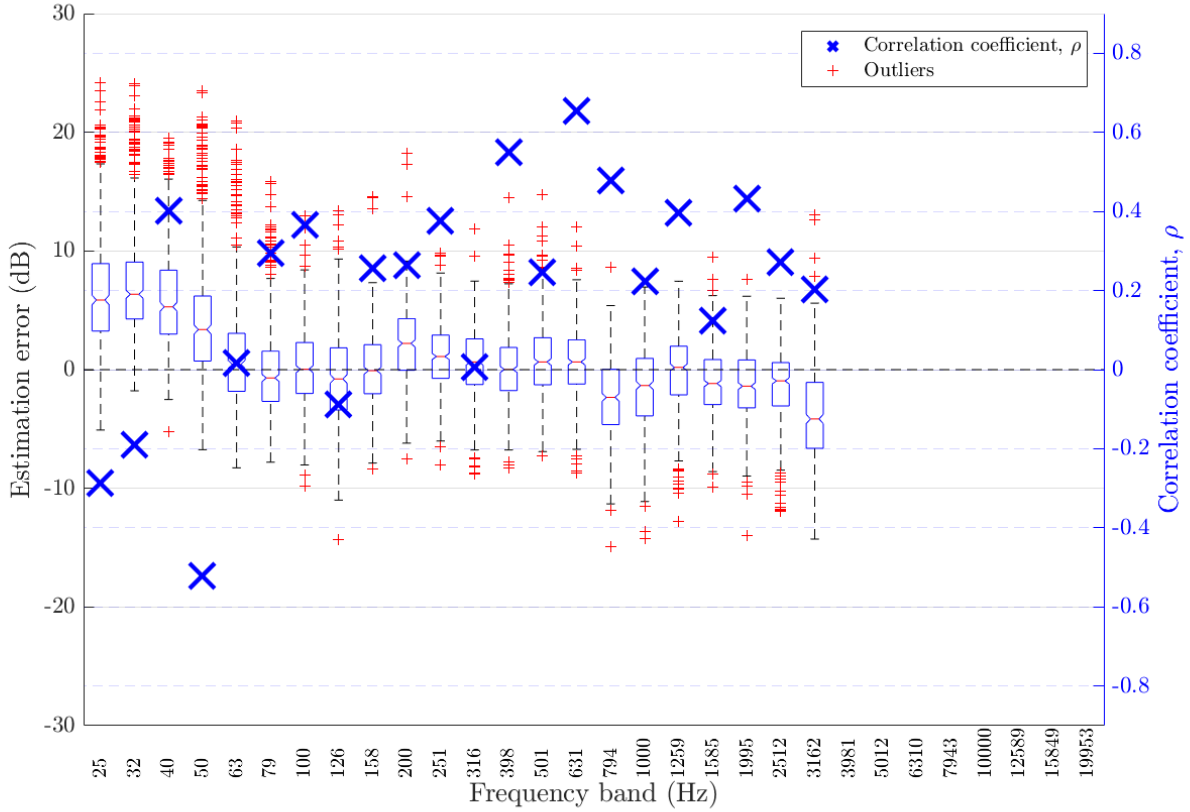

Figure 86: Frequency-dependent DRR estimation error in fan noise at -1 dB SNR for algorithm Particle Velocity [8]

Table 82: Frequency-dependent DRR estimation error in fan noise at $-1\,\mathrm{dB}$ SNR for algorithm Particle Velocity [8]

Freq. band	Centre Freq. (Hz)	Bias	MSE	ρ
1	25.12	6.8	72.14	-0.287
2	31.62	7.455	78.9	-0.19
3	39.81	6.075	55.28	0.4025
4	50.12	4.507	49.85	-0.5202
5	63.10	1.368	25.83	0.01604
6	79.43	-0.09664	15.99	0.2945
7	100.00	0.228	11.85	0.3664
8	125.89	-0.6912	16.52	-0.08779
9	158.49	0.03129	11.16	0.2558
10	199.53	2.087	14.03	0.2636
11	251.19	1.118	9.479	0.377
12	316.23	0.4814	10.35	0.00513
13	398.11	0.2001	9.138	0.5485
14	501.19	0.9111	11.69	0.2467
15	630.96	0.6737	9.642	0.653
16	794.33	-2.361	17.37	0.4788
17	1000.00	-1.593	15.72	0.2228
18	1258.93	-0.1792	10.81	0.3957
19	1584.89	-1.115	10.13	0.1225
20	1995.26	-1.244	10.04	0.4323
21	2511.89	-1.36	10.79	0.2724
22	3162.28	-3.863	30	0.2019

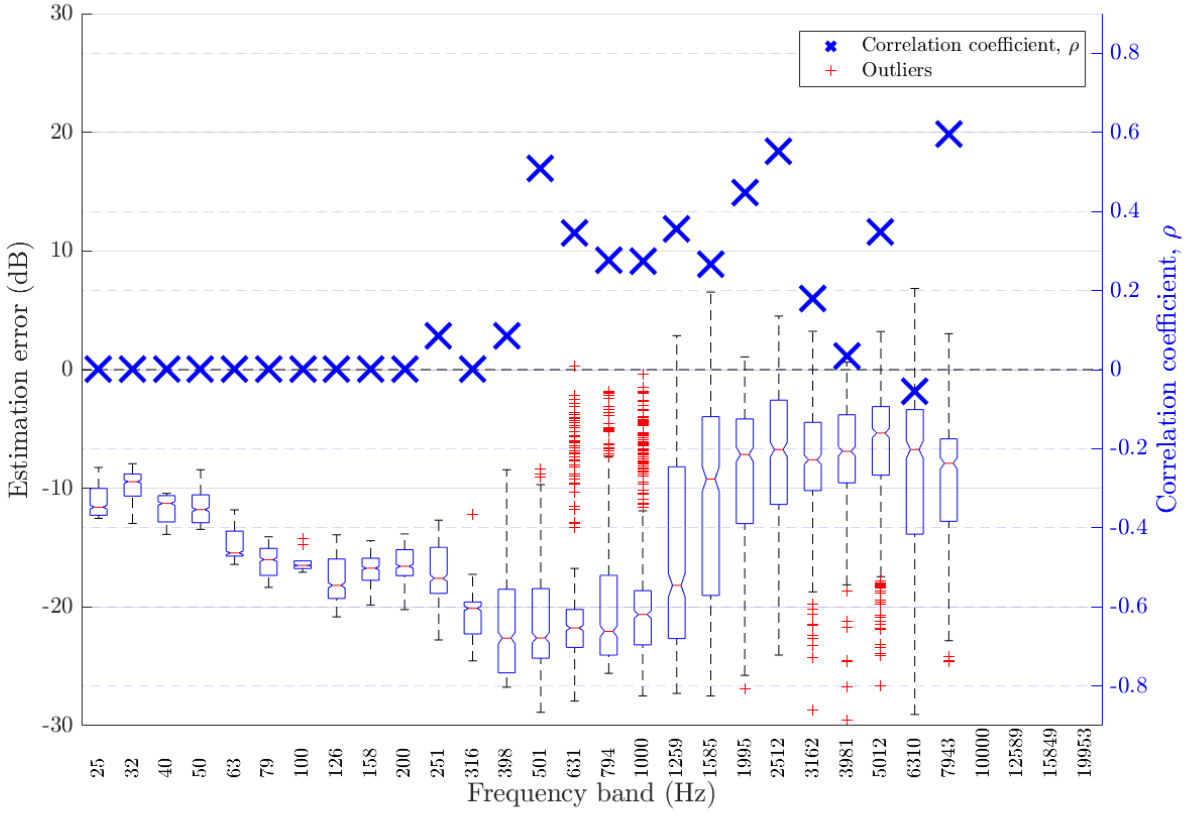

Figure 87: Frequency-dependent DRR estimation error in fan noise at -1 dB SNR for algorithm DENBE with FFT derived subbands [7]

Table 83: Frequency-dependent DRR estimation error in fan noise at $-1\,\mathrm{dB}$ SNR for algorithm DENBE with FFT derived subbands [7]

Freq. band	Centre Freq. (Hz)	Bias	MSE	ρ
1	25.12	-11.07	124.4	0
2	31.62	-9.93	100.8	0
3	39.81	-11.69	138.1	0
4	50.12	-11.55	135.4	0
5	63.10	-14.82	221.5	0
6	79.43	-16.09	260.6	0
7	100.00	-16.18	262.6	0
8	125.89	-17.74	318.4	0
9	158.49	-16.76	283.2	0
10	199.53	-16.72	282.9	0
11	251.19	-17.65	321.3	0.0866
12	316.23	-19.99	410	0
13	398.11	-22.1	502.3	0.08582
14	501.19	-21.71	484.2	0.509
15	630.96	-21.11	472.3	0.346
16	794.33	-20.42	446.5	0.2772
17	1000.00	-19.35	421.9	0.2746
18	1258.93	-15.99	322.6	0.3556
19	1584.89	-11.44	211.3	0.2663
20	1995.26	-9.818	149.7	0.4475
21	2511.89	-7.989	113.3	0.5531
22	3162.28	-7.629	86.07	0.1787
23	3981.07	-7.42	80.61	0.03488
24	5011.87	-7.202	96.03	0.3475
25	6309.57	-10.12	195.3	-0.05608
26	7943.28	-10.14	155.3	0.5944

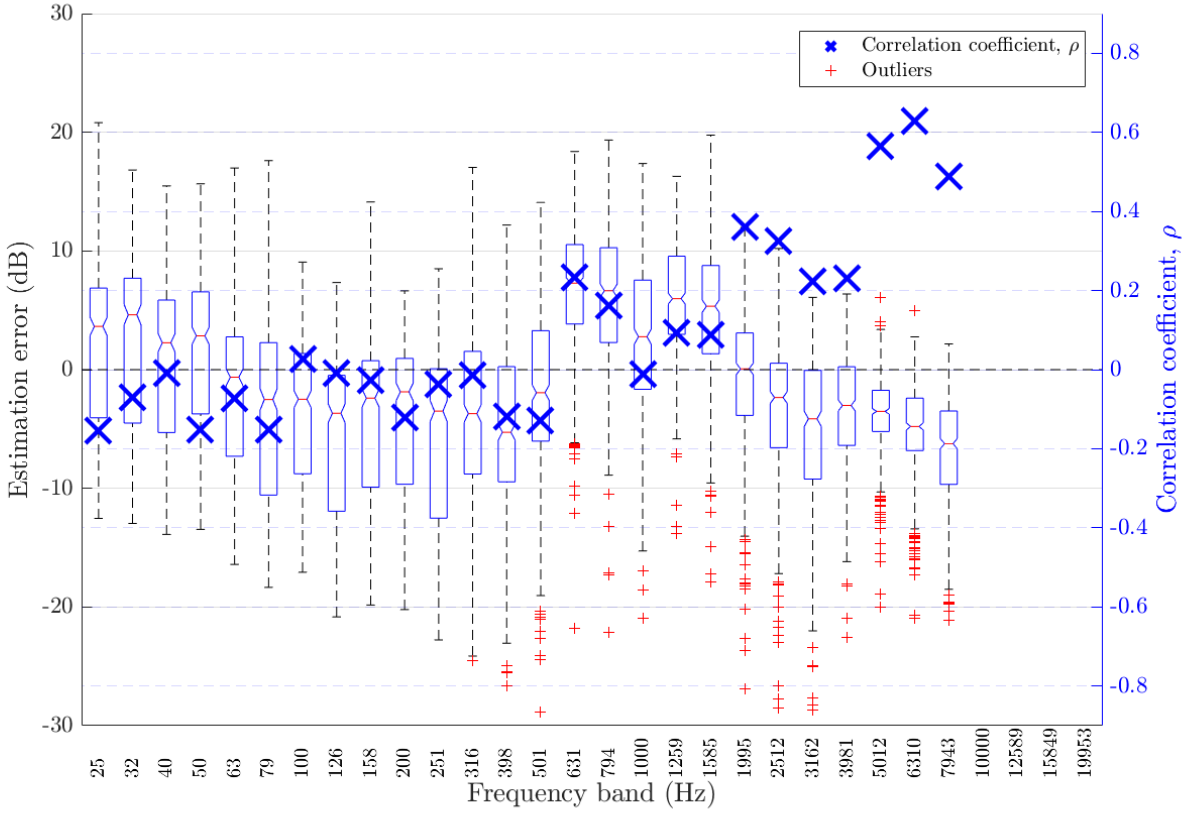

Figure 88: Frequency-dependent DRR estimation error in fan noise at -1 dB SNR for algorithm DENBE with filtered subbands [7]

Table 84: Frequency-dependent DRR estimation error in fan noise at $-1\,\mathrm{dB}$ SNR for algorithm DENBE with filtered subbands [7]

Freq. band	Centre Freq. (Hz)	Bias	MSE	ρ
1	25.12	1.193	59.71	-0.1535
2	31.62	2.184	62.21	-0.07125
3	39.81	0.1626	53.79	-0.009991
4	50.12	0.8293	54.66	-0.1506
5	63.10	-2.534	63.23	-0.07202
6	79.43	-3.812	87.12	-0.1506
7	100.00	-4.249	67.75	0.02707
8	125.89	-5.983	89.82	-0.009966
9	158.49	-4.554	78.42	-0.02563
10	199.53	-4.572	75.23	-0.1223
11	251.19	-5.887	95.82	-0.03686
12	316.23	-4.265	85.56	-0.01496
13	398.11	-5.381	95.37	-0.1178
14	501.19	-1.976	58.09	-0.1292
15	630.96	6.768	71.35	0.2326
16	794.33	6.021	72.37	0.162
17	1000.00	2.513	48.16	-0.01271
18	1258.93	5.994	58.64	0.09297
19	1584.89	4.96	62.21	0.08827
20	1995.26	-0.658	35.28	0.3601
21	2511.89	-3.467	51.26	0.3254
22	3162.28	-5.099	63.05	0.2232
23	3981.07	-3.56	31.75	0.2298
24	5011.87	-3.682	24.87	0.5644
25	6309.57	-5.057	40.37	0.6292
26	7943.28	-6.982	71.56	0.4892

References

[1] J. Eaton, N. D. Gaubitch, A. H. Moore, and P. A. Naylor, "The ACE Challenge - corpus description and performance evaluation," in *Proc. IEEE Workshop on Applications of Signal Processing to Audio and Acoustics (WASPAA)*, New Paltz, NY, USA, 2015.

[2] ——, "Proc. ACE challenge workshop, a satellite of IEEE-WASPAA," New Paltz, NY, USA, 2015. [Online]. Available: http://arxiv.org/abs/1510.00383

[3] H. W. Löllmann, E. Yilmaz, M. Jeub, and P. Vary, "An improved algorithm for blind reverberation time estimation," in *Proc. Intl. on Workshop Acoust. Echo and Noise Control (IWAENC)*, Tel-Aviv, Israel, Aug. 2010, pp. 1–4.

[4] P. P. Parada, D. Sharma, T. van Waterschoot, and P. A. Naylor, "Evaluating the non-intrusive room acoustics algorithm with the ACE challenge," in *Proc. ACE Challenge Workshop, a satellite of IEEE-WASPAA*, New Paltz, NY, USA, Oct. 2015.

[5] N. D. Gaubitch, H. W. Löllmann, M. Jeub, T. H. Falk, P. A. Naylor, P. Vary, and M. Brookes, "Performance comparison of algorithms for blind reverberation time estimation from speech," in *Proc. Intl. Workshop on Acoustic Signal Enhancement (IWAENC)*, Aachen, Germany, Sept. 2012.

[6] M. Jeub, C. M. Nelke, C. Beaugeant, and P. Vary, "Blind estimation of the coherent-to-diffuse energy ratio from noisy speech signals," in *Proc. European Signal Processing Conf. (EUSIPCO)*, Barcelona, Spain, 2011, pp. 1347–1351.

[7] J. Eaton and P. A. Naylor, "Direct-to-reverberant ratio estimation on the ACE corpus using a two-channel beamformer," in *Proc. ACE Challenge Workshop, a satellite of IEEE-WASPAA*, New Paltz, NY, USA, Oct. 2015.

[8] H. Chen, P. N. Samarasinghe, T. D. Abhayapala, and W. Zhang, "Estimation of the direct-to-reverberant energy ratio using a spherical microphone array," in *Proc. ACE Challenge Workshop, a satellite of IEEE-WASPAA*, New Paltz, NY, USA, Oct. 2015.

[9] H. W. Löllmann, A. Brendel, P. Vary, and W. Kellermann, "Single-channel maximum-likelihood T_{60} estimation exploiting subband information," in *Proc. ACE Challenge Workshop, a satellite of IEEE-WASPAA*, New Paltz, NY, USA, Oct. 2015.

[10] *Acoustics - Measurement of the Reverberation Time of Rooms with Reference to Other Acoustical Parameters*, Intl. Org. for Standardization (ISO) Recommendation ISO-3382, May 2009.

[11] T. de M. Prego, A. A. de Lima, R. Zambrano-López, and S. L. Netto, "Blind estimators for reverberation time and direct-to-reverberant energy ratio using subband speech decomposition," in *Proc. IEEE Workshop on Applications of Signal Processing to Audio and Acoustics (WASPAA)*, New Paltz, NY, USA, 2015.

[12] J. Eaton and P. A. Naylor, "Reverberation time estimation on the ACE corpus using the SDD method," in *Proc. ACE Challenge Workshop, a satellite of IEEE-WASPAA*, New Paltz, NY, USA, Oct. 2015.

[13] J. Eaton, N. D. Gaubitch, and P. A. Naylor, "Noise-robust reverberation time estimation using spectral decay distributions with reduced computational cost," in *Proc. IEEE Intl. Conf. on Acoustics, Speech and Signal Processing (ICASSP)*, Vancouver, Canada, May 2013, pp. 161–165.

[14] F. Xiong, S. Goetze, and B. T. Meyer, "Joint estimation of reverberation time and direct-to-reverberation ratio from speech using auditory inspired features," in *Proc. ACE Challenge Workshop, a satellite of IEEE-WASPAA*, New Paltz, NY, USA, Oct. 2015.

[15] M. Senoussaoui, J. F. Santos, and T. H. Falk, "SRMR variants for improved blind room acoustics characterization," in *Proc. ACE Challenge Workshop, a satellite of IEEE-WASPAA*, New Paltz, NY, USA, Oct. 2015.

[16] J. F. Santos, M. Senoussaoui, and T. H. Falk, "An improved non-intrusive intelligibility metric for noisy and reverberant speech," in *Proc. Intl. Workshop on Acoustic Signal Enhancement (IWAENC)*, Antibes, France, Sept. 2014, pp. 55–59.

[17] F. Lim, M. R. P. Thomas, and I. J. Tashev, "Blur kernel estimation approach to blind reverberation time estimation," in *Proc. IEEE Intl. Conf. on Acoustics, Speech and Signal Processing (ICASSP)*, no. 40, Brisbane, Australia, Apr. 2015, pp. 41–45.

[18] F. Lim, M. R. P. Thomas, P. A. Naylor, and I. J. Tashev, "Acoustic blur kernel with sliding window for blind estimation of reverberation time," in *Proc. IEEE Workshop on Applications of Signal Processing to Audio and Acoustics (WASPAA)*, New Paltz, NY, USA, Oct. 2015.

[19] T. H. Falk, C. Zheng, and W.-Y. Chan, "A non-intrusive quality and intelligibility measure of reverberant and dereverberated speech," *IEEE Trans. Audio, Speech, Lang. Process.*, vol. 18, no. 7, pp. 1766–1774, Sept. 2010.

[20] J. Y. C. Wen, E. A. P. Habets, and P. A. Naylor, "Blind estimation of reverberation time based on the distribution of signal decay rates," in *Proc. IEEE Intl. Conf. on Acoustics, Speech and Signal Processing (ICASSP)*, Las Vegas, USA, Apr. 2008, pp. 329–332.

[21] Y. Hioka and K. Niwa, "PSD estimation in beamspace for estimating direct-to-reverberant ratio from a reverberant speech signal," in *Proc. ACE Challenge Workshop, a satellite of IEEE-WASPAA*, New Paltz, NY, USA, Oct. 2015.

[22] Y. Hioka, K. Furuya, K. Niwa, and Y. Haneda, "Estimation of direct-to-reverberation energy ratio based on isotropic and homogeneous propagation model," in *Proc. Intl. Workshop on Acoustic Signal Enhancement (IWAENC)*, Sept. 2012.

[23] Y. Hioka, K. Niwa, S. Sakauchi, K. Furuya, and Y. Haneda, "Estimating direct-to-reverberant energy ratio using D/R spatial correlation matrix model," *IEEE Trans. Audio, Speech, Lang. Process.*, vol. 19, no. 8, pp. 2374–2384, Nov. 2011.

[24] J. Eaton, A. H. Moore, P. A. Naylor, and J. Skoglund, "Direct-to-reverberant ratio estimation using a null-steered beamformer," in *Proc. IEEE Intl. Conf. on Acoustics, Speech and Signal Processing (ICASSP)*, Brisbane, Australia, Apr. 2015, pp. 46–50.

[25] T. H. Falk and W.-Y. Chan, "Temporal dynamics for blind measurement of room acoustical parameters," *IEEE Trans. Instrum. Meas.*, vol. 59, no. 4, pp. 978–989, 2010.